

UC Santa Cruz

UC Santa Cruz Electronic Theses and Dissertations

Title

Spt5 facilitates transcription through nucleosomes in vivo

Permalink

<https://escholarship.org/uc/item/750390zm>

Author

Doody, Michael Jake

Publication Date

2022

Peer reviewed|Thesis/dissertation

UNIVERSITY OF CALIFORNIA
SANTA CRUZ

Spt5 facilitates transcription through nucleosomes *in vivo*

A dissertation submitted in partial satisfaction
of the requirements for the degree of

DOCTOR OF PHILOSOPHY

In

Molecular, Cell and Developmental Biology

By

Michael Jake Doody

March 2022

The Dissertation of Michael Jake Doody is
approved:

Professor Grant Hartzog, chair

Professor Hinrich Boeger

Professor Rohinton Kamakaka

Peter Biehl
Vice Provost and Dean of Graduate Studies

Table of Contents

1. List of figures and tables.....	vi
2. Abstract.....	ix
3. Dedications and acknowledgements.....	xi
4. Chapter 1: introduction.....	1
I. General foundations of transcription, RNA polymerase, and gene structure..	1
II. Spt5: a multi-domain transcription elongation factor.....	2
III. Regulation of transcription elongation: rate and processivity.....	2
IV. RNA pol transcription elongation states.....	3
V. Positive and negative transcription regulation by Spt5.....	4
VI. Temporal association of Spt5.....	5
VII. Recruitment of Spt5.....	6
VIII. Histones and histone like proteins.....	8
IX. Nucleosomes are barriers to transcription elongation in vitro.....	9
X. Do nucleosomes inhibit transcription <i>in vivo</i> ?.....	10
XI. Nucleosome fate during transcription.....	12
XII. Nucleosome states alter transcription in vitro.....	13
XIII. Spt5 and the nucleosomal barrier.....	14
5. Chapter 2: A novel class of histone H3 mutations supports an <i>in vivo</i> role for Spt5 in promoting transcription through nucleosomes.....	22
I. Abstract.....	22
II. Introduction.....	23
III. Results.....	25
i. Screening for histone mutations that suppress a cold-sensitive allele of SPT5.....	25

ii.	Mutations altering residues in four distinct regions of histone H3 suppress <i>spt5-242</i>	26
1.	Mutations that alter N-terminal tail of H3.....	26
2.	Mutations that alter the N-terminal alpha helix of H3.....	26
3.	Mutations that disrupt residues in the vicinity of super-helical location (SHL) 2.5.....	27
4.	Mutations that alter residues near the C-terminal alpha helix of histone H3.....	27
iii.	Histone mutations exhibit growth, transcription, and potential DNA replication defects.....	27
iv.	Histone mutations that suppress <i>spt5-242</i> are distinct from <i>Irs</i> and <i>sin/bur</i> alleles of H3.....	29
v.	A conserved H3.3-like function in budding yeast--need a better section title.....	30
vi.	Nucleosome occupancy at the 3' end of yeast genes depends on a histone H3 surface.....	32
vii.	Predicted nucleosome thermodynamic stability affects nucleosome occupancy in vivo.....	33
viii.	<i>Spt5</i> and chromatin structure.....	36
IV.	Discussion.....	38
6.	Chapter 3: Epistatic relationships between transcription elongation factors and histone H3.....	81
I.	Introduction.....	81
II.	Results.....	83
i.	Identification of <i>hht2-G90R</i> , <i>R128S</i> genetic suppressors.....	83
ii.	Histone chaperones are essential in <i>hht2-G90R</i> , <i>R128S</i>	84

iii.	Chd1 nucleosome assembly specifically affects transcription elongation.....	86
iv.	<i>hht2</i> suppressors distinctly affect cryptic initiation.....	87
v.	Ubp10 has multiple enzymatic targets in vivo that act on transcribed chromatin.....	88
vi.	SAGA mediated Sgf73 function.....	90
III.	Discussion.....	94
7.	Chapter 4: Conclusion.....	125
8.	Appendices.....	131
I.	A genetic model for Spt5/Spt6/Spt16 nucleosomal transcription elongation.....	131
i.	Results.....	131
ii.	Overexpression of Spt2 rescues <i>spt5-242</i>	131
iii.	Dominant <i>SPT6</i> suppressors of <i>spt5-242</i>	133
iv.	Genetic evidence for disrupted <i>spt5/spt16</i> function.....	135
v.	Intramolecular suppression of <i>spt5-242</i>	137
vi.	Genetic model of nucleosomal transcription elongation.....	137
II.	List of plasmids.....	164
III.	List of strains.....	169
IV.	Materials and Methods.....	182
9.	References.....	189

List of Figures and Tables

Figure 1-1 Enclosure of transcribed DNA by NusG NGN domain.....	17
Figure 1-2 Structural Domains of Spt5.....	19
Figure 1-3 adapted catalytic cycle of RNA pol.....	21
Table 2-1 Identification of single, or double plasmid borne <i>spt5-242</i> <i>hht</i> -supp amino acid changes isolated in our screen or acquired from the indicated source.....	44
Table 2-2 Genetic interactions of <i>spt5-242</i> and the Hir and Caf complex.....	46
Figure 2-1 Chimera figure showing locations on the nucleosome of amino acid residues altered by <i>hht2</i> -supp mutations.....	48
Figure 2-2 <i>hht2 spt5-242</i> suppressor mutations have pleiotropic phenotypes.....	50
Figure 2-3 <i>hht2</i> mutations that suppress <i>spt5Cs</i> - have a strong cryptic initiation phenotype.....	52
Figure 2-4 <i>spt5-242 hht1-T118I</i> double mutants are inviable.....	54
Figure 2-5 yH3.1 and yH3.3 genetic interactions.....	56
Figure 2-6 Mapping mono-nucleosomes in <i>hht2-S87P, G90R</i> cells.....	58
Figure 2-7 Testing models for 3' nucleosome loss.....	60
Figure 2-8 <i>hht2-S87P, G90R</i> nucleosome occupancy.....	63
Figure 2-9 Predicted average nucleosome stability relative to RNA pol II active site (net-seq) under Spt5 non-depletion (mock) and depletion conditions.....	65
Figure 2-10 <i>spt5</i> cryptic initiation mutations predominantly occur in a novel Spt5 region.....	67

Figure 2-S1 <i>hht2 spt5Cs</i> - suppressor mutations generally do not disrupt telomeric silencing.....	69
Figure 2-S2 <i>hht2 spt5-242</i> suppressor mutations do not disrupt silencing at the mating type locus.....	71
Figure 2-S3 Histone H3 mutations near SH2.5 have a <i>bur</i> phenotype.....	73
Figure 2-S4 yH3.3 cryptic initiation is suppressed by yH3.1.....	75
Figure 2-S5 3' Nucleosome loss is still observed in genes that have not been observed to exhibit chromatin disruption phenotypes.....	77
Figure 2-S6 AlphaFold predictions of the Spt5 NPR from multiple species.....	80
Figure 3-1 <i>hht2</i> suppressors have different suppression phenotypes.....	102
Figure 3-2 <i>hht2</i> depends on transcription elongation histone chaperone function for viability.....	104
Figure 3-3 <i>chd1Δ</i> is epistatic to <i>rad6Δ</i> and <i>chd1</i> nucleosome assembly activity inhibits <i>chd1</i> phenotypes.....	106
Figure 3-4 <i>hfi1</i> decreases and <i>ubp10</i> increases non-allelic <i>hht2</i> cryptic initiation phenotypes.....	108
Figure 3-5 Ubp10 has multiple enzymatic targets that act in chromatin regulation.....	110
Figure 3-6 <i>hfi1</i> disrupts SAGA integrity and Sgf73 function.....	112
Table 3-1 Genetic characterization of SAGA functional domains.....	114
Table 3-2 Relative SAGA complex protein abundances purified from <i>hfi1</i> mutants.....	116
Figure 3-S1 Histone <i>h2b</i> has dominant phenotypes in <i>hht2</i>	118

Figure 3-S2 Sgf73 has Ubp8 independent function that inhibits <i>hht2</i> growth.....	120
Figure 3-S3 <i>sgf73</i> that fails to associate with SAGA displays incomplete suppression of <i>hht2</i>	122
Figure 3-S4 Epistatic relationships between the SAGA HAT-module and <i>hht2</i> suppressors.....	124
Table A1-1 <i>spt5-242</i> yH3.1 genetically interacts with known <i>spt5</i> suppressors.....	141
Figure A1-1 Overexpression of Spt2 rescues <i>spt5-242</i>	143
Table A1-2 Spt5 overlaps with Spt6 function.....	145
Figure A1-2 <i>spt6</i> mutations that suppress <i>spt5-242</i> cluster in the acidic N-terminus and disrupt chromatin function.....	147
Figure A1-3 All <i>spt6</i> alleles are dominant suppressors of <i>spt5-242</i>	149
Figure A1-4 <i>spt16</i> suppressors of <i>spt5-242</i> cluster in the Spt16 Mid-domain.....	151
Figure A1-5 Proximity of <i>h3</i> and <i>spt16</i> alleles during transcription.....	153
Table A1-3 Functional redundancy between <i>hht2-L61W</i> and <i>spt5-242</i>	155
Table A1-4 Genetic interactions between <i>spt5</i> , <i>h3</i> , <i>spt16</i> , <i>spt6</i>	157
Figure A1-6 Intramolecular suppressors of <i>spt5-242</i> suppress many phenotypes.....	159
Figure A1-7 Model for eukaryotic nucleosomal transcription elongation.....	161
Figure A1-S1 Functional overlap between Spt5 NPR and KOW2.....	163

Abstract

Spt5 facilitates transcription through nucleosomes *in vivo*

Michael Jake Doody

The key proteins that function during eukaryotic transcription elongation are likely to have all been identified, but *in vitro* reconstitution of this process remains incomplete. Nucleosomes inhibit transcription elongation *in vitro* and *in vivo*. However, actively transcribed genes *in vivo* remain nucleosomal. Thus, there must be some mechanism(s) that overcomes the nucleosomal barrier to transcription elongation and subsequently restores nucleosomes. Spt5 is a universally conserved transcription elongation factor thought to play a role in this process. However, the *in vivo* relevance of Spt5 for transcription through nucleosomes remains uncertain.

Here we present evidence that Spt5 facilitates transcription through nucleosomes *in vivo*. Chapter 1 summarizes the literature and current gaps in our knowledge of transcription elongation through chromatin. Chapter 2 presents a novel class of histone H3 mutations that suppress *spt5-242*, a transcription elongation defective mutation that genetically interacts with chromatin regulators. These H3 mutations disrupt transcribed chromatin, and result in reduced nucleosome density at the 3' ends of genes. Single-molecule analysis of one of these mutations revealed that nucleosomes predicted to be stable are selectively lost from the body of *PHO5* when it is actively transcribed. The selective loss of stable nucleosomes is also observed genome wide. Furthermore, we describe *spt5* mutations with chromatin disruption phenotypes that cluster in a poorly conserved region of Spt5 that we name the NGN-Proximal Region (NPR). AlphaFold predicts that the Spt5 NPR has structure in many organisms. We propose that the NPR functions as a hinge to dynamically facilitate transcription through nucleosomes.

Chapter 3 describes genetic suppressors of one of the *h3* mutations described in chapter 2. Loss of *sgf73/hfi1* SAGA, *ubp10*, *chd1*, or *spt5* function all suppress the temperature sensitive growth defect of this histone mutation. We establish an epistatic relationship between the *h3* genetic suppressors and key enzymes that function during transcription elongation: Rad6 and Gcn5. These results suggest that RSC chromatin remodeler and/or Spt16 function work in collaboration with Spt5 to transcribe through nucleosomal DNA.

The concluding Chapter 4 summarizes the main findings throughout this work and its relation to the knowledge gaps identified in Chapter 1.

Dedication and Acknowledgments

I'd like to dedicate this body of work to Grant Hartzog. You took a gamble on me twice and are the perfect mentor. If I were to do it all over again, I wouldn't change a thing. Maybe I'd tell myself to be a little more bold with letting you know my desire to stay at UCSC during my first run at grad school – I'm glad you convinced me to leave the nest, though. Somehow, I still got lucky and was able to cash in my winning ticket from 2008.

To everyone else who helped make this work possible, helped me throughout grad school, or helped me become who I am today – thank you. Most of you were able to see my defense live and my attempt to thank/embarrass you in the acknowledgments portion. For those of you that couldn't make it, I'll regale the tale next time I see you.

Chapter 1

Introduction

Diversification and specialization of gene regulation is a common evolutionary strategy in development. In general, an input (or condition) is interpreted by regulatory macromolecules and an output is produced. This scheme is used at: the different stages of RNA transcription, protein translation, post-transcriptional and post-translational events during gene expression. Defective gene regulation can result in human pathologies and is associated with many cancers. This thesis focuses on understanding the mechanisms of Eukaryotic RNA transcription in *S. cerevisiae* (budding yeast) with an emphasis on RNA transcription elongation.

General foundations of transcription, RNA polymerase, and gene structure

Eukaryotes express at least three different forms of RNA polymerase each of which transcribes a distinct region of the genome. RNA polymerase I (pol I) transcribes 25S ribosomal RNA, and RNA polymerase III (pol III) transcribes tRNA genes. In contrast to pol I and pol III, which transcribe a small number of genes and RNA polymerase II (pol II) transcribes the many thousands of protein coding genes, as well as non-coding RNA (ncRNA), and some small structural RNAs.

RNA transcription is generally regulated at three consecutive steps: initiation, elongation, and termination.

Gene architecture dictates transcription regulation. A promoter functions to recruit RNA pol and defines where transcription initiates. At the promoter, RNA polymerase undergoes abortive transcription initiation and has repetitive rounds of short RNA synthesis until a transcript of sufficient length is made and RNA pol clears the promoter. Once RNA pol has escaped the promoter, it transitions into transcription elongation and normally continues

transcription until a transcription termination signal is encountered. Once the transcription termination signal is encountered, the enzyme undergoes another transition into a termination state and subsequently halts transcription.

Both transcription initiation and termination are regulated by DNA sequence. General transcription factors recognize promoter elements through their DNA-binding-domains (DBDs). This recognition of a nucleic acid sequence (cis) by a protein (trans) is referred to as a cis/trans regulatory system. During transcription elongation the RNA polymerase will transcribe a region of DNA that encodes a cis-element that is recognized in the transcribed RNA – the poly-adenylation signal. The trans Cleavage and Polyadenylation Stimulating factors (CPSF) recognizes this cis element. CPSF cleaves the nascent RNA chain, releasing it from RNA pol II and setting the stage for transcription termination. In contrast to initiation and termination, transcription elongation is not known to be regulated by cis elements in genes.

Spt5: a multi-domain transcription elongation factor

Spt5/NusG is the only known transcription elongation factor that is universally conserved and essential for life. Phylogenetic comparisons show that the minimal form of Spt5 contains an unstructured N-terminus, the NGN domain that binds over the large RNA pol cleft (Fig. 1-1), and a Kyrpides, Ouzounis, Woese (KOW) domain (Kyrpides *et al.* 1996). KOW domains have also been found in some ribosomal proteins and have been shown to bind RNA. Whereas NusG functions as a monomer, eukaryotic and Archaeal Spt5 associate with a small zinc-finger protein, Spt4 (Hartzog *et al.* 1998; Guo *et al.* 2008) eukaryotes Spt5 has expanded the number of KOW domains and has gained a post-translationally modifiable carboxy terminal repeat (CTR) region (Fig 1-2).

Regulation of transcription elongation: rate and processivity

RNA polymerases must transcribe from the beginning to the end of a gene to make a functional product. In budding yeast, RNA pol II genes can vary from ~50-15,000 nucleotides in length while the longest gene in humans, dystrophin, is ~1.7 million bp (Tennyson *et al.* 1995). There are at least two mechanisms by which transcription elongation is regulated: alteration of transcription elongation rate or processivity. Transcription elongation rate determines the time it takes to synthesize the RNA transcript and processivity refers to the ability of the enzyme to transcribe from the site of transcription initiation to the correct site of transcription termination.

Pol II transcription elongation processivity may vary between organisms but stabilizing RNA pol/DNA engagement appears to be conserved across evolution. There are five core RNA pol II subunits conserved across eubacteria, archaea, and eukaryotes. Six additional subunits are present in eukaryotes/archaea and only eukaryotes have a seventh additional subunit- Rpb9 (Barba-Aliaga *et al.* 2021). The catalytic center of pol II is primarily set by Rpo21 (Rpb1) and different *rpo21* mutations have been found that can either increase or decrease the transcription elongation rate (Viktorovskaya *et al.* 2013; Qiu *et al.* 2016), and RNA pol transcription elongation rate can be allosterically regulated (Žumer *et al.* 2021). RNA pol has a dedicated nucleotide funnel 'below' the polymerase that delivers nucleotides to the active site. RNA pol that is transcriptionally engaged with DNA has a large 'open cleft' where the downstream DNA, unwound non-transcribed DNA, and recently rewound upstream DNA is exposed and not covered by the polymerase (Fig. 1-1A). The NGN domain of NusG/Spt5, Spt5 from here on out, binds RNA pol at the open cleft (Fig. 1-1B) and acts as a processivity factor to keep the RNA pol engaged with actively transcribed genes. This protein also engages with and stabilizes the upstream DNA duplex (Kang *et al.* 2018).

RNA pol transcription elongation states

Both transcription elongation rate and processivity depend upon the catalytic cycle of RNA chain synthesis by RNA pol. The RNA pol can transition between a pre- and post-DNA translocation state, depending on whether a rNTP has entered the active site, upon which, nucleic acid synthesis can occur with the correct rNTP and the cycle repeats until transcription terminates, or the enzyme enters a non-productive 'paused' state (Fig. 1-3). The paused state is a native state the enzyme can enter. Pausing can also be provoked by DNA sequence transcribed or barriers to transcription such as nucleosomes or DNA lesions. Paused polymerases are prone to backtracking. In this backtracked state the RNA pol moves backwards, across the DNA sequence which it previously transcribed and single-stranded RNA pokes out through the nucleotide funnel. In vitro studies suggest that RNA polymerase is unable to recover from backtracking on its own. Rather, an accessory factor, TFIIS, stimulates cleavage of the exposed RNA in the nucleotide funnel, resetting RNA pol in a productive elongation state. This process conserved in evolution (Lisica *et al.* 2016).

Spt5 regulates transcription elongation by modulating RNA pol pausing and promoting forward translocation. Bacterial Spt5 inhibits entry into the pre-DNA translocation state from the post-DNA translocation state and entry into long-lived paused states (Herbert *et al.* 2010). Human Spt5 also promotes transcription *in vitro* under limiting nucleotide concentrations (Wada *et al.* 1998). This suggests that Spt5 can distinctly affect both the processivity and elongation rate of RNA pol during transcription elongation.

Positive and negative transcription regulation by Spt5

Spt5 is essential for life. This limits in vivo analyses to examination of partial loss of function mutations or the effects of acute depletion of Spt5. Depletion of Spt5 results in decreased transcription elongation in many organisms (Shetty *et al.* 2017; Henriques *et al.* 2018; Uzun *et al.* 2021) and at candidate genes (Komori *et al.* 2009; Quan and Hartzog 2010; Diamant *et al.* 2016; Kramer *et al.* 2016), consistent with a role in positively regulating

transcription elongation. Interestingly, Spt5 can also negatively regulate transcription elongation.

Spt5 was originally identified as a mutation that genetically suppressed the transcription defects associated with insertion of the Ty retrotransposon (suppressor of Ty; *SPT*) at the *HIS4* and *LYS2* genes in budding yeast (Winston *et al.* 1984). *In vitro* experiments showed that Spt5 and Spt4 is necessary for inhibition of transcription elongation by 5,6-dichlor-1- β -D-ribofuranosylbenzimidazole (DRB), a compound which causes RNA pol to pause and/or prematurely terminate transcription elongation, and was coined DRBsensitivity-inducing factor (DSIF) (Wada *et al.* 1998). DRB inhibits a kinase, P-TEFb, which phosphorylates the CTR of Spt5 (Kim and Sharp 2001; Yamada *et al.* 2006), the CTD of RNA pol II (Marshall *et al.* 1996), and the protein complex Negative Elongation Factor (NELF) (Fujinaga *et al.* 2004). NELF binding to RNA pol elongation complexes (EC) distorts the EC and hinders rNTP binding and restrains RNA pol mobility by binding the trigger loop and can contact the exiting transcribed RNA and Spt5 KOW domains (Vos *et al.* 2018). Further, NELF prevents TFIIIS from binding the EC *in vitro* (Vos *et al.* 2018). The CTR plays an important role in metazoan RNA pol promoter proximal pausing. However, the CTR is not essential for viability (Komori *et al.* 2009; Shetty *et al.* 2017) and PTEF-b can phosphorylate the Linker-3 region of human Spt5 (Sansó *et al.* 2016). Consistent with this, NELF is not universally conserved across eukaryotes nor present in prokaryotes and archaea. Further, promoter-proximal pausing of RNA pol is not observed in every organism. Lastly, Spt5 has been shown to suppress anti-sense transcription (Peters *et al.* 2012; Booth *et al.* 2016; Henriques *et al.* 2018).

Temporal association of Spt5

Spt5 is proposed to function after transcription initiation. Under conditions in which transcription initiation is inhibited in human cells, RNA pol II is dynamically turned over at

gene promoters and Spt5 does not associate with these complexes (Erickson *et al.* 2018). *In vitro* microscopy experiments with yeast nuclear extracts show that Spt5 associates with pol II when NTPs are added and transcription occurs (Rosen *et al.* 2020). In eukaryotes, the pol II binding site for general transcription factor TFIIE involved in formation of the pol II initiation complex overlaps that for Spt5. Similarly, in archaea, the TFIIE homolog TFE competes with Spt5 for binding the clamp domain of archaea RNA pol (Grohmann *et al.* 2011). Genomic studies also show a temporal transition of RNA pol complexes and association and dissociation of the many proteins that function during transcription (Mayer *et al.* 2010). In prokaryotes there is an observed correlation with Spt5 association and the length of the bacterial transcription unit (Mooney *et al.* 2009). In Archaea and Eukaryotes, Spt5 associates with RNA pol throughout the transcribed gene body (Rahl *et al.* 2010; Mayer *et al.* 2010; Smollett *et al.* 2017).

Recruitment of Spt5

How Spt5 is recruited to RNA pol remains unclear. Some Prokaryotes have a Spt5 paralog, RfaH, which recognizes a short hairpin structure – *ops* – in the non-transcribed DNA sequences at a subset of genes (Artsimovitch and Landick 2002; Kang *et al.* 2018). The *ops* sequence is present just downstream the transcriptional start-site and induces RNA pol to pause at this sequence, allowing RfaH recruitment. While the NGN of Spt5 does not recognize the *ops*, it does contact the non-transcribed DNA strand (Meyer *et al.* 2015; Crickard *et al.* 2016; Ehara *et al.* 2017; Bernecky *et al.* 2017). However, this does not appear to be a universal Spt5 recruitment mechanism.

Physical interaction between Spt5 and RNA may be necessary for eukaryotic Spt5 recruitment. Spt5 binds more tightly to RNA pol when RNA is synthesized (Cheng and Price 2008; Bernecky *et al.* 2017), nascent RNA is required for yeast (Crickard *et al.* 2016) and fly (Missra and Gilmour 2010) Spt5 to bind the elongation complex *in vitro*. While the KOW

domains adopt a similar structure, not all Spt5 KOW domains directly interact with nucleic acids. One study showed that only KOW1-Linker1 region of yeast Spt5 interacts with nucleic acids (Meyer *et al.* 2015), a different study showed that human KOW4 preferentially binds single-stranded RNA (Zuber *et al.* 2018), and a final study showed that the conserved NGN domain and Spt4 binding interface is sufficient for Spt5/RNA physical interaction (Blythe *et al.* 2016).

Both protein-protein and protein-RNA interactions appear to be necessary for Spt5 recruitment. In different human cell lines, the MYC transcription factor physically interacts with Spt5 through Spt5's N-terminus and recruits Spt5 to promoters (Balupuri *et al.* 2019). Spt5 physically interacts with many different proteins that function at different stages of transcription elongation (Krogan *et al.* 2002b; Lindstrom *et al.* 2003; Joo *et al.* 2019); Spt5 may be co-recruited with proteins that function during early transcription elongation. For example, Spt5 associates with and stimulates the capping enzyme, which adds the 5' cap to mRNA transcripts as they emerge from pol II (Rasmussen and Lis 1993; Chiu *et al.* 2002). Spt5 also binds the Polymerase Associated Factor 1 complex (Paf1C), a large multi-protein complex that associates with RNA pol II and also functions as a transcription elongation factor (Hou *et al.* 2019; Francette *et al.* 2021). Both the mRNA capping enzyme and Paf1C, are recruited to pol II via its phosphorylated CTD (Squazzo *et al.* 2002; Lindstrom *et al.* 2003; Kachaev *et al.* 2020; Francette *et al.* 2021). However, the Paf1C is not essential for viability in yeast and *in vitro* time course experiments that block CTD phosphorylation show that Spt5 is still recruited to pol II (Joo *et al.* 2019). Spt5 makes multiple contacts with pol II and associated factors, it remains to be determined which of these mediates recruitment. Outside of Spt4, a systematic study examining what proteins Spt5 physical interacts with when not engaged with RNA pol II has not been reported.

Two themes are consistent across studies from all domains of life with respect to Spt5 recruitment to RNA pol.

I) RNA polymerase must shed transcription initiation factors before Spt5 association

As mentioned previously, TFIIE/TFE and Spt5 binding to RNA pol is mutually exclusive. Similarly, the σ general transcription factors in prokaryotes and Spt5 binding to RNA is also mutually exclusive (Yang *et al.* 2021).

II) A physical/structural barrier to RNA pol transcription elongation.

Spt5 in archaea and eukaryotes binds to genes just after the promoter and is present across the transcribed gene body (Rahl *et al.* 2010; Mayer *et al.* 2010; Smollett *et al.* 2017). In contrast, Spt5 in prokaryotes appears to bind genes stochastically and is correlated with gene length (Mooney *et al.* 2009). Difficult to transcribe DNA, structured hairpins in the non-transcribed sequences, and nascent RNA folding can halt RNA transcription in prokaryotes (Wang and Artsimovitch 2021). Nucleic acid sequence barriers can explain prokaryotic Spt5 recruitment. One clear example is the *ops* element that recruits RfaH (Kang *et al.* 2018). In *E. coli* and *B. subtilis* there are consensus pausing motifs which cause RNA pol to pause transcription (Larson *et al.* 2014; Yakhnin *et al.* 2020). Longer genes may be enriched with pausing sequences compared to shorter genes, which can explain the correlation between Spt5 gene association and gene length in prokaryotes. In yeasts there is some evidence for nucleic acid mediated Spt5 function (Blythe *et al.* 2016; Shetty *et al.* 2017), but this does not appear to be a genome-wide process or seen in other eukaryotes. However, protein barriers to transcription elongation are present in both archaea and eukaryotes over gene bodies and can provide a temporal window for Spt5 recruitment to paused RNA pol after transcription initiation.

Histones and histone like proteins

Eukaryotes package DNA into a chromatin (DNA/protein) structure. The principal unit of chromatin is the nucleosome: 147 bp of DNA wrapped around an octameric protein core.

Histones comprise this protein core and four histones are present in two copies each. There is a common structure to each histone: an acidic N-terminal tail, a histone-fold-domain. Each histone is minimally bound as a dimer through a histone-fold-domain interface. Histone H3 dimerizes with histone H4 and histone H2A dimerizes with histone H2B. In the context of the nucleosome, two histone H3-H4 dimers form a tetramer through the C-terminal alpha-helix of histone H3 and two histone H2A-H2B dimers flank the H3-H4 tetramer which creates a symmetrical dyad structure.

The principal chromatin system of archaea, prokaryotes, and viral vectors is largely distinct. Archaea have a diverse set of proteins which can bind, bend, and package DNA (Henneman *et al.* 2018; Laursen *et al.* 2021). Structural comparison of archaeal HMfB shows the same histone-fold-domain interface seen in eukaryotic histones (Bailey *et al.* 2002). Most archaea histone like proteins lack an acidic N-terminal tail (Laursen *et al.* 2021). Interestingly, HMfB can form nucleosome like structures with three HMfB dimers wrapping around 90 bp of DNA (Mattioli *et al.* 2017). Prokaryotes employ Nucleoid-Associated Proteins (NAP) to organize their genome. These proteins are small and have generally have a basic charge (Dame and Tark-Dame 2016). One interesting NAP is the histone-like nucleoid structuring (H-NS) protein. H-NS has target nucleation sites in the *E. coli* genome, where it can spread and form bridged filamentous structures (Kotlajich *et al.* 2015; Grainger 2016). Nuclear DNA viruses can assemble their genomes into chromatin inside their host, but, do not have nucleosome assembled DNA in their capsid (Lieberman 2008). Some nucleocytoplasmic large DNA viruses contain histone-like proteins that have homologs of histone H4 fused to H3 and histone H2B fused to H2A and form nucleosome-like structures (Liu *et al.* 2021). Viral encoded proteins have been coopted in dinoflagellates, a unicellular eukaryotic algae, and may explain the dinoflagellates unique chromatin divergence (Irwin *et al.* 2018).

Nucleosomes are barriers to transcription elongation *in vitro*

RNA polymerase is capable of synthesizing transcripts from naked DNA under appropriate reaction conditions, but the presence of nucleosomes inhibits RNA pol. A single nucleosome is sufficient to block transcription elongation *in vitro* (Izban and Luse 1991). The histone H3-H4 tetramer, which wraps the majority of the DNA in the nucleosome (Luger *et al.* 1997), is sufficient to provide a major barrier to transcribing RNA pol (Chang and Luse 1997). Nucleosomes wrapped with different DNA sequences have different barrier strengths to transcribing RNA pol (Bondarenko *et al.* 2006). Interestingly, the bacteriophage SP6 RNA polymerase is not inhibited by nucleosomes *in vivo* (Bondarenko *et al.* 2006). This suggests that nucleosomal inhibition to transcription elongation is not a general feature of RNA polymerase. Interestingly, both archaea RNA pol elongation is inhibited by HTkB histone isoforms (Sanders *et al.* 2019) and prokaryotic RNA pol elongation is inhibited by H-NS (Kotlajich *et al.* 2015) *in vitro*.

Do nucleosomes inhibit transcription *in vivo*?

Most eukaryotic DNA is wrapped in nucleosomes and presents a repeating barrier over the transcribed gene body. Unlike gene bodies, promoters are often depleted of nucleosomes and are sometimes referred to as Nucleosome Depleted Regions (NDRs). DNA sequence can facilitate NDR formation. Genome-wide nucleosome reconstitution experiments in yeast show that *in vitro* NDRs are similar to *in vivo* nucleosome mapping (Kaplan *et al.* 2009). Transcription activators can directly and indirectly form NDRs. A systematic study in yeast has shown that transcription factors can have varying strengths in displacing nucleosomes (Yan *et al.* 2018). While access to DNA wrapped around the nucleosome is restricted, some transcription factors can directly interact with nucleosomal DNA and structurally reorganize the complex (Morgunova and Taipale 2021). For transcription factors that can't bind to nucleosomal sequences or displace nucleosomes on their own, transcriptional activators can recruit ATP-dependent chromatin remodelers. Nucleosome formation is thermodynamically favorable (Mack *et al.* 2012). By expending ATP

energy, these chromatin remodelers can overcome this energy barrier and either slide nucleosomes away from transcription factor binding sites or physically disassemble the nucleosome (Hirschhorn *et al.* 1992; Kwon *et al.* 1994; Boeger *et al.* 2004; Lorch *et al.* 2011).

The nucleosome is a general repressor of transcription *in vivo*. Depletion of histone H4 in yeast can induce the expression of individual reporter genes (Han and Grunstein 1988), and can either increase or decrease the expression of a subset of genes using microarrays (Wyrick *et al.* 1999). An analogous study depleting histone H3 from yeast used modern techniques (MNase-seq, RNA-seq) identified that ~2,500 genes become de-repressed and that nucleosomes are more likely to be lost over promoters (Gossett and Lieb 2012). This is consistent with *in vitro* experiments that show nucleosomes inhibit transcription initiation (Knezetic and Luse 1986). Altering the expression levels of histones *in vivo* affects transcription (Clark-Adams *et al.* 1988) and can lead to in-viability (Libuda and Winston 2006).

Direct disruption of nucleosome function can result in loss of gene repression. The positively charged N-terminal histone tails help stabilize the nucleosome and aid in formation of compacted higher-order nucleosome structures (Iwasaki *et al.* 2013; Ghoneim *et al.* 2021; Stormberg *et al.* 2021). Truncation of the histone H4 N-terminus decreases chromatin compaction in yeast (Hsieh *et al.* 2015) while truncation of the histone H3 N-terminus can de-repress genes and lead to transcription hyperactivation (Mann and Grunstein 1992). Both H3 and H4 N-termini are simultaneously essential for viability (Ling *et al.* 1996).

Mutagenic screens in yeast have identified several different classes of histone mutations that function in gene repression. Mutant screens of histone H2B and H2A function have been reported and a searchable histone mutant database exists (Huang *et al.* 2009). However, this work focuses on histone H3 and H4. The *lrs*- class of mutations affect telomeric, rDNA, and mating type locus silencing (Park *et al.* 2002). The *sin*- class of

mutations bypasses the Swi/Snf chromatin remodeler function for transcription activation (Kruger *et al.* 1995). The *bur-* class of mutations bypasses the need for up-stream activating sequences that are targets for transcription activators (Prelich and Winston 1993). Screens for general transcription (Duina and Winston 2004), cryptic transcription initiation (Cheung *et al.* 2008), and transcription-couple nucleosome occupancy (Hainer and Martens 2011) defects have also been reported.

Nucleosome fate during transcription

Nucleosome dynamics and occupancy is context specific *in vivo*. At active promoters nucleosomes have high turnover rates (Dion *et al.* 2007; Rufiange *et al.* 2007). This suggests that nucleosomes that are removed by chromatin remodelers at promoters are replaced with new nucleosomes. When histones are not assembled into nucleosomes, they can form insoluble aggregates *in vitro*. Histone chaperones can interact with histone dimers and tetramers and increase histone solubility as well as facilitate both nucleosome assembly. In contrast to promoter nucleosomes, only histone H2A/H2B dimers appear to exchange in the ORF and the (H3-H4)₂/nucleosome core appear 'static' and have limited turnover relative (Dion *et al.* 2007; Rufiange *et al.* 2007). Even though nucleosomes are strong barriers to transcription elongation *in vitro* and promote gene repression *in vivo*, actively transcribed gene bodies remain associated with nucleosomes which are not evicted (Radman-Livaja *et al.* 2011; Brown *et al.* 2013). pol II must recruit auxiliary factors that aid in nucleosomal bypass *in vivo* during transcription elongation.

There are two mechanisms for removal of the RNA pol nucleosomal barrier *in vitro*. Histone chaperones can disassemble nucleosomes to decrease the nucleosome barrier to transcription *in vitro*. FACT (Facilitates Chromatin Transactions) was identified as an *in vitro* factor that allowed RNA polymerase to transcribe through nucleosomal DNA (Orphanides *et al.* 1998). Interestingly, FACT also acts with p-TEFb to relieve DSIF's negative transcription

elongation function in a dose-dependent manner *in vitro* (Wada *et al.* 2000). RNA polymerase can occasionally directly transcribe through nucleosomes *in vitro*. The spontaneous unwrapping of DNA from the nucleosome core can facilitate access for RNA pol (Li *et al.* 2005) and nucleosomes can be either ejected from DNA or retained (Lorch *et al.* 1987; Kulaeva *et al.* 2009).

RNA polymerase transcription through the nucleosome alters the state of the nucleosome. Histone H2A/H2B dimers often dissociate and a nucleosome 'hexamer' containing the (H3-H4)₂ tetramer and one H2A-H2B dimer remain associated with the transcribed DNA (Kireeva *et al.* 2002). Formation of the hexamer is critical for RNA polymerase nucleosome retention through an upstream DNA-loop transfer mechanism (Kulaeva *et al.* 2009). Transcription elongation rate alters the formation of hexamers. As the RNA transcription elongation rate increases so does the generation of retained hexamers (Bintu *et al.* 2011).

Nucleosome states alter transcription *in vitro*

The nucleosomal state affects mechanisms of RNA polymerase transcription through the nucleosome. Removal of the proximal histone H2A-H2B dimer can stall transcription through the nucleosome (Kulaeva *et al.* 2009). This proximal histone H2A-H2B dimer also the first major nucleosomal barrier to RNA pol, followed by the histone (H3-H4)₂ tetramer (Bondarenko *et al.* 2006). The *sin* histone mutations that derepress promoter chromatin increase the transcription rate through the nucleosome. Optical tweezer experiments show that histone H3 and H4 *sin* alleles increase transcription through the nucleosome and decrease nucleosomal RNA pol pausing (Bintu *et al.* 2012). Bulk *in vitro* analysis suggests that the increased nucleosomal transcription in *sin* mutants leads to increased nucleosome eviction, instead of the observed retention in the optical tweezer experiments (Hsieh *et al.* 2010; Bintu *et al.* 2012).

Histones are targets for post-translational modification (PTM) during transcription. Histone H2B is ubiquitinated (H2B-Ub) by the Rad6/Bre1 ubiquitin conjugation pathway during transcription elongation (Wood *et al.* 2003; Xiao *et al.* 2005) and in part, H2B-Ub functions in promotes FACT nucleosome reassembly *in vivo* (Fleming *et al.* 2008). Further, the human Rad6/Bre1 homologs cooperate with FACT in promoting RNA pol transcription through nucleosomes (Pavri *et al.* 2006) and FACT promotes nucleosome survival (Hsieh *et al.* 2013) *in vitro*. Interestingly, H2B-Ub increases both the proximal H2A-H2B dimer and (H3-H4)₂ tetramer nucleosomal barrier to pol II (Chen *et al.* 2019). While H2B-Ub increased the time that RNA pol took to transcribe through the nucleosome, H2B-Ub also increases the probability that RNA pol transcribes through the nucleosome when compared to unmodified wild type nucleosomes (Chen *et al.* 2019)

Spt5 and the nucleosomal barrier

Spt5 can stimulate RNA pol II transcription into the nucleosomal barrier. Recombinant Spt4/Spt5 and purified Spt4-TAP/Spt5 complexes from yeast specifically decrease the (H3-H4)₂ tetramer nucleosomal barrier to pol II (Crickard *et al.* 2017). Recently it has been shown that a region in the unstructured N-terminus of Spt5 has histone H3-H4 chaperone activity (Evrin *et al.* 2022). This may explain why Spt4/Spt5 does not decrease the H2A-H2B dimer barrier. Spt4/Spt5 also affects DNA rewinding around the nucleosome and the strength of nucleosomal DNA association affects Spt4/Spt5 function (Crickard *et al.* 2017).

Spt4/Spt5 in collaboration with transcription elongation factors stimulates nucleosomal transcription *in vitro*. Elf1 is a small protein that was identified as being essential for viability when *tfiis* is absent, and was shown to have chromatin phenotypes when mutated (Prather *et al.* 2005). The addition of Elf1 to Spt4/Spt5 *in vitro* transcription reactions greatly stimulates nucleosomal transcription and decreases the H2A-H2B nucleosomal barrier

(Ehara *et al.* 2019). Cryo-EM models show that Elf1 resides below the NGN domain of Spt5, suggesting that Spt4 and Elf1 are stabilizing NGN association over the open pol II cleft. And, may be regulating interaction between the NGN and non-transcribed DNA sequence (Crickard *et al.* 2016). With respect to the nucleosome and RNA pol II, Spt4/Spt5/Elf1 appear to be decreasing non-productive ‘tight’ physical association that was previously observed when the elongation factors were absent (Kujirai *et al.* 2018). A cryo-EM model of Spt4/Spt5 and FACT nucleosomal transcription has been solved as well. Consistent with the prior study, the addition of FACT stimulates Spt4/Spt5 transcription through the nucleosome *in vitro* (Farnung *et al.* 2021). In the structural model, DNA is unwrapped from the proximal H2A-H2B and is instead bound by a C-terminal region of FACT and leads to retention of the proximal H2A-H2B dimer. This is consistent with the prior *in vitro* work showing that retention of this histone dimer is required for transcription through the nucleosome.

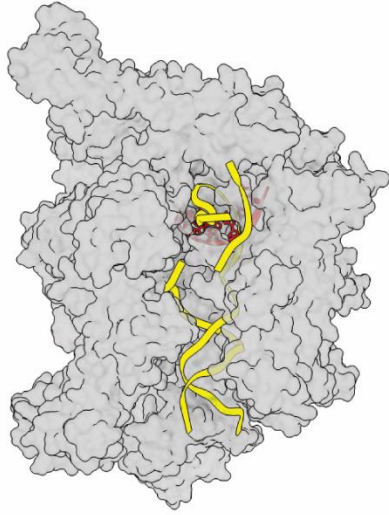
The structural models and mechanisms of Spt5-mediated nucleosomal transcription remains incomplete. There are currently no models for the predicted nucleosome bypass/disassembly intermediates, predicted nucleosome reassembly, and regions of Spt5 that are essential for viability (Evrin *et al.* 2022) are unresolved. Genetic tests that are informed from the provided structural information can provide insight into these remaining nucleosomal transcription elongation states and structures.

Figure 1-1. Enclosure of transcribed DNA by NusG NGN domain

The minimal enclosure of transcribed DNA by prokaryotic RNA pol is shown (PDB: 6C6U). Only the main RNA pol body (grey surface with transparency), DNA (yellow ribbon), RNA (red ribbon with nucleotide rings), or NusG (pink surface) are represented.

- A.) The large open cleft clearly shows the downstream DNA which is about to be transcribed.
- B.) The conserved NGN domain of NusG sits atop the large cleft and encloses the transcribed DNA with RNA pol.

A.



B.

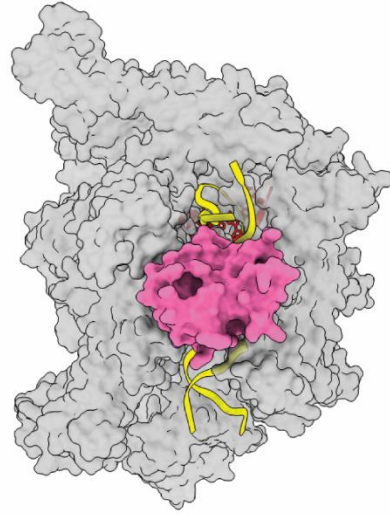


Figure 2-2. Structural Domains of Spt5

Spt5 has four structural motifs. An unstructured N-terminus, the NGN domain, KOW domains, linker regions between the KOW domains, and the C-terminal repeat (CTR). The minimal form of Spt5 consists of N-terminus, NGN, and KOW1. Eukaryotes have up to six KOW domains, with budding yeast having five. The CTR across eukaryotes also contains varying numbers of a post-translationally modifiable repeat sequence (CTR-phospho*). DNA is yellow ribbon and RNA is red ribbon with nucleic acids shown. Protein is displayed as a surface representation and described in the key. Linkers are abbreviated as L. PDB structure 6TED.

A.) A direct view through the downstream DNA. The modifiable carboxy-terminal domain (CTD) of Rpb2 can be viewed.

B.) A top-down view. Transcribed RNA can be seen.

C.) A lateral view of the right side of the RNA pol.

Key:

- Rpb1 & Rpb2
- NGN & KOW1 (NusG)
- L1 & L1-structured
- KOW2-KOW3
- L2
- KOW4
- L3
- KOW5
- CTR
- CTR-phospho*

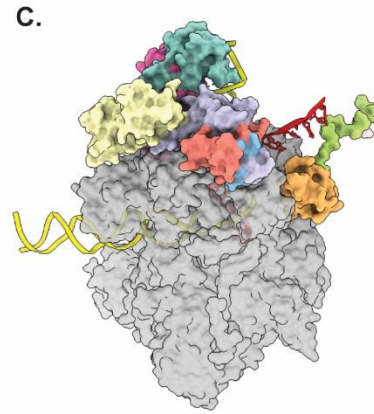
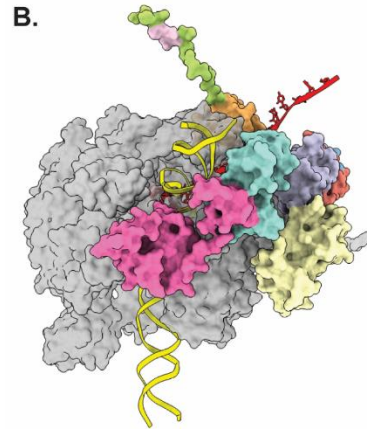
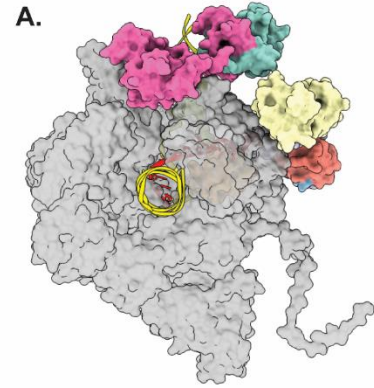
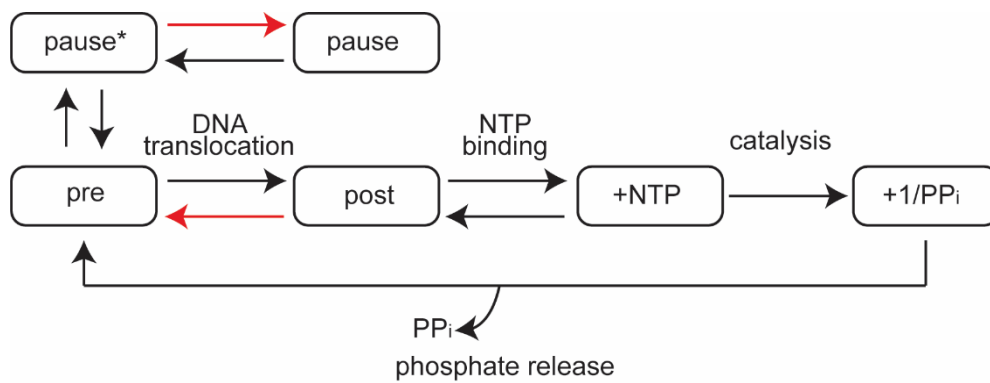


Figure 1-3. adapted catalytic cycle of RNA pol

RNA pol can reversibly transition between three states: pre-DNA translocation, post-DNA translocation, and NTP bindings. RNA chain synthesis (catalysis) and phosphate release are irreversible steps. Phosphate release resets the catalytic cycle in the pre-DNA translocation state. An additional state can be entered through the pre-DNA translocation state, the elemental pause state (pause*). Additional, longer-lived pause/backtracked states can be entered through the elemental pause state. Red arrows indicate transitions that NusG inhibits *in vitro*. This figure has been adapted from Herbert et al. 2010.



Chapter 2

A novel class of histone H3 mutations supports an *in vivo* role for Spt5 in promoting transcription through nucleosomes.

Michael Doody, Araceli Ortiz, Tiffani Quan, Lourdes Valenzuela, Nancy Sanchez, Robert Shelansky, Sol Katzman, Myra Gordon, Hinrich Boeger, Grant Hartzog

This chapter will be submitted as a manuscript to the Genetics journal. The above authors contributed to different experiments described below. An original description of the histone mutations can be found in Tiffani Quan's thesis: Maintaining chromatin structure during transcription elongation in *Saccharomyces cerevisiae*. Permission from Tiffani Quan has been given for presenting any overlapping material.

Abstract

Nucleosomes present a strong repeating barrier to RNA polymerase II during transcription elongation. *In vitro*, transcription elongation factor Spt4/Spt5 reduces transcription pausing and arrest and can increase the ability of RNA polymerase to transcribe into or through single nucleosomes. However, the mechanisms underlying these activities and their relevance to Spt4/Spt5's *in vivo* functions remain to be determined. Previously, we identified a cold-sensitive allele of *SPT5* that decreases the rate of RNA polymerase II elongation and causes processivity defects *in vivo*. Here we report a genetic screen for alleles of histone H3 that suppress this cold-sensitive *spt5* allele. These histone H3 suppressor mutations alter amino acids that cluster in four different structural regions of histone H3. Curiously, our H3 mutations are genetically distinct from previously described histone mutations that derepress transcription or abolish gene silencing in yeast. Genetic assays, as well as genome-wide and single molecule analysis of nucleosome positions of two of the histone mutants suggest that these mutations disrupt chromatin over transcribed sequences. Thermodynamic predictions

of nucleosome stabilities suggested that these histone mutations cause nucleosome loss at DNA sequences that, on average, are predicted to form more stable nucleosomes. We suggest that Spt5 promotes RNA polymerase II transcription through stable nucleosomes that would otherwise block its progress in vivo, and that the mutations that we describe here preferentially affect nucleosomes at these positions.

Introduction

Nucleosomes, the fundamental subunit of chromatin, permit efficient packaging of genomes, but at the price of repressing gene expression. In addition to blocking binding of transcription factors at promoters, nucleosomes form a repeating barrier to transcribing RNA polymerases. An average human gene can be assembled with ~60-90 nucleosomes – but a single nucleosome acts as a protein barrier and strongly inhibits RNA polymerase transcription in vitro (Izban and Luse 1991). However, actively transcribed genes remain associated with nucleosomes, indicating that there must be mechanisms by which elongating RNA polymerases can transcribe nucleosomal DNA without persistently disrupting or removing nucleosomes (Dion *et al.* 2007; Radman-Livaja *et al.* 2011).

One factor that may assist in elongating RNA polymerase II (pol II) to overcome nucleosomes is Spt5, the only known universally conserved transcription accessory factor. Eukaryotic Spt5 exists as a dimer with Spt4 and associates with pol II soon after transcription initiation (Hartzog *et al.* 1998; Wada *et al.* 1998). Metazoan Spt4/Spt5, DSIF, is necessary for the paused polymerases observed near the transcription start sites of many genes (Decker 2020) Furthermore, depletion of Spt5 in fission yeast abolishes transcription elongation and leads to an accumulation of pol II over the beginning of transcribed genes (Shetty *et al.* 2017), and in budding yeast Spt4/Spt5 may regulate RNA polymerase stalling between the +1 and +2 nucleosome (Badjatia *et al.* 2021). Biochemical studies of Spt4/Spt5 and Spt5's bacterial homolog, NusG, show that it suppresses entry into long lived transcriptionally

paused states, polymerase backtracking and transcription arrest (Herbert *et al.* 2010; Crickard *et al.* 2016) Furthermore, *in vitro* studies have shown that nucleosomes can provoke TFIIIS dependent transcription arrest (Kireeva *et al.* 2005), and that Spt4/5 can facilitate pol II transcription into, but not completely through, nucleosomes *in vitro* (Crickard *et al.* 2017; Ehara *et al.* 2019). Collectively, these data suggest a model in which Spt5 functions to protect pol II from transcription pausing or arrest events provoked by nucleosomes.

In previous studies, we characterized *spt5-242*, which causes a cold-sensitive (Cs-) growth defect and decreases the rate of pol II elongation and pol II processivity *in vivo* (Hartzog *et al.* 1998; Quan and Hartzog 2010). To further explore the function of Spt5, we selected for genetic suppressors of the *spt5-242* Cs- growth defect. In addition to mutations in the catalytic core of pol II, we identified suppressor mutations affecting members of the Paf1 complex, chromatin remodeling enzyme Chd1, histone methyltransferases Set1 and Set2, the Rpd3S histone deacetylase complex, as well as other chromatin-related factors (Hartzog *et al.* 1998; Squazzo *et al.* 2002; Simic *et al.* 2003; Quan and Hartzog 2010). Each of these factors is implicated in transcription elongation and maintenance of normal chromatin structure over transcribed genes. We also showed that mutations that alter histone H3 residues lysine 4 and lysine 36, which are targeted by Set1 and Set2, suppressed *spt5-242* (Quan and Hartzog 2010). This final observation led us to ask in this study if mutations altering other residues of histone H3 could also suppress the *spt5-242* Cs- growth defect.

Here we present the identification of a new class of histone H3 mutations that genetically suppress the cold-sensitive and transcription elongation defective *spt5-242* allele. Structurally, these mutations cluster to four distinct nucleosomal regions. In addition, all display phenotypes that are typically seen when chromatin is disrupted. We focused our studies on mutations that alter amino acids whose different identities in histones H3.1 and H3.3 isoforms in many eukaryotes define their respective functions in replication-dependent and replication-independent nucleosome assembly pathways (Ahmad and Henikoff 2002).

Genome-wide nucleosome mapping of this class of H3 mutants revealed a nucleosome occupancy defect at the 3' end of transcribed genes that scaled with gene length. Single molecule analysis of the *PHO5* gene demonstrates that decreased nucleosome occupancy occurs over DNA sequences which are predicted to form more stable nucleosomes - which we can also observe globally in our genome-wide data. In contrast to our genome-wide data, single-molecule nucleosome occupancy defects can occur throughout the *PHO5* gene and not just at the 3' end. Together, these data are consistent with a model where Spt5 facilitates the pol II elongation through nucleosomes that would otherwise impede or block transcription.

Results

Screening for histone mutations that suppress a cold-sensitive allele of *SPT5*

Given our prior observations that mutations that alter the histone H2 lysine 4 or 36 residues suppress *spt5-242*, we set out to identify additional histone H3 mutations that suppress *spt5-242*. We reasoned that these mutations would identify residues or nucleosomal surfaces that genetically interact with Spt5 and thus, may function during transcription elongation. They could potentially disrupt sites of post-translational modifications, histone deposition pathways, nucleosome spacing, and/or overall nucleosome stability. To identify such mutations, we PCR mutagenized a plasmid borne copy of *HHT2* and then screened for mutations that suppressed the Cs- growth defect of *spt5-242*. In addition, we screened histone H3 alleles that had previously been isolated by others and generated additional mutations by site directed mutagenesis. We identified a large collection of plasmids that conferred suppression of *spt5-242*. Following plasmid rescue and sequencing we focused on a set 23 of these plasmids with mutations that altered at most two amino acids in histone H3. This set of plasmids contained mutations in 25 out of the 135 residues in histone H3 (Table 1). Although mutations affecting several residues were

repeatedly isolated, our screen was likely not saturated, as mutations of lysines 4 and 36 were not identified.

Mutations altering residues in four distinct regions of histone H3 suppress *spt5-242*

Mapping the *hht2* suppressor (*hht-supp*) mutations onto the crystal structure of the yeast nucleosome (1id3) revealed that they primarily alter amino acids in four distinct regions of histone H3: (I) residues in the amino-terminal tail, (II) amino-acids in the N-terminal alpha helix, (III) alterations in amino acid residues that map near super helical location 2.5 of the nucleosome, and (IV) mutations in the C-terminal helix (White *et al.* 2001) (Fig. 1 and Table 1)

1 - Mutations that alter N-terminal tail of H3

We previously showed that mutation of H3K4 or K36 leads to suppression of the *spt5-242* phenotype. In addition, several double mutants altered residues in the H3 N-terminal tail. One of these— H3K18E,K23E— alters residues targeted by the Gcn5 acetyltransferase (Tse *et al.* 1998; Kuo and Andrews 2013). However, these two mutations were not separated and thus, their individual influence on Spt5 function remains to be determined. Finally, we found the mutation of H3 lysine 37 to glutamate suppressed *spt5-242*. This residue has been reported to be a target for the Set7 histone methyltransferase in *Schizosaccharomyces pombe* (Shen *et al.* 2019).

2 - Mutations that alter the N-terminal alpha helix of H3

Three mutations altered the N-terminal alpha helix of H3. We obtained an H3-R49K single mutation, as well as H3-A29G, -R53G and -H39R, S87F double mutations. The amino acid changes in the double mutants were not separated, so the individual contributions of the H3-A29G and -H39R mutations to suppression of *spt5-242* are uncertain. However, it is

interesting to note that the N-terminal alpha helix of H3 appears to make a number of stabilizing interactions with the minor grooves of the DNA as it enters and exits the nucleosome (superhelical location 6.5(SHL6.5)) Further, alterations in this helix, including at amino acids 39 and 49 have been reported to alter nucleosome stability and susceptibility to remodeling by the Chd1 or RSC chromatin remodeling enzymes (Somers and Owen-Hughes 2009).

3 - Mutations that disrupt residues in the vicinity of super-helical location (SHL) 2.5

The next class of mutations includes residues L60, I62, K64, L65, S87, G90, and E94, which define a surface that occurs near SHL2.5. These residues appear to be solvent accessible and, with the exception of K64 and L65, do not contact DNA (White *et al.* 2001).

4 - Mutations that alter residues near the C-terminal alpha helix of histone H3.

The last class of mutations altered residues involved at or near sites of histone-histone contacts. This class included mutations that altered amino acid F104, which is found at the histone H3-histone H4 dimer interface. Additionally, we found multiple mutations that alter residues in the H3 C-terminal helix, which serves as an interface between the two H3-H4 dimers. This suggests that mutations that disrupt overall nucleosome stability may lead to suppression of the *spt5* phenotype (Sinha *et al.* 2017; Armache *et al.* 2019).

Histone mutations exhibit growth, transcription, and potential DNA replication defects

We selected representative members of the four classes of *hht-supp* mutations for further phenotypic analysis. Because yeast is sensitive to the dosage of histones (Clark-Adams *et al.* 1988), we integrated these mutations at the endogenous *HHT2* locus and confirmed their ability to suppress *spt5-242*. The mutations were also carried through backcrosses to ensure that the observed phenotypes co-segregated with the *hht2* mutation. In an otherwise wild type strain, a subset of the mutations showed general growth defects at

15°C, 22°C, and 30°C (Fig. 2A). In addition, many of the mutations caused temperature sensitivity at 37°C and 39°C. Several of the mutations also resulted in hydroxyurea sensitive phenotypes, indicating potential DNA replication defects (Fig. 2B).

To determine if any of the mutations cause transcription defects, we screened for the Spt- (Suppressor of Ty) phenotype. In Spt+ cells carrying the Ty delta insertion mutation *lys2-128d*, *LYS2* transcripts are truncated, resulting in a Lys- growth defect. In Spt- cells, the *LYS2* transcription initiation site shifts downstream, resulting in a functional transcript and Lys+ phenotype (Swanson *et al.* 1991). We found that several of our mutations have transcription defects, as evidenced by a Lys+/Spt- phenotype (Fig. 2C).

In addition to the Spt- phenotype, we tested our mutants for cryptic initiation defects. Previous studies revealed that mutations which disrupt chromatin can cause aberrant transcripts to initiate from within the body of transcribed genes. These mutations frequently fall in histone genes or in genes encoding factors that regulate chromatin over transcribed sequences (Cheung *et al.* 2008). To test for cryptic initiation, we transformed plasmids carrying a subset of our histone suppressor mutations into a strain lacking chromosomal copies of histones H3 and H4 and carrying previously characterized reporter of cryptic initiation in which the *GAL1* promoter drives expression of the *FLO8* gene fused to *HIS3* coding region. Transcription initiation from the normal *GAL1* start site creates a transcript in which *HIS3* is out of frame. In contrast, initiation from the well-characterized cryptic promoter in the interior of *FLO8* produces a transcript that can be translated to produce His3 protein and a His+ phenotype (Cheung *et al.* 2008). Using this reporter, we found that these mutants displayed moderate to strong cryptic initiation defects (Fig. 3), and that several resulted in cryptic initiation phenotypes stronger than that produced by H3K36R, which was previously reported to cause a strong cryptic initiation phenotype (Quan and Hartzog 2010; Du and Briggs 2010).

Histone mutations that suppress *spt5-242* are distinct from *lrs* and *sin/bur* alleles of H3

Spt5-242 reduces the rate and processivity of RNA pol II *in vivo* (Quan and Hartzog 2010). Given this, we considered the possibility that histone suppressors of *spt5-242* derepress transcription. Several genetic screens have identified histone mutations with this effect. Among these, *sin/bur* mutations suppress transcription defects associated with loss of the Snf/Swi chromatin remodeler and deletion of the *SUC2* UAS (Prelich and Winston 1993; Kruger *et al.* 1995). In contrast, *lrs* mutations constitute a distinct set of histone H3 and H4 mutations that relieve silencing of RNA pol II transcribed genes rDNA, telomeres and the silent mating type loci (Park *et al.* 2002).

The H3 mutations that cause Sin/Bur or Lrs phenotypes alter amino acid residues distinct from those that suppress *spt5-242*, suggesting that our suppressors interrupt a function of H3 that is different from those altered by *sin/bur* and *lrs* mutations. Indeed, in a prior study, we showed that a *lrs* mutation, H3K79A, enhances rather than suppresses the *spt5* phenotype (Quan and Hartzog 2010). To further test this idea, we asked if there is phenotypic overlap between our *spt5-242* suppressors and *sin/bur* or *lrs* mutations. To test a *sin/bur* H3 allele for suppression of *spt5-242*, we integrated *hht2-T118I* into the second genomic copy (*HHT2*) of histone H3 while maintaining the wild type *HHT1* locus (H3T118I is recessive lethal). This newly integrated allele displayed the same phenotypes as the original *hht1-T118I* mutation (Prelich and Winston 1993). In genetic crosses between *HHT1 hht2-T118I* and *HHT1 HHT2 spt5-242* strains, we were only able to recover *HHT1 hht2-T118I spt5-242* double mutants when a wild type copy of histone H3 was provided on a *URA3* plasmid. Furthermore, these strains were both 5FOA and cold-sensitive, showing that *hht2-T118I* is an enhancer of *spt5-242* phenotypes (Fig. 4). Thus, neither a *lrs* nor a *sin/bur* mutation suppresses *spt5-242*, distinguishing them from our *hht-supp* mutations.

Do H3 mutations that suppress *spt5-242* cause *Sin*⁻/*Bur*⁻ or *Lrs*⁻ phenotypes? We tested a panel of H3 suppressors of *spt5-242* for an *Lrs*⁻ phenotype, derepression of a *URA3* reporter gene inserted in the subtelomeric region of chromosome VII, using a plasmid shuffle assay. In contrast to the *Lrs*⁻ H3K79A mutation and two other mutations previously shown to disrupt telomeric silencing, H3K4R and H3K56G (Krogan *et al.* 2002a; Xu *et al.* 2007), the H3 suppressors of *spt5-242* did not derepress expression of the reporter gene (Fig. S1). Similarly, we found that, in contrast to *Lrs* mutations, the histone H3 suppressors of *spt5-242* do not cause mating defects, suggesting that they do not derepress the silent mating type loci (Fig. S2A, B). We also crossed a representative panel of the H3 suppressors to a *suc2ΔUAS* strain to test for the *Bur*⁻ phenotype and observed a variety of phenotypes in the resulting double mutants. These ranged from no suppression of *suc2DUAS* (H3 K18E,K23E), to moderate suppression, to strong suppression equivalent to that of H3T118I (Fig. S3). Thus, the histone H3 suppressors of *spt5-242* are distinct from the *Lrs* and *sin/bur* classes of histone H3 mutations.

A conserved H3.3-like function in budding yeast

Most eukaryotes express at least two non-centromeric variants of histone H3, H3.1 and H3.3, which, consistently, differ from each other at residues 31, 87, 89, and 90 (Elsaesser *et al.* 2010). Histone H3.1 is expressed and incorporated into chromatin during DNA replication, whereas H3.3 is expressed throughout the cell cycle and can be incorporated via both the replication and transcription-dependent pathways (Ahmad and Henikoff 2002). *S. cerevisiae* is unusual in that it only expresses a single non-centromeric form of H3. However, the histone chaperones that discriminate between H3.1 and H3.3 in higher eukaryotes, Asf1-Caf1 and Asf1-HirA, are conserved in yeast, suggesting conservation of both assembly pathways (Elsaesser *et al.* 2010). Consistent with this hypothesis, Cho and colleagues have found that human H3.3 is preferentially incorporated into transcribed chromatin of *S. cerevisiae* cells that are arrested in the G1 phase of the cell

cycle (Song *et al.* 2013). They found that this preference depends upon H3 residues 87, 89 and 90, as well as the Hir complex. Furthermore, replication independent incorporation of yeast H3 was reduced to background levels when residues 89 and 90 were mutated. Similarly, yeast H3 carrying mutations that increase its resemblance to metazoan H3.1 (I89V, G90M) increased incorporation relative to wild type yeast H3.3, whereas mutations that increased the resemblance of yeast H3 to metazoan H3.1, reduced its incorporation to background levels.

Interestingly, our third class of suppressor mutations, those that alter residues near SHL2.5, includes mutations affecting residues 87 and 90 as well as other residues in their general vicinity, suggesting that this class of mutation may alter histone incorporation. To test this idea, we created versions of yeast H3 that resembled histone H3.1 (yH3.1; S31A, I89V, G90M) or H3.3 (yH3.3; S87A) and integrated them into the *HHT2* locus in a strain lacking *HHT1*, so that they were the sole form of histone H3 in these strains. Both strains grew indistinguishably from wild type cells. Interestingly however, the yH3.3 mutation caused a cryptic initiation defect that was recessive to the wild type and yH3.1 forms of histone H3 (Fig. 5A, Fig. S4). Furthermore, genetic crosses revealed that yH3.3 suppresses the Cs-phenotype of *spt5-242*, whereas yH3.1 *spt5-242* double mutants are inviable (Figure 5B). Combined with the earlier observations of Cho and colleagues, these observations suggested that *spt5-242* cells can be genetically suppressed by increased replication-independent incorporation of histone H3 and are inviable when this incorporation pathway is absent. We tested this hypothesis by combining *spt5-242* with deletions of genes encoding subunits of the Caf and Hir complexes as well as *ASF1*. When a *spt5-242* mutant was crossed to strains carrying deletions of any one of several different Hir complex subunits, the resulting double mutants were inviable (Table 2), as predicted by our model. Furthermore, *spt5-242 asf1D* double mutants were also inviable. In contrast, a *spt5-242* strain lacking the Cac1 subunit of

the Caf1 complex was viable, but still cold-sensitive. We conclude that *spt5-242* sensitizes cells to the efficiency of replication-independent histone incorporation.

Nucleosome occupancy at the 3' end of yeast genes depends on a histone H3 surface

We reasoned that the *spt5-242* suppressor mutations that alter H3 residues near SHL2.5 alter nucleosome positioning or density *in vivo*. To test this, we sequenced mono-nucleosomal DNA to determine nucleosome positioning and occupancy genome-wide in an *hht2-S87P*, *G90R* and a wild type control strain. When the genes were aligned by their 5' transcriptional start site, the pattern of nucleosome densities observed in the *hht2-S87P*, *G90R* strain was not clearly distinct from our wild type control (Fig. 6A). We also did not observe any significant differences in nucleosome density or positions between wild type and mutant cells when we stratified genes by expression rate, SAGA or TFIID dependency, or length (data not shown).

In contrast, when we aligned genes by their poly-adenylation site (Park *et al.* 2014), we observed a significant decrease in nucleosome occupancy in the histone mutant versus wild type cells (Fig. 6B). Furthermore, the observed nucleosome occupancy defect at the 3' end of genes scaled with gene length (Fig. 6B). More nucleosomes on average were lost at the ends of the longest genes than were lost at shorter genes. Genome-wide nucleosome positioning and occupancy has been measured in many different organisms and contexts. A 3' end defect has been observed in FACT and H3-K56 single and double mutant cells, but an occupancy defect that scaled with gene length was not reported (McCullough *et al.* 2019). Interestingly, in a previous study of Chd1 function in nucleosome dynamics, we found that histone exchange at the 3' end of genes also scaled with gene length (Radman-Livaja *et al.* 2012). However, the previously reported pattern of nucleosome distribution in *chd1* mutants (Gkikopoulos *et al.* 2011; Ocampo *et al.* 2016) is clearly distinct from that we observe for

hht2-S87P, G90R, refuting the simple model that this mutation merely disrupts Chd1-nucleosome binding or remodeling.

Predicted nucleosome thermodynamic stability affects nucleosome occupancy *in vivo*

We considered 3 models to explain the preferential loss of nucleosomes from the 3' ends of genes in *hht2-S87P, G90R* cells. First, we considered the possibility that this alteration was due to cryptic initiation events. This model is consistent with the observations that cryptic initiation is associated with chromatin disruption and that the *hht2-S87P, G90R* mutation causes a robust cryptic initiation phenotype (Fig. 3). Furthermore, assuming that cryptic promoters are randomly distributed across the genome, longer genes should be more likely to have cryptic promoters. However, when we removed from our analysis those genes that have previously been annotated to have the potential to give rise to cryptic transcripts (e.g., genes with Set2 repressed antisense transcripts (Venkatesh *et al.* 2016), stable unannotated transcripts (Xu *et al.* 2009), cryptic unstable transcripts (Xu *et al.* 2009), or Xrn1-dependent unstable transcripts (van Dijk *et al.* 2011), we still observed a length dependent 3' end defect in nucleosome occupancy (Fig. S5).

In the second model, nucleosomes are lost specifically from the 3' ends of genes and replaced only slowly, if at all, leaving a gap at the 3' end. In the third model, nucleosomes can be lost from any location within a gene, with nucleosomes sliding in the 3' to 5' direction to fill the gap (Fig. 7A). This third model had two interesting implications. First, as nucleosomes slide 5' to fill gaps caused by nucleosome loss, the gaps are propagated to the 3' ends of genes. Second, because longer genes have a greater number of nucleosomes, they will have more frequent or more apparent gaps. Unfortunately, if nucleosome sliding is fast relative to nucleosome loss, these two models cannot be easily distinguished by bulk analysis of nucleosome positioning. That is, models two and three are both expected to give a picture of an average nucleosome loss at the 3' ends of genes.

To distinguish between these models, we turned to single molecule analysis of nucleosome positioning on the *PHO5* gene (Brown *et al.* 2013). In contrast to MNase analysis, which reports the average position of nucleosomes across a population of cells, this method can show the locations of both nucleosomal and nucleosome-free DNA across individual gene molecules. This approach allows a test of our models, which predict that gaps will only occur at the 3' end of genes (model two) or that nucleosome loss should be observable throughout individual gene molecules (model three). That is, if the third model is correct, nucleosome gaps should be observed throughout genes prior to or during gap propagation to the 3' end of the gene.

We analyzed single *PHO5* gene molecules in two different gene expression conditions - in the presence of the *PHO5* negative regulator *PHO80* (*PHO5* repressed) and in its absence (*pho80Δ*; *PHO5* expressed) (Korber and Barbaric 2014). For these experiments, we analyzed *hht2-G90R*, *R128S*, which behaves identically to *hht2-S87P*, *G90R* in genetic assays but appears to be less susceptible to suppressor mutations.

We first examined the average distribution of nucleosomes across *PHO5*. When *PHO5* was transcriptionally repressed, the *hht2-G90R*, *R128S* mutation did not alter the distribution of *PHO5* nucleosomes relative to that in wild type cells (Fig. 7B). In contrast, when *PHO5* expression was activated, the *hht2-G90R*, *R128S* mutation resulted in a modest decrease in nucleosome density over the 5' and 3' ends of the transcribed body of the gene (Fig. 7B).

To test for nucleosome loss on individual copies of *PHO5*, we extracted all nucleosome free DNA sequences between 87 and 167 bp in length. These sequences are large enough to accommodate pre-nucleosomes (Fei *et al.* 2015) or complete, but do not. In the *hht2-G90R*, *R128S* mutant, nucleosome gaps occurred more frequently over the *PHO5* promoter and at several discrete locations along the transcribed region of *PHO5* (Fig. 7C).

These observations are not compatible with the model that nucleosome loss in *hht2-G90R*, *R128S* cells is limited to the 3' ends of genes. The observations are compatible with our model that *hht2-G90R*, *R128S* can result in nucleosome loss throughout a gene body.

While ATP-dependent chromatin remodelers are thought to mediate nucleosome assembly and disassembly at promoters, the mechanisms of nucleosome disassembly and assembly over transcribed genes are less clear (Li *et al.* 2007; Venkatesh and Workman 2015). We hypothesized that the regions of elevated nucleosome loss may represent sites of decreased nucleosome stability. We used a probabilistic model, previously shown to accurately predict the position of nucleosomes *in vivo*, to predict the free energy of nucleosome formation across the entire *PHO5* gene sequence (Heijden *et al.* 2012). Sites with lower free energy correspond to those locations that favor nucleosomes. Unexpectedly, we found that the nucleosome gaps that we observed in *hht2-G90R*, *R128S* cells occurred at positions where nucleosomes are predicted to be more stable, relative to adjacent flanking sequences, over the transcribed gene body (Fig. 7C). Conversely, an increase in nucleosome gaps was less apparent at *PHO5* sequences that were predicted to be less favorable for nucleosome formation. This suggests that relatively stable nucleosomes are specifically disrupted by *hht2-G90R*, *R128S* and that RNA pol II transcription through stable nucleosomes is impaired in *spt5-242* cells.

The data above can be explained by the model that Spt5 is required to overcome the nucleosomal barrier to elongation. By destabilizing particularly stable nucleosomes, the *hht-supp* mutations may permit transcription elongation even though Spt5 function is reduced. This behavior is not limited to *PHO5*. When we examined our *hht2-S87P*, *G90R* genome-wide nucleosome mapping data we observed that locations where nucleosomes were predicted to form more stable nucleosomes displayed lower nucleosome occupancy in *hht2-S87P*, *G90R* cells (Fig. 8A).

As an alternative test of this model, we manipulated histone tail acetylation in the cells expressing H3-S87P, G90R. Histone tails can stabilize nucleosomes by promoting DNA wrapping around the nucleosome core and aid in the formation of compact chromatin structures, both of which can be regulated by post-translational modifications (PTM) of histone tails (Annunziato and Hansen 2018; Ghoneim *et al.* 2021). Acetylation of histone H3, a prominent PTM found over actively transcribed genes, keeps chromatin in an accessible open state. One way tail acetylation opens chromatin is by neutralizing the electrostatic interactions between the positively charged histone tail and the negatively charged DNA (Fletcher and Hansen 1995; Bannister and Kouzarides 2011; Gebala *et al.* 2019). We previously studied a form of histone H3 that cannot be post-translationally modified at 4 residues that are major acetylation targets- H3-K9, 14, 18, 23R. This form of H3, which is predicted to form more stable nucleosomes, causes lethality when combined with *spt5-242* (Quan and Hartzog 2010). We generated a form of histone H3 that contained both these histone tail mutations and the SHL2.5 *S87P*, *G90R* mutations. The SHL2.5 mutations rescued the synthetic lethal interaction between *H3-K9, K14, K18, K23R* and *spt5-242*, as predicted by the model that *hht2-S87P, G90R* disrupts stable nucleosomes Fig. 8B).

To further test of the idea that Spt5 promotes elongation through nucleosomes, we examined published NET-Seq data for *S.cerevisiae* (Uzun *et al.* 2021) and *S.pombe* (Shetty *et al.* 2017) strains in which Spt5 was depleted from the nucleus. NET-seq identifies the sequences where transcribing RNA pol II is located across the genome. When Spt5 was depleted from the nucleus, RNA pol II in these two studies accumulated at sites predicted to form more stable nucleosomes (Fig. 9).

Spt5 and transcribed chromatin structure

During preparation of this manuscript a study was published that demonstrated that a region in the Spt5 N-terminus of budding yeast can bind histone H3 and H4, is essential for

viability, and results in decreased histone H3-K4-me3 at the 5' end of transcribed genes that was interpreted as a measure for nucleosome reassembly defects during transcription elongation (Evrin *et al.* 2022). This is consistent with the reported *spt5 FLO8-HIS3* cryptic initiation phenotype (Cheung *et al.* 2008) and the nucleosome mediated repression of the *SER3* gene (Pruneski *et al.* 2011). The *spt5-194* allele used in those studies is defective in physical association with Spt4, and *spt4* Δ cells have a cryptic initiation and *SER3* phenotype (Cheung *et al.* 2008; Guo *et al.* 2008; Pruneski *et al.* 2011). This poses the question on whether these chromatin phenotypes are due to loss of mechanistic functions of Spt5 or loss of Spt4 function in context of the transcription elongation complex.

We performed a plasmid borne *spt5* screen to identify regions of Spt5 that have a cryptic initiation phenotype. The mutation locations predominantly occur in an NGN-proximal region (NPR) (Fig. 9A). While we did not identify any mutations in the N-terminal histone H3-H4 binding sequence of Spt5, this could be an artifact of our mutagenesis conditions or because this region is important for viability. Interestingly, a charge reversal at a solvent exposed location in KOW2 (E546K), a charge introduction at the KOW3 Rpb4/Rpb7 stalk interface (G587D), and a nonsense mutation at Q887 that removes the CTR were also identified. Our genetic screen was not saturating. The residues of the *spt5-242* allele (A268V) and the *spt5-194* allele (S324F) were not identified in our screen, suggesting that there may be additional Spt5 residues important for maintaining chromatin structure during transcription elongation.

The Spt5 NPR, when present in the Spt5 constructs used, is not visualized in structural studies. AlphaFold is a machine learning computational program that predicts protein structure and a publicly available database contains many protein structural predictions across many organisms (Jumper *et al.* 2021; Varadi *et al.* 2022). We aligned the yeast Spt5 AlphaFold structural prediction to a cryo-EM model of Spt5 bound RNA pol II

transcribing through a nucleosome (Fig. 10B). Only a portion of the acidic N-terminus through KOW3 of the AlphaFold Spt5 structure is displayed. Interestingly, the yeast Spt5 NPR is predicted to be structured and may be capable of interacting with Spt4. While the NPR of Spt5 is poorly conserved, this region of Spt5 is predicted to be structured in different organisms and a cluster of conserved residues just before the NGN domain appear to have the most structural similarity (Fig. S6). The acidic Spt5 residues which are required for Spt5 to interact with histone H3-H4 are capable of reaching upstream and downstream DNA sequences. As noted in previous structural studies, the Spt5 N-terminus is well placed to interact with the downstream DNA/histones and in one study electron density of the Spt5 N-terminus contacting exposed histone H2A/H2B has been observed (Ehara *et al.* 2019; Farnung *et al.* 2021). Loss of *spt5* function at the adjacent NPR causes chromatin disruption phenotypes. The Spt5 NPR may be the most immediate portion of Spt5 that can sense transcription through a nucleosome to coordinate RNA pol II transcription elongation.

Discussion

During transcription elongation in eukaryotes many molecular processes are coupled or co-regulated on a spatial and temporal scale - e.g. pre-mRNA processing, chromatin function, and transcription elongation rate and processivity. Genetic and biochemical experiments implicate Spt5, the only universally conserved transcription regulatory factor, in virtually all of these processes (Decker 2020). The molecular mechanism(s) by which Spt5 influences these processes are largely undetermined. In this work, we used a genetic approach to investigate the connections between Spt5 and chromatin.

The Spt4/Spt5 complex is thought to promote transcription elongation through chromatin (Hartzog and Fu 2013; Decker 2020). This model predicts that loss of function mutations in *SPT5* should be genetically suppressed by mutations that disrupt chromatin structures that repress or interfere with transcription. We tested this prediction by comparing

our *hht-supp* mutations to two classes of mutations known to relieve chromatin-mediated repression of transcription. *Sin/bur* mutations relieve nucleosome-mediated repression of gene promoters (Prelich and Winston 1993; Kruger *et al.* 1995) and *Irs* mutations disrupt chromatin mediated repression of expression from rDNA, subtelomeric, and mating-type loci (Park *et al.* 2002). The *sin/bur*, *Irs* histone and *spt5-242* suppressor H3 mutations alter distinct sets of amino acid residues and tend to form spatially distinct clusters on the nucleosome structure (Fig. S6). While a subset of our *hht-supp* mutations do share phenotypes with *sin/bur* and *Irs* H3, others do not. Furthermore, rather than suppressing *spt5-242* growth defects, the *sin/bur* and *Irs* histone mutations that we tested enhance or cause synthetic lethality in combination with *spt5-242*. Thus, the *hht-supp* mutations appear to be functionally distinct from previously described H3 alleles that disrupt chromatin. In addition, neither the *spt6-50* nor the *spt16-197* histone chaperone mutations, both of which broadly disrupt chromatin structure (Kaplan *et al.* 2003; Feng *et al.* 2016), suppress the *spt5-242* mutation (unpublished). Thus, the growth defect imposed by *spt5-242* is not generally relieved by chromatin disruption.

What aspect of histone H3 function is disrupted by the *hht-supp* mutations? Spt5 associates with and regulates elongating RNA pol II, suggesting that the *hht-supp* mutations are likely to affect nucleosomes over transcribed regions. Several observations reported here support this prediction: (i) the *hht-supp* mutations cause cryptic initiation (Fig. 3), suggesting that chromatin is altered over gene bodies; (ii) they genetically interact with mutations affecting several other transcription elongation factors (data not shown), (iii) they can alter nucleosome positioning over transcribed genes genome-wide (Fig. 6A); and (iv) they cause nucleosome loss over the *PHO5* ORF when it is transcriptionally active, but not when it is repressed (Fig. 7B). These observations can be explained by 2 models. In the first, the *hht-supp* mutations alter nucleosomes, reducing their ability to block RNA pol II transcription elongation in *spt5-242* strains. In the second, particularly stable nucleosomes are lost (as we

observed in *PHO5*, Fig. 7C), so that they are not present to interfere with transcription elongation in *spt5-242* cells.

The models presented above do not require that *hht-supp* mutations all act in the same way. Indeed, it is possible that the different classes of *hht-supp* mutations suppress *spt5-242* through multiple mechanisms. For example, consistent with our prior work demonstrating that loss of the Set2/Rpd3s histone deacetylase pathway genetically suppresses *spt5-242*, we isolated a N-terminal hyperacetylated histone mimic *H3-K18E,K23E*, as an *hht-supp* allele. We also isolated mutations affecting the N-terminal alpha helix of H3 at the DNA entry/exit site of the nucleosome. Changes in this helix were previously shown to modulate Chd1 and RSC chromatin remodeler activity (Somers and Owen-Hughes 2009). Both remodelers are thought to function over transcribed chromatin (Zentner *et al.* 2013; Spain *et al.* 2014) and we previously showed that *chd1* mutations suppress *spt5-242*. Another class of *hht-supp* mutations alter residues at the H3-H4 dimer (*F104L*) or the (H3-H4)₂ tetramer (I124L; R128G; L130I) interfaces. These mutations may subtly destabilize nucleosome structure or stability, or alternatively, alter exchange of H3-H4 over transcribed sequences. The final class of *hht-supp* mutations, those altering residues near SHL2.5, likely affect histone exchange or nucleosome assembly. Many eukaryotes have histone H3 isoforms which are assembled in a replication-dependent (H3.1; Asf1/CAF complex) or a replication-independent (H3.3; Asf1/HIR complex) pathway that are distinguished by the histone H3 residues occupying SHL2.5 and unique histone chaperones complexes (Nakatani *et al.* 2004; Grover *et al.* 2018). Although *S. cerevisiae* only has a single non-centromeric histone H3 isoform, Asf1, the CAF and HIR complexes are conserved and mutations of SHL2.5 residues interfere with nucleosome assembly (Song *et al.* 2013). We previously reported that the *hht2-S87P, G90S* mutation, which alters 2 of the residues that distinguish H3.1 and H3.3 suppresses *spt5-242* (Radman-Livaja *et al.* 2012). We predicted that this mutation interfered with replication-independent histone exchange and

showed that it leads to profound growth defects when combined with a deletion of the H3 N-terminal tail, which is required for replication-dependent nucleosome assembly.

To gain greater insight into the defects caused by the *hht-supp* mutations affecting the SHL2.5 region, we carried out bulk and single molecule analyses of chromatin. Genome-wide mapping of mono-nucleosomes in a *hht2-S87P,G90S* strain showed decreased nucleosome occupancy defect at the 3' ends of genes that scales with gene length. The 3' loss could not be clearly explained by cryptic initiation, as even genes that lack documented cryptic promoters showed 3' nucleosome loss in *hht2-S87P, G90R* cells (Fig S5). We considered two other models that explain a 3' nucleosome occupancy defect: the 'direct model' simply states that the occupancy defect is specifically localized to the 3' ends of genes whereas a 'treadmill model' predicts that an occupancy defect can occur anywhere over the RNA pol II transcribed gene body but that nucleosomes migrate 3' to 5' to occupy the vacant DNA, leaving the observed 3' gap. Further, the 'treadmill model', and not the 'direct model', is readily compatible with the correlation of gene length with the magnitude of the 3' loss; longer genes have more opportunities to lose nucleosomes across the entire gene body. In our single molecule analysis, we observed that nucleosome sized gaps occur throughout *PHO5* under transcriptionally active conditions, as predicted by the 'treadmill model'. Strikingly these gaps were most often observed at DNA sequences predicted to form more thermodynamically stable nucleosomes. Similarly, in our genome-wide data, we observe that the nucleosomes most likely to be lost in the *hht-supp* strains are those nucleosomes that are predicted to form the most stable nucleosomes (Fig. 8B).

Why the SHL2.5 sub-class of *hht-supp* mutations predominantly affects nucleosomes predicted to be thermodynamically stable remains less clear. We do not favor the model that these mutations directly alter histone-DNA contacts and nucleosome stability. Few of the residues altered by the *hht-supp* mutations contact DNA, and the effects of these mutations are only apparent when transcription is active. A more intriguing idea is that these *hht-supp*

mutations result in nucleosomes that are more susceptible to eviction. A recent study demonstrated that while the yeast RSC chromatin remodeler mobilizes partially unwrapped nucleosomes, it evicts nucleosomes over strong positioning sequences (Schlichter *et al.* 2020). SHL2.5 *hht-supp* mutations may make nucleosomes more susceptible to nucleosome ejection by RSC, some other chromatin remodeler, or elongating RNA pol II. Alternatively, SHL2.5 *hht-supp* mutations may decrease the probability that a nucleosome is reassembled at these stable sites following passage of elongating RNA pol II.

A recent study identified a histone H3-H4 binding region in the Spt5 N-terminus that is essential for life. Surprisingly, *spt5* mutation of this domain does not prevent RNA polymerase II from transcribing genes but does result in significant loss of nucleosomes from transcribed genes (Evrin *et al.* 2022). When Spt5 is depleted from the nucleus in *S. cerevisiae* and *S. pombe*, RNA pol II accumulates at DNA sequences predicted to form more stable nucleosomes. This is a key prediction of the model that Spt5 promotes RNA pol II transcription through nucleosomes in vivo (Fig. 8A). We have identified a region of Spt5, the NPR, which is a predominant hotspot for mutations in *spt5* that have a cryptic initiation phenotype, contains the *spt5-242* allele, and may be structured.

Further work will be needed to address how Spt5 is mechanistically coupled to transcription elongation through nucleosomes. Some interesting questions are: (i) does Spt5 directly aid in disassembly of the downstream nucleosome and/or reassembly of the upstream nucleosome? (ii) does the Spt5 NPR/N-terminus act as a platform to coordinate histone chaperone activity of FACT and Spt6/Spn1? (iii) can the NPR/N-terminus act as a toggle to control the binding of the Spt5 NGN domain to RNA pol II to alter transcription elongation rate? Based on this and prior work, we favor a model in which the Spt5 NPR/N-terminus dynamically coordinates and stabilizes RNA pol II as it encounters nucleosomes during elongation.

Table 2-1. Identification of single, or double plasmid borne *spt5-242 hht-supp* amino acid changes isolated in our screen or acquired from the indicated source.








Mutation class	AA change	source
<u>I: Amino terminus</u>	K18E, K23E	
	Δ4-30	pRM430, Grunstein
<u>II: Histone-DNA interactions</u>	K37E	Andrea Duina
	R49K	
	A29G, R53G	
<u>III: Nucleosome surface</u>	L65I, E94G	
	L65S, E94V	
	S87P, G90S	
	I62V, L65S	
	L60P, R131S	
	G90R, R128S	
	L60M	
	K64R	
	L65S	
	L65V	
	G90R	
	E94G	
	Q68R	Andrea Duina
	Q93R	Andrea Duina
L60P, F84L	Andrea Duina	
<u>IV: Histone-Histone interactions</u>	I124L	
	R128G	
	L130I	
	F104L	

Table 2-2. Genetic interactions of *spt5-242* and the Hir and Caf complex.

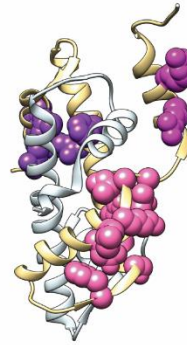
Growth at 30C

		<u>asf1Δ</u>	<u>cac1Δ</u>	<u>hir1Δ</u>	<u>hir2Δ</u>	<u>hir3Δ</u>	<u>hpc2Δ</u>
<i>spt5-242</i>	+/-	-	+/-	-	-	-	-

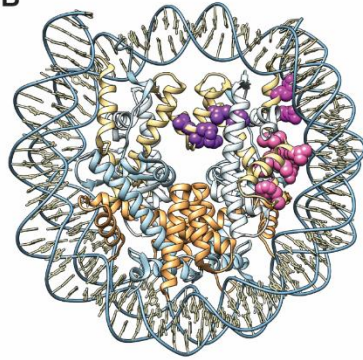
Figure 2-1. Chimera figure showing locations on the nucleosome of amino acid residues altered by hht2-supp mutations.

key	
histone	mutation class
 H3	 II
 H4	 III
 H2A	 IV
 H2B	

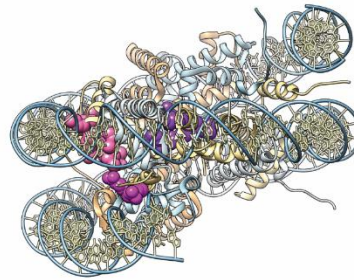
A



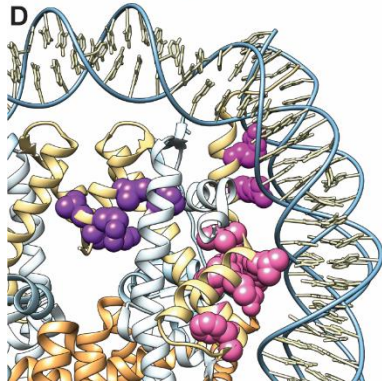
B



C



D



E

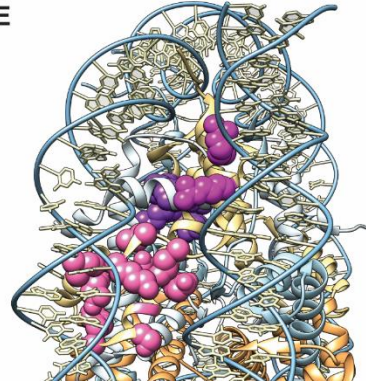


Figure 2-2. *hht2 spt5-242* suppressor mutations have pleiotropic phenotypes

Representative *hht2 spt5-242* suppressor mutations were integrated at *HHT2* with histones H3 and H4 being solely expressed from the *HHT2-HHF2* locus. The indicated genotypes were serially diluted onto the indicated media and incubated at the given temperatures.

A.) *hht2* mutants have different tolerances to decreased or increased constitutive growth temperatures on YPD. From left to right plates were incubated for 5 days, 4 days, 1 day, 1 day, and 1 day at their respective temperature.

B.) *hht2* mutants are sensitive to replication stress at elevated growth temperatures. YPD + 0.1 mM hydroxyurea (H.U.) plates were incubated for 4 days at 30C or 7 days at 37C.

C.) *hht2* mutants that are outside of the H3 N-terminus tail have a modest *spt-* phenotype. The sc-lys plate was incubated for 2 days.

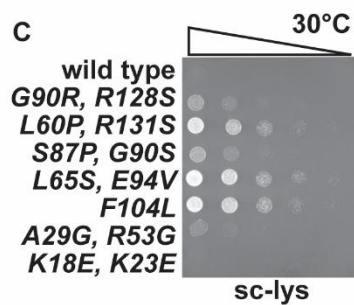
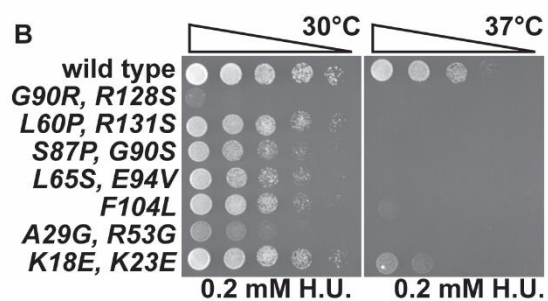
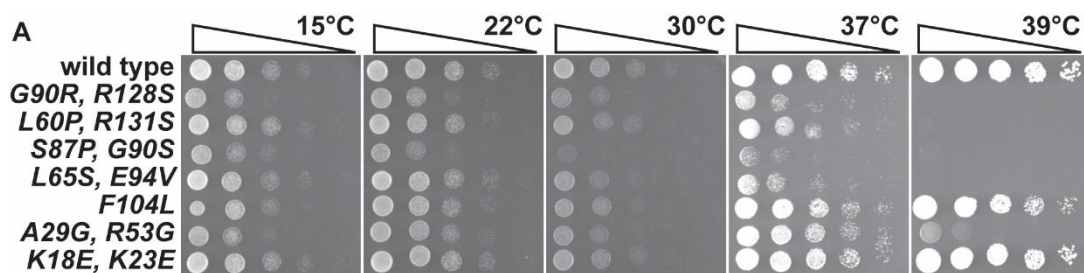


Figure 2-3. *hht2* mutations that suppress *spt5Cs-* have a strong cryptic initiation phenotype.

Histone H3 alleles were transformed into a histone shuffle strain with the *FLO8-HIS3* reporter gene and passed over 5FOA to remove a *CEN3 URA3 HHT1-HHF1* plasmid. Strains were serially diluted onto sc-trp, sc-his, and sc-his + gal. All plates were incubated for 3.5 days at 30C.

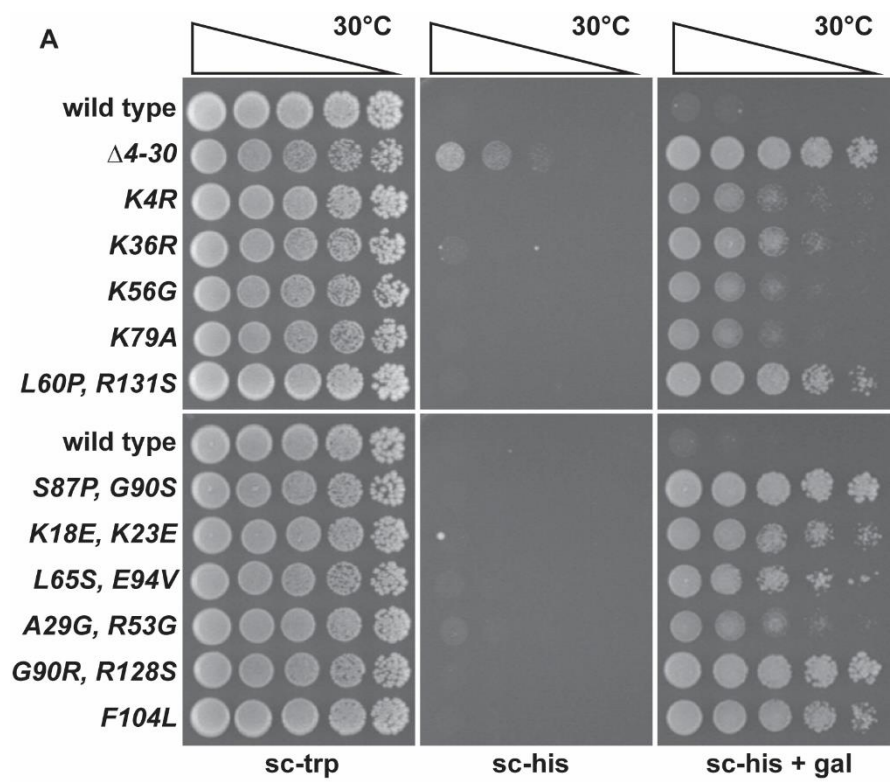


Figure 2-4. *spt5-242 hht1-T118I* double mutants are inviable.

Strains with the indicated genotypes and carrying a *CEN URA3 HHT1-HHF1* plasmid were serially diluted onto SC-URA and 5FOA and incubated at 30° C for 3 days.

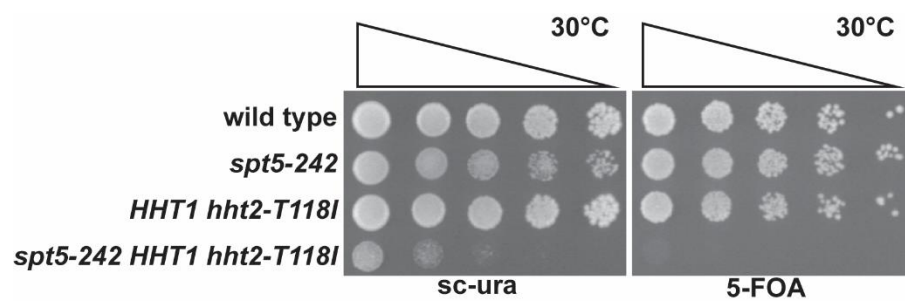


Figure 2-5. yH3.1 and yH3.3 genetic interactions.

A.) yH3.1 (*hht2* - S31A, I89V, G90M) and yH3.3 (*hht2* - S87A) are viable and display modest transcriptional phenotypes. The indicated strains lack copy 1 of the H3-H4 locus, contain the *pGAL-FLO8-HIS3* reporter gene, and were serially diluted onto the respective media. YPD was incubated for 2 days, sc-his + gal and sc-lys were incubated for 3 days.

B.) yH3.3 genetically suppresses *spt5-242* growth defects while yH3.1 results in synthetic lethality. The indicated strains contain a *CEN URA3 SPT5* plasmid and were serially diluted onto sc-ura or 5FOA and incubated at 30C for 2 days.

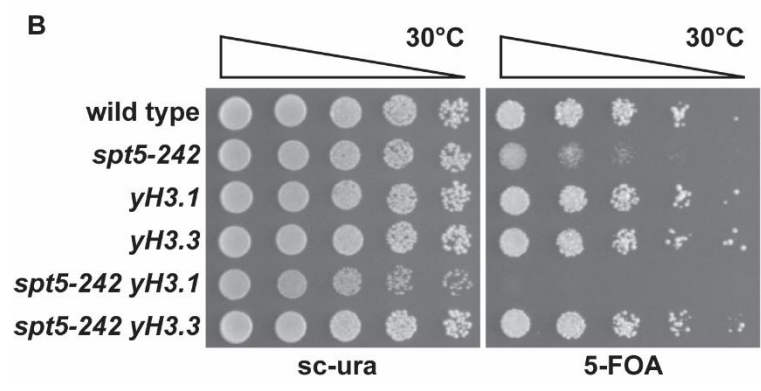
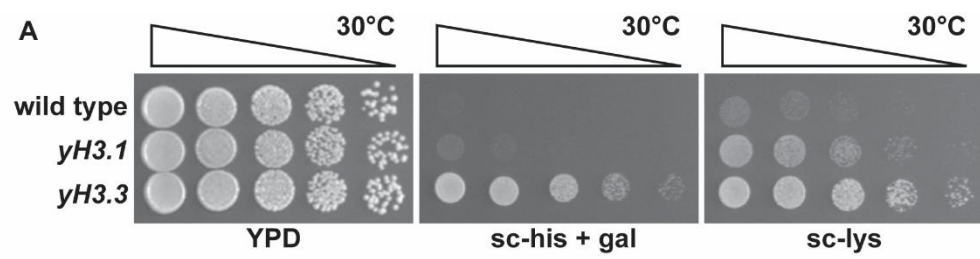


Figure 2-6. Mapping mono-nucleosomes in *hht2-S87P*, *G90R* cells

Chromatin from log-phase *hht2-S87P*, *G90R* cell cultures was digested by MNase and mono-nucleosome sized DNA fragments were gel purified and sequenced. 4,974 RNA pol II transcribed genes with both a mapped transcription start site (TSS) and poly-adenylation site (pA) were selected for subsequent analysis.

A) Nucleosome density is decreased near the pA site of genes and are progressively delocalised downstream the TSS. Metagene analysis with average mononucleosome MNase-seq signal for *hht2-S87P*, *G90R* (shades of green) and WT (purple) nucleosomes with respect to the TSS or pA.

B) Decreased nucleosome density at the pA site scales with the length of the transcription unit. The geneset with defined TSS and pA coordinates were parsed into quartiles based off of the base pair distance between the TSS and pA sites.

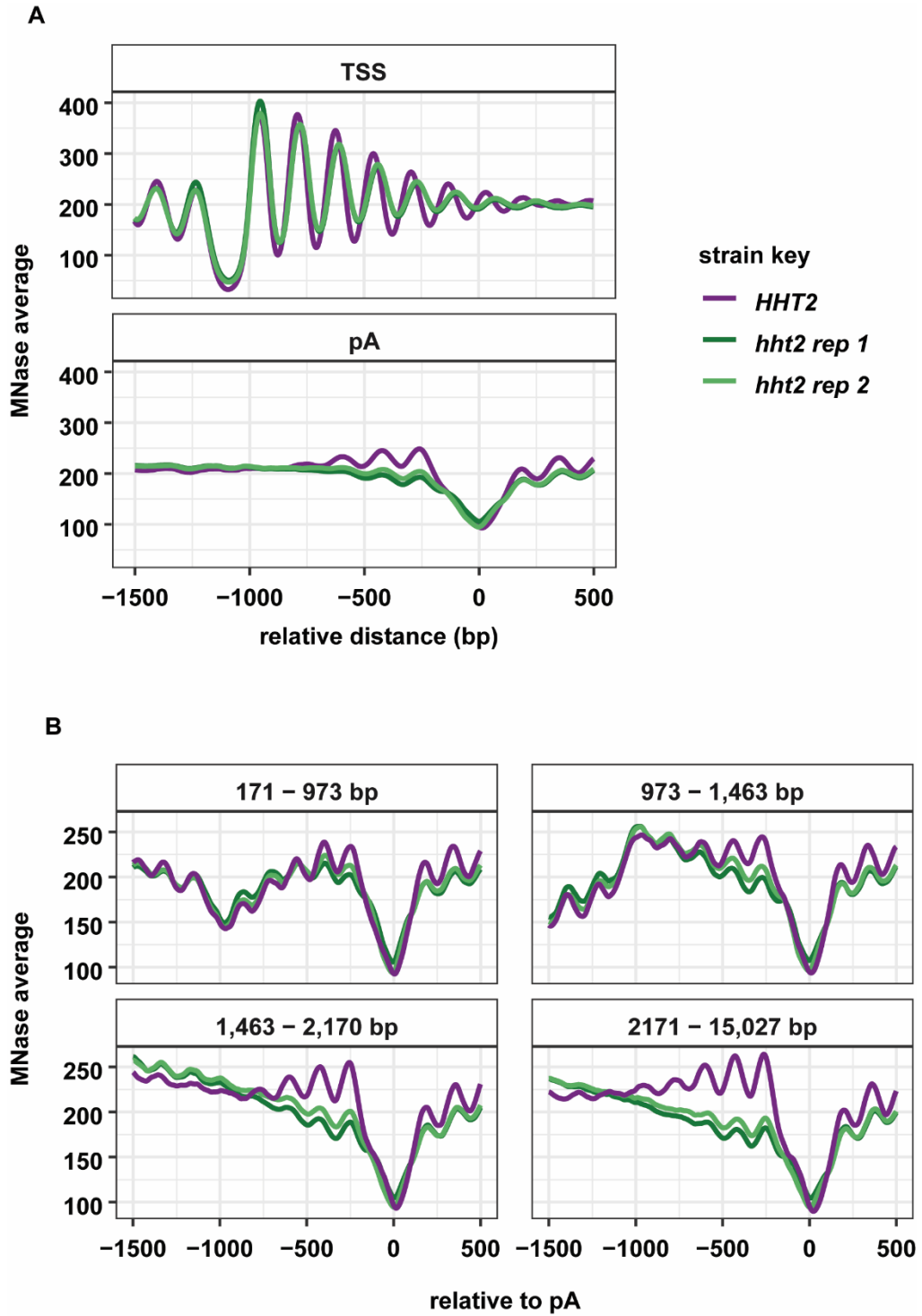
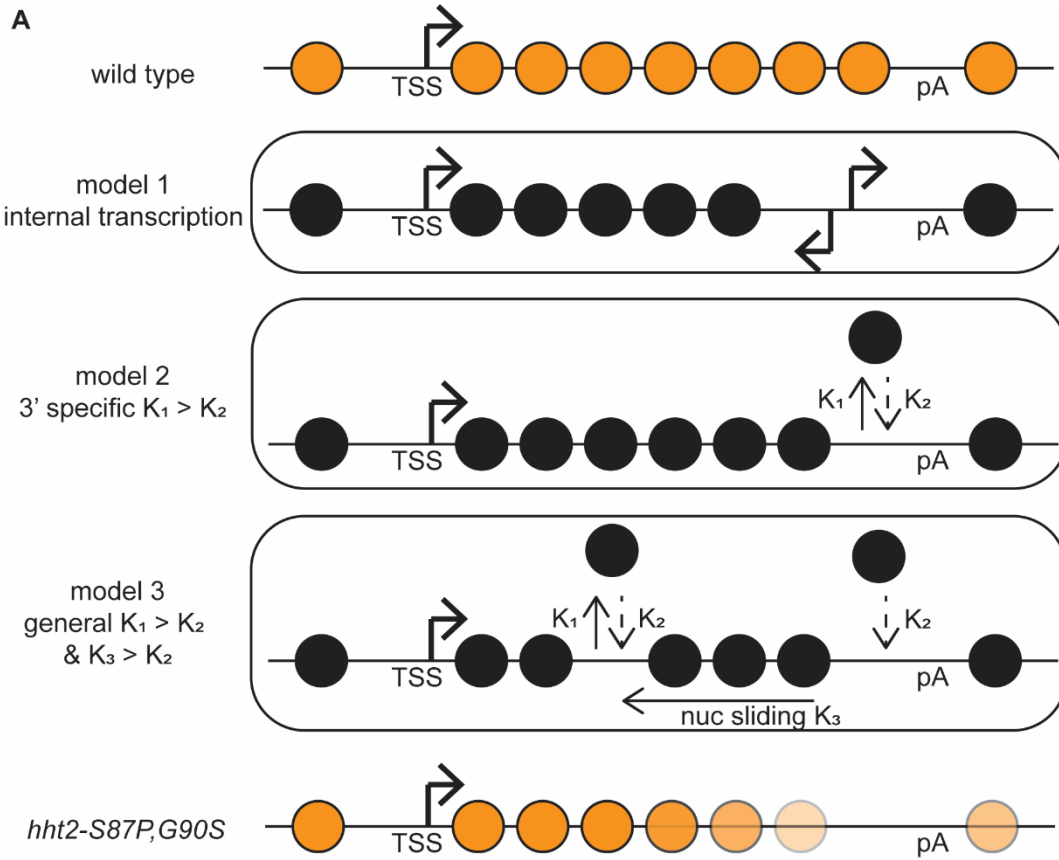


Figure 2-7. Testing models for 3' nucleosome loss

A) Three models that predict 3' end nucleosome loss. Model 1: internal transcription initiation over transcribed gene bodies results in nucleosome loss. Model 2: nucleosome dynamics are specifically affected at the 3' ends of genes, the rate of nucleosome disassembly and/or complete removal (K_1) is greater than the rate of nucleosome reassembly and/or new assembly (K_2). Model 3: nucleosome can be disrupted at any location over the transcribed gene body and the rate of retrograde nucleosome sliding (K_3) is greater than the rate of nucleosome assembly (K_2) leading to apparent 3' loss.

B) Single molecule analysis of nucleosome loss over *PHO5* in *hht2-G90R*, *R128S* cells (showing repressed and de-repressed *PHO5* data). Single molecule analysis demonstrates that nucleosome occupancy decreases at the promoter, 5' end, and 3' end of the constitutively activated *PHO5* gene in *hht2-G90R*, *R128S* strains. 170 molecules of repressed and 213 molecules of active *PHO5* gene electron micrographs (EM) were digitized to give base pair resolution of whether a DNA sequence is nucleosomal (bubble) or not (linear DNA). Average nucleosome occupancy (R-value) is plotted for active (black line) and repressed (tan space fill) gene molecules relative to the *PHO5* TSS. Genomic locations are annotated from left to right: RS-element, UAS1, UAS2, TATA box, TSS, 5' UTR, ORF, 3' UTR, p/TTTS region, LexA binding site.

C) Nucleosome sized gaps in *PHO5* occur at sites predicted to form less stable nucleosomes. Frequency of pre-nucleosome to nucleosome sized free-DNA 'gaps' increases in *hht2-G90R*, *R128S* strains at locations predicted to form relatively more stable nucleosomes over the transcribed *PHO5* gene. The frequency of linear DNA between 87 and 167 base pairs in length for wild type (grey space fill) [CB/HB] and *hht2-G90R*, *R128S* strains (black line) as well as the predicted free energy of tetramer/DNA wrapping (purple line) are plotted relative to the *PHO5* TSS.



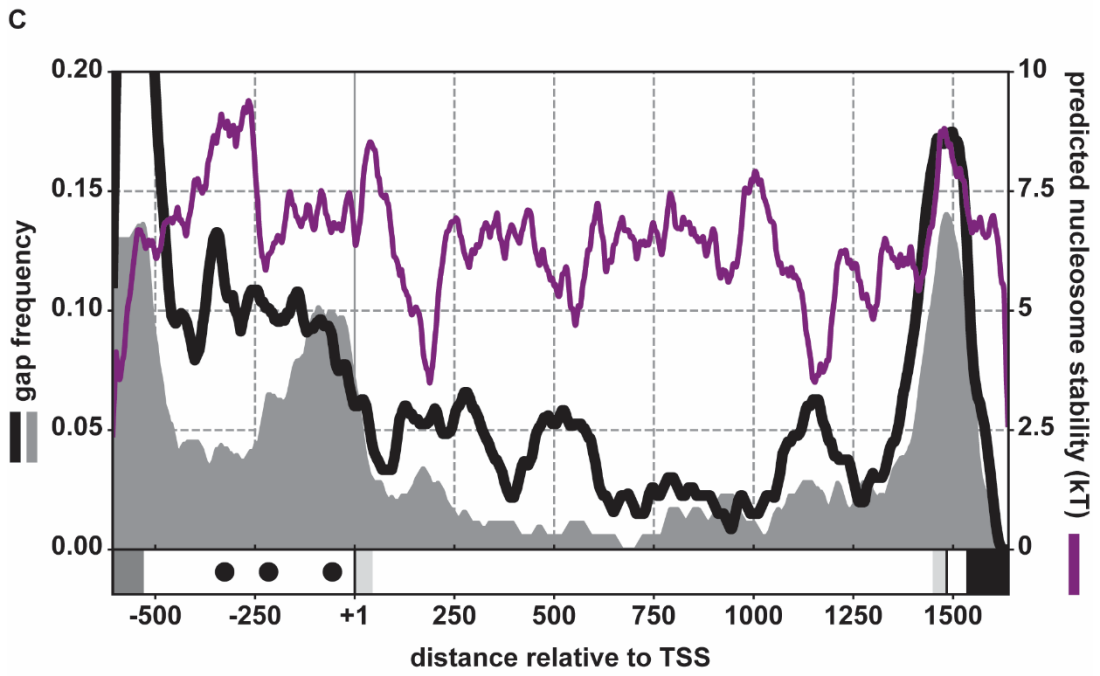
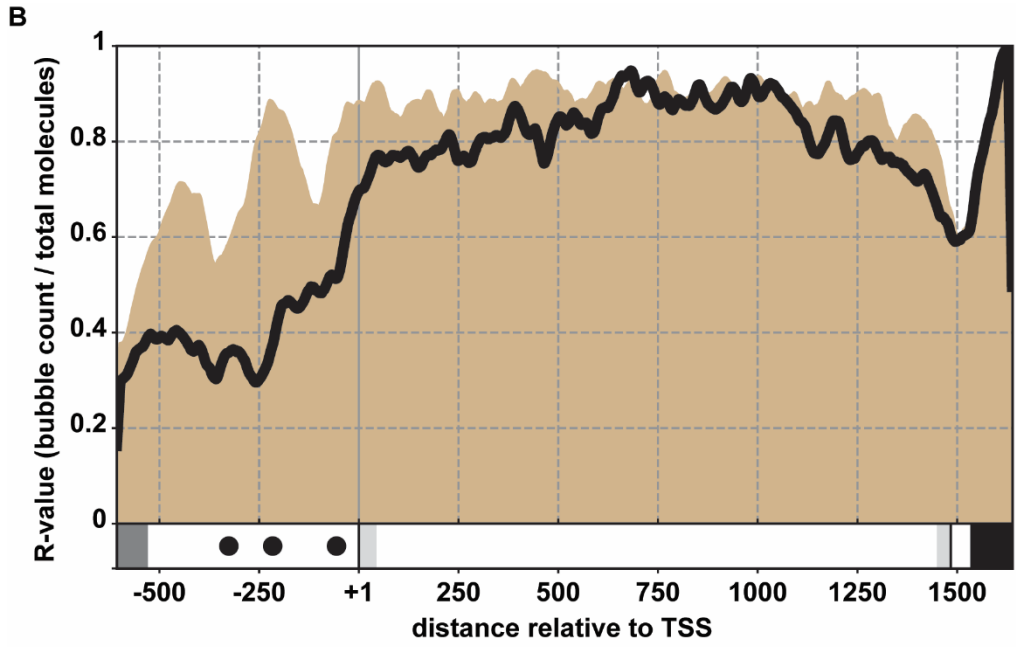


Figure 2-8. *hht2-S87P, G90R* nucleosome occupancy

A) Genome-wide nucleosome loss in *hht2-S87P, G90R* cells is most common at sites predicted to form more stable nucleosomes. 22,507 WT nucleosome dyads over the transcription unit of genes at least 1,400 bp in length were oriented in the direction of transcription and split into four quartiles determined by the ratio of mutant to WT MNase signal at the WT dyad location (shown in the bottom set of panels with arbitrary units). The top set of panels shows the average predicted free energy of nucleosome formation at these locations.

B) *hht2-S87P, G90R* rescues synthetic lethality caused by the inability to acetylate/post-translationally modify H3-K9,14,18,23 in *spt5-242* cells. Strains with the indicated *SPT5* genotype, *CEN TRP1 HHT2* allele plasmid, and *CEN URA3 HHT1* plasmid were serially diluted onto the indicated plates and temperatures for 2 days.

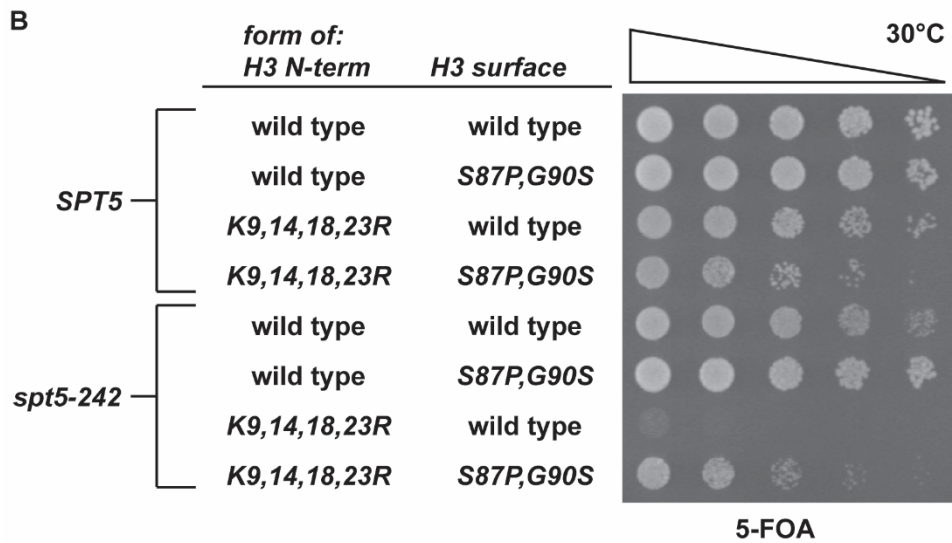
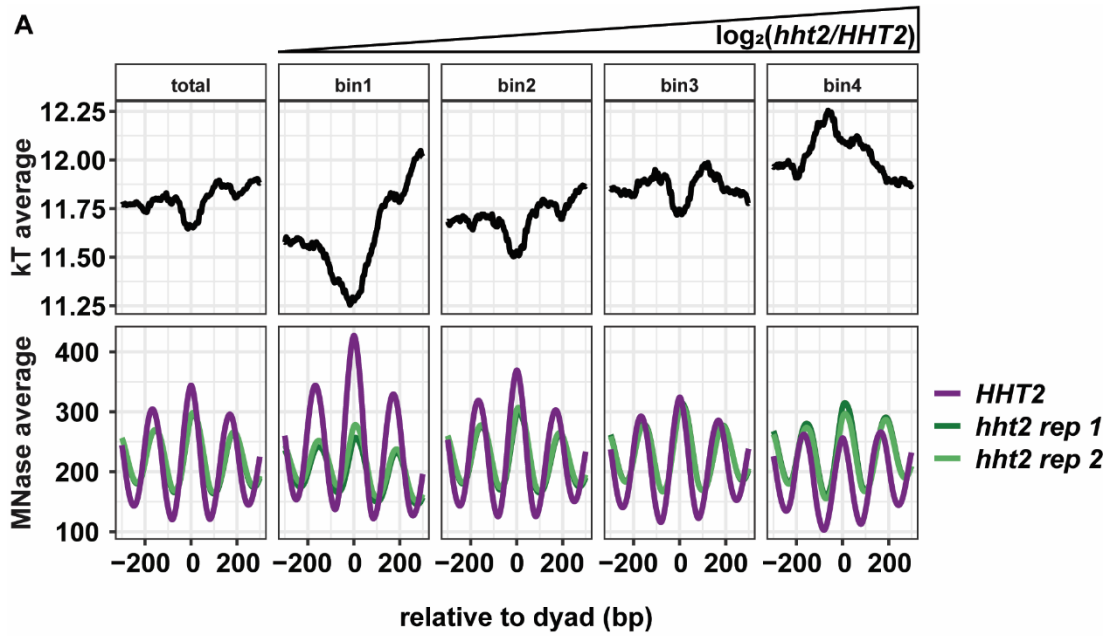


Figure 2-9. Predicted average nucleosome stability relative to RNA pol II active site (net-seq) under Spt5 non-depletion (mock) and depletion conditions.

Only the *S.cerevisiae* net-seq data ([Uzun et al. 2021](#)) which overlaps with the 4,974 geneset and *S.pombe* net-seq data ([Shetty et al. 2017](#)) which overlaps with the gene transcription unit defined in ([Eser et al. 2016](#)) were used.

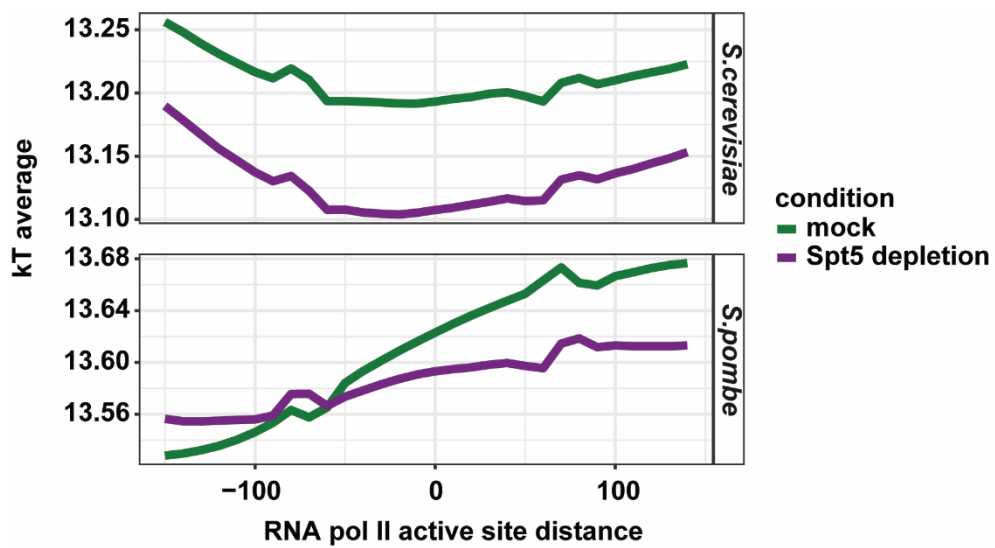


Figure 2-10. *spt5* cryptic initiation mutations predominantly occur in a novel Spt5 region

Plasmid born *spt5* mutations that have a cryptic initiation phenotype were identified and mapped relative to Spt5 structure.

A) Most *spt5* cryptic initiation mutations occur in an NGN-proximal region (NPR). Mutations in KOW2, KOW3 and that truncate the CTR have also been identified. The *spt5-242* allele is in bold. The location of the three amino acids important for binding histone H3-H4 are noted with *.

B) AlphaFold predicts that the Spt5 NPR is structured. PDB:6J4Y was used as a model to align the AlphaFold predicted Spt5 structure. Amino acids identified in the *spt5* cryptic initiation screen and that function in binding histone H3-H4 are displayed as spheres.

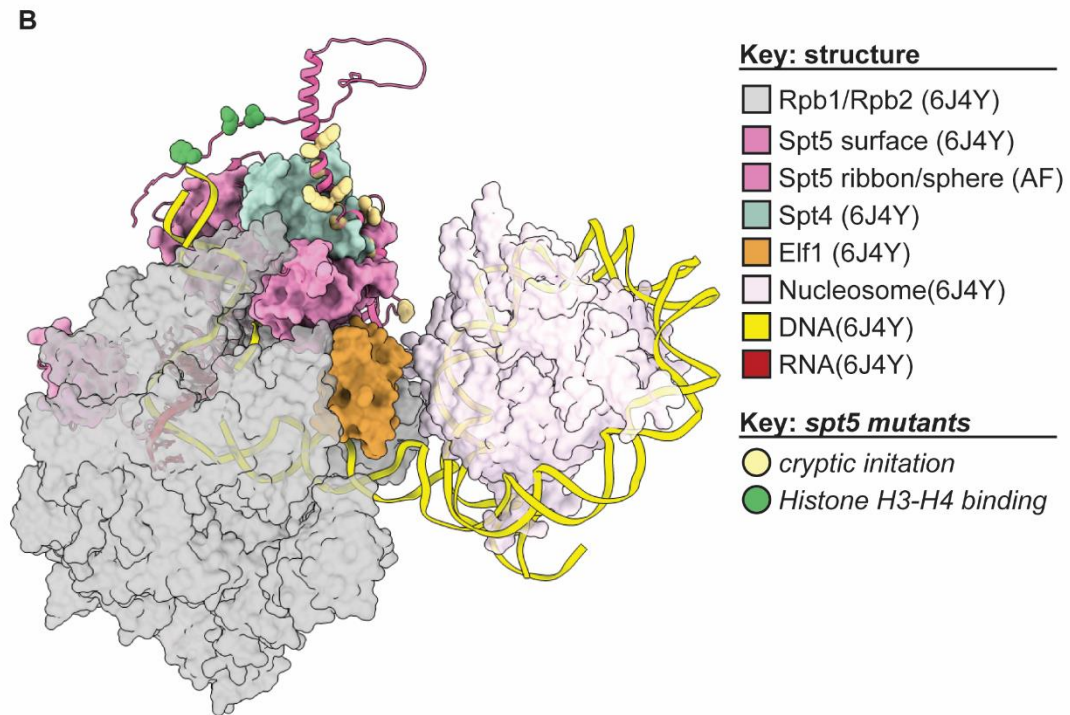
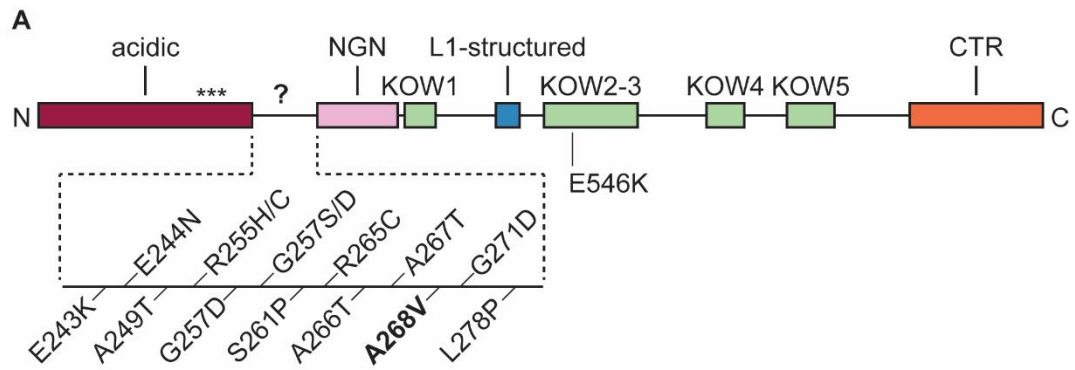


Figure 2-S1. *hht2 spt5Cs*- suppressor mutations generally do not disrupt telomeric silencing.

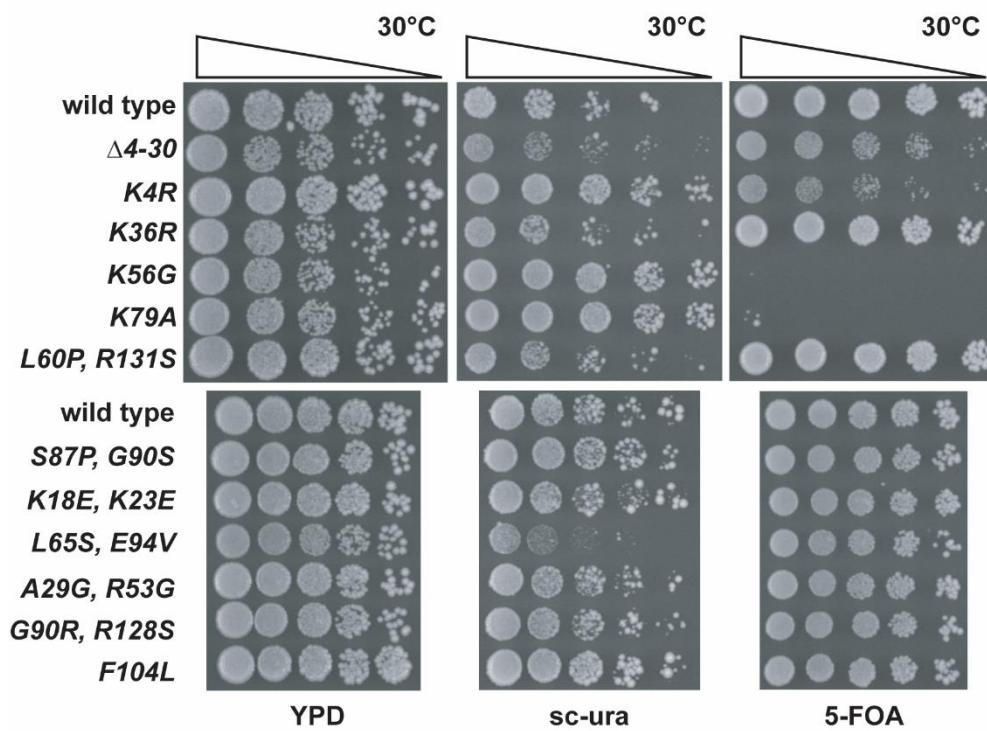


Figure 2-S2. *hht2 spt5-242* suppressor mutations do not disrupt silencing at the mating type locus.

A.) *hht2-supp* mutations do not interfere with mating to wild type yeast cells. Histone shuffle strains were transformed with a *TRP1 CEN HHT2* plasmid that contains the indicated *hht2* allele (except *sir2D*) and serially diluted onto YPD or a lawn of wild type cells of the opposite mating type for one day of growth before replica plating to SD plates. YPD plates were incubated for 3 days and SD plates were incubated for 2 days.

B.) Normal mating efficiency is observed in *hht2-supp* x *hht2-supp* crosses. *hht2** corresponds to histone H3 allele of the lawn or the indicated row of cells for the respective dilution spot. The matings were replica plated to SD and incubated for 2 days.

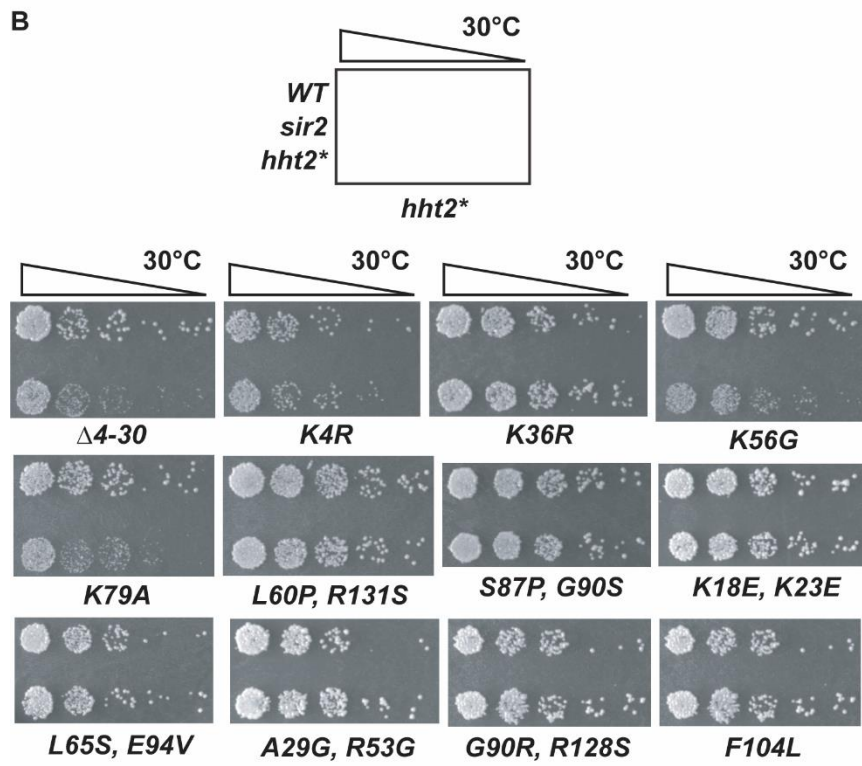
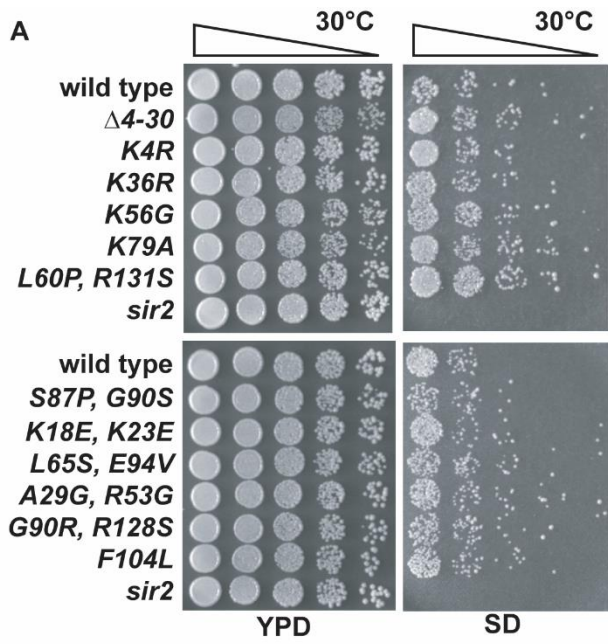


Figure 2-S3. Histone H3 mutations near SH2.5 have a *bur* phenotype.

All strains have copy 1 of the H3-H4 locus deleted and only *SUC2* does not contain the *suc2DUAS* allele. The indicated strains were directly struck out to YP + sucrose + 1 mM antimycin A for 2 days.

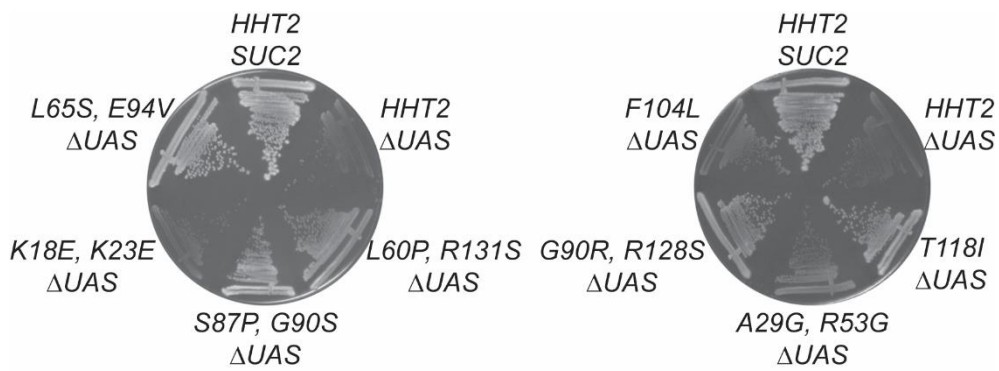


Figure 2-S4. yH3.3 cryptic initiation is suppressed by yH3.1.

Diploids that were homozygous for H3-H4 copy 1 deletions and heterozygous for the indicated *HHT2* allele were serially diluted on the indicated media and growth conditions. YPD plates were incubated for 2 days and sc-his + gal for 3 days.

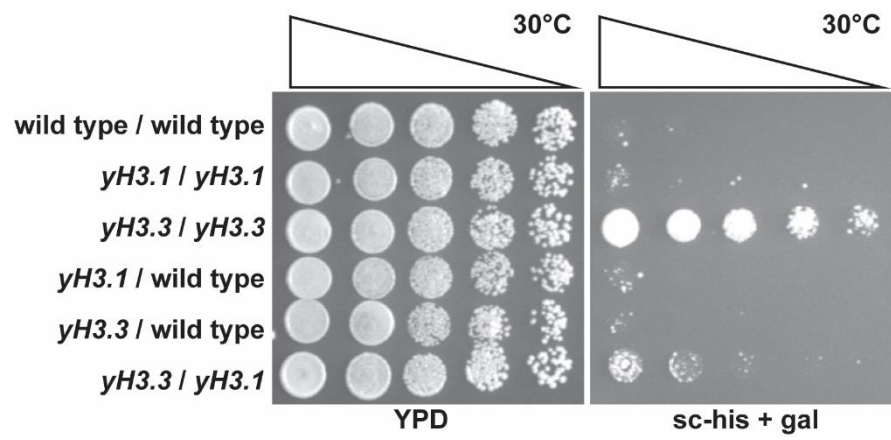
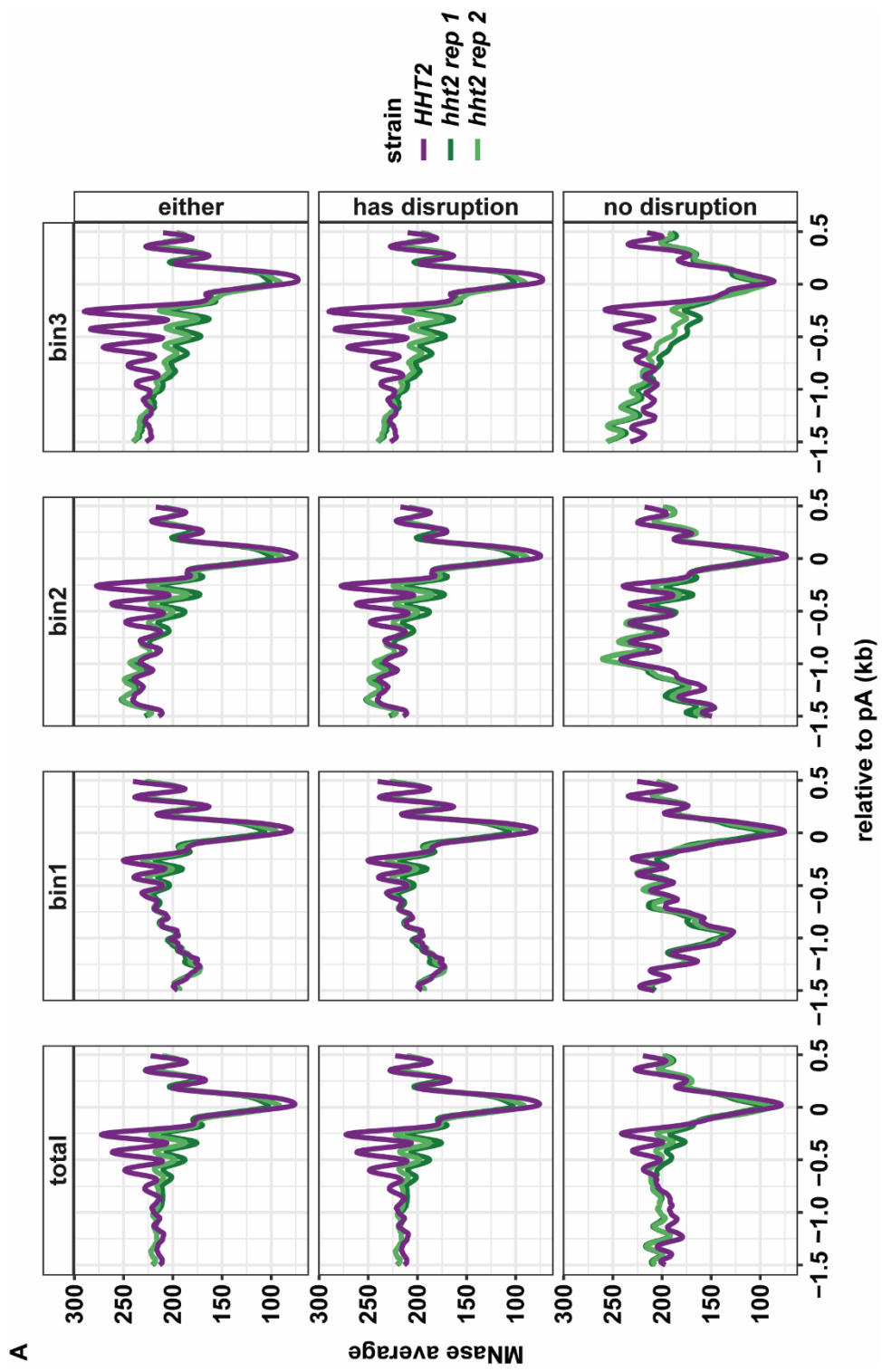


Figure 2-S5. 3' Nucleosome loss is still observed in genes that have not been observed to exhibit chromatin disruption phenotypes.

The 4,974 genes with mapped TSS and pA sites were split into two groups depending on whether they have a reported chromatin disruption phenotype ('has disruption': cryptic initiation, Set2 repressed anti-sense transcripts, stable unannotated transcripts, or cryptic unstable transcripts), or have yet to be reported as being disrupted ('no disruption'). These groups were then split into two more subgroups based on whether the genes overlap with other genomic features (e.g. ARS, tRNA genes, transposable elements, other genes) shown below and parsed by transcribed gene length

A) Subgroup of genes with no overlapping yeast genomic features. The gene counts for each panel are as follows (total, bin1, bin2, bin3): either (2,827, 943, 942, 942), has disruption (1,677, 599, 599, 599), no disruption (1,150, 384, 384, 384).

B) Subgroup of genes with overlapping yeast genomic features. The gene counts for each panel are as follows (total, bin1, bin2, bin3): either (2,146; 716, 715, 715), has disruption (1,031; 344; 344; 343), no disruption (1,115; 372, 372, 371).



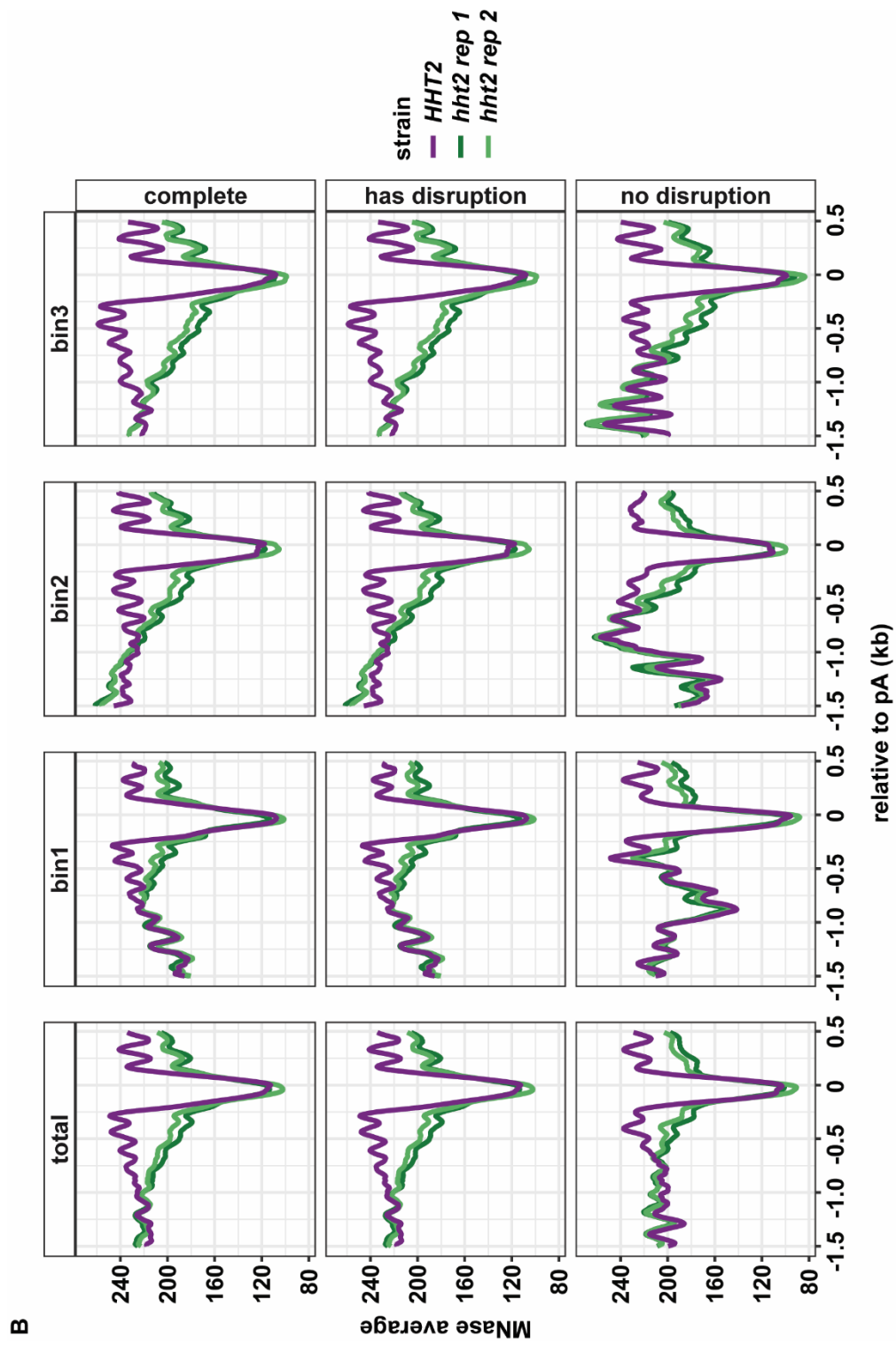
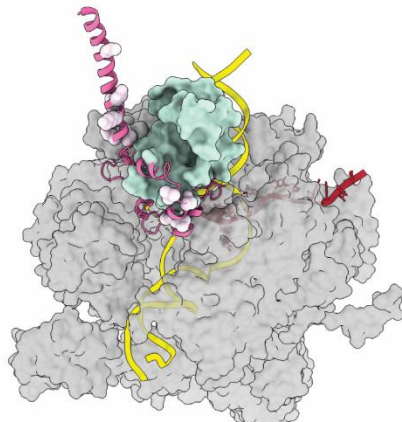


Figure 2-S6. AlphaFold predictions of the Spt5 NPR from multiple species.

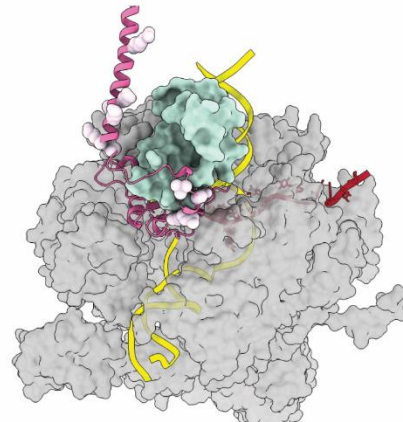
AlphaFold Spt5 predictions were aligned to PDB:6J4Y and Spt5 structure not part of the NPR-NGN is hidden from view. Amino acids which are conserved across these species are shown as spheres.

Key:

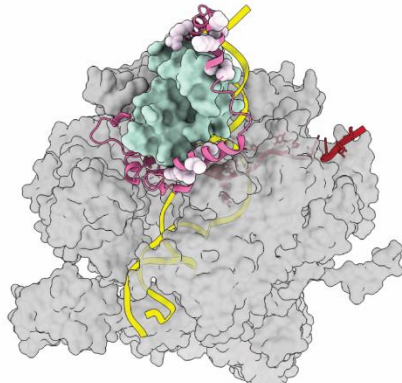
□ Rpb1/Rpb2 ■ AlphaFold Spt5 □ conserved residue ■ Spt4 ■ DNA ■ RNA



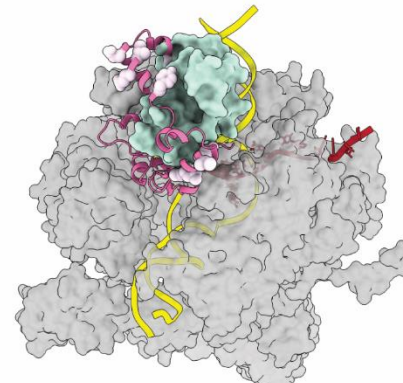
S. cerevisiae



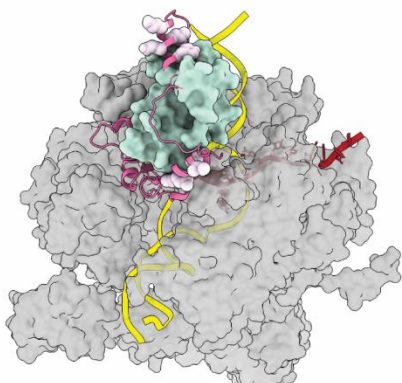
S. pombe



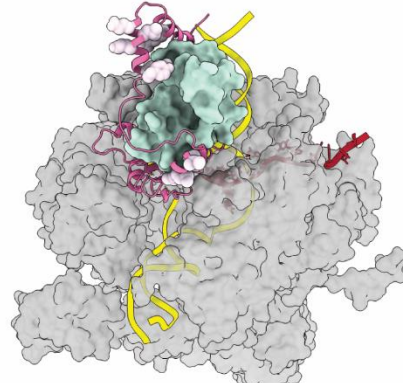
C. elegans



D. melanogaster



M. musculus



H. sapiens

Chapter 3

Epistatic relationships between transcription elongation factors and histone H3

Introduction

A wealth of knowledge exists for many genes and the *in vivo* molecular pathways in which they function. The protein products of a subset of these genes have been characterized *in vitro* to elucidate mechanistic details of how they may function *in vivo*. A further limited subset have established biochemical systems to interrogate multi-step/multi-protein mechanisms (Nagai *et al.* 2017; Yang *et al.* 2022). However, not all proteins are amenable to biochemical studies, or *in vitro* conditions required for their function have yet to be identified. Further, while advances in cryo-electron microscopy (cryo-EM) have led to a boon in visualizing multi-protein complexes, critical unstructured regions of proteins in these complexes remain unresolved. Genetic and biochemical methods have been a powerful combination of experimental approaches and results from each technique can aid the other. Mutant hunts remain an important tool to identify unknown relationships between genes and to discover new gene properties (Winston and Koshland 2016).

We previously isolated a class of histone H3 alleles that suppress the cold-sensitive and transcription elongation defective *spt5-242* allele. Spt5 is a universally conserved, multi-domain transcription elongation factor that is essential for life (Hartzog and Fu 2013). The NGN domain of Spt5 binds over the large central cleft of RNA pol. Along with its protein binding partner, Spt4, the Spt5 NGN domain functions as a processivity factor that keeps RNA pol engaged with DNA. Nucleosomes inhibit both *in vivo* and *in vitro* transcription. Addition of Spt4/Spt5 and chromatin factors that act on nucleosomes to transcription reactions decreases the nucleosomal barrier to RNA pol *in vitro* transcription elongation. We have previously established a working model that Spt5 helps RNA pol II overcome the chromatin barrier to transcription elongation: loss of ATP-dependent chromatin remodeler

Chd1, the Rpd3S/Set2 histone deacetylase system, Set1 histone H3-K4 methylation, or the PAF1 complex function suppresses *spt5-242* (Squazzo *et al.* 2002; Simic *et al.* 2003; Quan and Hartzog 2010). Our *hht2* suppressors of *spt5-242* (*hht2*-supps) provide direct evidence that nucleosomes oppose Spt5 function during transcription elongation *in vivo*. While we demonstrated that the *hht2*-supps disrupt chromatin function over transcribed genes, and for 2 alleles examined, specifically affect the nucleosome occupancy over DNA sequences predicted to form more thermodynamically stable nucleosomes – the mechanism of *hht2* chromatin disruption is unknown.

Nucleosome structure is qualitatively described by the points of DNA/histone contact (super helical location; SHL) and the histone composition of the nucleosome core (Luger *et al.* 1997). One sub-class of our *hht2* alleles that suppress *spt5-242* alters amino acids located near SHL2.5, a region that is solvent exposed and is structurally distinct between many histone H3-isoforms. Histone chaperones can distinguish among histone H3-isoforms and facilitate post-translational modifications to histones (Rando and Winston 2012; Martire and Banaszynski 2020; Ray-Gallet and Almouzni 2021). Further, the Snf2 class of ATP-dependent chromatin remodelers engage with the nucleosomal DNA at the SHL2 and can make extensive contact with the nucleosome (Hauk and Bowman 2011; Nodelman and Bowman 2021). Thus, many different types of proteins and protein complex act on this nucleosome surface during transcription.

Do the SHL2.5 *hht2* mutations disrupt a specific protein-protein interaction, do they disrupt global SHL 2.5 function, or do the different SHL 2.5 alleles represent distinct and allelic protein disruption that led to *spt5-242* suppression? To better understand how this class of *hht2* alters chromatin function, we selected for and identified extra-genic suppressors of the SHL2.5 *hht2* temperature-sensitive phenotype. We identified mutations in the HFI and UBP10 genes both of which encode components of the SAGA histone acetyl transferase complex. We found that *spt5-242* is a mutual suppressor of *hht2* and that nucleosome

assembly of Chd1 inhibits *hht2* and *spt5*. Analysis *hht2* suppressors suggest that *hfi1* disrupts a Sgf73 SAGA-independent function, Ubp10 has non-Rad6 ubiquitinated targets *in vivo*, *hht2* suppressors don't decrease the dependence on transcription elongation chaperone function for viability in *hht2*, and that the SHL2.5 *hht2* alleles are predicted to alter FACT and/or RSC chromatin function *in vivo*.

Results

Identification of *hht2-G90R, R128S* genetic suppressors

The *hht2-G90R, R128S* mutation was previously isolated as a genetic suppressor of *spt5-242*. Our prior analysis of this mutation (Chapter 2) indicates that it disrupts transcribed chromatin. To further investigate this histone mutation, we took a genetic approach. In cells with wild type Spt5, *hht2-G90R, R128S* causes several mutant phenotypes, including temperature sensitive growth defect. We therefore selected for Ts⁺ revertants and identified 7 complementation groups that restore *hht2* temperature-sensitive growth. Our main assumption was that the suppressors of this histone mutation would alter transcribed chromatin. However, that *hht2-G90R, R128S* has pleiotropic phenotypes, and it remains possible that the genetic suppressors alter chromatin processes distinct from those relevant to transcription elongation.

We subsequently identified the genes represented by 2 of these complementation groups (Fig. 3-1A). One genetic suppressor from the screen is *hfi1-L305P*, a helix-breaker mutation in the histone-fold-domain of a SAGA structural integrity protein. The other genetic suppressor from the screen is *ubp10-270^{ter}*, a nonsense mutation that truncates an a de-ubiquitinase with multiple targets *in vivo*. We also identified several other suppressors of *hht2-G90R, R128S* by taking a candidate approach (Fig. 3-1). Interestingly, the mutation used to identify *hht2-G90R, R128S* – *spt5-242* – is a genetic suppressor of the *hht2-G90R, R128S* Ts⁻ phenotype. Furthermore, deletion of ATP-dependent chromatin remodeler gene

CHD1, also suppresses *hht2-G90R, R128S*. The *hht2* genetic suppressors also suppress replication stress (hydroxy urea), caffeine, and high-salt phenotypes of *hht2-G90R, R128S* (Fig. 3-1B). The variability in genetic suppression of *hht2* phenotypes (Fig. 3-1B) suggests that *hfi1-L305P*, *ubp10-270^{ter}*, *chd1Δ*, and *spt5-242* may suppress *hht2-G90R, R128S* by distinct mechanisms.

Histone chaperones are essential in *hht2-G90R, R128S*

Glycine 90 of yeast histone H3 is located at the solvent exposed SHL2.5 in the nucleosomal structure. In many eukaryotes, this histone H3 region is distinct between two non-centromeric isoforms of histone H3 – H3.1 and H3.3. These H3 isoforms are each bound by a distinct set of histone chaperone complexes that are used to form nucleosomes in a replication-dependent (H3.1) or replication-independent (H3.3) process, respectively. Although budding yeast only encode a single non-centromeric form of histone H3, they do express the chaperones that distinguish H3.1 and H3.3 in other eukaryotes, and mutations affecting these chaperones and the SHL2.5 region of yeast H3 can selectively interfere with replication independent nucleosome assembly (Cho paper). Furthermore, we previously demonstrated that the SHL2.5 region in yeast has a role in nucleosome assembly (Radman-Livaja *et al.* 2012) and mutations that alter this region affect nucleosome occupancy over transcribed genes (Chapter 2).

An appealing hypothesis is that SHL2.5 mutations interfere with the ability of one or more histone chaperones to function *in vivo*. To test this hypothesis genetically, we first conducted a 2 μ high-copy suppressor screen of *hht2* with a yeast genomic tiling library (Jones *et al.* 2008) but isolated no candidate plasmids. We then took a candidate approach to identify histone chaperones that are necessary for viability in *hht2*. In yeast, histone chaperone function is largely redundant, and loss of multiple histone chaperones functions are required for synthetic lethality or strong phenotypes. When we generated double mutants

between *hht2-G90R*, *R128S* and *spt6-50*, *spt16-197*, *hir1*, *asf1* or *rtt106*. All double mutants were inviable in the absence of a wild type copy of histone H3 (i.e., either the chromosomal *HHT1* gene or a plasmid borne copy of *HHT2*). (Fig. 3-2A). These genetic interactions are not allele specific, as we also observed synthetic lethality when a second histone H3 suppressor of *spt5-242*, *hht2-L65S*, *E94V*, was combined with these histone chaperone mutations (data not shown). In contrast, when we disrupted replication-dependent histone chaperone function with *cac1Δ*, double mutant cells were viable in the absence of wild type histone H3 (Fig. 3-2B).

Histone H3 acetylation regulates replication-coupled nucleosome assembly (Burgess *et al.* 2010). Gcn5 predominately acetylates the histone H3 tail, but does have non-histone targets *in vivo*, while Rtt109 targets H3-K56 in globular domain of histone H3 (Park *et al.* 2008). Neither of these enzymes are essential for viability in *hht2-S87P*, *G90R* (Fig. 3-2C). Interestingly, Rtt106 is thought to specifically assemble nucleosomes that have histone H3-K56 acetylation (Zunder *et al.* 2012; Fazly *et al.* 2012), which is achieved by Rtt109 (Park *et al.* 2008; Zhang *et al.* 2018). The observation that *hht2* double mutants with *rtt106Δ* but not *rtt109Δ* are inviable suggests that either Rtt106 has a H3-K56 independent function or that H3-K56 can be acetylated by other histone H3 HATs which has not been reported in the literature. Overall, the *hht2* mutants strongly interact with histone chaperones and loss of transcription-coupled histone chaperone function is essential for viability.

We used the *hht2* histone chaperone double mutants as a genetic tool to perform epistasis tests with a subset of *hht2* genetic suppressors. No *hht2* genetic suppressor strongly rescued the synthetic lethality between *hht2* and *spt16-197* (Fig. 3-2C). The observed growth on 5-FOA is likely due to spontaneous genetic suppressors which is frequently observed with our *hht2* strains (data not shown). We also performed the same epistasis tests with *spt6-50*, *asf1Δ*, and *hir1Δ* and did not observe rescue of viability (data not

shown). This suggests that the *hht2* suppressors do not decrease the dependence of histone chaperone function in *hht2* cells.

Chd1 nucleosome assembly specifically affects transcription elongation

Chd1 is an ATP-dependent chromatin remodeler can functionally slide and assemble nucleosomes *in vitro* (Torigoe *et al.* 2013; Nodelman and Bowman 2021). ChIP experiments show that it is located at gene promoters, transcribed gene bodies, and sites of transcription termination (Simic *et al.* 2003; Hauk and Bowman 2011). Loss of *chd1Δ* function has many reported phenotypes across the entire gene unit. Similarly, our *hht2* mutations have multiple chromatin phenotypes at distinct gene locations. *hht2* has a cryptic transcription initiation phenotype over the transcribed gene body of the *FLO8-HIS3* genetic reporter and *sin/bur* phenotype at the *suc2* promoter in transcription activator sequence reporters.

To address which genic location loss of *chd1* function suppresses *hht2* temperature-sensitivity, we performed epistasis tests with enzymes that function at known gene locations during transcription. The histone H3 methyltransferases Set1 and Dot1 function at the 5' and 3' end of transcribed gene bodies, respectively. Rad6 is a histone H2B E2-ubiquitin conjugation enzyme that can ubiquitinate histone H2B across the entire gene. Further, histone H2B ubiquitination is required for Set1 and Dot1 function in a 'trans-histone' crosstalk mechanism (Chandrasekharan *et al.* 2010). Neither *set1Δ*, *dot1Δ*, nor *rad6Δ* suppress *hht2* at elevated temperatures (Fig. 3A). *chd1Δ hht2* temperature-sensitivity suppression is epistatic to *set1Δ* and *dot1Δ*, suggesting that neither Set1 nor Dot1 is required for the suppression of *hht2* by *chd1* (Fig. 3-3A). Interestingly, *rad6Δ* is epistatic to *chd1Δ* (Fig. 3-3A). We note that it remains possible that *set1Δ dot1Δ* double mutant yeast could be epistatic to *chd1Δ*, but a histone H2B ubiquitination function is a more direct explanation. While Rad6 can ubiquitinate histone H2B across the gene, our work with histone H2B de-ubiquitinases suggests that it is

loss of *rad6* function across the transcribed gene body and not the promoter that is necessary for *chd1* Δ suppression (see below).

Chd1 has two functions, nucleosome sliding and nucleosome assembly. To determine if loss of either of these could explain the *hht* suppression mechanism, we took advantage of *chd1-W932A*. This form of Chd1 lacks the ability to slide nucleosomes *in vitro*, but retains partial assembly activity (Torigoe *et al.* 2013). We generated a *chd1-W932A* mutant and integrated it at the *CHD1* chromosomal locus. Like *chd1* Δ , the *chd1-W932A* mutant has a cryptic initiation phenotype with the *FLO8-HIS3* genetic reporter (Fig. 3-3C) and partially suppresses the Ts- phenotype of *hht2* (Fig. 3-3D) and Cs- phenotype of *spt5-242*, an *spt5* allele that impairs transcription elongation (Simic *et al.* 2003; Quan and Hartzog 2010) (Fig. 3-3E). However, in each case, *chd1-W932A* was a weaker suppressor of these phenotypes than was *chd1* Δ . Thus, loss of Chd1's nucleosome sliding activity is not sufficient to explain the observed interactions of *chd1* Δ with *hht2* and *spt5-242*, nor its cryptic initiation phenotype.

***hht2* suppressors distinctly affect cryptic initiation**

One prediction of the *hht2* suppressors is that they restore disrupted chromatin function over transcribed gene bodies. To test this hypothesis, we generated histone shuffle strains that contain the cryptic initiation *FLO8-HIS3* reporter and either *hfi1-L305P* or *ubp10* Δ *hht2* suppressor mutations. A variety of histone H3 mutations that we have previously shown to activate the *FLO8-HIS3* reporter were then introduced to these strains using the plasmid shuffle strategy. In addition to *hht2-G90R*, *R128S*, we examined point mutations at post-translationally modified histone residues and a representative set of *hht2* mutations that suppress *spt5-242* (chapter 2).

Surprisingly, our two different *hht2* suppressors had opposing effects in this assay, *hfi1-L305P* reduced growth of these histone mutant strains on galactose -His plates while

ubp10Δ increased growth of most, but not all, of the histone mutants (Fig. 3-4). The apparent enhancement of cryptic initiation by the *ubp10Δ* mutation is consistent with a previous study that demonstrated the same phenotype enhancement between *ubp10* and *spt16* or *pob3* mutants (Nune *et al.* 2019).

SAGA is a transcriptional co-activator of galactose regulated genes (Bhaumik and Green 2001; Larschan and Winston 2001) and the *GAL1* promoter drives the *FLO8-HIS3* reporter gene (Cheung *et al.* 2008). Therefore, decreased SAGA function in *hfi1-L305P* cells may explain the decrease in the observed cryptic initiation phenotypes observed in the *hfi1-L305P hht2* strains. The relative strength of promoter transcription activation has been shown to affect cryptic initiation phenotypes (Silva *et al.* 2012) and deletion of the histone H3 tail *hht2-Δ4-30* which de-represses galactose genes (Mann and Grunstein 1992) has a decreased cryptic initiation phenotype in *hfi1-L305P* cells (Fig. 3-4). Further, *hfi1-L305P* genetically suppresses the *sin/bur* phenotype of *hht2-G90R, R128S* (data not shown). Like known SAGA mutants, *hfi1-L305P* likely decreases promoter activation.

Ubp10 has multiple enzymatic targets *in vivo* that act on transcribed chromatin

The histone H2B deubiquitinase Ubp10 was originally identified as a regulator of telomeric and sub-telomeric gene repression (Kahana and Gottschling 1999; Gardner *et al.* 2005). Ubp10 physically interacts with Sir4 to mediate telomeric silencing and *ubp10-270^{ter}* creates a truncated *ubp10* protein that lacks catalytic activity but is predicted to physically interact with Sir4 (Kahana and Gottschling 1999). A complementation test with previously characterized *ubp10* mutants demonstrates that it is the loss of general *ubp10* enzymatic activity and not Sir4 mediated catalytic activity which suppresses *hht2* (Fig. 3-5B). The catalytically inactive *ubp10-C371S* allele fails to complement both *ubp10Δ* and *ubp10-270^{ter}* while the defective Sir4 binding but catalytically active *ubp10^{Δ94-250}* does complement *ubp10* suppression of *hht2* (Fig. 3-5B). Ubp8 is another histone H2B de-ubiquitinase and *ubp8Δ*

ubp10Δ double mutants have increased *in vivo* H2B-Ub than either single mutant (Gardner *et al.* 2005). Interestingly, Ubp8 and Ubp10 have target H2B-Ub at different genomic locations across the gene body (Schulze *et al.* 2011). In *ubp10Δ* and not *ubp8Δ* mutants there is elevated H2B-Ub at the 3' ends of gene bodies, a transcribed region where we observe prominent *hht2* nucleosome occupancy defects (Chapter 2). However, we do not observe *hht2* suppression in *ubp8Δ* cells nor enhanced genetic suppression in *ubp8Δ ubp10Δ* cells (Fig. 3-5A, data not shown).

Recent work has demonstrated an expanded functional role for Ubp10 *in vivo*. Ubp10 physically associates with and de-ubiquitinate PCNA (Gallego-Sánchez *et al.* 2012) and Rpa190 (Richardson *et al.* 2012), the largest subunit of RNA pol I. Like histone H2B ubiquitination, PCNA ubiquitination requires Rad6 function (Gallego-Sánchez *et al.* 2012) and a non-peer reviewed pre-print suggests that Rad6 plays a predominant role in Rpa190 ubiquitination (Ibars *et al.* 2021). Ubp10 also physically interacts with (Buszczak *et al.* 2009; Richardson *et al.* 2012) and alters the abundance (Isasa *et al.* 2015) of many proteins that function during transcription elongation. To determine if the Rad6 E2-ubiquitin conjugation pathway is required for the *ubp10* suppression mechanism we performed an epistasis test between *rad6Δ* and *ubp10-270^{ter}*. We still observe Ts+ in *hht2-G90R, R128S ubp10-270^{ter} rad6Δ* cells, although, it is an intermediate phenotype when compared to *hht2 ubp10* double mutants (Fig. 3-5C).

The intermediate phenotype observed in *hht2-G90R, R128S ubp10-270^{ter} rad6Δ* cells could be attributed to: (i) negative genetic interactions between loss of the entire Rad6 pathway and *hht2 ubp10*, or (ii) Ubp10 de-ubiquitinates different sets of proteins that are targeted by distinct E2-ubiquitin conjugating enzymes. We transformed two versions of histone H2B into different *hht2* strains to test whether histone H2B-Ub, and thus the Rad6 pathway, has a role in the *ubp10* suppression mechanism. Additional copies plasmid borne

H2A-H2B leads to decreased growth in *hht2* and *hht2 ubp10* cells. Further, if the added histone H2B cannot be ubiquitinated (*htb1-K123R*), the dominant negative interaction is stronger (Fig. 3-S1). This suggests that the genetic suppression observed in *hht2 ubp10 rad6* is due to increased ubiquitination in non-Rad6 E2-ubiquitin conjugating enzymes and the intermediate phenotype is because of the loss of Rad6 histone H2B ubiquitination.

SAGA mediated Sgf73 function

SAGA is a large protein complex with multiple functions during gene expression. Hfi1 is a structural integrity protein in SAGA and interacts with Taf12 through a histone-fold domain (Sterner *et al.* 1999; Gangloff *et al.* 2000; Wu *et al.* 2004; Papai *et al.* 2020; Wang *et al.* 2020). We hypothesized that *hfi1-L305P* disrupts a specific SAGA function, during cloning of this allele it displayed less severe phenotypes than *hfi1Δ* and *hfi1Δ* does not suppress *hht2*. We systematically examined most non-essential SAGA genes to identify loss of function mutations in a specific SAGA functional module that phenocopies *hfi1-L305P hht2* suppression (Table 3-1).

hfi1-L305P suppression of the *sin/bur* and cryptic initiation phenotypes of *hht2* can be explained by decreased SAGA function in promoter activation. SAGA's Spt3 and Spt8 subunits shuttle TBP to promoters where they recruit RNA pol II. Decreased TBP shuttling would reduce transcription at all RNA pol II transcribed genes. However, neither *spt3Δ* or *spt8Δ* suppress *hht2*. This suggests that *hfi1-L305P* is not abolishing SAGA TBP shuttling. The histone acetyl transferase (HAT) and histone H2B de-ubiquitinase (DUB) enzymatic modules both function at gene promoters to activate transcription. However, we have showed that loss of *gcn5Δ* or *ubp8Δ* function does not suppress *hht2* (Fig. 2B, data not shown).

Gcn5, the catalytic subunit of the SAGA and the closely related ADA complex, acetylate different lysine residues in the histone H3 N-terminal tail as well as non-histone proteins. Loss of a specific sub-set of SAGA/ADA functions may be sufficient to suppress

hht2. Deletion of the ADA-specific subunit Ahc1, abolishes this complex (Eberharter *et al.* 1999; Lee *et al.* 2011). However, an *ahc1Δ* mutation did not suppress *hht2* (Fig/Table). Gcn5 HAT function is augmented by different HAT-module proteins. Ada3 allows Gcn5 to acetylate nucleosomal histones instead of just core histones and expands the selection of lysine's in the histone H3 N-terminal tail for Gcn5 acetylation (Balasubramanian *et al.* 2002). Sgf29 has a general function in Gcn5 HAT function and contains a tandem Tudor domain that binds H3-K4me3 which aids in SAGA recruitment to promoters (Bian *et al.* 2011). Neither loss of *ada3Δ* or *sgf29Δ* HAT-module sub-function suppresses *hht2* (Fig.????).

Like Gcn5, Ubp8 could have SAGA-dependent and -independent enzymatic activities, or there are DUB-module regulated functions that are not disrupted in *ubp8Δ* cells. Loss of a sub-function and not global *ubp8* function could suppress *hht2*. The DUB-module functions in mRNA export through Sus1 which is part of both the SAGA and TREX-2 mRNA export complexes (Rodríguez-Navarro *et al.* 2004). Sus1 also has a role in H2B de-ubiquitination (Köhler *et al.* 2006) and formation of pre-initiation complexes at promoters (Durairaj *et al.* 2014). Complete loss of *sus1Δ* function does not suppress *hht2*. Sus1 depends on Sgf11 for association with SAGA but not for association with TREX-2 (Klößner *et al.* 2009). Specific loss of SAGA Sus1 function in *sgf11Δ* does not genetically suppress *hht2*. Further, Sgf11 contains a zinc finger domain that binds nucleosomal DNA and Sgf11 has a functional role in Ubp8 enzymatic activity (Samara *et al.* 2012; Koehler *et al.* 2014; Morgan *et al.* 2016) and loss of these *sgf11Δ* functions does not suppress *hht2*. Lastly - Sgf73 anchors the DUB-module to the SAGA complex (Köhler *et al.* 2008; Lee *et al.* 2009). Surprisingly, loss of *sgf73Δ* function genetically suppressed *hht2* and to a similar extent as *hfi1-L305P* (Fig. 3-6A).

A key prediction of our systematic analysis in identifying non-essential *saga* gene deletions which phenocopy *hfi1-L305P* is that *hfi1-L305P* should have overlapping

phenotypes with the *saga* gene deletion. The DUB-module regulates yeast replicative lifespan (RLS) and *sgf73Δ* have the largest DUB-module extension of increased yeast RLS (McCormick *et al.* 2014). We used the same method to measure yeast RLS between a wild type and *hfi1-L305P* strain and found that *hfi1-L305P* strains do have an increased RLS (Fig. 3-6B). Mutations of *sgf73* distinctly affect SAGA composition in mass-spec analysis (Han *et al.* 2014; Durand *et al.* 2014).

To do/examine what, we purified Spt7-TAP SAGA complex from strains that expressed *HFI1* or the *hfi1-L305P hht2* suppressor, or that entirely lacked *HFI1* (Fig. 6C). These complexes were then analyzed by mass-spectrometry to identify their protein constituents. We identified the protein composition of each Spt7-TAP purification and normalized the SAGA protein abundances relative to Spt7-TAP to compare changes to SAGA complex composition. Spt7-TAP SAGA purified from *hfi1Δ* grossly disrupts the HAT-module, DUB-module, Tra1, Spt3, and as predicted – Taf12 association (Table 3-2). This is consistent with prior studying showing that SAGA is grossly disrupted in from *hfi1Δ* strains (Wu and Winston 2002; Lee *et al.* 2011) (Fig./Table??). In contrast, Spt7-TAP SAGA purified from *hfi1-L305P* has about 50% less HAT-module association, 60% less DUB-module association, 75% less association of Tra1 and Spt3, little change in Spt8 association, and a 40% decrease in *hfi1-L305P* and 65% decrease in Hfi1 interaction partner Taf12 (Fig. 3-6C) (Table 3-2). While our mass-spec results cannot rule-out whether these relative protein abundances in *hfi1-L305P* represent alterations to or formation of SAGA sub-complexes, our data has similarity to SAGA purified from *sgf73Δ2A*. Ignoring the abundance of Sgf11 and Sus1 which have low spectral averages, our mass-spec suggests that either 25% of all SAGA complexes have a complete complex and *in vivo* SAGA function is globally reduced or there are multiple mixed SAGA complex compositions that have distinctly altered *in vivo* function.

What Sgf73 function is disrupted in *hfi1-L305P*? We performed epistasis crosses to generate *hht2 sgf73Δ ubp8Δ* and *hht2 hfi1-L305P ubp8Δ* strains to test whether Sgf73-independent activity of Ubp8 or altered SAGA-independent activity of Ubp8 could explain *hht2* suppression. Both strains suppress *hht2* (Fig. 3-S2 & data not shown) and any potential SAGA/Sgf73-independent activity of Ubp8 cannot explain the suppression mechanism. While *sus1Δ* disrupts a SAGA/TREX-2 function it leaves TREX-2 SAGA-independent function intact, and as mentioned previously, *sgf73Δ* disrupts the composition of the TREX-2 complex (Köhler *et al.* 2008). To test whether disruption of TREX-2 could explain genetic suppression of *hht2* we crossed deletions of non-essential TREX-2 genes in *hht2* strains. Both *sac3Δ* and *thp1Δ* are synthetic lethal with *hht2*. Further, *hfi1-L305P/sgf73Δ* rescues synthetic lethality between TREX-2 gene deletions and *hht2*. These results are inconsistent with the simple model that *hfi1-L305P/sgf73Δ* selectively disrupts TREX-2 complex function. Consistent with our mass-spec and *hfi1-L305P* suppression of *hht2* cryptic initiation and *sin/bur* phenotypes, SAGA may have reduced global activity in gene expression. SAGA was originally proposed to regulate ~10% of the yeast genome at stress-related genes (Huisinga and Pugh 2004). With new experimental techniques that measured and compared nascent transcription, SAGA function was shown to have a predominant function across the gene body and acts a general cofactor for global RNA pol II transcription (Bonnet *et al.* 2014; Baptista *et al.* 2017). While a global decrease in SAGA activity in *hfi1-L305P/sgf73Δ* can explain *hht2* suppression, SAGA function is still required. Loss of HAT function with *ada3Δ* or *gcn5Δ* and TBP recruitment with *spt3Δ* eliminates *hfi1-L305P* suppression of *hht2*, but this could be a consequence of SAGA function being required for RNA pol II and *sgf73Δ gcn5Δ/ada3Δ* and *sgf73Δ spt3Δ* have negative genetic interactions.

The remaining Sgf73 function is its role in stress-inducible transcript export from the nucleus (Kim *et al.* 2019). Interestingly, the synthetic lethal interactions between TREX-2

mutants and *hht2* suggest that redundant TREX-2 function may be disrupted in *hht2*. In addition to chromatin specific functions, histone H2B-Ub has a prominent role in the formation of proper mRNA-protein (mRNP) complexes for nuclear export (Moehle *et al.* 2012; Vitaliano-Prunier *et al.* 2012). Epistasis crosses with *rad6Δ* and *hfi1-L305P* show that *rad6Δ* is epistatic to *hfi1-L305P* and is required for *hht2* suppression (data not shown; should probably make figure?). Interestingly, *sgf73Δ* and not other DUB-module deletions genetically suppress mRNA export mutants (Kim *et al.* 2019), and Sgf73 but not other DUB-module proteins is required for Hog1 stress-response expression of the *PAU* genes in hypoxic conditions (Hickman *et al.* 2011). Complementation tests with *sgf73Δ2A* and *sgf73Δ4* alleles show that *SGF73* and *sgf73Δ4*, complement *sgf73Δ hht2* suppression and *sgf73Δ2A* fails to complement *sgf73Δ* at 30°C (Fig. 3-S3). Interestingly, at elevated temperatures *sgf73Δ2A* does complement *sgf73Δ hht2* suppression. Taken together this suggest that loss of Sgf73 SAGA association is important for *hht2* suppression and that Sgf73 may have a post-SAGA independent function. The model proposed by Kim *et al.* proposes that Sgf73 can facilitate canonical mRNA export with proper loading of Yra1 onto RNA at gene promoters or activate Mex67-mediated non-canonical mRNA export which bypasses mRNA quality control. The disrupted promoter and ORF phenotypes of *hht2* may disrupt promoter and/or transcription-coupled mRNP export complex formation and *sgf73/hfi1-L305P* restores a disrupted balance between disrupted mRNP export pathways.

Discussion

The *hht2* alleles were originally identified as suppressers of the cold-sensitive transcription elongation factor *spt5-242*. Thus, they are hypothesized to disrupt chromatin structure/function over the transcribed gene body. In Chapter 2 we show that these *hht2* mutations do decrease nucleosome occupancy and do alter chromatin function over gene bodies. Comparison of the different structural classes of *hht2* and the literature in Chapter 2

suggests that there are multiple molecular pathways that *hht2* disrupts during transcription elongation, but they remained to be tested. We used the strong temperature-sensitive phenotype of the SHL2.5 *hht2* alleles as a genetic tool to identify extra-genic suppressor mutations in molecular pathways that overlap with *hht2*.

There are several possible classes of *hht2* suppressors that we could identify: (i) restore direct physical interaction between *hht2* and *suppressor*; (ii) break *hht2* and *suppressor* physical interaction; (iii) decrease the dependence of *hht2* function; (iv) bypass *hht2* function; (v) indirect/act downstream of *hht2* affected processes.

We have identified five extragenic suppressors of SHL2.5 *hht2*: *spt5*, *chd1*, *ubp10*, *hfi1*, and *sgf73* (Fig 1A). In aggregate, the *hht2* suppressors function at promoters (Chd1, Hfi1/Sgf73) and transcribed gene bodies (Spt5, Ubp10, Chd1, Hfi1/Sgf73). Pairwise permutations in *hht2* double suppressor strains all have enhanced *hht2* temperature-sensitive suppression (data not shown) which suggests that each *hht2* suppressor has a distinct mechanism/pathway. However, they are all likely to restore some aspect of disrupted chromatin function over transcribed genes. The Set2/Rpd3s pathway functions to restore closed/un-acetylated ORF chromatin during transcription elongation and deletion of *set2Δ* in *hht2 suppressor* double mutants decreases the strength of temperature-sensitive suppression (data not shown).

The epistatic relationship between the *hht2* suppressors and *rad6Δ* highlight the various functional rolls that histone H2B ubiquitination has during transcription and provide new insight into known protein function. One key function of histone H2B-Ub is FACT mediated nucleosome reassembly during transcription elongation (Fleming *et al.* 2008). The *hht2* strains have a strong dependence on histone chaperone function for viability (Fig. 2A) and presumed decreased FACT nucleosome reassembly in *rad6Δ* is consistent with the increased sickness of *hht2 rad6Δ* cells (Fig. 3A). The *chd1-W932A* allele can assemble but

not slide nucleosomes *in vitro* and has decreased *hht2* suppression compared to *chd1Δ* (Fig. 3A). Chd1 has a known function in replication-independent nucleosome assembly of histone H3.3 (Konev *et al.* 2007; Siggins *et al.* 2015; Zhang *et al.* 2016; Schoberleitner *et al.* 2021) but also functions in inhibiting histone turnover in yeast (Radman-Livaja *et al.* 2012; Smolle *et al.* 2012), possibly by promoting nucleosome reassembly. Interestingly, *rad6Δ* is epistatic to *chd1Δ* in *hht2* suppression (Fig. 3A). This suggests that Chd1 may negatively regulate FACT-mediated nucleosome reassembly. Chd1 could function directly with FACT in nucleosome reassembly dynamics or Chd1 could function in nucleosome reassembly mediated through other histone chaperones. Recent work supports a model in which FACT directly associates with chromatin during transcription elongation starting at the +1 nucleosome and spreads throughout the gene body in a Chd1 dependent process (Jeronimo *et al.* 2021) that may be mediated through the Chd1 N-terminus (Farnung *et al.* 2021).

Histone H2B-Ub levels are elevated in *ubp10Δ* strains. An argument has been made that H2B-Ub contributes to nucleosome stability, there is more soluble histone H3 in NaCl treated nuclei when histone H2B-Ub is absent than when histone H2B-Ub is elevated (Chandrasekharan *et al.* 2009). Interestingly, we do see enhanced NaCl *hht2* suppression by *ubp10-270^{ter}* when compared to the other *hht2* suppressors. However, we observe decreased nucleosome occupancy at DNA sequences predicted to form more stable nucleosomes (Chapter 2). More intriguing is recent work that demonstrates FACT mediated de-ubiquitination activity of Ubp10 (Nune *et al.* 2019). The model proposed by Nune *et al.* states that FACT destabilizes or binds to already destabilized nucleosomes which contain H2B-Ub and that FACT assisted Ubp10 de-ubiquitinase activity serves as an assembly checkpoint for activation of FACT nucleosome assembly. This model predicts that *hht2* has decreased FACT nucleosome association and that elevated histone H2B-Ub by *ubp10Δ* restores FACT nucleosome binding at the expense of regulated nucleosome assembly activity. Interestingly, *rad6Δ* is incompletely epistatic to *ubp10 hht2* suppression, suggesting that in addition to

Rad6 E2-ubiquitin conjugation there may be another E2-ubiquitin conjugation pathway that Ubp10 targets which functions in a chromatin pathway.

An alternative model to histone H2B-Ub/FACT function is that elevated histone H2B-Ub in *ubp10Δ* may be inhibiting RSC function over transcribed gene bodies. Histone H2B-Ub opposes RSC function in fission yeast at the *ste11* gene (Materne *et al.* 2016) and recent RSC/nucleosome structures suggest that H2B-Ub should occlude or diminish RSC's ability to bind to the nucleosome (Ye *et al.* 2019; Patel *et al.* 2019). RSC in budding yeast has a sub-complex that remodels accessible nucleosomes which can lead to RSC-mediated nucleosome ejection over DNA sequences form more stable nucleosomes (Schlichter *et al.* 2020). The SHL2.5 *hht2* mutants have decreased nucleosome occupancy at DNA sequences predicted to form more thermodynamically stable nucleosomes and increased H2B-Ub in *ubp10D* could stabilize *hht2* occupancy by opposing RSC function on these nucleosomes. Further, Ubp10 primarily targets H2B-Ub at the 3' ends of long genes (Schulze *et al.* 2011) and is consistent with the observed correlation between *hht2* nucleosome occupancy defects and gene length (Chapter 2).

The *hfi1/sgf73* suppressors can also explain a H2B-Ub independent decrease in RSC activity. Histone H3 N-terminal acetylation increases RSC nucleosome binding (Ferreira *et al.* 2007; Chatterjee *et al.* 2011) and stimulates RSC's ability to remove the nucleosomal barrier to RNA pol II *in vitro* (Carey *et al.* 2006). The global SAGA complex reduction in *hfi1-L305P* and decreased HAT activity in *sgf73Δ* would lead to reduced RSC recruitment and decrease the frequency of RSC nucleosome ejection in *hht2*. Rsc4 functions in a autoregulatory mechanism – Rsc4 tandem bromodomains can bind to either itself when acetylated by Gcn5 or to acetylated histone H3-K14 when Rsc4 is not acetylated (Kasten *et al.* 2004; VanDemark *et al.* 2007). This may explain the epistatic relationship between *gcn5* and *hfi1-L305P hht2* suppression. Loss of *gcn5* HAT-independent activity leads to stimulated RSC activity and

functionally related histone H3 HATs supply histone H3 acetylation. Recently it has been reported that histone acetylation has the ability to actually stabilize nucleosomes and inhibit RSC function at +1 nucleosomes (Lorch *et al.* 2018). Un-acetylated nucleosomes are ejected by RSC and transferred to the Nap1 histone chaperone. Histone acetylation prevents RSC nucleosome transfer to Nap1 and increases RSC associated with the nucleosome. The *ada3Δ* epistatic relationship with *hfi1-L305P hht2* suppression can be explained by this +1 nucleosome RSC function. Gcn5 HAT-module function is decreased in *ada3Δ* which leads to under-acetylated +1 nucleosomes that are ejected by RSC and causes unregulated pol II transcription activation. Consistent with this, *gcn5Δ* is epistatic to *ubp10 hht2* suppression but *ada3Δ* shows incomplete epistasis. Suggesting that increased H2B-Ub may compensate for decreased SAGA HAT activity under this model.

Our *saga* complex purifications and analysis of *sgf73 hht2* suppression suggests that *hfi1-L305P* has *sgf73Δ* phenotypes and can disrupt SAGA-mediated Sgf73 recruitment and affect post-SAGA Sgf73 function. Like *sgf73Δ* (McCormick *et al.* 2014), *hfi1-L305P* extends yeast RSL (Fig. 3-6B) and purified *hfi1-L305P* SAGA complexes have broad disruptions that overlap with *sgf73Δ2A* – an allele that prevents DUB-module association – SAGA complex compositions (Han *et al.* 2014). Interestingly, *sgf73Δ2A* complements *sgf73Δ* at elevated temperatures and is consistent with a Sgf73 SAGA independent function previously reported (Kim *et al.* 2019). Promoter bound Sgf73 is suggested to regulate whether canonical or non-canonical mRNA export occurs from a given gene. Even though *sgf73Δ2A* does not stably associate with SAGA *in vitro*, transient associations *in vivo* may still be possible and restore mRNA export regulation. Consistent with this, histone H2B-Ub has a prominent role in mRNP regulation (Vitaliano-Prunier *et al.* 2012) and *rad6Δ* is epistatic to *hfi1-L305P*. Further work will determine if *hfi1-L305P* and *sgf73Δ* are distinct *hht2* suppressors or if *in vivo hfi1-L305P* disrupts Sgf73 SAGA-independent mRNA export function. Interestingly, we previously shown

that *spt4* suppresses mRNA export mutants (Burckin *et al.* 2005). While previously tested SAGA mutants are synthetic lethal or very sick when combined with *spt5-242* (Quan and Hartzog 2010), *sgf73Δ* is a weak genetic suppressor of *spt5-242* (data not shown).

There is an interesting genetic relationship between *spt5*, *hht2*, and *chd1*. Both *chd1* and *hht2* were isolated as suppressors of transcription elongation defective *spt5-242* (Simic *et al.* 2003; Quan and Hartzog 2010). Here we show that *spt5-242* and *hht2* are mutual genetic suppressors and that *chd1* also suppresses *hht2* (Fig. 3-1, Fig. 3-3). Recent work has shown that yeast Spt5 has a histone H3-H4 binding domain in its N-terminus and this histone binding region is essential for yeast viability. However, the *spt5-242* mutation is not located in this region (Chapter 2). Spt5 physically interacts with Chd1 (Simic *et al.* 2003) and the *hht2* alleles may be acting as *chd1* bypass mutations which can explain why both *chd1* and *hht2* both suppress *spt5-242*. This cannot explain the *chd1 hht2* suppression and enhanced suppression in *spt5-242 chd1 hht2* cells (data not shown). The FACT subunit Spt16 may provide the missing link in our genetic suppression analysis.

We have previously shown that Spt5 physically interacts with Spt16 (Lindstrom) and Spt5 N-terminal fragments containing the histone binding region associate with FACT and histones *in vivo* (ZZ). Cryo-EM models of Spt5/pol II nucleosomal transcription with FACT or Chd1 show that FACT and Chd1 mutually exclude each other for binding the downstream nucleosome. *chd1* alleles which have *in vitro* nucleosome assembly – but no nucleosome sliding – activity show decreased *spt5-242* and *hht2* suppression. While no Chd1 nucleosome disassembly activity has been reported that enzymatic activity remains formally possible and the *in vitro* conditions and co-factors that remain to be identified – are present *in vivo*. The above biochemical interactions and our genetic interactions suggest that Spt5 collaborates with Spt16/Chd1 in nucleosome disassembly of the downstream nucleosome and nucleosome reassembly in the wake of RNA pol II. There is separation of function alleles of

both *pob3* and *spt16* in yeast FACT that have allele specificity with different histone mutations. The *pob3-Q308K* allele has hyper-active nucleosome reorganization activity but increased nucleosome retention compared to *POB3 in vitro*. Mutations to histone H4 that genetically suppress *pob3-Q308K* were identified and shown to decrease *pob3-Q308K* nucleosome retention. Interestingly, *hht2-L65I* was isolated as the sole histone H3 suppressor of *pob3-Q308K* and this histone H3 allele overlaps with our SHL2.5 *hht2* alleles that suppress *spt5-242*. Further, *hht2-L61W* is an allele that has increased Spt16 chromatin association and is synthetic lethal with *spt5-242* (Duina, personal communication). This implies that our *hht2* suppressors of *spt5-242* have decreased Spt16 association and our identification of *ubp10* as a genetic suppressor of *hht2* is consistent with this interpretation. Additionally, we have identified *spt16* genetic suppressors of *spt5-242* (Chapter 4) which is a prediction of the above model. The primary transcription elongation defect of *hht2* is suggested to be FACT/nucleosome disruption and that *spt5*, *chd1*, *ubp10*, *hfi1/sgf73* either restore FACT/H3 co-function or decrease the dependence on proper FACT/H3 interactions.

Figure 3-1 *hht2* suppressors have different suppression phenotypes

Serial dilution different *hht2* temperature-sensitive suppressors spotted different phenotype growth medium

(A) The *hht2* suppressors were originally identified based on the ability to restore growth at elevated temperatures. Photos for both plates are after 2 days of growth.

(B) Hydroxy-urea (H.U.), caffeine, or NaCl were added at the indicated concentrations for each respective plate. H.U. photos are after 2 days growth and both caffeine and NaCl are after 5 days growth.

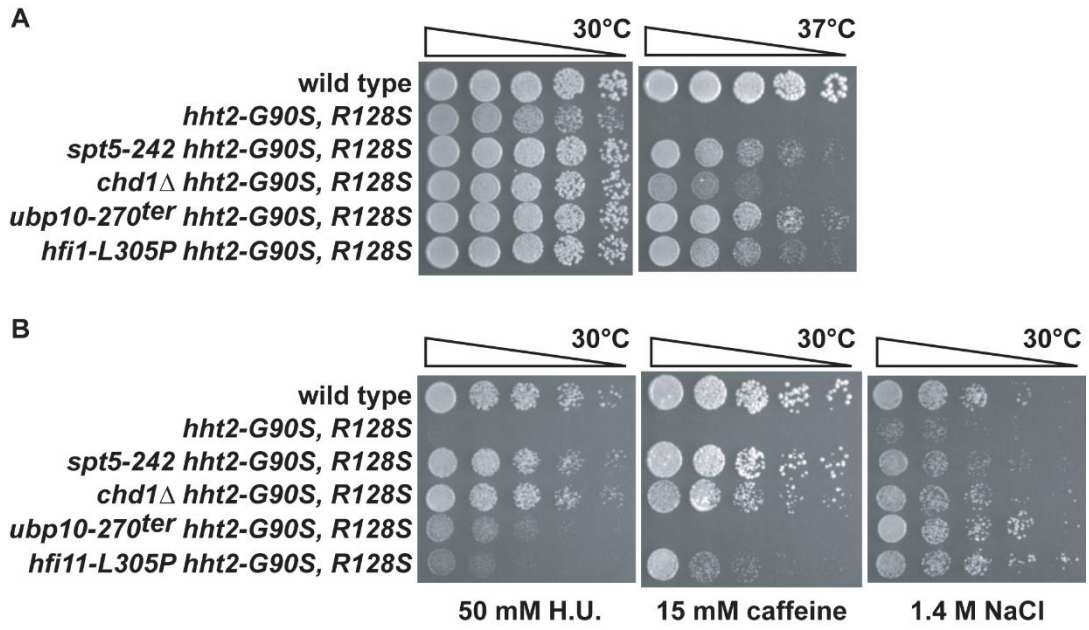


Figure 3-2 *hht2* depends on transcription elongation histone chaperone function for viability

The indicated *hht2* strains with the indicated histone chaperone, histone H3 HAT, and *hht2* suppressors were generated from different yeast crosses in the presence of pDM9 (*URA3 HHT1-HHF1* CEN) and spotted onto the indicated yeast media to supply wild type histone (sc-ura; pDM9) or only genomic *hht2* (5FOA) at the indicated growth temperature.

(A) Wild type histone H3 is essential for viability when mutant transcription elongation histone chaperones are combined with *hht2*. Sc-ura represents 3 days growth and 5FOA represents 2 days growth.

(B) Wild type histone H3 is not essential for viability when the replication-dependent complex *cac1Δ* mutant or loss of replication-coupled histone H3 HATs *gcn5Δ* or *rtt109Δ* are combined with *hht2*. Sc-ura represents 2 days of growth and 5FOA represents 3 days of growth.

(C) The addition of *hht2* suppressors does not strongly or reproducibly restore viability in *hht2 spt16-197* strains when wild type histone H3 is absent. Sc-ura represents 2 days of growth and 5FOA represents 3 days of growth.

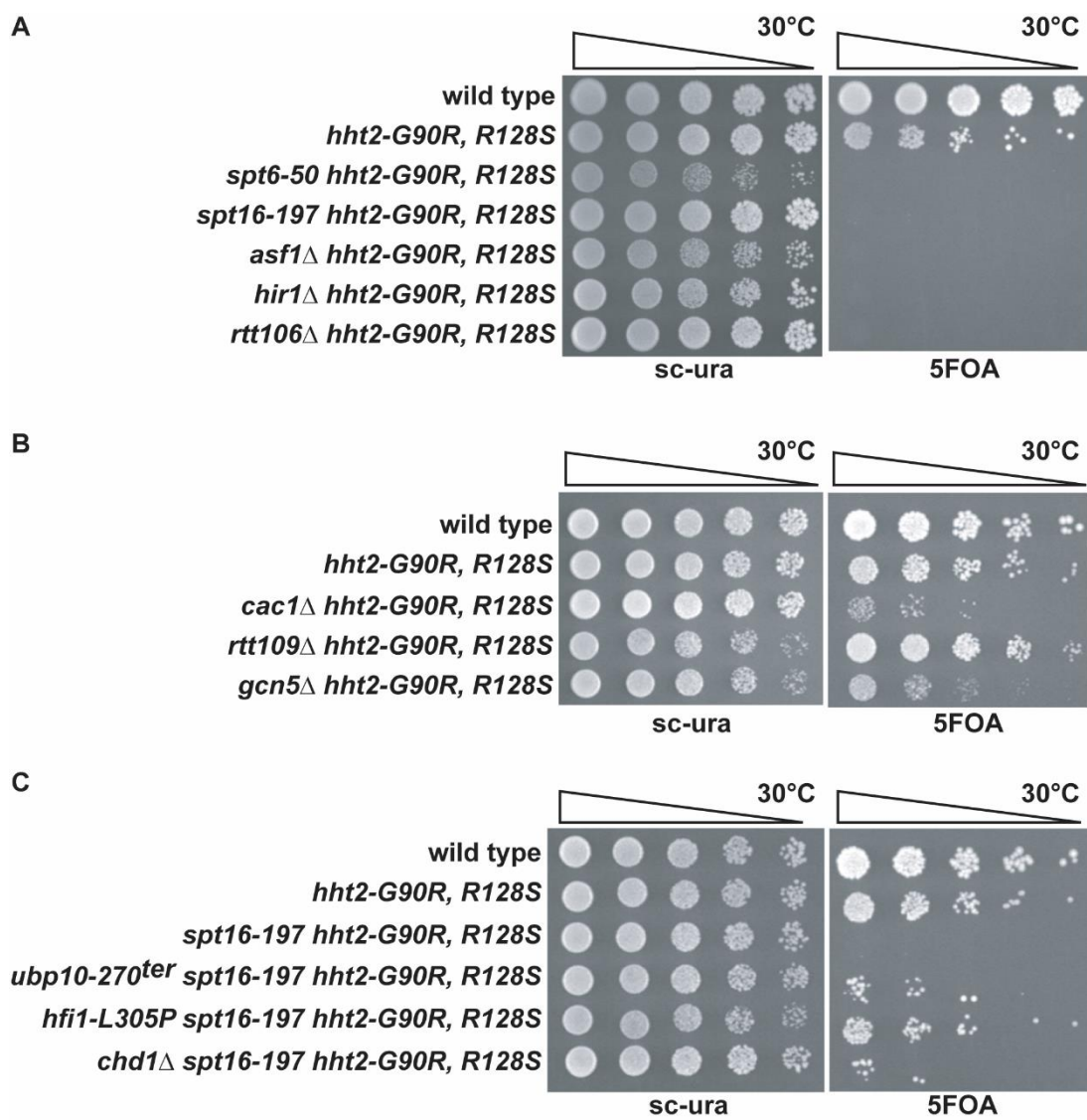


Figure 3-3 *chd1Δ* is epistatic to *rad6Δ* and *chd1* nucleosome assembly activity inhibits *chd1* phenotypes.

Yeast crosses were performed to generate the indicated genotypes and serially diluted onto the indicated growth media at the indicated temperatures.

(A) In the absence of wild type histone H3 (5FOA) *chd1Δ* is epistatic to *rad6Δ* in *hht2* suppression. The epistatic relationship does not depend on loss of *set1* or *dot1* function which act downstream of Rad6. Sc-ura represents 2 days growth and 5FOA represents 2 days of growth.

(B) Representation of *chd1-W932A* *in vitro* biochemical activity.

(C) The addition of nucleosome assembly activity decreases the strength of *chd1-W932A* chromatin disruption. *chd1-W932A* was integrated into the yeast genome and crossed with a strain carrying the cryptic initiation reporter. Sc-his + gal is growth conditions that measure cryptic initiation with this reporter and the photo represents 3 days of growth.

(D & E) Presumed Chd1 nucleosome assembly negatively regulates *hht2* (D) and *spt5* (E) *in vivo*. The photo in (D) represents 2 days of growth and the photo in (E) represents 3 days of growth.

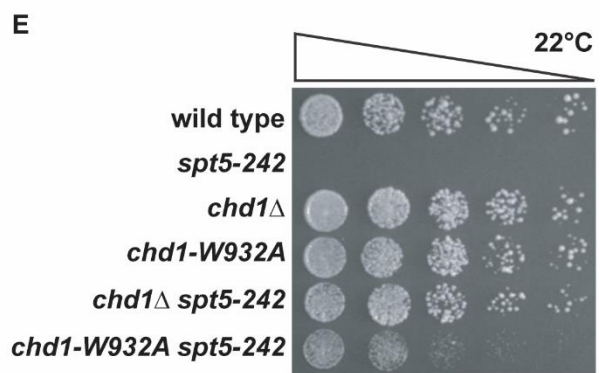
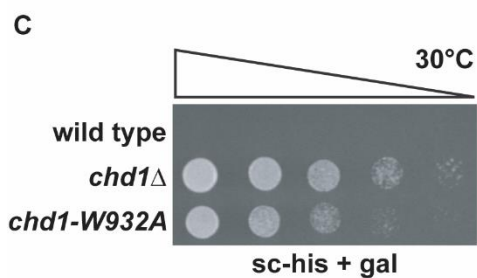
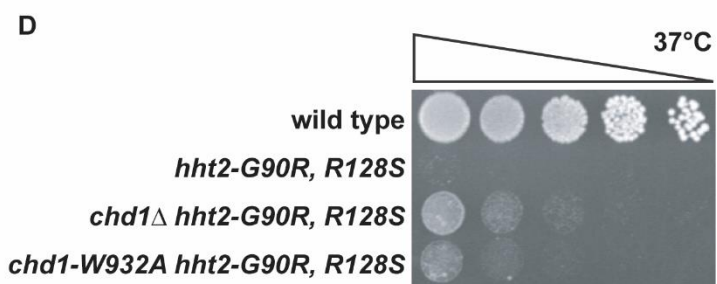
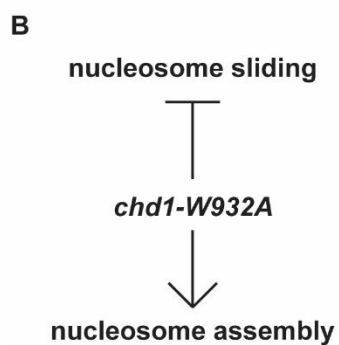
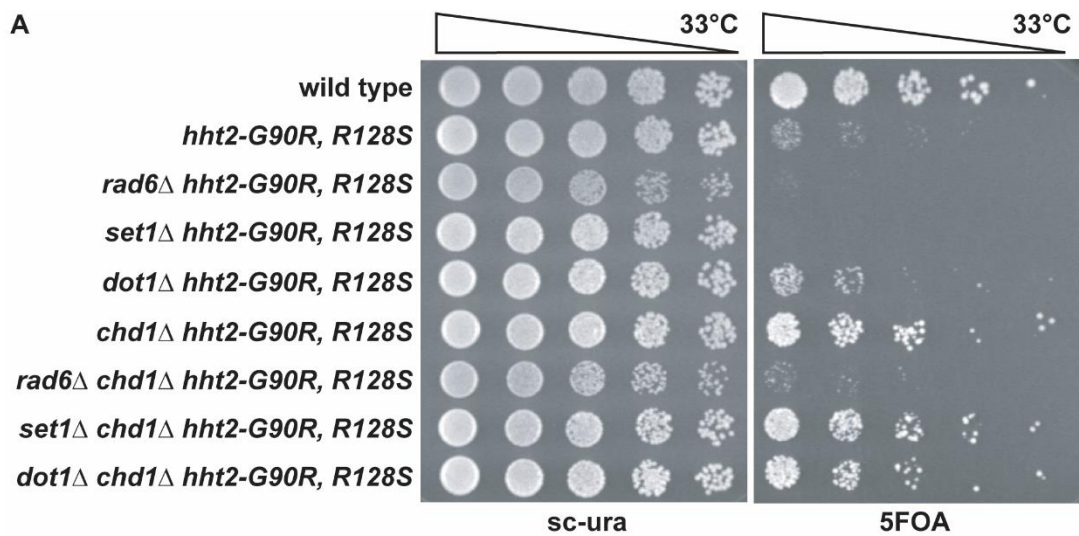


Figure 3-4 *hfi1* decreases and *ubp10* increases non-allelic *hht2* cryptic initiation phenotypes

Histone H3 shuffle strains (*hht1-hhf1* Δ *hht2-hhf2* Δ pGAL-FLO8-HIS3 + pDM9) in wild type*, *hfi1-L305P*, or *ubp10* Δ background were generated and the indicated plasmid born *hht2* mutant was transformed and wild type H3 (pDM9) was counter-selected against on 5FOA media before dilution spotting onto sc-his + gal at the indicated temperature to measure expression of the cryptic initiation reporter. *hfi1-L305P* and *ubp10* Δ represents 3.5 days of growth. * this data is from Chapter 2 and used as a point of reference for *hht2* cryptic initiation.

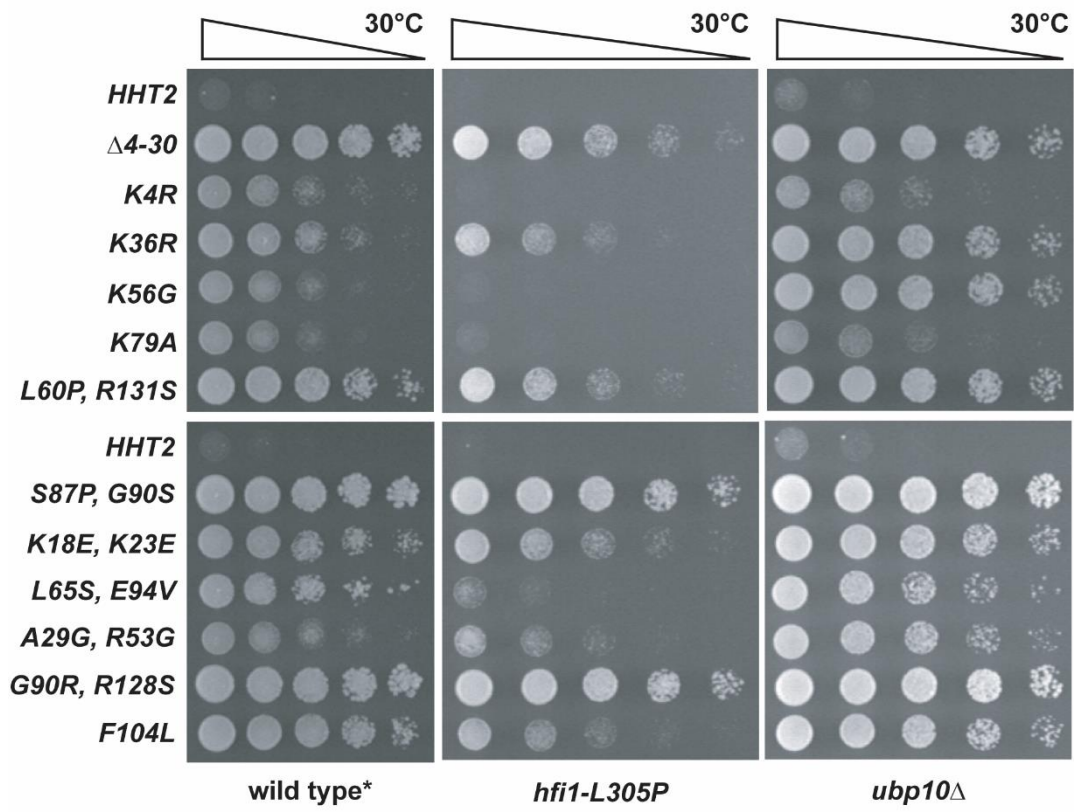


Figure 3-5 Ubp10 has multiple enzymatic targets that act in chromatin regulation

Ubp10 and not Ubp8 enzymatic activity negatively regulates *hht2* and Ubp10 has ubiquitinated targets from non-Rad6 E2-ubiquitin conjugation. The indicated strains were generated from yeast crosses or plasmid transformations and serially diluted, or replica plated to the indicated media and temperatures.

(A) *ubp10* and not *ubp8* suppresses the *hht2* temperature-sensitivity.

(B) Loss of catalytic *ubp10* function and not the inability to physically interact with Sir4 suppresses *hht2*. Only the catalytically inactive *ubp10-C371S* fails to complement *ubp10 hht2* suppression.

(C) Ubp10 has non-Rad6 ubiquitinated targets *in vivo*. Direct streak-outs of the indicated genotypes were replica plated to elevated growth temperatures and *hht2 ubp10 rad6* has an intermediate phenotype.

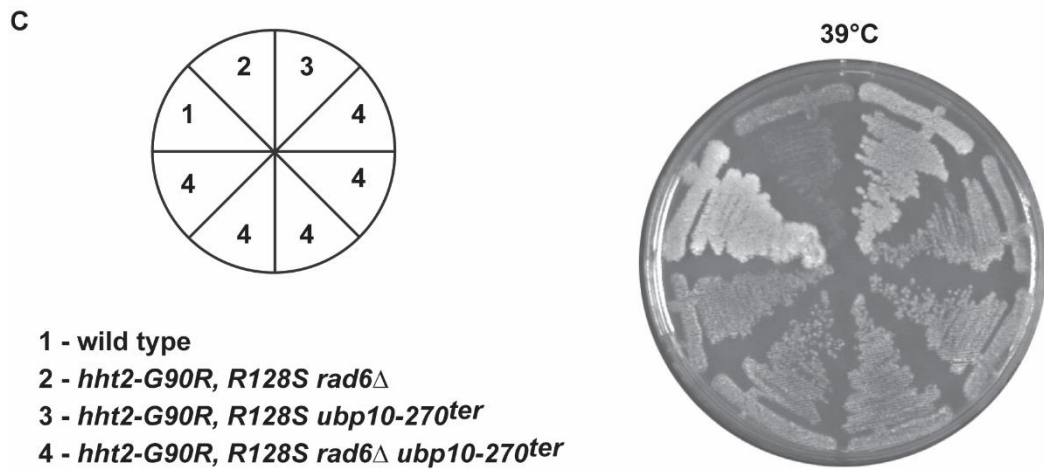
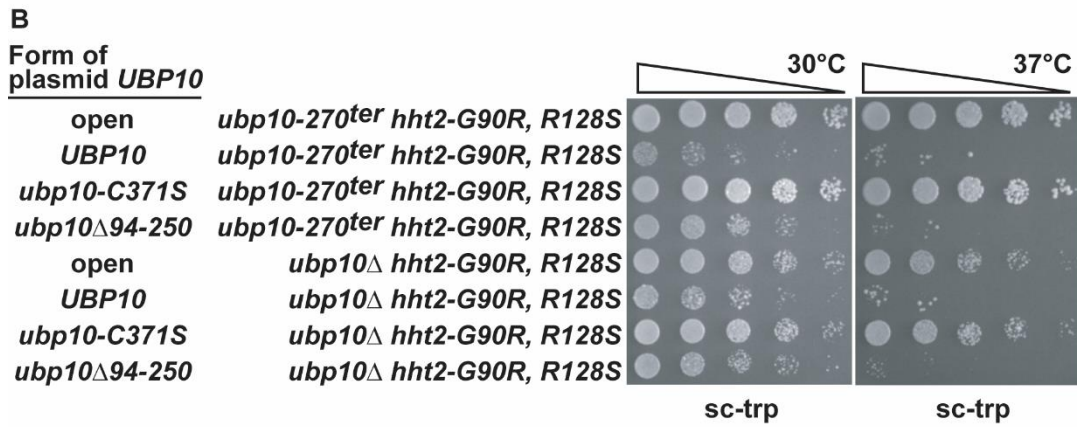
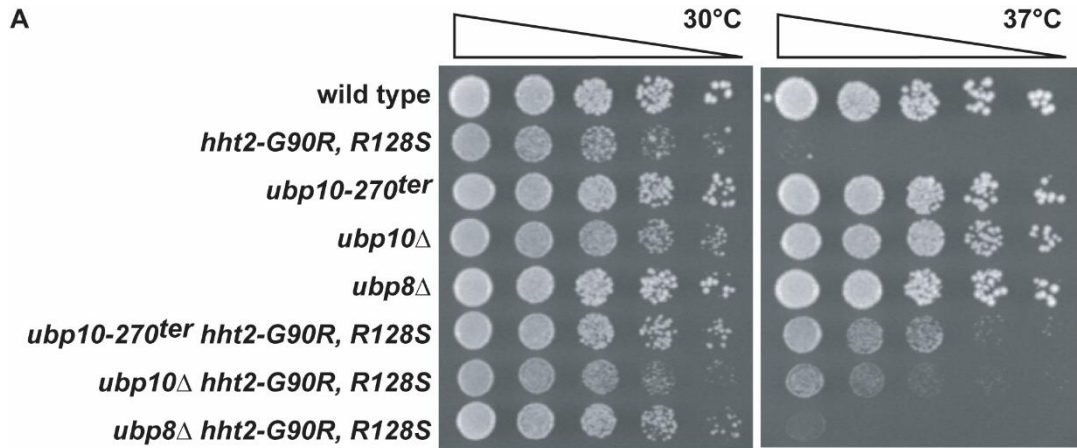


Figure 3-6 *hfi1* disrupts SAGA integrity and Sgf73 function

hfi1 and *sgf73* share similar phenotypes and SAGA complex disruptions, suggesting that *hfi1-L305P* functions as a *sgf73Δ* *in vivo*.

(A) *sgf73Δ* phenocopies *hfi1-L305P hht2* suppression. Strains were generated by crosses and the indicated strains were serially diluted on growth media at the indicated temperature for 3 days of growth.

(B) *hfi1-L305P* increases yeast replicative life span.

(C) SAGA complex composition is disrupted in *hfi1* cells. Spt7-TAP was used to purify SAGA and associated proteins and a fraction of purified protein was run out on an acrylamide gradient gel and then stained with Coomassie brilliant blue before silver staining. General locations of SAGA proteins in the gel are indicated.

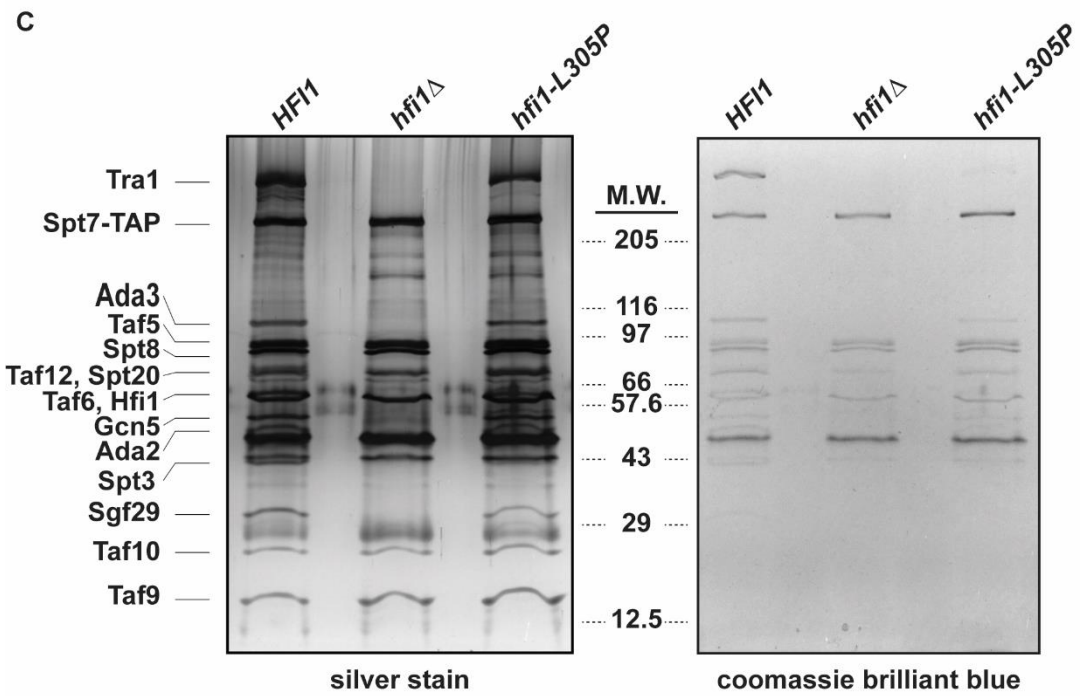
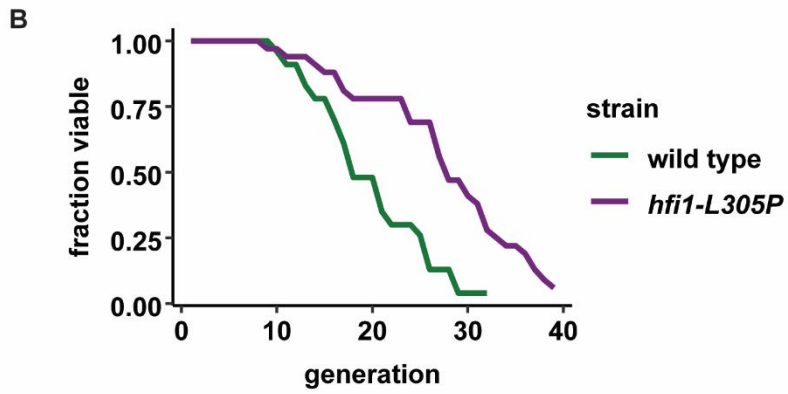
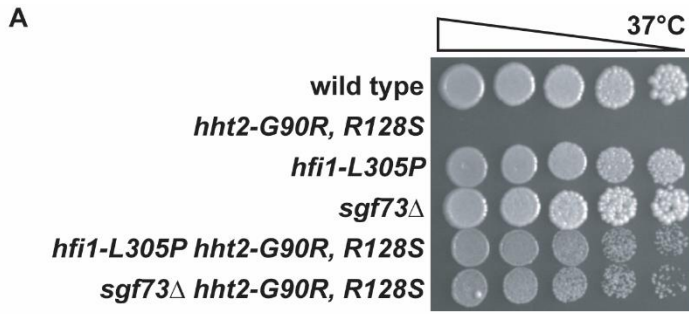


Table 3-1 Genetic characterization of SAGA functional domains

Double mutant strains between *hht2* and *saga* single mutants were generated with crosses and growth at 37°C is presented.

	wild type	HAT				DUB				TBP		core	
		<i>gcn5</i> Δ	<i>ada3</i> Δ	<i>sgf29</i> Δ	<i>ahc1</i> Δ	<i>ubp8</i> Δ	<i>sgf11</i> Δ	<i>sgf73</i> Δ	<i>sus1</i> Δ	<i>spt3</i> Δ	<i>spt8</i> Δ	<i>spt7</i> Δ	<i>hfi1</i> Δ
<i>hht2-G90R, R128S</i>	-	-	-	-	-	-	-	+/-	-	-	-	-	-

Table 3-2 Relative SAGA complex protein abundances purified from *hfi1* mutants

Spt7-TAP purified SAGA complexes in different *hfi1* strains were purified and associated protein abundance was determined with mass-spec. To qualitatively compare purified SAGA spectral counts were normalized to the level of Spt7-TAP (*).

		HFI1 spectral average	<i>hfi1</i> Δ / HFI1 %	<i>hfi1</i> -L305P / HFI1 %
HAT	Gcn5	371.5	7.32	50.07
	Ada2	326.5	4.90	56.76
	Ada3	741.5	3.34	48.39
	Sgf29	237	2.87	50.02
DUB	Ubp8	352	1.82	39.71
	Sgf73	400.5	1.40	41.93
	Sgf11	39.5	0.00	7.92
	Sus1	42	0.00	24.01
SPT	Tra1	2198.5	1.15	26.14
	Spt3	353	0.91	23.24
	Spt8	645	88.68	90.99
	Spt7	1624	100.00	100.00 *
	Spt20	759	98.85	82.22
	Hfi1	527	2.50	57.66
TAF	Taf5	1242.5	102.11	87.14
	Taf6	568.5	85.35	78.77
	Taf9	143	93.64	88.01
	Taf10	258	56.24	55.12
	Taf12	516.5	4.33	35.07

Figure 3-S1 Histone *h2b* has dominant phenotypes in *hht2*

Additional copies of plasmid borne histone H2B appear to have a dominant negative interaction with *hht2* and loss of histone H2B ubiquitination in *h2b-K123R* is even more severe. Dilution spots temperature growth conditions represent 2 days of growth.

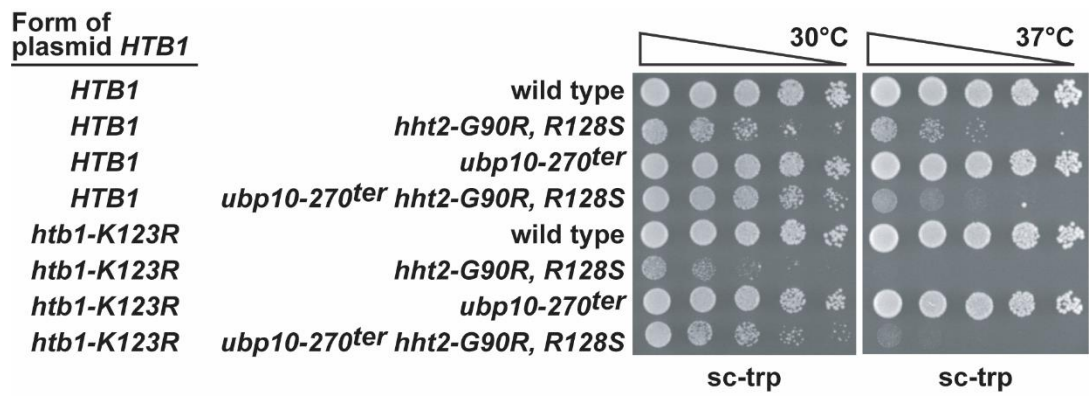


Figure 3-S2 Sgf73 has Ubp8 independent function that inhibits *hht2* growth

The indicated yeast strains were generated with crosses and then serially diluted to growth media at the indicated temperature for 2 days.

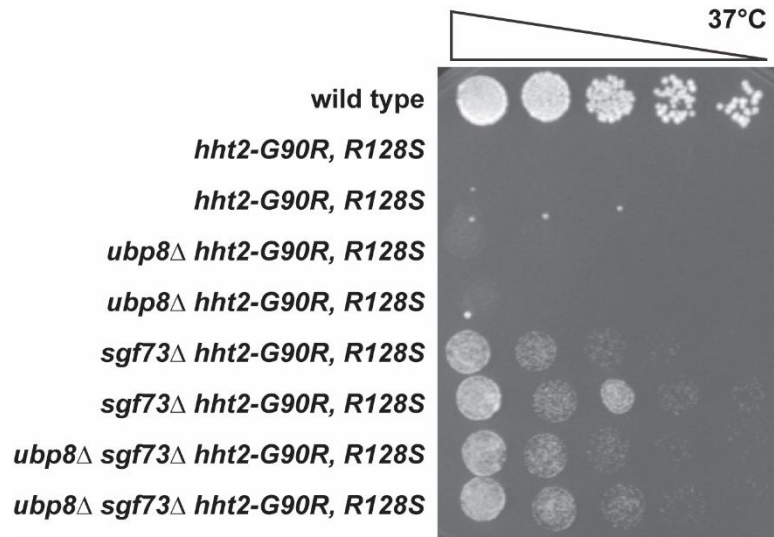


Figure 3-S3 *sgf73* that fails to associate with SAGA displays incomplete suppression of *hht2*.

hht2 sgf73Δ strains were transformed with different plasmids that did or did not contain previously characterized *sgf73* alleles. The transformants were directly struck out to growth media at 37°C for 2 days or 39°C for 4 days.

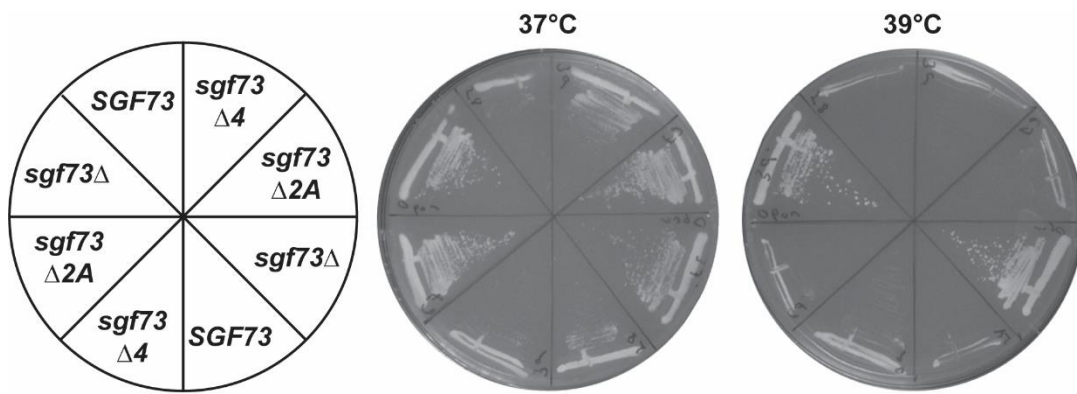


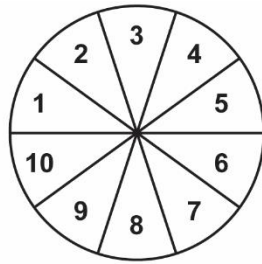
Figure 3-S4 Epistatic relationships between the SAGA HAT-module and *hht2* suppressors

The indicated genotypes were generated by yeast crosses and were directly struck out to the indicated growth temperature (A) or subsequently replica plated to elevated temperatures (B) after sufficient growth at 30°C.

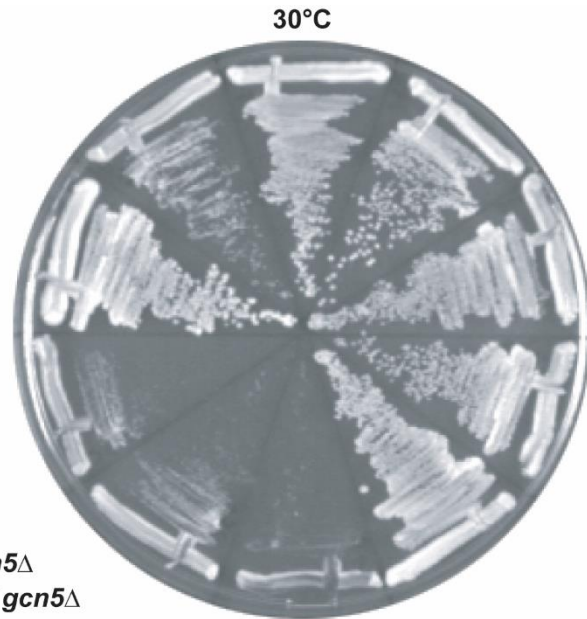
(A) *gcn5* is epistatic to both *hfi1-L305P* and *ubp10-270^{ter}* in *hht2* strains. The direct streak-out represents 2 days growth.

(B) *ada3* is epistatic to *hfi1-L305P* and decreases but does not eliminate *ubp10-270^{ter} hht2* suppression. The replica-plating represents 2 days growth.

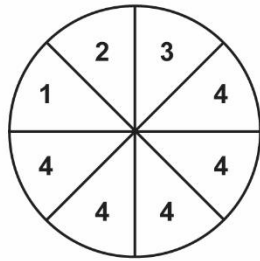
A



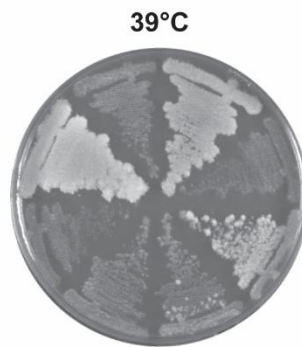
- 1 - wild type
- 2 - *hht2-G90R, R128S*
- 3 - *hfi1-L305P*
- 4 - *ubp10-270^{ter}*
- 5 - *gcn5 Δ*
- 6 - *hht2-G90R, R128S hfi1-L305P*
- 7 - *hht2-G90R, R128S ubp10-270^{ter}*
- 8 - *hht2-G90R, R128S gcn5 Δ*
- 9 - *hht2-G90R, R128S hfi1-L305P gcn5 Δ*
- 10 - *hht2-G90R, R128S ubp10-270^{ter} gcn5 Δ*



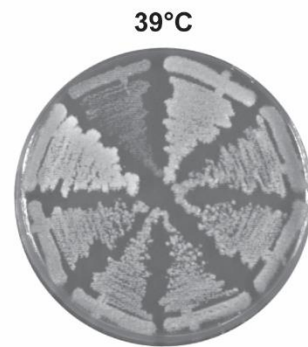
B



- 1 - wild type
- 2 - *hht2-G90R, R128S ada3 Δ*
- 3 - *hht2-G90R, R128S hht2-supp*
- 4 - *hht2-G90R, R128S hht2-supp ada3 Δ*



hfi1-L305P



ubp10-270^{ter}

Chapter 4

Concluding remarks

Spt5 aids transcription through nucleosomes *in vitro* (Crickard *et al.* 2017; Ehara *et al.* 2019; Farnung *et al.* 2021) and binds to histone H3 and H4 *in vivo* (Evrin *et al.* 2022). However, a role for Spt5 in facilitating nucleosomal transcription *in vivo* was uncertain. The *spt5-242* allele has a transcription elongation defect (Quan and Hartzog 2010), depends on TFIIIS for viability during constitutive growth (Hartzog *et al.* 1998), and interacts with chromatin regulators (Squazzo *et al.* 2002; Lindstrom *et al.* 2003; Simic *et al.* 2003; Quan and Hartzog 2010). In Chapter 2 we present a large body of work that supports a model for Spt5 promoting transcription through nucleosomes *in vivo*.

Nucleosomes that are predicted to be thermodynamically stable pose a specific challenge to elongating RNA polymerase II when *spt5* is defective. When we mapped nucleosomes genome wide in *hht2-S87P*, *G90R* mutant yeast, nucleosomes appeared to be selectively lost at the 3' ends of transcribed genes, and the extent of this loss was proportional to gene length. A 3' end nucleosome occupancy defect has been previously reported in FACT complex mutants (McCullough *et al.* 2019), but the authors did not comment on how gene length contributed to the reported phenotype. We considered three models that could explain our genome wide 3' occupancy defect. By restricting our analysis of nucleosome loss to genes that do not display cryptic transcription when chromatin is disrupted, we ruled out internal transcription at the 3' ends of genes. Using single molecule analysis of the *PHO5* gene, we asked if nucleosome loss in our *hht2-* is necessarily restricted to the 3' end of the gene. We found that nucleosomes can be lost throughout the gene body of actively transcribed, but not repressed, full length *PHO5* single gene molecules. Analysis of the predicted free energy of nucleosome formation across the *PHO5* gene (Heijden *et al.* 2012) demonstrated that the positions of nucleosome loss over the transcribed

PHO5 gene body correspond with positions of increased nucleosome stability. When we applied this free energy of nucleosomes formation model genome wide, we observed that *h3* nucleosomes occupancy was also lost at stable sequences.

Why does selective loss of stable nucleosomes suppress *spt5-242*? With respect to nucleosomes being physical protein barriers to transcription elongation by RNA pol II a rational argument can be made. Stable nucleosomes take more energy to unwrap than less stable nucleosomes and when Spt5 is defective, the energy penalty becomes too large to overcome. However, it is not obvious why stable nucleosomes are selectively lost from *hht2-S87P*, *G90S*. The mutated residues are solvent exposed and do not make direct contact with DNA or other histones but may directly perturb nucleosome stability in a manner we have yet to test. Interestingly, the nucleosome SHL2.5 functionally interacts with chromatin remodelers (Zofall *et al.* 2006; Gangaraju *et al.* 2009; Hada *et al.* 2019). Something about SHL2.5 and Blaine Bartholomew's working showing remodeler interactions at that location? Yeast have a RSC chromatin remodeler subtype that selectively remodels partially unwrapped nucleosomes (Schlichter *et al.* 2020). This RSC subtype also ejects nucleosomes when they are slid over DNA sequences predicted to form more stable nucleosomes (Schlichter *et al.* 2020). Thus, it is possible that our mutations make nucleosomes more susceptible to ejection by RSC. Among our histone *h3* suppressors of *spt5-242* are alleles that alter residues in the N-terminal alpha-helix of histone H3. Mutations in this alpha-helix are predicted to disrupt nucleosome wrapping and have been shown to increase the activity of several chromatin remodelers and RSC (Somers and Owen-Hughes 2009; Chatterjee *et al.* 2011). Thus, it may be that our *h3* mutations create a more permissive environment for RSC chromatin remodeling which leads to suppression of defective *spt5* function during transcription elongation.

Genetic analysis of the extragenic suppressors of the *h3* temperature-sensitivity phenotype is also consistent with *h3* mutants altering RSC function. Gcn5 is part of the HAT-

module of SAGA and targets histone H3 for acetylation (Tse *et al.* 1998 ; Kuo and Andrews 2013). RSC has increased binding affinity to acetylated nucleosomes and Gcn5 also acetylates and regulates RSC function (Kasten *et al.* 2004; Carey *et al.* 2006; VanDemark *et al.* 2007). Interestingly, disruption of *gcn5* or its associated proteins *ada3* and *sgf29* is an enhancer of *h3* growth defects. This may be explained by loss of HAT-independent acetylation (Kim *et al.* 2010; Downey *et al.* 2015; Rössl *et al.* 2019). We identified a *hfi1* allele that disrupts global SAGA function and appears to be phenotypically like a *sgf73* null. Through decreased global SAGA activity in *hfi1* or decreased HAT-module function in *sgf73Δ* (Shukla *et al.* 2006; Han *et al.* 2014) there would be decreased general RSC activity over transcribed gene bodies in *h3* cells. We also *ubp10* as a genetic suppressor of *h3*. Curiously, mutations of *UBP8*, which encodes a histone deubiquitinase that associates with SAGA, did not suppress the *h3* mutation. Histone H2B ubiquitination (H2B-Ub) has been shown to oppose RSC function over promoters in *S. pombe* (Materne *et al.* 2016) and H2B-Ub is predicted to sterically clash with RSC in nucleosome bound RSC cryo-EM models (Ye *et al.* 2019; Patel *et al.* 2019). A detailed *in vitro* study on Rad6/Bre1 mediated H2B-Ub and RSC function has yet to be reported, though. Interestingly, *rad6* mutations are epistatic to *hfi1* and *ubp10* in *h3* genetic interactions. H2B-Ub has a documented role in FACT nucleosome mediated reassembly (Fleming *et al.* 2008) and promoting *in vitro* nucleosomal transcription elongation (Pavri *et al.* 2006). This suggests that the *rad6* epistasis is due to the loss of FACT function in *h3* cells.

The *h3* alleles that disrupt SHL2.5 depend upon the function of several histone chaperones for viability. This suggests that these *h3* alleles are disrupting nucleosome dynamics *in vivo*. There is broad functional redundancy between histone chaperones, and we have not systematically tested our *h3* mutants for specific defects in H3-chaperone binding. However, yeast histone 'isoforms' that look histone H3.3 (yH3.3) or H3.1 (yH3.1) are both viable and display no growth defects. Interestingly, yH3.3 has a cryptic initiation phenotype

and genetically suppresses *spt5-242* while yH3.1 does not have a cryptic initiation phenotype and is synthetic lethal with *spt5-242*. Consistent with this, *hir* complex mutations are also synthetic lethal with *spt5-242*. We have yet to identify *hir* or *asf1* mutations that may act to phenocopy a replication-independent nucleosome assembly proficient yH3.3 (Song *et al.* 2013). This may be due to the observation that yeast Hpc2 would be predicted to discriminate yH3.1/yH3.3 (Ricketts *et al.* 2015). Altered Asf1/Hir complex function in yH3.3 and yH3.1 cells would be from physical interactions with Hpc2 and not the other associated complex proteins.

FACT directly interacts with all 4 core histones and can both disassemble and reassemble nucleosomes (Kemble *et al.* 2015; McCullough *et al.* 2015, 2018; Valieva *et al.* 2016; Sivkina *et al.* 2022). Interestingly, *spt16-197* has a strong chromatin disruption phenotype does not genetically interact with *spt5-242*. Given that our chromatin suppressors of *spt5-242* have a chromatin disruption phenotype, this suggesting that there are specific chromatin transactions that are defective in *spt5-242*. The *h3-L61W* allele was identified as a cold-sensitive histone mutation and was demonstrated to increase the associate of Spt16, a FACT subunit, with chromatin. This histone mutation when combined with *spt5-242* leads to synthetic lethality, suggesting Spt16 chromatin association is defective in *spt5-242*. Histone mutations that suppress *fact* phenotypes (McCullough *et al.* 2013), alter Spt2/Spt6/Sp16 genomic occupancies (Hainer and Martens 2016), and are defective in in transcription-coupled nucleosome occupancy (Hainer and Martens 2011). Our histone mutations that suppress *spt5-242* (SHL2.5, N-terminal alpha helix) may be also disrupting FACT function. The H3 L61 residue is adjacent to SHL2.5 and the N-terminal alpha helix and both *fact* and *h3* mutants have nucleosome occupancy defects that can scale with gene length (data not shown). Nucleosomes are dynamic structures and artificially making the nucleosome more rigid alters chromatin remodeling outcomes (Sinha *et al.* 2017). Further work will be needed to determine if our *h3* mutations disrupt the mechanics of FACT function. FACT does not

require ATP to disrupt the nucleosome structure (Sivkina *et al.* 2022). It is interesting to speculate that our SHL2.5 *h3* alter FACT's ability to unwrap or rewrap nucleosome DNA.

The poorly characterized N-terminus of Spt5 is likely to facilitate nucleosomal transactions during transcription elongation. This region of the protein has yet to be unambiguously imaged by cryo-EM or x-ray crystallography (Bernecky *et al.* 2017; Vos *et al.* 2018; Ehara *et al.* 2019; Farnung *et al.* 2021; Žumer *et al.* 2021). Recent work has demonstrated that residues in the acidic Spt5 N-terminus bind histone H3 and H4 (Evrin *et al.* 2022), but are dispensable for transcription elongation through nucleosomes *in vivo*. However, this Spt5 H3-H4 binding region is necessary for viability and mutations that disrupt it cause nucleosome loss during transcription elongation. In chapter 2, we identified the unstructured NGN-Proximal Region (NPR) of Spt5 that is sensitive to chromatin disruption phenotypes and contains the *spt5-242* allele. AlphaFold predicts that the NPR is structured in many organisms. Further, we have independently identified the NPR as a region that harbors intra-molecular *spt5* suppressors of *spt5-242*. This region is likely to be dynamic and we predict that Spt5-242 protein, which alters a single amino acid in the NPR, is delayed or stuck in specific state(s) during nucleosomal transcription elongation.

Our previous work demonstrated that *spt5-242* suppressors fall in two mechanistic classes: mutations that decrease transcription elongation rate and mutations that alter chromatin. By decreasing the transcription elongation rate, *spt5-242* may not enter non-productive structural states or it gives the transcription elongation apparatus time to rectify any stalled complex. Analysis of our *h3* suppressors of *spt5-242* suggests that RSC and/or FACT have defective function in *spt5-242*. Physical interaction between RSC and Spt5 has not been reported, but RSC does function to remodel and promote transcription elongation (Biernat *et al.* 2021). We have previously reported that Spt16 physically interacts with Spt5 (Lindstrom *et al.* 2003) and Spt5 H3-H4 interaction occurs with Spt16 (Evrin *et al.* 2022). The work presented in this thesis suggests that Spt5 facilitates transcription through stable

nucleosomes via RSC and/or FACT. How Spt5 coordinates nucleosome reassembly and if transcribed nucleosomes are treated the same remain important questions, which, we now have identified key proteins for future study.

Appendix – 1

A genetic model for Spt5/Spt6/Spt16 nucleosomal transcription elongation

Results

One main prediction of the model that Spt5 mediates chromatin transactions is that Spt5 has histone chaperone activity and/or collaborates with histone chaperones during transcription elongation. A recent study has reported that a Spt5 N-terminal region can bind histones H3 and H4 and is essential for viability in yeast. However, mutations to this region that prevent *spt5* histone binding does not prevent RNA pol II transcription elongation. This *spt5* mutation does result in nucleosome loss over transcribed gene bodies, though. Spt5 has an apparent function in nucleosome reassembly during transcription elongation and not nucleosome disassembly ahead of RNA pol II. Histone chaperones then must disassemble or bypass the downstream nucleosomal barrier to RNA pol II and Spt5 coordinates these histone chaperones during nucleosome reassembly in the wake of RNA pol II.

Which histone chaperones disassemble or bypass nucleosomes ahead of RNA pol II? Histone chaperone function is highly redundant *in vivo*, and more than one histone chaperone may disassemble nucleosomes ahead of pol II. In yeast the Hir, Spt16/Pob3/Nhp6 (FACT), Spt6/Spn1 complexes and single the individual Nap1, Rtt106, Spt2, and Vps75 proteins are histone chaperones that function during transcription elongation.

Overexpression of Spt2 rescues *spt5-242*

In chapter 2 we reported that the yH3.1 histone isoform has a synthetic lethal interaction with *spt5-242*. This allele is predicted to not physically interact with the Hir complex which functions in replication-independent nucleosome assembly. Consistent with this, single deletions of each *hir* complex member are also synthetic lethal with *spt5-242*. Importantly, *hir1Δ yH3.1* strains are viable. This suggests that yH3.1 is recognized by other

histone chaperones *in vivo*. *yH3.1* dominantly interacts with *spt5-242*. The presence of wild type histone H3 in *HHT1-HHF1 yH3.1 spt5-242* still results in synthetic lethality (Table A1-1). This gave us an opportunity to take an unbiased approach to screen for 2 μ plasmid suppressors from a genomic library. If *yH3.1* is disrupting physical interactions between some protein X and *spt5-242*, over-expression of that target protein may restore functional physical interactions by mass-action, or we may identify proteins which bypass the need for *spt5-242* to interact with protein X. As a control we first crossed *yH3.1 spt5-242* to known suppressors of *spt5-242* to test whether it is possible to rescue *yH3.1 spt5-242* synthetic lethality. From a representative set of original *spt5-242* suppressors we can rescue *yH3.1 spt5-242* synthetic lethality (Table A1-1). We further crossed the *yH3.1 spt5-242 set2 Δ* triple mutant to determine if the *set2* suppression is due to hyperacetylation of the present wild type histone H3 or not. When just *yH3.1* is present, *set2* still rescues synthetic lethality between *yH3.1* and *spt5-242* (Table A1-1). The less severe *HHT1-HHF1 yH3.1 spt5-242* strain was used for the 2 μ plasmid screen to increase the chance of identifying candidates.

Overexpression of *SPT2* was the only identified and confirmed candidate that rescued *HHT1-HHF1 yH3.1 spt5-242* synthetic lethality. *Spt2* is a HMG-like protein and *spt2 Δ* genetically interacts with many transcription elongation factors (Nourani *et al.* 2006). Crystal structures have been solved of a truncated human *Spt2* that binds to the (H3-H4)₂ histone tetramer and alterations to this binding surface in yeast *spt2* causes cryptic transcription and increased histone turnover (Chen *et al.* 2015). Overexpression of *SPT2* can suppress *spt5-242* cold-sensitive growth and suppress *spt5-242* cryptic initiation (Fig A1-1). Interestingly, increased levels of *SPT2* on its own has a cryptic initiation phenotype. The mutual cryptic initiation suppression in 2 μ *SPT2 spt5-242* may be due to compensatory changes on nucleosome reassembly or some other mechanism.

SPT2 is not an essential gene and therefore cannot be the primary histone chaperone that disassembles nucleosomes ahead of RNA pol II during transcription elongation. Spt2 physically interacts with Spt6 (Bhat *et al.* 2013). During transcription elongation, disruption of *spt6* function reduces Spt2 chromatin association and disruption of *spt2* function reduces Spt6 chromatin association (Nourani *et al.* 2006; Thebault *et al.* 2011). Spt6 is essential for life in budding yeast and may be the missing link that connects nucleosome disassembly ahead of RNA pol II with Spt5 mediated nucleosome reassembly. However, Spt6 is not essential for life in fission yeast (Kiely *et al.* 2011). Fission yeast with *spt6Δ* are extremely sick and the decreased dependence on Spt6 function may be organismal specific. Given this and our 2μ *SPT2* result, we went ahead and screened for *spt6* suppressors of *spt5-242*.

Dominant *SPT6* suppressors of *spt5-242*

First, we tested for genetic interactions between previously characterized *spt6* alleles and *spt5-242*. The different *spt6* alleles have overlapping and distinct phenotypes (Clark-Adams and Winston 1987; Swanson and Winston 1992; Kaplan *et al.* 2005; Diebold *et al.* 2010b). The two alleles which are synthetic lethal in combination with *spt5-242* (Table A1-2) have distinct phenotypes in 3' mRNA processing (*spt6-14*) or are predicted to greatly decrease RNA pol II binding (*spt6-50*). While *spt6-140* does have chromatin disruption phenotypes it has a neutral genetic interaction with *spt5-242*. As Spt6 is a large protein that functions in many transcriptional processes, the region that positively interacts with *spt5-242* likely not represented in the previously characterized *spt6* alleles and a new *spt6* screen should be done.

From our screen to identify *spt6* suppressors of *spt5-242* we found and characterized six candidates. The bulk of the *spt6* alleles fall within the acidic N-terminus of Spt6 and the last candidate is an amino acid deletion between the HhH and DLD domain (Figure A1-2A).

In the acidic N-terminus there is a small region that binds the histone chaperone Spn1 (Diebold *et al.* 2010a; McDonald *et al.* 2010). This region of Spt6 is critical for *in vitro* nucleosome binding and the presence of Spn1 inhibits Spt6/nucleosome binding (McDonald *et al.* 2010). Interestingly, the *spt6-YW* allele disrupts Spt6/lws1 binding (Diebold *et al.* 2010a) and *spt6-YW* has been reported to suppress the cold-sensitive phenotype of *spt5-242* (Viktorovskaya *et al.* 2021). This suggests that our *spt6* alleles in this region may be behaving similarly. Spt6 is heavily phosphorylated by the Casein Kinase 2 (CK2) complex at serine residues in the acidic N-terminus (Gouot *et al.* 2018; Dronamraju *et al.* 2018). The phosphorylation state affects both Spn1 and Spt2 binding to Spt6 (Bhat *et al.* 2013; Dronamraju *et al.* 2018). Dephosphorylated Spt6 associates with Spt2 *in vitro* and Spt6 phosphorylation by CK2 releases Spt6 (Bhat *et al.* 2013). When phosphorylated, Spt6 interaction with Spn1 is strongly stabilized and both *spt6* phosphomimetic (S to E) and hypomimetic (S to A) disrupt chromatin function (Gouot *et al.* 2018; Dronamraju *et al.* 2018). As many of our *spt6* alleles are predicted to disrupt Spn1 binding, and one is a known CK2 target (S206) we determined if they also have a cryptic initiation phenotype. Surprisingly the *spt6* allele in the Spn1 binding region failed to display a cryptic initiation phenotype, *S206F* has a mild phenotype, and *D1017Δ* also has no phenotype (Fig. A1-2B). All our known suppressors of *spt5-242* have a cryptic initiation phenotype. Determining whether chromatin disruption is necessary for suppression of *spt5-242*, if this reporter is not sensitive enough, or we are observing gene-dependent effects will require future work.

During our initial characterization of our isolated *spt6* mutations we noticed that many were dominant suppressors of *spt5-242*. We performed a dominance test by expressing the *spt6* suppressors on a CEN marked plasmid over genomic *SPT6* in *spt5-242* strain with the *FLO8-HIS3* cryptic initiation reporter. Interestingly, the addition of an extra wild type *SPT6* plasmid makes *spt5-242* sicker (Fig. A1-3A). All *spt6* mutants restore cold-sensitive growth and *D197H* and *D243N* suppress the strongest. Surprisingly, most *spt6* mutants also restore

suppression of cryptic initiation that is un-correlated with cold-sensitive suppression and *D1017Δ* enhances the *spt5-242* cryptic initiation phenotype (Fig. A1-3B). It remains to be tested whether the mutual suppression of the cryptic initiation phenotype in *spt6 spt5* strains is related to our Spt2 results.

If the observation that Spt6 is dispensable for viability in fission yeast is not a fission yeast artifact, then a different histone chaperone is the main target for nucleosome disassembly ahead of RNA pol II during transcription elongation. It may be that the dominant phenotype of the *spt6* suppressors is bypassing some function of this to be determined histone chaperon in *spt5-242* cells. We have previously shown that Spt5 physically interacts with both Spt6 and Spt16 (Lindstrom *et al.* 2003). In yeast Spt16 associates with Pob3 and NHP6 to form FACT. FACT was originally identified for its biochemical activity to promote RNA pol II transcription through nucleosomes *in vitro* (Orphanides *et al.* 1998). Subsequent work from many groups have established FACT's ability to disassemble, reassemble, and alter nucleosome states both *in vitro* and *in vivo*. Like Spt6, Spt16 is a modular protein and the well-studied *spt16-197* (G132D) allele has a neutral genetic interaction with *spt5-242*.

Genetic evidence for disrupted *spt5/spt16* function

We performed a plasmid *spt16* mutagenesis screen to identify *spt16* alleles that suppress *spt5-242*. All the candidates that we isolated were single mutations in the Mid domain of Spt16 (Fig A1-4A). Crystal structures of the human FACT Mid-domain engaging the histone (H3-H4)₂ tetramer have been solved as well as a cryo-EM model of human FACT engaging with the nucleosome (Tsunaka *et al.* 2016; Liu *et al.* 2020). A cryo-EM model has been determined for FACT engagement with the nucleosome during transcription elongation (Farnung *et al.* 2021). The *spt16* suppressors of *spt5-242* mostly cluster in a long alpha-helix & unstructured region that can interact with the nucleosomal surface adjacent to SHL2.5 (Fig. A1-4B). The potential physical overlap between *hht2* alleles that suppress *spt5-242* and the

spt16 alleles is apparent when looking at mapped mutations relative to the proximal histone H3 in the engaged nucleosome (Fig. A1-4B). While the *hht2* alleles in the distal histone H3 appear to not be engaging with Spt16, *hht2-R49A* can contact a region of Spt16 (Fig. A1-4B).

The Mid-domain of Spt16 functions in transcription-coupled nucleosome occupancy and Spt16 release from chromatin *in vivo*. *hht2-L61W* is a cold-sensitive mutation that increase Spt16 chromatin association (Duina and Winston 2004; Duina *et al.* 2007). *spt16* mutations in the Mid-domain suppress *hht2-L61W* cold-sensitivity and decrease Spt16 chromatin association (Duina *et al.* 2007; Myers *et al.* 2011). Transcription from the *SRG1* promoter represses *SER3* and defective transcription-coupled nucleosome assembly activates *SER3* (Martens *et al.* 2004; Thebault *et al.* 2011 p. 2; Hainer and Martens 2011; Pruneski *et al.* 2011). A screen for *spt16* alleles that activated a *SER3-HIS3* reporter identified many mutations in the Mid-domain (Hainer *et al.* 2012). The *spt16 hht2-L61W* suppressors are distinct from *spt16 SER3* alleles, no *spt16 SER3* allele suppressed *hht2-L61W* cold-sensitivity (Hainer *et al.* 2012). Interestingly, *spt16-D787N* and *spt16-E790D* suppress *hht2-L61W* and were independently identified as *spt5-242* suppressors.

spt5-252 and *hht2-L61W* have overlapping phenotypes and *spt5-242 hht2-L61W* double mutants are inviable (Table A1-3). This suggests that Spt5 and histone H3 are making independent physical interactions with Spt16. Spt6 and Spt16 have many overlapping and collaborative chromatin functions *in vivo* (Jeronimo *et al.* 2015, 2019; McCullough *et al.* 2015; Viktorovskaya *et al.* 2021). When *spt5*, *h3*, *spt16* is defective, presumed loss of *spt6/pol II* association is synthetically lethal; when *spt16* has chromatin association defects it can rescue *spt5* and *h3* mutations (Table A1-4). The histone H3 residues that are distinct between *yH3.1* and *yH3.3* are in proximity to H3-L61 and may also be augmenting Spt16 function or chromatin association (Fig. A1-5).

Intramolecular suppression of *spt5-242*

Spt5 is a large multi-domain protein, and it remains possible that the different Spt5 domains cooperate *in vivo*. We tested the hypothesis that *spt5* is stuck in a physical conformation by screening for intramolecular (I.M.) suppressors of *spt5-242* (A268V) cold-sensitivity. Surprisingly, all the I.M. suppressors are near A268V and not in the KOW domains or the CTR, which would be predicted for locked long-range structural states (Fig. A1-6A). In addition to cold-sensitive suppression, the I.M. suppressors restore repression of cryptic initiation (Fig. A1-6B). This suggests that chromatin function is restored in *spt5*. TFIIIS (*PPR2*) promotes nucleosomal transcription *in vitro* and Hir1 functions in replication-independent nucleosome assembly. Both *ppr2Δ* and *hir1Δ* when combined with *spt5-242* is synthetically lethal. Consistent with restored chromatin function from I.M. *spt5*, *spt5* viability is largely restored in *ppr2Δ* and *hir1Δ* strains.

We previously identified the NGN-Proximal Region (NPR) as a hot-spot for *spt5* mutants that have a cryptic initiation phenotype. *spt5-242* and the I.M. suppressors, except for R313K, are in the NPR. Further, S261 and G271 residues were identified in both the cryptic initiation and I.M. suppression screens. To further characterize Spt5 structure/function we generated new *spt5* mutants that contained *spt5-242* and *kow* double mutations. We chose *kow* alleles that have (KOW2; E546K) and don't have (KOW5; *kow5Δ*) a cryptic initiation phenotype. Interestingly, *spt5-A68V*, *kow5Δ* double mutants behave as *spt5-A268V* single mutants during normal growth conditions but *spt5-A268V*, *E546K* double mutants are very sick (Fig. A1-S1A). Increased growth temperature restores *spt5-A268V* constitutive growth but *spt5-A268V*, *E546K* remain sick and slow growing at 39°C (Fig. A1-S1B). This suggests that Spt5 may have overlapping chromatin function at the NPR and KOW2 domain.

Genetic model of nucleosomal transcription elongation

We have identified several histone chaperone pathways which can genetically suppress *spt5-242*. Overexpression of *SPT2*, point mutations to *spt6* and yH3.3 are all

dominant suppressors of *spt5-242* cold-sensitive growth (Fig. A1-1, Fig. A1-3A, data not shown). In addition, these dominant suppressors also can restore repression of cryptic transcription from the *FLO8-HIS3* reporter (Fig. A1-1, Fig. A1-3B, data not shown). The repression of cryptic transcription is a mutual genetic interaction, suggesting that Spt2/Spt6/yH3.3 and Spt5 have compensatory or opposing roles in nucleosome reassembly. The *spt16* mutations that suppress *spt5-242* cold-sensitive growth are recessive mutations and some of our *spt16* alleles were independently identified as suppressors of *hht2-L61W* cold-sensitive growth (Fig. A1-4, Table A1-4). Spt16 has increased chromatin association in *hht2-L61W* and the overlapping *spt16* alleles lead to decreased chromatin association. This suggests that *spt5-242* may also lead to increased Spt16 chromatin association. The dominant *spt5-242* suppressors may be either bypassing Spt5/Spt16 function or promote Spt16 chromatin release.

From this work, a model of eukaryotic nucleosomal transcription elongation can be proposed (Fig. A1-7). Spt16 disassembles the downstream nucleosome inhibiting RNA pol II progression. In collaboration with Spt6, Spt16 reassembles the nucleosome at upstream DNA sequence. Spt5 negatively regulates nucleosome reassembly through Spt16. This ensures that co-transcriptional nucleosomal modifications may occur and that pol II does not engage with another nucleosome before the currently engaged nucleosome is reassembled. Spt16 disengagement with Spt5 may promote pol II to engage the next downstream nucleosome and/or Spt16 disengagement from pol II signals complete nucleosome reassembly and transcription elongation can continue. Histone replacement is compatible with this model and Spt5, Spt6, or Sp16 could be targets for regulating this mechanism.

Spt16 (FACT) functions in nucleosome reassembly during both DNA replication and RNA transcription. Histone H3.1 and H3.3 isoforms may be augmenting the fidelity of nucleosome reassembly by FACT in opposing ways. At the expense of the rate of FACT nucleosome disassembly H3.1 would promote the retention of H3.1 marked with repressive

PTM during DNA replication and unregulated/inappropriate transcription elongation. In contrast, H3.3 would increase the rate of FACT nucleosome disassembly which promotes nucleosome loss. This would allow for increased nucleosome turnover during DNA replication to titrate out H3.3 marked with activating PTM that are no longer needed during DNA replication and increased transcription elongation rate and/or efficient removal of specific nucleosomes at stalled pol II complexes.

Table A1-1 *spt5-242 yH3.1* genetically interacts with known *spt5* suppressors

The indicated strains were crossed with known suppressors of *spt5-242* in the presence of pMS4 (*URA3 SPT5 CEN*) and tested for viability on 5FOA media. Results are shown in the table (- no growth; +/- strong growth; -/+ weak growth; N.D. was not conducted).

	wild type	<i>spt5</i> suppressor			
		<i>set2</i> Δ	<i>chd1</i> Δ	<i>rtf1</i> Δ	<i>rpb1-244</i>
<i>spt5-242 HHT1-HHF2 yH3.1</i>	-	+/-	+/-	+/-	+/-
<i>spt5-242 (hht1-hhf2)Δ yH3.1</i>	-	-/+	N.D.	N.D.	N.D.

Figure A1-1 Overexpression of Spt2 rescues *spt5-242*

spt5-242 is no longer cold-sensitive when Spt2 is overexpressed and overexpression of Spt2 in *spt5-242* mutually suppresses the cryptic initiation phenotype. Open vector or *SPT2* plasmids were transformed into wild type and *spt5-242* strains bearing the *FLO8-HIS3* cryptic initiation reporter and then serially diluted onto the indicated plates at the indicated temperatures for growth. Sc-trp 30C and 22C represents 2 or 3 days of growth, respectively. Sc-trp + gal represents 2 days of growth and sc-trp, his + gal represents 4 days of growth.

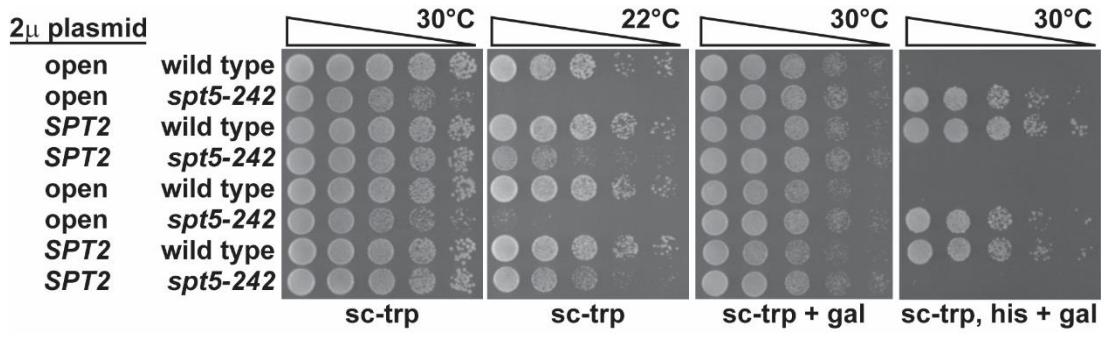


Table A1-2 Spt5 overlaps with Spt6 function

Spt5 overlaps with a sub-set of Spt6 function *in vivo*. Double mutants were generated from a cross that unambiguously identified double mutants that were also covered with a UR3 marked *SPT6* plasmid. 5FOA was used to test for double mutant viability.

	wild type	spt6-140 ; L653P	spt6-14 ; S952F	spt6-50 ; K1274ter
<i>spt5-242</i>	+/-	+/-	-	-

Figure A1-2 *spt6* suppressors of *spt5-242* mostly cluster in the acidic N-terminus and disrupt chromatin function

Disruption of the Spn1 binding domain and adjacent residues in *spt6* suppresses *spt5-242* and most *spt6* mutations have a cryptic initiation phenotype. The *spt6-YW* (Y255A, W257A) was previously described in Viktorovskaya *et al.* 2021 and reported to suppress *spt5-242*.

(A) A schematic representation of the *spt6* mutations relative to known Spt6 domains described in Close *et al.* 2011. Most identified alleles are point mutations in or adjacent to the Spn1 binding region. One allele results in a residue deletion between the HhH and DLD domains.

(B) Not all *spt6* alleles have a cryptic initiation phenotype. The *spt6* alleles were transformed into a *SPT6* shuffle strain that contained the cryptic initiation reporter, passed over 5FOA to knockout the wild type *SPT6* plasmid, and patched to YPD before replica plating to the indicated media. No growth was observed on sc-his (data not shown). YPD, gal, and sc-his + gal represent 2, 3, and 3 days of growth, respectively.

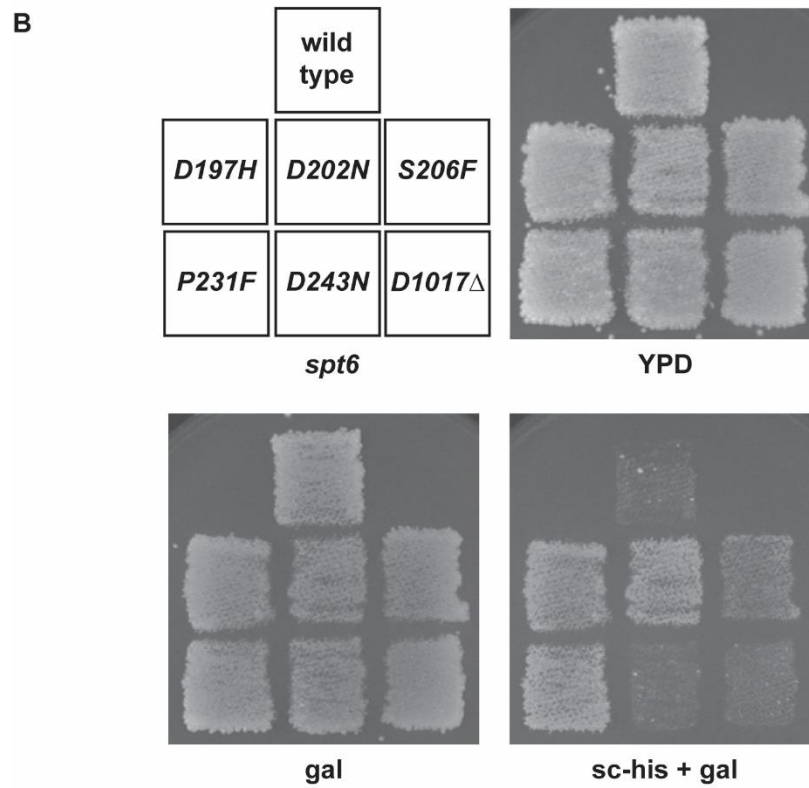
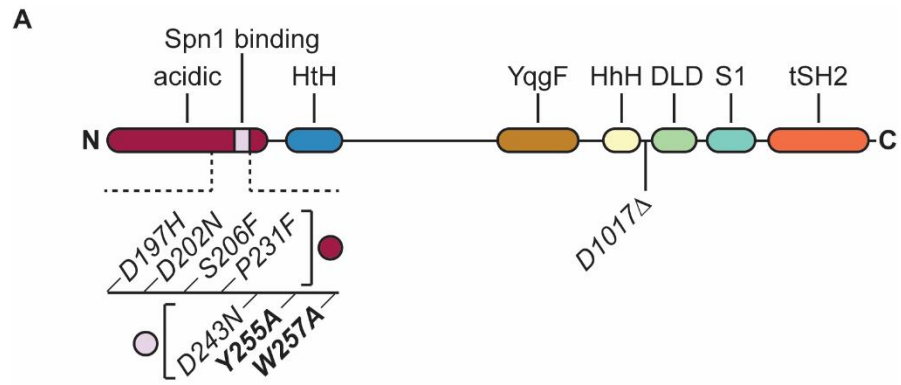


Figure A1-3 All *spt6* alleles are dominant suppressors of *spt5-242*

SPT6 spt5-242 FLO8-HIS3 strains were transformed with the indicated pRS414 (*TRP CEN*) plasmid and serially diluted to the indicated media and growth temperature.

(A) Adding an additional *SPT6* copy makes *spt5-242* sicker but the addition of all *spt6* alleles dominantly suppresses *spt5-242* cold-sensitive growth. Growth at 30°C and 22°C represent 2 and 4 days, respectively.

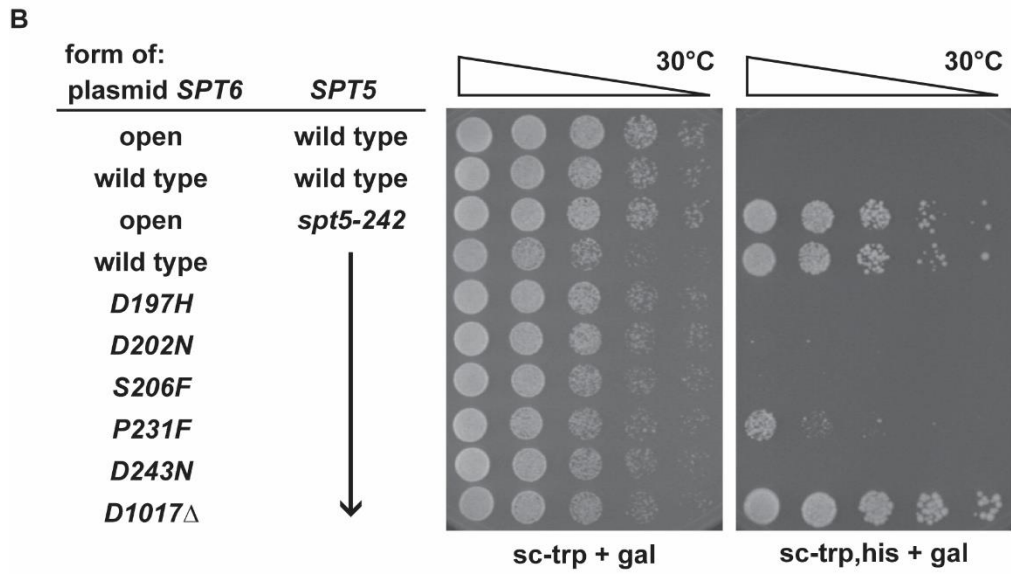
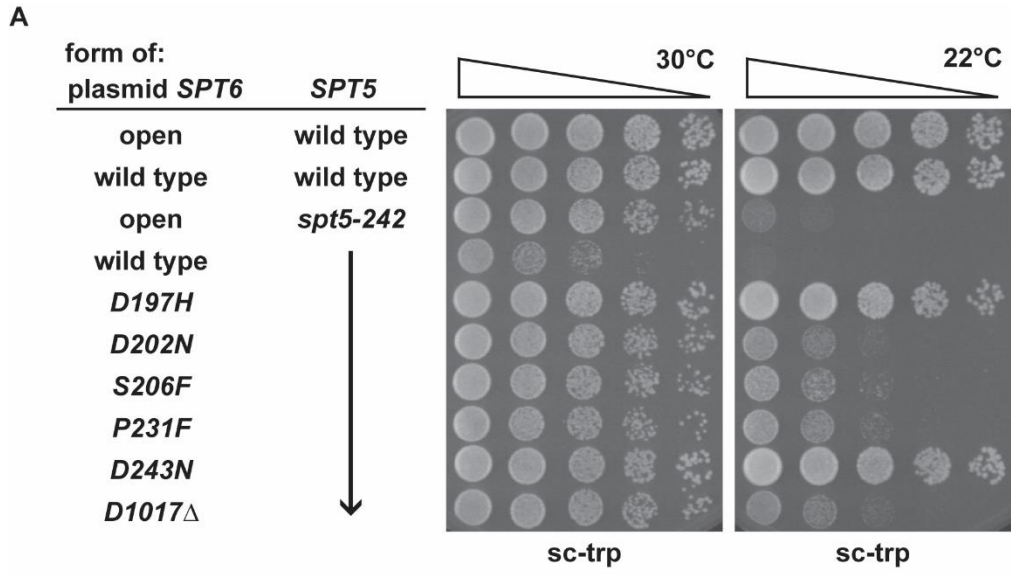


Figure A1-4 *spt16* suppressors of *spt5-242* cluster in the Spt16 Mid-domain.

(A) *spt16* alleles are mapped relative to known Spt16 domains from Kemble *et al.* 2013.

(B) The *spt16* alleles physically cluster in a long alpha-helix and an adjacent unstructured region that can engage with the nucleosome. *D918N* is located at a region that points back towards RNA pol II. PDB: 7NKY is the reference structure.

(C) The long alpha-helix and unstructured region structurally overlaps with the *hht2* mutations that suppress *spt5-242*. Overlap and/or physical interaction may be histone H3 dimer specific. PDB: 7NKY is the reference structure.

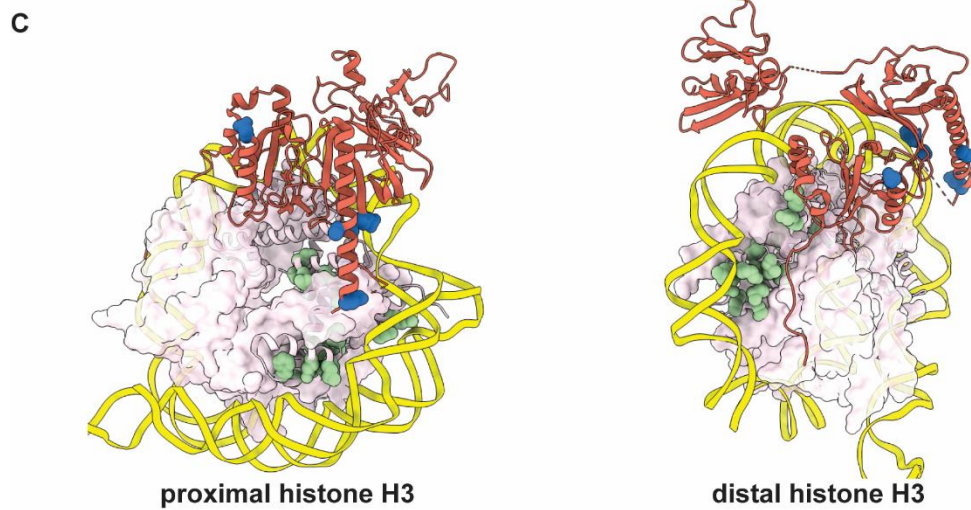
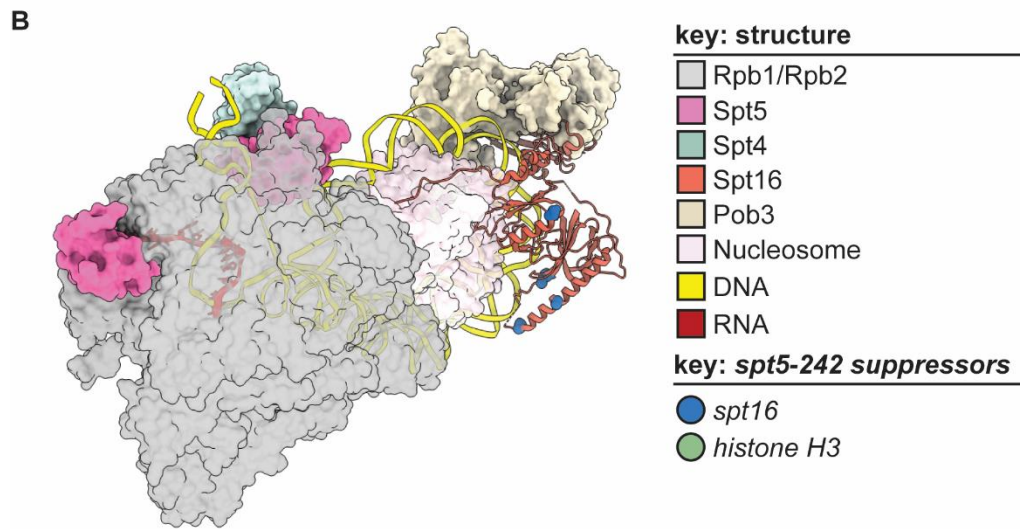
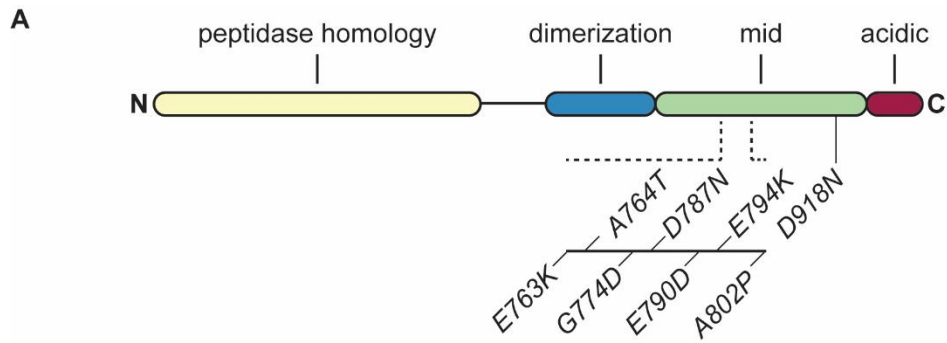
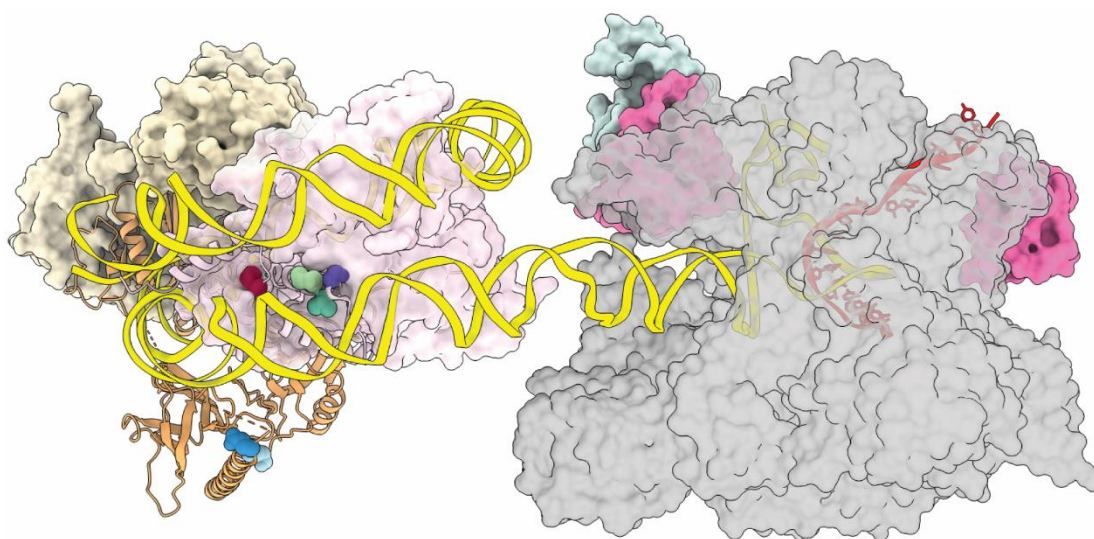


Figure A1-5 Proximity of *h3* and *spt16* alleles during transcription

Histone H3 residues that genetically interact with *spt5-242* and Spt16 residues that genetically interact with *spt5-242* and/or *hht2-L61W* are displayed. PDB: 7NKY is the reference structure.



key: structure

- Rpb1/Rpb2
- Spt5
- Spt4
- Spt16
- Pob3
- Nucleosome
- DNA
- RNA

key: H3 residues

- L61
- S87
- A89
- G90

key: Spt16 residues

- E790
- E794

Table A1-3 Functional redundancy between *hht2-L61W* and *spt5-242*

Summary of known phenotypes and genetic interactions from the literature. Abbreviations: not determined (N.D.), no growth (-), some growth (-/+), modest growth (+/-), robust growth (+), mycophenolic acid (MPA), 6-azauracil (6AU).

	15°C	30°C	37°C	15°C + MPA/6AU
<i>hht2-L61W</i>	-	-/+	-	-/+
<i>spt5-242</i>	-	+/-	+	+/-
<i>spt5-242 hht2-L61W</i>	N.D.	-	N.D	N.D

Table A1-4 Genetic interactions between *spt5*, *h3*, *spt16*, *spt6*

Summary of pairwise genetic suppression or interaction phenotypes. Abbreviations: synthetic lethal (S.L.), not determined (N.D.), modest phenotype suppression (+/-), no change (N.C.), self (-).

	<i>spt5-242</i>	<i>hht2-L61W</i>	<i>hht2-yH3.1</i>	<i>hht2-yH3.3</i>	<i>spt16-E790D</i>	<i>spt16-E794K</i>	<i>spt6-50</i>
<i>spt5-242</i>	-	S.L.	S.L.	+/-	+/-	+/-	S.L.
<i>hht2-L61W</i>		-	N.D.	N.D.	+/-	N.D.	N.D.
<i>hht2-yH3.1</i>			-	+/-	N.D.	N.D.	S.L.
<i>hht2-yH3.3</i>				-	N.D.	N.D.	S.L.
<i>spt16-E790D</i>					-	N.D.	N.C.
<i>spt16-E794K</i>						-	S.L.
<i>spt5-50</i>							-

Figure A1-6 Intramolecular suppressors of *spt5-242* suppress many phenotypes

Intramolecular suppressors were generated by plasmid mutagenesis of plasmids bearing *spt5-242* (A268V) and selected for by restoration of cold-sensitive growth. Non-revertant alleles were further characterized.

(A & B) The intramolecular *spt5-242* suppressors restore cold-sensitive growth (A) and suppress the cryptic initiation phenotype (B) of *spt5-242*. Indicated *LEU2 CEN spt5* plasmids were transformed into *spt5Δ FLO8-HIS3* + pMS4 (*URA3 CEN SPT5*) and subsequently passed over 5FOA to select against pMS4. The transformants were then serially diluted to indicated plates and growth temperatures. (A) 30°C and 22°C represent 2 and 3 days of growth, respectively. (B) sc-leu + gal and sc-leu, his + gal represent 2 and 4 days of growth, respectively.

(C) Most intramolecular suppressors restore *spt5-242* viability when TFIIIS or Hir complex function is absent. The same plasmids in A & B were transformed into *spt5Δ ppr2Δ* (*URA3 CEN SPT5*) or *spt5Δ hir1Δ* (*URA3 CEN SPT5*) strains. Transformants were serially diluted onto 5FOA to test for *spt5* genetic interactions with the indicated gene deletions. *ppr2* represents 4 days of growth and *hir1* represents 3 days of growth.

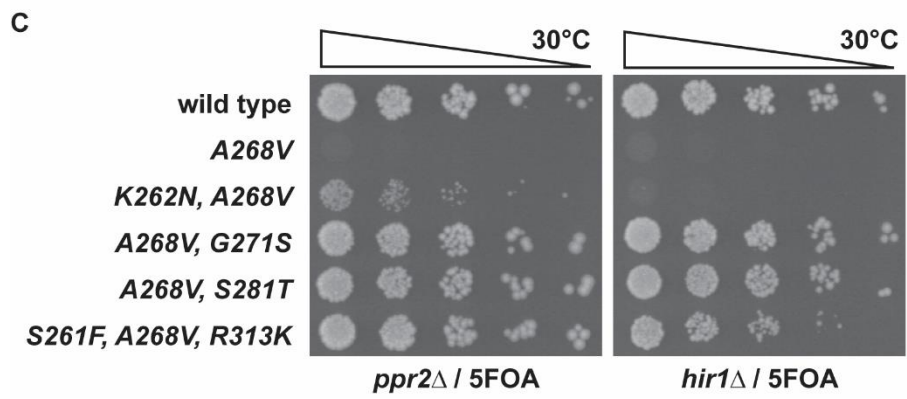
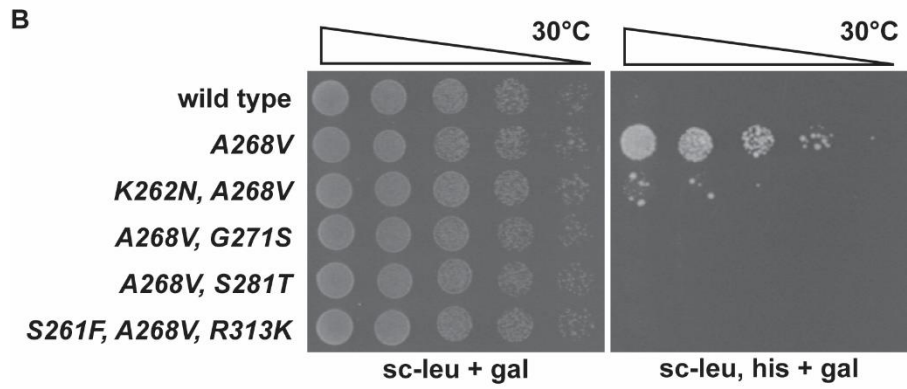
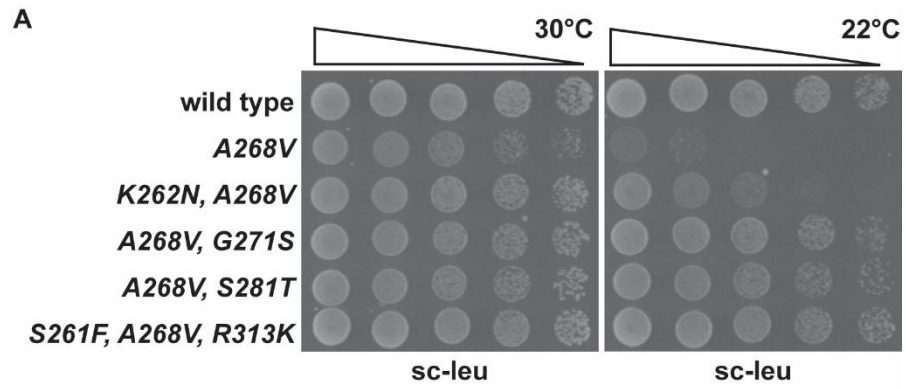


Figure A1-7 Model for eukaryotic nucleosomal transcription elongation

The nucleosomal barrier to RNA pol II during transcription elongation is overcome by Spt16 (FACT). After the nucleosome ahead of pol II is disassembled, Spt6/Spt16/Spt5 facilitate nucleosome reassembly in the wake of pol II. Spt16 disengages from the nucleosome which resets pol II for progressive transcription elongation. γ H3.3 and γ H3.1 have opposing functions of Spt16 function. This could serve as a checkpoint/efficiency system in eukaryotic transcription. Inhibition of Spt16 function by H3.1 decreases the frequency of inappropriate transcription and increases the probability of nucleosome reassembly if inappropriate transcription proceeds. Promotion of Spt16 function by H3.3 facilitates efficient nucleosome transactions in post-mitotic gene expression. Spt16 and/or Spt5 can then be targets for post-translational modification (PTM) regulation of nucleosome reassembly. Spt5 delays nucleosome reassembly. This allows time for transcription coupled histone PTM. Spt16 functions with Spt5 in delaying reassembly and functions with Spt6 in promoting reassembly. Spt16 release from Spt5 & the nucleosome signals the completion of nucleosome reassembly and transcription elongation continues.

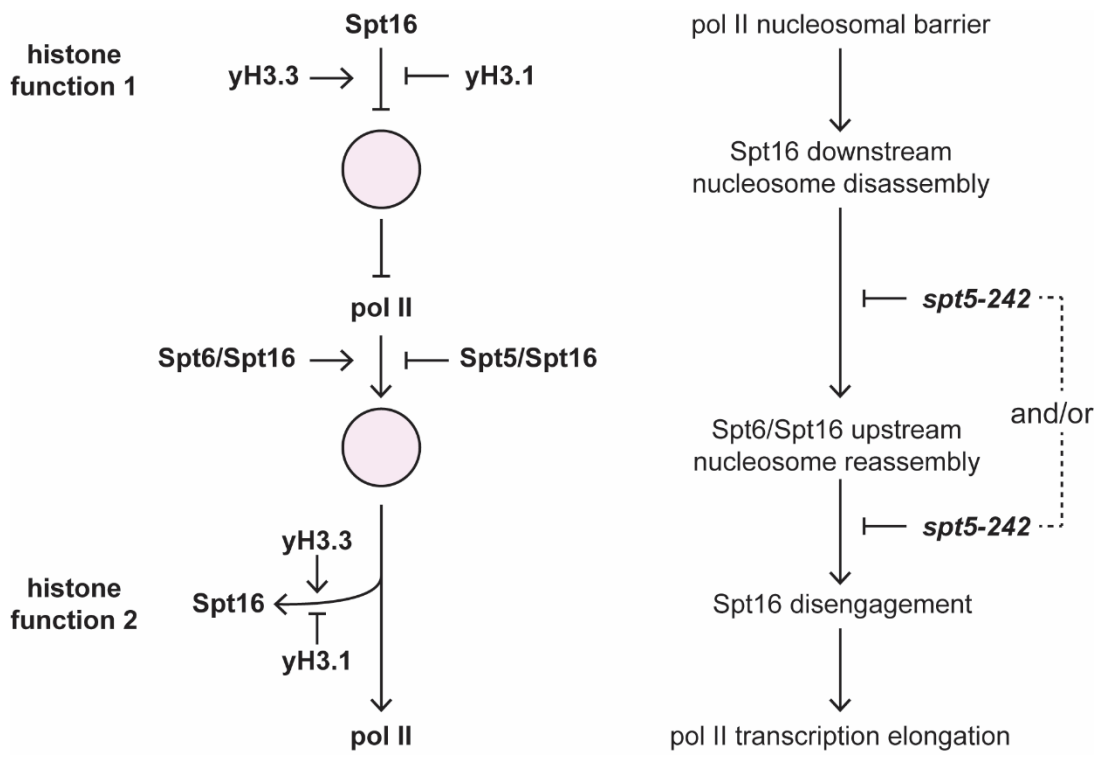
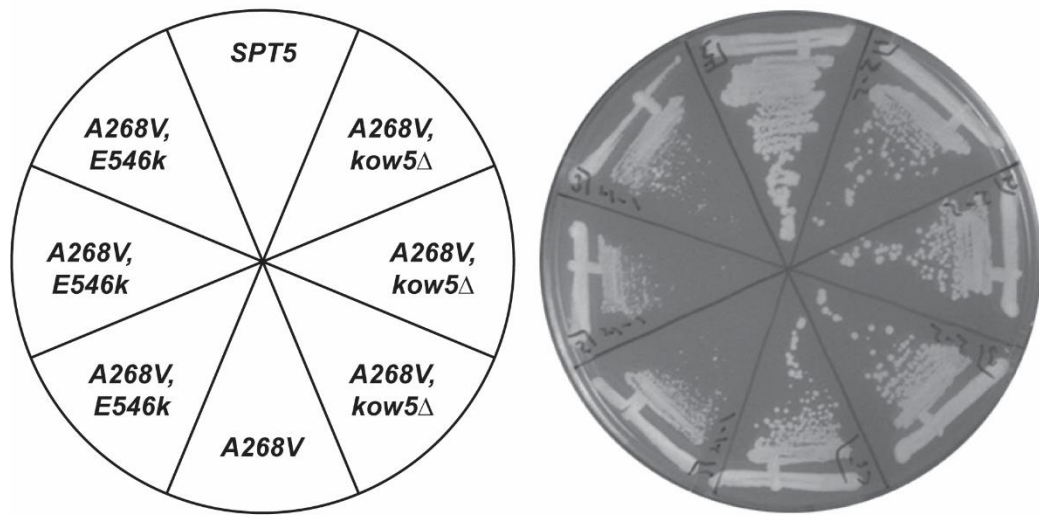


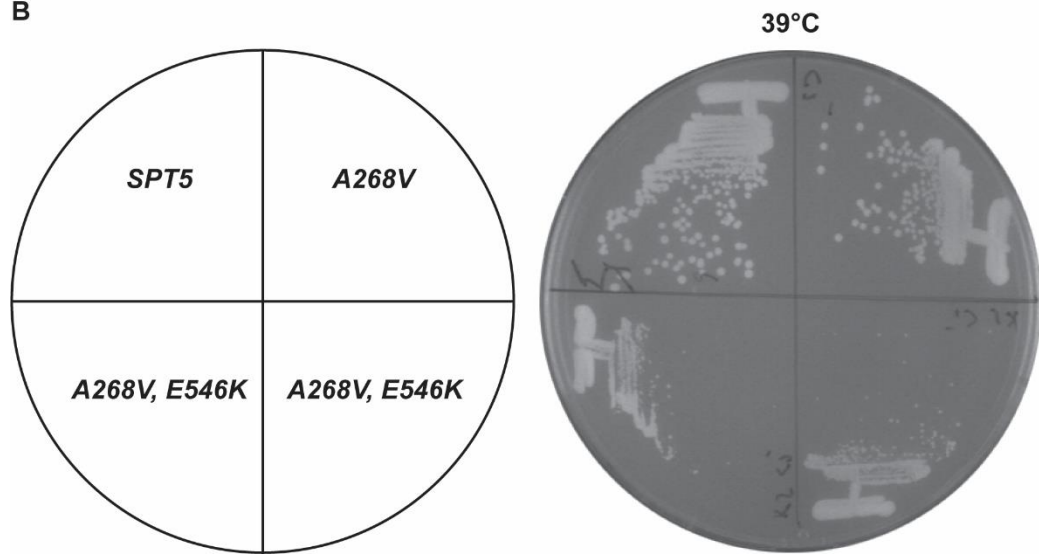
Figure A1-S1 Functional overlap between Spt5 NPR and KOW2

spt5-A268V,E546K are very sick and growth is not restored at elevated temperatures. The indicated *spt5* plasmids (*spt5 CEN LEU*) were transformed into a *spt5Δ* shuffle strain and passed over 5FOA. Candidates were directly struck out to plates and incubated at the indicated growth temperatures. 30°C represents 3 days of growth and 39°C represents 2 days of growth.

A



B



Appendix – 2

List of Plasmids

<u>plasmid</u>	<u>genotype</u>	<u>source</u>	<u>ch</u>
pMS4	<i>SPT5 URA3 CEN AMP</i>	Hartzog lab	2
pAAD49	<i>AMP CEN TRP1 HHF2-hht2-49 (K37E)</i>	Andrea Duina	2
pGH336	<i>TRP1 CEN Ampr HHF2 hht2-22-2 (H3 R49K)</i>	Hartzog lab	2
pJH18-AO32	<i>TRP1 CEN hht2-AO32 (I62V L65S) HHF2</i>	Hartzog lab	2
pJH18-AO23	<i>TRP1 CEN hht2-AO23 (A24 SILENT, L60R) HHF2</i>	Hartzog lab	2
pJH18-AO29	<i>TRP1 CEN hht2-AO29 (R17 SILENT, E94G) HHF2</i>	Hartzog lab	2
pAAD41	<i>AMP CEN TRP1 HHF2-hht2-41 (Q68R)</i>	Andrea Duina	2
pAAD44	<i>AMP CEN TRP1 HHF2-hht2-44 (Q93R)</i>	Andrea Duina	2
pGH327	<i>TRP1 CEN Ampr HHF2 hht2-3-1 (H3 I124L)</i>	Hartzog lab	2
pGH328	<i>TRP1 CEN Ampr HHF2 hht2-8-4b (H3 R128G)</i>	Hartzog lab	2
pGH329	<i>TRP1 CEN Ampr HHF2 hht2-10-1 (H3 L130I)</i>	Hartzog lab	2
pJH18-AO19	<i>TRP1 CEN hht2-AO19 (E59 SILENT, L60M) HHF2</i>	Hartzog lab	2
pJH18-AO20	<i>TRP1 CEN hht2-AO20 (G90R, L100 SILENT) HHF2</i>	Hartzog lab	2

pJH18-AO33	<i>TRP1 CEN hht2-AO33 (L65S, V117 SILENT) HHF2</i>	Hartzog lab	2
pJH18-AO5	<i>TRP1 CEN hht2-ac5 (K64R) HHF2</i>	Hartzog lab	2
pJH18-AO8	<i>TRP1 CEN hht2-ac8 (L65V) HHF2</i>	Hartzog lab	2
pGH359	<i>CEN TRP1 hht2-T118I HHF2</i>	Hartzog lab	2
pHHT2-K9,14,18,23R	<i>TRP1 CEN Ampr HHF2 hht2-K9,14,18,23R</i>	LeeAnne Howe	2
pMD73	<i>TRP1 CEN Ampr HHF2 hht2-K9,14,18,23R,S87P,G90S</i>	Hartzog lab	2
pGH356	<i>CEN TRP1 hht2-S87A HHF2</i>	Hartzog lab	2
pMD7	<i>Trp Cen Amp HHF2-hht2-S31A</i>	Hartzog lab	2
pGH374	<i>AMP TRP1 CEN hht2-S31A-I89V, G90M</i>	Hartzog lab	2
pM51.1	<i>pho5D::URA3 AMP</i>	Hinrich Boeger	2
pM53.1	<i>PHO5-LexA-RS AMP</i>	Hinrich Boeger	2
pM67.6	<i>pho80D::HIS3 AMP</i>	Hinrich Boeger	2
pSH17	<i>TEF2p:LexA-TAP, GAL1p:R-Recombinase (Z. rouxii), LEU2-RS</i>	Hinrich Boeger	2
pMD1	<i>URA3 CEN HFI1 AmpR</i>	Hartzog lab	3
pMD2	<i>Trp Cen Amp SuppE</i>	Hartzog lab	3
pMD3	<i>Suppl LEU2 2um KanR</i>	Hartzog lab	3
pMD4	<i>UBP10 LEU2 2micron KanR</i>	Hartzog lab	3
Str4	<i>AMP CEN TRP STR4 = UBP10</i>	Daniel Gottschling	3
Str4-1	<i>AMP CEN TRP STR4 = UBP10</i>	Daniel Gottschling	3
Str4-5	<i>AMP CEN TRP STR4 = UBP10</i>	Daniel Gottschling	3
pRS416	<i>URA3 CEN Ampr</i>	Hartzog lab	3

pRS314-HTB1- Flag	<i>TRP1 CEN Amp HTB1-Flag</i>	Mary Ann Osley	3
pRS314- htb1K123R- Flag	<i>TRP1 CEN Amp -htb1K123R-Flag</i>	Mary Ann Osley	3
pRS414	<i>TRP1 CEN Ampr</i>	Hartzog lab	3
pJH18	<i>HHT2-HHF2 TRP1 CEN Ampr</i>	Mary Bryk	2, 3
pDM9	<i>HHT1-HHF1 URA3 CEN AMP</i>	Lisa Laprade/Winston	2, 3
pJH18-AO14	<i>TRP1 CEN hht2-ac14 (K18E, K23E) HHF2</i>	Hartzog lab	2, 3
pJH18-AO35	<i>TRP1 CEN hht2-AO35 (L65S E94V) HHF2</i>	Hartzog lab	2, 3
pJH18-AO6	<i>TRP1 CEN hht2-ac6 (S87P,G90S) HHF2</i>	Hartzog lab	2, 3
pJH18-AO1	<i>TRP1 CEN hht2-ac1 (L60P,R131S) HHF2</i>	Hartzog lab	2, 3
pJH18-AO18	<i>TRP1 CEN hht2-AO18 (G90R, R128S, R131 SILENT, G132 SILENT) HHF2</i>	Hartzog lab	2, 3
pJH18-AO38	<i>TRP1 CEN hht2-AO38 (P30 SILENT, F104L) HHF2</i>	Hartzog lab	2, 3
pRM430	<i>hht2Δ4-30 HHF2 TRP1 CEN Ampr</i>	Michael Grunstein	2, 3
MBB257	<i>hht2K4R-HHF2 TRP1 CEN Ampr</i>	Mary Bryk	2, 3
MBB286	<i>hht2K36R-HHF2 TRP1 CEN Ampr</i>	Mary Bryk	2, 3
PWZ414-F13- K79A	<i>hht2-K79A HHF2 CEN TRP1 Amp</i>	Kevin Struhl	2, 3

pFX04-K56G	<i>TRP1 CEN hht2-K56G HHF2</i>	Michael Grunstein	2, 3
pJH18-AO30	<i>TRP1 CEN hht2-AO30 (A29G, R53G) HHF2</i>	Hartzog lab	2, 3
pMD10	<i>CEN AMP LEU2 spt5-G257S</i>	Hartzog lab	A1-1
pMD11	<i>CEN AMP LEU2 spt5-E546K</i>	Hartzog lab	A1-1
pMD12	<i>CEN AMP LEU2 spt5-L278P</i>	Hartzog lab	A1-1
pMD13	<i>CEN AMP LEU2 spt5-E243K</i>	Hartzog lab	A1-1
pMD14	<i>CEN AMP LEU2 spt5-R265C</i>	Hartzog lab	A1-1
pMD15	<i>CEN AMP LEU2 spt5-G602S, S809F</i>	Hartzog lab	A1-1
pMD16	<i>CEN AMP LEU2 spt5-G271D</i>	Hartzog lab	A1-1
pMD17	<i>CEN AMP LEU2 spt5-R255H</i>	Hartzog lab	A1-1
pMD18	<i>CEN AMP LEU2 spt5-G587D</i>	Hartzog lab	A1-1
pMD19	<i>CEN AMP LEU2 spt5-Q788ter</i>	Hartzog lab	A1-1
pMD20	<i>CEN AMP LEU2 spt5-R255C</i>	Hartzog lab	A1-1
pMD21	<i>AMP CEN LEU2 chd1-W932A</i>	Hartzog lab	A1-1
pMD22	<i>CEN AMP LEU2 spt5-G257D</i>	Hartzog lab	A1-1
pMD23	<i>CEN AMP LEU2 spt5-A267T</i>	Hartzog lab	A1-1
pMD24	<i>CEN AMP LEU2 spt5-A267T (G121 silent)</i>	Hartzog lab	A1-1
pMD25	<i>CEN AMP LEU2 spt5-R265C</i>	Hartzog lab	A1-1
pMD26	<i>CEN AMP LEU2 spt5-E244N</i>	Hartzog lab	A1-1
pMD27	<i>CEN AMP LEU2 spt5-S261P</i>	Hartzog lab	A1-1
pMD28	<i>CEN AMP LEU2 spt5-A249T</i>	Hartzog lab	A1-1
pMD29	<i>CEN AMP LEU2 spt5-A266T</i>	Hartzog lab	A1-1
pMD30	<i>CEN AMP LEU2 spt5-E504K</i>	Hartzog lab	A1-1

pMD33	<i>KANr 2u LEU2 [BUR6, tR(ACG)E, YER160C, YER159C-A, SPT2]</i>	Hartzog lab	A1-1
pMD49	<i>TRP1 ampR 2u SPT2</i>	Hartzog lab	A1-1
pMD50	<i>TRP1 ampR CEN SPT6</i>	Hartzog lab	A1-1
pMD51	<i>TRP1 ampR CEN SPT16</i>	Hartzog lab	A1-1
pMD52	<i>URA3 ampR CEN suppE</i>	Hartzog lab	A1-1
pMD54	<i>TRP1 ampR CEN spt6-6 (S206F)</i>	Hartzog lab	A1-1
pMD55	<i>TRP1 ampR CEN spt6-8 (D1017del)</i>	Hartzog lab	A1-1
pMD56	<i>TRP1 ampR CEN spt6-9 (P231F)</i>	Hartzog lab	A1-1
pMD57	<i>TRP1 ampR CEN spt6-10 (P231F)</i>	Hartzog lab	A1-1
pMD58	<i>TRP1 ampR CEN spt6-12 (D202N)</i>	Hartzog lab	A1-1
pMD59	<i>TRP1 ampR CEN spt6-17 (R882C)</i>	Hartzog lab	A1-1
pMD60	<i>TRP1 ampR CEN spt6-18 (D197H)</i>	Hartzog lab	A1-1
pMD61	<i>TRP1 ampR CEN spt6-20 (D243N)</i>	Hartzog lab	A1-1
pMD62	<i>TRP1 ampR CEN spt16-2 (D918N)</i>	Hartzog lab	A1-1
pMD63	<i>TRP1 ampR CEN spt16-9 (D787N)</i>	Hartzog lab	A1-1
pMD64	<i>TRP1 ampR CEN spt16-8</i>	Hartzog lab	A1-1
pMD65	<i>TRP1 ampR CEN spt16-13 (E790D)</i>	Hartzog lab	A1-1
pMD66	<i>TRP1 ampR CEN spt16-16 (P334L, G773D)</i>	Hartzog lab	A1-1
pMD67	<i>TRP1 ampR CEN spt16-18 (A802P)</i>	Hartzog lab	A1-1
pMD68	<i>TRP1 ampR CEN spt16-30 (E763K)</i>	Hartzog lab	A1-1
pMD69	<i>TRP1 ampR CEN spt16-35 (?)</i>	Hartzog lab	A1-1
pMD70	<i>TRP1 ampR CEN spt16-36 (E794K)</i>	Hartzog lab	A1-1
pMD71	<i>TRP1 ampR CEN spt16-42 (G774D)</i>	Hartzog lab	A1-1
pMD72	<i>TRP1 ampR CEN spt16-47 (A764T)</i>	Hartzog lab	A1-1

Appendix – 3

List of strains

<u>name</u>	<u>#</u>	<u>a/b</u>	<u>genotype</u>	<u>source</u>	<u>ch</u>
OY	98	b	<i>his3Δ200 lys2-128δ leu2Δ1 trp1Δ63 ura3-52</i>	FY603/Fred Winston	2
GHY	619	b	<i>his3D200 lys2-128d leu2D0 ura3D0 trp1D63</i>	Hartzog Lab	2
GHY	823	a	<i>his3Δ200 lys2-128δ leu2Δ1 ura3-52 trp1Δ63 (hht1-hhf1)Δ::LEU2 (hht2-hhf2)Δ::HIS3 pDM9</i>	FY1716/Fred Winston	2
GHY	827	b	<i>his3Δ200 lys2-128δ leu2Δ1 ura3-52 trp1Δ63 spt5-242</i>	Hartzog Lab	2
GHY	735	b	<i>his3Δ200 lys2-128δ leu2Δ1 ura3-52 trp1Δ63 (hht1-hhf1)Δ::LEU2</i>	Hartzog Lab	2
GHY	736	a	<i>his3Δ200 lys2-128δ leu2Δ1 ura3-52 trp1Δ63 (hht2-hhf2)Δ::HIS3</i>	Hartzog Lab	2
GHY	840	b	<i>his3Δ200 lys2-128δ leu2Δ1 ura3-52 trp1Δ63 (hht1-hhf1)Δ::LEU2 (hht2-hhf2)Δ::HIS3 pDM9</i>	Hartzog Lab	2
GHY	842	a	<i>his3Δ200 lys2-128δ leu2Δ1 ura3-52 trp1Δ63 spt5-242 (hht1-hhf1)Δ::LEU2 (hht2- hhf2)Δ::HIS3 pDM9</i>	Hartzog Lab	2

			<i>his3Δ200 lys2-128δ leu2Δ1 ura3-52 trp1Δ63</i>		
GHY	843	b	<i>spt5-242 (hht1-hhf1)Δ::LEU2 (hht2-hhf2)Δ::HIS3 pDM9</i>	Hartzog Lab	2
GHY	844	b	<i>his3Δ200 lys2-128δ leu2Δ1 ura3-52 trp1Δ63 spt5-242 (hht1-hhf1)Δ::LEU2 pDM9</i>	Hartzog Lab	2
GHY	1779	b	<i>his3Δ200 lys2-128δ leu2Δ(0 or 1) ura3(-52 or Δ0) trp1Δ63 hht2Δ1::URA3</i>	Hartzog Lab	2
GHY	1867	b	<i>hisΔ200 lys2-128d leu2Δ(0or1) trp1Δ63 ura(-52 or Δ0) (hht1-hhf1)Δ::LEU2 hht2-F104L</i>	Hartzog Lab	2
GHY	1868	a	<i>hisΔ200 lys2-128d leu2Δ(0or1) trp1Δ63 ura(-52 or Δ0) (hht1-hhf1)Δ::LEU2 hht2-F104L</i>	Hartzog Lab	2
GHY	1869	b	<i>hisΔ200 lys2-128d leu2Δ(0or1) trp1Δ63 ura(-52 or Δ0) (hht1-hhf1)Δ::LEU2 hht2-K18E,K23E</i>	Hartzog Lab	2
GHY	1870	a	<i>hisΔ200 lys2-128d leu2Δ(0or1) trp1Δ63 ura(-52 or Δ0) (hht1-hhf1)Δ::LEU2 hht2-K18E,K23E</i>	Hartzog Lab	2
GHY	1871	b	<i>hisΔ200 lys2-128d leu2Δ(0or1) trp1Δ63 ura(-52 or Δ0) (hht1-hhf1)Δ::LEU2 hht2-L60P,R131S</i>	Hartzog Lab	2
GHY	1872	a	<i>hisΔ200 lys2-128d leu2Δ(0or1) trp1Δ63 ura(-52 or Δ0) (hht1-hhf1)Δ::LEU2 hht2-L60P,R131S</i>	Hartzog Lab	2
GHY	1891	b	<i>his3Δ200 lys2-128δ leu2Δ(0 or 1) trp1Δ63 ura3(-52 or 0) (hht1-hhf1)Δ::LEU2 hht2-A29G,R53G</i>	Hartzog Lab	2

			<i>his3Δ200 lys2-128δ leu2Δ(0 or 1) trp1Δ63</i>		
GHY	1892	a	<i>ura3(-52 or 0) (hht1-hhf1)Δ::LEU2 hht2-A29G,R53G</i>	Hartzog Lab	2
			<i>his3Δ200 lys2-128δ leu2Δ(0 or 1) trp1Δ63</i>		
GHY	1893	a	<i>ura3(-52 or 0) (hht1-hhf1)Δ::LEU2 hht2-G90R,R128S pDM9</i>	Hartzog Lab	2
			<i>his3Δ200 lys2-128δ leu2Δ(0 or 1) trp1Δ63</i>		
GHY	1894	b	<i>ura3(-52 or 0) (hht1-hhf1)Δ::LEU2 hht2-G90R,R128S pDM9</i>	Hartzog Lab	2
			<i>his3Δ200 lys2-128δ leu2Δ(0 or 1) trp1Δ63</i>		
GHY	1895	a	<i>ura3(-52 or 0) (hht1-hhf1)Δ::LEU2 hht2-S87P,G90S</i>	Hartzog Lab	2
			<i>his3Δ200 lys2-128δ leu2Δ(0 or 1) trp1Δ63</i>		
GHY	1896	b	<i>ura3(-52 or 0) (hht1-hhf1)Δ::LEU2 hht2-S87P,G90S</i>	Hartzog Lab	2
			<i>his3Δ200 lys2-128δ trp1Δ63 ura3(-52or Δ0)</i>		
GHY	1912	b	<i>leu2Δ(1 or 0) (hht1-hhf1)Δ::LEU2 hht2-L65S,E94V (pDM9=HHT1-HHF1 URA3)</i>	Hartzog Lab	2
			<i>his3Δ200 lys2-128δ trp1Δ63 ura3(-52or Δ0)</i>		
GHY	1913	a	<i>leu2Δ(1 or 0) (hht1-hhf1)Δ::LEU2 hht2-L65S,E94V (pDM9=HHT1-HHF1 URA3)</i>	Hartzog Lab	2
			<i>his3Δ200 lys2-128δ leu2Δ1 ura3-52 trp1Δ63</i>		
GHY	2006	b	<i>(hht1-hhf1)Δ::LEU2 pGAL1-FLO8-HIS3::KANMX</i>	Hartzog Lab	2

			<i>his3Δ200 lys2-128δ leu2Δ1 ura3-52 trp1Δ63</i>		
GHY	2007	a	<i>(hht1-hhf1)Δ::LEU2 pGAL1-FLO8-HIS3::KANMX</i>	Hartzog Lab	2
			<i>his3Δ200 lys2-128δ leu2Δ1 ura3-52 trp1Δ63</i>		
GHY	2010	a	<i>(hht1-hhf1)Δ::LEU2 (hht2-hhf2)Δ::NAT pGAL1-FLO8-HIS3::KANMX [pDM9=URA3 CEN HHT1-HHF1]</i>	Hartzog Lab	2
			<i>his3D1 leu2D0 met15D0 ura3D0</i>		
GHY	2244	a	<i>sir2D0::KANMX</i>	Hartzog Lab	2
			<i>his3D200 lys2-128d leu2D(1 or 0) ura3(-52 or D0) trp1D63 (hht1-hhf1)D::LEU2 suc2DUAS(-1900/-390) hht2-L60P,R131S [pDM9 = HHT1-HHF1 URA3 CEN AMP]</i>	Hartzog Lab	2
			<i>his3D200 lys2-128d leu2D(1 or 0) ura3(-52 or D0) trp1D63 (hht1-hhf1)D::LEU2 suc2DUAS(-1900/-390) hht2-A29G,R53G [pDM9 = HHT1-HHF1 URA3 CEN AMP]</i>	Hartzog Lab	2
			<i>his3D200 lys2-128d leu2D(1 or 0) ura3(-52 or D0) trp1D63 (hht1-hhf1)D::LEU2 suc2DUAS(-1900/-390) hht2-S87P,G90S [pDM9 = HHT1-HHF1 URA3 CEN AMP]</i>	Hartzog Lab	2
			<i>his3Δ200 lys2-128δ leu2Δ(0 or 1) trp1Δ63 ura3(-52 or 0) hht2-3.1 spt5-242 pMS4</i>	Hartzog Lab	2
			<i>his3Δ200 lys2-128δ leu2Δ(0 or 1) trp1Δ63 ura3(-52 or 0) (hht1-hhf1)Δ::LEU2 hht2-3.1 pGAL1-FLO8-HIS3::KANMX</i>	Hartzog Lab	2

			<i>his3Δ200 lys2-128δ leu2Δ(0 or 1) trp1Δ63</i>		
GHY	2842	b	<i>ura3(-52 or 0) (hht1-hhf1)Δ::LEU2 hht2-3.1</i> <i>pGAL1-FLO8-HIS3::KANMX</i>	Hartzog Lab	2
			<i>his3Δ200 lys2-128δ leu2(Δ1 or 0) ura3(-52 or</i>		
GHY	2853	b	<i>Δ0) trp1Δ63 (hht1-hhf1)Δ::LEU2 hht2-3.3</i> <i>pGAL1-FLO8-HIS3::KANMX</i>	Hartzog Lab	2
			<i>his3Δ200 lys2-128δ leu2(Δ1 or 0) ura3(-52 or</i>		
GHY	2854	a	<i>Δ0) trp1Δ63 (hht1-hhf1)Δ::LEU2 hht2-3.3</i> <i>pGAL1-FLO8-HIS3::KANMX</i>	Hartzog Lab	2
			<i>his3Δ200 lys2-128δ leu2Δ1 ura3-52 trp1Δ63</i>		
GHY	2862	b	<i>spt5-242 hht2-T118I pDM9</i>	Hartzog Lab	2
			<i>his3Δ200 lys2-128δ leu2Δ1 ura3-52 trp1Δ63</i>		
GHY	2867	b	<i>hht2-T118I pDM9</i>	Hartzog Lab	2
			<i>his3Δ200 lys2-128δ leu2Δ1 ura3-52 trp1Δ63</i>		
GHY	2868	a	<i>(hht1-hhf1)Δ::LEU2 hht2-T118I pDM9</i>	Hartzog Lab	2
			<i>his3Δ200 lys2-128δ leu2Δ(0 or 1) trp1Δ63</i>		
GHY	2803	b	<i>ura3(-52 or 0) (hht1-hhf1)Δ::LEU2 hht2-3.1</i> <i>spt5-242</i>	Hartzog Lab	2
			<i>his3Δ200 lys2-128δ leu2Δ(0 or 1) trp1Δ63</i>		
GHY	2807	b	<i>ura3(-52 or 0) (hht1-hhf1)Δ::LEU2 hht2-3.3</i> <i>spt5-242</i>	Hartzog Lab	2
			<i>his3D200 lys2-128d leu2D(1 or 0) ura3(-52 or</i>		
GHY	3000	a	<i>D0) trp1D63 suc2DUAS(-1900/-390) hht2-</i> <i>T118I [pDM9 = HHT1-HHF1 URA3 CEN AMP]</i>	Hartzog Lab	2
			<i>his3D200 lys2-128d leu2D(1 or 0) ura3(-52 or</i>		
GHY	3001	b	<i>D0) trp1D63 (hht1-hhf1)D::LEU2 suc2DUAS(-</i>	Hartzog Lab	2

			1900/-390) <i>hht2-L65S,E94V</i> [pDM9 = HHT1-HHF1 URA3 CEN AMP]		
			<i>his3D200 lys2-128d leu2D(1 or 0) ura3(-52 or D0) trp1D63 (hht1-hhf1)D::LEU2 suc2DUAS(-1900/-390) hht2-K18E,K23E</i> [pDM9 = HHT1-HHF1 URA3 CEN AMP]		
GHY	3003	b		Hartzog Lab	2
			<i>his3D200 lys2-128d leu2D(1 or 0) ura3(-52 or D0) trp1D63 (hht1-hhf1)D::LEU2 suc2DUAS(-1900/-390) hht2-G90R,R128S</i> [pDM9 = HHT1-HHF1 URA3 CEN AMP]		
GHY	3005	a		Hartzog Lab	2
			<i>his3D200 lys2-128d leu2D(1 or 0) ura3(-52 or D0) trp1D63 (hht1-hhf1)D::LEU2 suc2DUAS(-1900/-390) hht2-F104L</i> [pDM9 = HHT1-HHF1 URA3 CEN AMP]		
GHY	3006	a		Hartzog Lab	2
			<i>his3D200 lys2-128d leu2D1 ura3-52 trp1D63 (hht1-hhf1)D::LEU2 suc2DUAS(-1900/-390)</i>		
GHY	3007	b		Hartzog Lab	2
			<i>his3Δ200 leu2Δ1 lys2Δ0 met15Δ0 ura3-167 trp1Δ63 ade2::his (hht1-hhf1)Δ::NATMX (hht2-hhf2)Δ::HYGMX RDN1::mURA3/HIS3 RDN1::TY1-MET15 TELV::ADE2 [pJP11=HHT1-HHF1 LYS2 CEN]</i>		
OY	411	a		Jeff Boeke	2
			<i>his3Δ200 lys2-128δ leu2Δ1 ura3-52 trp1Δ63 (hht1-hhf1)Δ::LEU2</i>		
GHY	835	b		Hartzog Lab	3
			<i>his3Δ200 lys2-128δ leu2Δ(0 or 1) trp1Δ63 ura3(-52 or 0) spt5-242 (hht1-hhf1)Δ::LEU2 hht2-15R (15R=G90R,R128S)</i>		
GHY	1945	b		Hartzog Lab	3

			<i>his3Δ200 lys2-128δ leu2Δ(0 or 1) trp1Δ63</i>		
GHY	2019	a	<i>ura3(-52 or 0) (hht1-hhf1)Δ::LEU2 hht2-15R</i> <i>suppressor cand. E (pRS314= TRP1 CEN)</i> <i>his3Δ(200 or 1) lys2(D1 or -128δ) leu2Δ(0 or</i> <i>1) ura3(-52 or Δ0) trp1Δ63 (hht1-</i>	Hartzog Lab	3
GHY	2180	a	<i>hhf1)Δ::LEU2 hht2-15R hfi1Δ::KAN pDM9</i> <i>(=URA3 CEN HHT1-HHF1) pAO9-3 (=TRP1</i> <i>CEN HFI1)</i>	Hartzog Lab	3
GHY	2182	a	<i>his3Δ200 leu2Δ(0 or 1 or D::PET56) ura3(-52</i> <i>or Δ0) trp1Δ63 (hht1-hhf1)Δ::LEU2 hht2-15R</i> <i>gcn5Δ::KAN pDM9 (=URA3 CEN HHT1-</i> <i>HHF1)</i>	Hartzog Lab	3
GHY	2565	b	<i>his3D(0 or 200) lys2-128d leu2D(0 or 1)</i> <i>trp1D63 ura3(-52 or D0) (hht1-hhf1)D::LEU2</i> <i>hht2-15R ubp10D0::HIS3 ubp8D0::KANMX</i> <i>[pDM9=HHT1-HHF1 URA3 CEN AMPR]</i>	Hartzog Lab	3
GHY	2265	a	<i>his3Δ200 lys2-128δ leu2Δ(0 or1) ura3(-52 or</i> <i>Δ0) trp1Δ63 (hht1-hhf1)Δ::LEU2 hht2-15R</i> <i>suppl</i>	Hartzog Lab	3
GHY	2286	b	<i>his3D200 lys2-128d leu2D(1 or 0) ura3-52</i> <i>trp1D63 (hht1-hht2)D::LEU2 (hht2-</i> <i>hhf2)D::URA3 suppE [pDM9=URA3 CEN</i> <i>H3/H4]</i>	Hartzog Lab	3
GHY	2288	a	<i>his3D200 lys2-128d leu2D(1 or 0) ura3-52</i> <i>trp1D63 (hht1-hht2)D::LEU2 (hht2-</i>	Hartzog Lab	3

		<i>hht2</i>)D::HIS3 suppl [pDM9=URA3 CEN H3/H4]			
			<i>his3Δ200 leu2(Δ1 or 0) lys2-128δ ura3(-52</i>		
GHY	2381	a	<i>or Δ0) trp1Δ63 (hht1-hhf1)Δ::LEU2 hht2-15R</i>	Hartzog Lab	3
			<i>ubp10Δ::KanMX [pDM9=(HHT1-HHF1)URA3]</i>		
			<i>his3Δ200 leu2(Δ1 or 0) lys2-128δ ura3(-52</i>		
GHY	2386	b	<i>or Δ0) trp1Δ63 (hht1-hhf1)Δ::LEU2 hht2-15R</i>	Hartzog Lab	3
			<i>spt16-197 [pDM9=(HHT1-HHF1)URA3]</i>		
			<i>his3Δ200 leu2(Δ1 or 0) lys2-128δ ura3(-52</i>		
GHY	2392	a	<i>or Δ0) trp1Δ63 (hht1-hhf1)Δ::LEU2 hht2-15R</i>	Hartzog Lab	3
			<i>spt16-197 suppl [pDM9=(HHT1-HHF1)URA3]</i>		
			<i>his3Δ200 leu2(Δ1 or 0) lys2-128δ ura3(-52</i>		
GHY	2394	a	<i>or Δ0) trp1Δ63 (hht1-hhf1)Δ::LEU2 hht2-15R</i>	Hartzog Lab	3
			<i>spt16-197 suppE [pDM9=(HHT1-HHF1)URA3]</i>		
			<i>his3Δ(200 or 0) leu2(Δ1 or 0) lys2-128δ</i>		
			<i>ura3(-52 or Δ0) trp1Δ63 (hht1-hhf1)Δ::LEU2</i>		
GHY	2396	a	<i>hht2-15R ubp8Δ::KanMX [pDM9=(HHT1-</i>	Hartzog Lab	3
			<i>HHF1)URA3]</i>		
			<i>his3Δ200 leu2Δ(1 or 0 or ::PET56) lys2-128δ</i>		
			<i>ura3(-52 or Δ0) trp1Δ63 (hht1-hhf1)Δ::LEU2</i>		
GHY	2401	a	<i>hht2-15R gcn5Δ::KAN suppE</i>	Hartzog Lab	3
			<i>[pDM9=(HHT1-HHF1)URA3]</i>		
			<i>his3Δ200 leu2Δ(0 or 1 or ::PET56) ura3(-52 or</i>		
			<i>Δ0) trp1Δ63 (hht1-hhf1)Δ::LEU2 hht2-15R</i>		
GHY	2403	a	<i>gcn5Δ::KAN suppl pDM9 (=URA3 CEN</i>	Hartzog Lab	3
			<i>HHT1-HHF1)</i>		

			<i>his3Δ(200 or 1) lys2-128δ leu2Δ(0 or 1)</i>		
GHY	2405	a	<i>ura3(-52 or 0) (hht1-hhf1)Δ::LEU2</i>	Hartzog Lab	3
			<i>ada3Δ0::KanMX hht2-15R pDM9</i>		
			<i>his3Δ200 lys2-128δ leu2(Δ1 or 0) ura3(-52 or</i>		
			<i>Δ0) trp1Δ63 (hht1-hhf1)Δ::LEU2 (hht2-</i>		
GHY	2410	b	<i>hhf2)Δ::NAT suppE pGAL1-FLO8-</i>	Hartzog Lab	3
			<i>HIS3::KANMX [pDM9=URA3 CEN HHT1-</i>		
			<i>HHF1]</i>		
			<i>his3Δ(1 or 200) lys2-128× leu2Δ(0 or 1)</i>		
GHY	2420	a	<i>ura3(Δ0 or -52) (hht1-hhf1)Δ::LEU2 hht2-</i>	Hartzog Lab	3
			<i>15R asf1Δ0::KANMX trp1Δ63 [pDM9=HHT1-</i>		
			<i>HHF1 URA3 CEN]</i>		
			<i>his3Δ(1 or 200) lys2-(128δ or 0) leu2Δ(0 or 1)</i>		
GHY	2422	b	<i>ura3(Δ0 or -52) hht2-15R, rad6Δ0::KAN,</i>	Hartzog Lab	3
			<i>[pDM9=HHT1-HHF1 URA3 CEN]</i>		
			<i>his3Δ(1 or 200) leu2Δ(0 or 1) ura3(Δ0 or -52)</i>		
GHY	2425	a	<i>trp1Δ63 cac1Δ::KANMX (hht1-hhf1)Δ::LEU2</i>	Hartzog Lab	3
			<i>hht2-15R [pDM9=HHT1-HHF1 URA3]</i>		
			<i>his3Δ200 lys2-128δ leu2(Δ1 or 0) ura3(-52 or</i>		
			<i>Δ0) trp1Δ63 (hht1-hhf1)Δ::LEU2 (hht2-</i>		
GHY	2431		<i>hhf2)Δ::NAT suppl pGAL1-FLO8-</i>	Hartzog Lab	3
			<i>HIS3::KANMX [pDM9=URA3 CEN HHT1-</i>		
			<i>HHF1]</i>		
			<i>his3Δ(200 or 1) lys2-128δ leu2Δ(0 or 1) ura3(-</i>		
GHY	2437	a	<i>52 or Δ0) trp1Δ63 (hht1-hhf1)Δ::LEU2 hht2-</i>	Hartzog Lab	3

			15R <i>rtt106Δ0::KAN pDM9 (=URA3 CEN</i>		
			<i>HHT1-HHF1)</i>		
			<i>his3Δ200 lys2-128δ leu2Δ1 ura3-52</i>		
GHY	2440	b	<i>trp1Δ63 chd1Δ::HIS3</i>	Hartzog Lab	3
			<i>(hht1-hhf1)Δ::LEU2 hht2-15R</i>		
			<i>his3Δ200 lys2-128δ leu2Δ(0 or 1) trp1Δ63</i>		
GHY	2441	a	<i>ura3(-52 or 0) (hht1-hhf1)Δ::LEU2 hht2-15R</i>	Hartzog Lab	3
			<i>spt6-50 pDM9</i>		
			<i>his3Δ200 lys2-128δ trp1Δ63 ura3(-52or Δ0)</i>		
GHY	2453	a	<i>leu2Δ(1 or 0) (hht1-hhf1)Δ::LEU2 hht2-15R</i>	Hartzog Lab	3
			<i>dot1Δ0::KAN (pDM9=HHT1-HHF1 URA3)</i>		
			<i>his3Δ200 lys2-128δ trp1Δ63 ura3(-52or Δ0)</i>		
GHY	2455	b	<i>leu2Δ(1 or 0) (hht1-hhf1)Δ::LEU2 hht2-15R</i>	Hartzog Lab	3
			<i>set1Δ0::KAN (pDM9=HHT1-HHF1 URA3)</i>		
			<i>his3Δ200 lys2-128δ trp1Δ63 ura3(-52or Δ0)</i>		
GHY	2457	a	<i>leu2Δ(1 or 0) (hht1-hhf1)Δ::LEU2 hht2-15R</i>	Hartzog Lab	3
			<i>set2Δ0::KAN (pDM9=HHT1-HHF1 URA3)</i>		
			<i>his3Δ200 lys2-128δ leu2Δ(0 or 1) trp1Δ63</i>		
GHY	2471	a	<i>ura3(-52 or 0) (hht1-hhf1)Δ::LEU2 hht2-15R</i>	Hartzog Lab	3
			<i>rtt109Δ0::KAN pDM9</i>		
			<i>his3Δ(200 or 1) lys2-(128δ op 0) leu2Δ(1 or 0)</i>		
GHY	2491	a	<i>ura3(-52 or 0) trp1Δ63 (hht1-hhf1)Δ::LEU2</i>	Hartzog Lab	3
			<i>hht2-15R ahc1D::KANMX pDM9</i>		
			<i>his3Δ(200 or 1) lys2-128δ leu2Δ(1 or 0) ura3(-</i>		
GHY	2497	a	<i>52 or 0) trp1Δ63 (hht1-hhf1)Δ::LEU2 hht2-15R</i>	Hartzog Lab	3
			<i>hir1Δ0::KAN pDM9</i>		

GHY	2573	a	<i>his3Δ200 leu2(Δ1 or 0) lys2-128δ ura3(-52 or Δ0) trp1Δ63 (hht1-hhf1)Δ::LEU2 hht2-15R spt16-197 chd1Δ::HIS3 [pDM9=(HHT1-HHF1)URA3]</i>	Hartzog Lab	3
GHY	2588	b	<i>his3Δ200 lys2-128δ leu2Δ(0 or 1 or Δ::PET56) ura3(-52 or Δ0) trp1Δ63 (hht1-hhf1)Δ::LEU2 hht2-15R gcn5Δ::KAN chd1Δ::HIS3 pDM9 (=URA3 CEN HHT1-HHF1)</i>	Hartzog Lab	3
GHY	2591	b	<i>his3Δ(1 or 200) lys2-(128δ or 0) leu2Δ(0 or 1) ura3(Δ0 or -52) hht2-15R rad6Δ0::KAN chd1Δ::HIS3 [pDM9=HHT1-HHF1 URA3 CEN]</i>	Hartzog Lab	3
GHY	2593	b	<i>his3Δ(200 or 1) lys2-128δ leu2Δ(0 or 1) ura3(-52 or Δ0) trp1Δ63 (hht1-hhf1)Δ::LEU2 ada3Δ0::KanMX chd1Δ::HIS3 hht2-15R pDM9</i>	Hartzog Lab	3
GHY	2599	b	<i>his3Δ200 lys2-128d trp1Δ63 ura3(-52or Δ0) leu2Δ(1 or 0) (hht1-hhf1)Δ::LEU2 hht2-15R dot1Δ0::KAN chd1Δ::HIS3 (pDM9=HHT1-HHF1 URA3)</i>	Hartzog Lab	3
GHY	2601	b	<i>his3Δ200 lys2-128d trp1Δ63 ura3(-52or Δ0) leu2Δ(1 or 0) (hht1-hhf1)Δ::LEU2 hht2-15R set2Δ0::KAN chd1Δ::HIS3 (pDM9=HHT1-HHF1 URA3)</i>	Hartzog Lab	3
GHY	2603	a	<i>his3Δ200 lys2-128d trp1Δ63 ura3(-52or Δ0) leu2Δ(1 or 0) (hht1-hhf1)Δ::LEU2 hht2-15R</i>	Hartzog Lab	3

			<i>set1Δ0::KAN chd1Δ::HIS3 (pDM9=HHT1-HHF1 URA3)</i>		
			<i>his3Δ(1 or 200) lys2-128d leu2Δ(0 or 1)</i>		
GHY	2611	a	<i>ura3(Δ0 or -52) trp1Δ63 hpc2Δ0::KANMX (hht1-hhf1)Δ::LEU2 hht2-15R pDM9(=HHT1-HHF1 URA3 CEN)</i>	Hartzog Lab	3
			<i>his3Δ200 lys2-128δ? leu2Δ1 ura3-52</i>		
GHY	2687	a	<i>met15D0? (hht1-hhf1)Δ::LEU2 hht2-15R sgfΔ73::KanMX pDM9</i>	Hartzog Lab	3
			<i>his3Δ200 lys2-128δ? leu2Δ1 ura3-52</i>		
GHY	2689	a	<i>met15D0? (hht1-hhf1)Δ::LEU2 hht2-15R sgfΔ29::KanMX pDM9</i>	Hartzog Lab	3
			<i>his3Δ200 lys2-128δ leu2Δ(0 or 1) trp1Δ63?</i>		
GHY	3059	a	<i>ura3(-52 or 0) (hht1-hhf1)Δ::LEU2 ubp8Δ::KanMX sgf73Δ::NatMX hht2-15R</i>	Hartzog Lab	3
			<i>his3Δ200 lys2-128δ leu2Δ(0 or 1) ura3(-52 or</i>		
GHY	3294	b	<i>Δ0) trp1Δ63 (hht1-hhf1)Δ::LEU2 hht2-15R suppE::NatMX rad6Δ0::KanMX</i>	Hartzog Lab	3
			<i>his3Δ200 lys2-128δ leu2Δ1 ura3-52</i>		
GHY	1998	a	<i>chd1Δ::HIS3 pGAL1-FLO8-HIS3::KANMX</i>	Hartzog Lab	3
			<i>his3Δ200 lys2-128δ leu2Δ1 ura3-52 trp1Δ63</i>		
GHY	2682	b	<i>chd1Δ::chd1W932A pGAL1-FLO8-HIS3::KANMX</i>	Hartzog Lab	3
			<i>his3Δ200 lys2-128δ leu2Δ1 ura3-52 trp1Δ63</i>		
GHY	2740	b	<i>spt5Δ4::TRP1 pGAL1-FLO8-HIS3::KANMX [pMS4]</i>	Hartzog Lab	3

			<i>his3Δ200 lys2-128δ leu2Δ(0 or 1) ura3(-52 or</i>		
GHY	3277	a	<i>Δ0) trp1Δ63 (hht1-hhf1)Δ::LEU2 hht2-15R</i>	Hartzog Lab	3
			<i>suppE::NatMX sac3Δ0::KanMX</i>		
			<i>his3D1 leu2D0 ura3D0 hfi1D::KANMX</i>		
GHY	3182	b	<i>sac3Δ::NatMX [pmD1=URA3 CEN HFI1]</i>	Hartzog Lab	3
			<i>his3D1 lys2-128δ leu2(D0 or 1) ura3D0 suppE</i>		
GHY	3187	a	<i>sac3Δ::NatMX</i>	Hartzog Lab	3
			<i>his3Δ200 lys2-128δ leu2Δ(0 or 1) trp1Δ63</i>		
GHY	3188	a	<i>ura3(-52 or 0) (hht1-hhf1)Δ::LEU2 hht2-15R</i>	Hartzog Lab	3
			<i>sac3Δ::KanMX pDM9</i>		
			<i>HA-SPT7-TAP::TRP1 ura3Δ0 leu2Δ1 trp1Δ63</i>		
GHY	3009	a	<i>his3Δ200 ada1Δ::HIS3 lys2-173R2 his4-917δ</i>	Hartzog Lab	3
			<i>pMD1</i>		
			<i>HA-SPT7-TAP::TRP1 ura3Δ0 leu2Δ1 trp1Δ63</i>		
GHY	3011	a	<i>his3Δ200 ada1Δ::HIS3 lys2-173R2 his4-917δ</i>	Hartzog Lab	3
			<i>pMD52</i>		
			<i>HA-SPT7-TAP::TRP1 ura3Δ0 leu2Δ1 trp1Δ63</i>		
GHY	3013	a	<i>his3Δ200 ada1Δ::HIS3 lys2-173R2 his4-917δ</i>	Hartzog Lab	3
			<i>pRS416</i>		
			<i>his3Δ200 lys2-128δ leu2Δ1 ura3-52</i>		
GHY	3296	b	<i>trp1Δ63 spt5-242 pGAL1-FLO8-</i>	Hartzog Lab	A1- 1
			<i>HIS3::NatMX</i>		
			<i>his4-912d lys2-128d leu2d1 ura3-52 trp1d63</i>		
GHY	3180	a	<i>spt6::LEU2 spt5-242::NAT (pCC11)</i>	Hartzog Lab	A1- 1

			<i>his4-912δ lys2-128δ trp1Δ63 ura3-52 leu2Δ1</i>		
GHY	3265	b	<i>spt16D::KanMX spt5-242::NAT</i> <i>(pcc58)</i>	Hartzog Lab	A1- 1
			<i>his3D(1 or 200) lys2-128d leu2D(0 or 1)</i>		
GHY	2730	b	<i>ura3(D0 or -52) trp1D63 spt5D4::TRP1</i> <i>ppr2D0::KAN [pMS4=SPT5 URA3 CEN]</i>	Hartzog Lab	A1- 1
			<i>his3Δ200 lys2-128δ leu2Δ1 ura3-52 trp1Δ63</i>		
GHY	2875	a	<i>spt5Δ4::TRP1 hir1 Δ::KANMX [pMS4]</i>	Hartzog Lab	A1- 1

Appendix - 4

Materials and Methods

Media and yeast genetic methods

All yeast media used is made as described previously (rose) and all strain construction methods were standard methods (rose). *S. Cerevisiae* strains used in this study are isogenic to S288C and are *GAL2+*(winston) and are listed in supporting information Table S1.

To integrate *hht2* mutants a 5-FOA/*URA3* counterselection strategy was used. The *HHT2* ORF in GHY-619 was recombined out in a high-efficiency transformation protocol and replaced with a PCR product that amplified the *URA3* sequence from pRS404 with flanking homology arms to DNA upstream (OGH-672) and downstream (OGH-673) the *HHT2* ORF. Transformants were plated on SC-URA and then screened via PCR for successful integration. This GHY-619 *hht2D1::URA3* intermediate strain was crossed to GHY-836 to generate the master histone H3 *hht2* integration strain GHY-1779. All histone H3 *hht2* mutants generated in this study are derivatives of plasmid pJH18 and selected mutants for integration were digested with either *BaeI* and *SaII* or *EagI* and *SaII* to generate a *hht2* dropout fragment for *URA3* replacement by replica plating to 5-FOA. PCR verified *hht2* integrants were crossed with GHY-823 and sequenced to ensure no new histone H3 or any histone H4 mutations were introduced during transformation.

Yeast strains GHY-2625 and GHY-2630 were generated by a series of homologous recombination events via high-efficiency transformation and a meiotic cross. First *PHO5* was replaced with *URA3* by transforming GHY-836 with *NotI* digested plasmid pM51.1 and plated to SC-URA. A Ura+ *pho5D::URA3* recombinant was identified by PCR and subsequently transformed with *NotI* digested plasmid pM53.1 containing the *PHO5-GC* cassette. Transformants that had replaced *pho5D::URA3* with *PHO5-GC* were selected on 5-FOA and verified by PCR. This intermediate strain was crossed with the below intermediate strain. The *LEU2* marker in GHY-1893 was switched to *NatMX* by transformation with (*hht1-hhf1*)*D::NatMX* PCR product amplified from OY410 genomic DNA. Leu- and Nat+ cells were transformed with *EcoRI* digested plasmid pM67.6 and plated to SC-HIS to replace *PHO80* with *HIS3*.

Isolation of *spt5* cryptic initiation mutants and *spt6* or *spt16* mutants that genetically suppress *spt5-242* was done with hydroxylamine mutagenized plasmids (rose).

Plasmids

A detailed list of the plasmids used in this study is listed in supporting information Table S2. To generate mutagenized histone H3 containing plasmids a recombination based approach was used. Plasmid pJH18 (*HHT2-HHF2 CEN TRP1*) was digested with *SalI* and *BamHI* to create a gapped plasmid backbone lacking *HHT2*. Separately, *HHT2* was PCR amplified from pJH18 under mutagenic conditions (Taq polymerase, 125 uM MnCl₂, 40 cycles: 94°C for 45 seconds, 55°C for 30 seconds, and 72°C for 2 minutes) using primer pair OGH587/OGH588 amplified. The pJH18 PCR mutagenesis template was digested with *MfeI* and *SacI* to prevent intact pJH18 from being transformed into yeast in subsequent steps. The mutagenized *hht2* amplicons contained ~200 bp of DNA overhangs homologous to the *SalI/BamHI* gapped pJH18. Equal masses of gapped pJH18 and mutagenized *hht2* DNA were co-transformed into yeast strains GHY842 and GHY843 and plated on SC-TRP

media. Candidate *hht2* suppressors were identified by replica plating to 15°C for growth at the restrictive temperature (both before and after plating to 5FOA). Colonies that grew at 15°C were purified, retested, and plasmids were rescued, and re-transformed to GHY842 or GHY843 to confirm that the Cs- suppression was plasmid linked. DNA sequencing was performed to identify the H3 mutations and confirm that the H4 gene on these plasmids still carried the wildtype sequence.

Plasmids pGH327, pGH328 and pGH329 were generated by a PCR mutagenesis, using oligonucleotides that randomized one codon at a time.

Plasmid pMD73 was generated by digesting plasmids pJH18-AO6 and pHHT2-K9,14,18,23R with *Bcl*I and *Bam*HI to drop out a 206 bp fragment containing 21 bp of *HHT2* promoter DNA up *HHT2-L61* sequence. The large plasmid backbone from the pJH18-AO6 containing *hht2-S87P*, *G90S* sequence was ligated with the 206 bp dropout from pHHT2-K19,14,18,23R containing the histone tail mutations and successful ligations were verified by sequencing.

Plasmids pGH356 (*hht2-S87A*; *yH3.3*), pGH359 (*hht2-T118I*), and pMD7 (*hht2-S31A*) were generated by site directed mutagenesis of pJH18. Plasmid pGH374 (*hht2-S31A,I89V,G90M*; *yH3.1*) was generated by site directed mutagenesis of plasmid pMD7.

Mono-nucleosome preparation

Yeast strains GHY835 and GHY1895 were grown overnight to mid log phase ($2 - 2.3 \times 10^7$ cells/ml) in 200 ml of YPD, cross-linked at room temperature for 15 minutes by adding formaldehyde to a final concentration of 1%, and quenched with 0.125 M glycine for 5-10 minutes. Cells were washed twice with ice cold PBS and stored at -80°C.

MNase titrations and recovery of digested DNA were carried out as previously described by Yuan et. al. 2005, with few modifications. Briefly, spheroplasts were prepared by first re-suspending defrosted cell pellets in Zymolyase Buffer (1 M Sorbitol, 50 mM Tris-HCl pH 7.4,

10 mM β-mercaptoethanol), then Zymolyase 100T was added to a final concentration of 0.25 mg/ml and cells were incubated at 30°C with 200 rpm shaking for 20-40 min. Spheroplasted cells were monitored until their measured OD_{600nm} (30 µl cell-reaction in 1 ml of 1% SDS) was 10-20% of the initial reading. Spheroplasts were washed with Zymolyase Buffer, re-suspended in NP-buffer (1 M Sorbitol, 50 mM NaCl, 10 mM Tris-HCl pH 7.4, 5 mM MgCl₂, 1 mM CaCl₂; 0.075% NP-40, 1 mM β-mercaptoethanol, and 0.5 mM spermidine added fresh) and split into five equal aliquots for titrated MNase digestions. MNase (S7 nuclease Roche), previously dissolved and stored in Dilution Buffer (50 mM Tris-HCl pH 7.4, 50 mM NaCl, 10 mM MgCl₂, 50% glycerol), was added at amounts ranging from 10U to 25U. Digestions were carried out at 37°C for 20 minutes and stopped with the addition of 50 mM EDTA and 5% SDS (10 mM EDTA and 1% SDS final concentration). To isolate MNase digested DNA fragments, 3 µl of 20 mg/ml proteinase K were added and proteins digested for 1 h at 55°C in a water bath, followed by an overnight incubation at 65°C to reverse formaldehyde cross-linking. DNA was phenol-chloroform-isoamyl alcohol (25:24:1) extracted, washed with chloroform and ethanol precipitated. Resuspended DNA was treated with DNase-free RNase at 37°C for 30 min, phenol-chloroform extracted, washed with chloroform, precipitated with ethanol, re-suspended in 50 µl of MQ water and stored at -80°C.

Mononucleosomal DNA was obtained by gel-purification using a modified protocol described in Shivaswamy et. al. 2008. In brief, MNase digested DNA samples were examined by gel electrophoresis and titrations which generated 80-90% mononucleosome sized DNA were chosen to be resolved on a 1.8% Low Range Ultra Pure Agarose gel in TAE buffer, alongside a 100 bp ladder, for 2 hr at 100 V. The 150-200 bp mononucleosomal size band was excised under long UV wavelength, transferred to a LoBind microcentrifuge tube and processed following the NucleoSpin Gel Extraction and PCR Clean-up kit (Macherey-Nagel) with the following modifications: NT1 buffer was added at a ratio of 4X volume to 1X volume of the gel slice and incubations were at room temperature for 30-45 min.

Genome-wide mapping of mono-nucleosomes

Mononucleosome sized DNA fragments were prepared for paired-end Illumina Sequencing, with the adapter ligated library going through 14 rounds of PCR amplification. Briefly, 150-200 ng purified mononucleosomal DNA were end repaired with 4.5U T4 DNA Polymerase, 2.5U Klenow Fragment and 25U T4 PNK at 20°C for 30 min and purified with a NucleoSpin column. End-repaired DNA was A-tailed with 15 units of Klenow exo- at 37°C for 30 min, NucleoSpin column purified, and then ligated at 25°C for 15 min with Illumina adapters and Quick T4 DNA ligase. Reactions were purified with a NucleoSpin column and resolved in a 1.8% Low Range Ultra Pure Agarose gel. A ~280 bp band corresponding to the ligated mononucleosomal DNA fragments was cut out of the gel, purified using a NucleoSpin Gel Extraction Kit with the modifications previously described, and stored at -80°C until needed. To amplify the mononucleosomal DNA library, 1U of Pfx enzyme (Invitrogen) and empirically determined diluted template that amplifies within the linear PCR range for 14 cycles were used. Amplified libraries were purified with a NucleoSpin column, visualized with a BioAnalyzer and quantified by qPCR before subjecting them to Illumina sequencing at the UCSC Berkeley Sequencing Facility.

Nucleosomes were mapped using DANPOS2 with standard settings.

Software and bioinformatic analysis

Simple bedtools commands were used to generate annotated genesets or identify nucleosome dyads over the transcription unit. A simplified python script from Heijden T. van der et al. was used to calculate the predicted kT of nucleosome formation across the yeast genome with the following parameters set: $w = 147$, $p = 10.1$, and $b = 0.2$. DANPOS2 was used to calculate the MNase or kT average for the displayed data. R-studio and ggplot2 were used to generate MNase and predicted kT of nucleosome formation figures. Chimera was used for protein structure figures.

***PHO5* single molecule analysis**

Chromatin ring purification, trimethylpsoralen crosslinking and denaturation, and electron microscopy were performed as previously described (Brown *et al.* 2013, 2015).

Briefly: The *PHO5* gene was engineered to have flanking DNA recombination sequences (RS) and an internal bacterial LexA DNA binding domain. Chromatinized *PHO5* genes were recombined out of the genome in vivo by galactose-controlled RS recombinase expression and then affinity purified with a LexA-TAP tagged protein. The purified *PHO5* chromatin was incubated with psoralen and UV-light irradiated, to crosslink DNA which is not wrapped around nucleosomes. Following deproteinization and DNA denaturation, the *PHO5* gene DNA is observed by electron microscopy and appears as a contiguous series of single stranded DNA 'bubbles' (DNA that is wrapped around nucleosomes) and double stranded DNA 'linear' segments (psoralen/UV crosslinked DNA not wrapped around nucleosomes). Pretreatment of purified psoralen UV-crosslinked DNA with a restriction enzyme that cuts in the RS gives a stereotyped structure at the 3' end of the *PHO5* gene and allows for a position specific record of nucleosomal or non-nucleosomal DNA on an electron micrograph

To test for nucleosome loss on individual copies of *PHO5*, we examined each molecule and extracted all 'linear' DNA that has a base pair length between 87 and 167 nucleotides in our single molecule datasets.

Custom python scripts were used to convert the hand-traced ImageJ files into a directional sequence of contiguous nucleosomal or non-nucleosomal associated DNA segments from the promoter to the pA site of the *PHO5* gene for computational analysis or data plotting data in figures 7B and 7C.

Purification of SAGA complexes

SAGA was purified as previously described (Wu and Winston 2002). Strain GHY-3009 was used to purify wild type *HFI1* complexes, strain GHY-3011 was used to purify *hfi1-L305P* complexes, and strain GHY-3013 was used to purify *hfi1Δ* complexes.

A gradient acrylamide gel was used with standard silver staining procedures. Mass-spec analysis was performed in collaboration with the John R Yates III lab.

References

- Ahmad K., and S. Henikoff, 2002 The Histone Variant H3.3 Marks Active Chromatin by Replication-Independent Nucleosome Assembly. *Mol. Cell* 9: 1191–1200. [https://doi.org/10.1016/S1097-2765\(02\)00542-7](https://doi.org/10.1016/S1097-2765(02)00542-7)
- Annunziato A. T., and J. C. Hansen, 2018 Role of Histone Acetylation in the Assembly and Modulation of Chromatin Structures. *Gene Expr.* 9: 37–61.
- Armache J. P., N. Gamarra, S. L. Johnson, J. D. Leonard, S. Wu, *et al.*, 2019 Cryo-EM structures of remodeler-nucleosome intermediates suggest allosteric control through the nucleosome, (C. Wolberger, S. H. Scheres, and S. H. Scheres, Eds.). *eLife* 8: e46057. <https://doi.org/10.7554/eLife.46057>
- Artsimovitch I., and R. Landick, 2002 The Transcriptional Regulator RfaH Stimulates RNA Chain Synthesis after Recruitment to Elongation Complexes by the Exposed Nontemplate DNA Strand. *Cell* 109: 193–203. [https://doi.org/10.1016/S0092-8674\(02\)00724-9](https://doi.org/10.1016/S0092-8674(02)00724-9)
- Badjatia N., M. J. Rossi, A. R. Bataille, C. Mittal, W. K. M. Lai, *et al.*, 2021 Acute stress drives global repression through two independent RNA polymerase II stalling events in *Saccharomyces*. *Cell Rep.* 34: 108640. <https://doi.org/10.1016/j.celrep.2020.108640>
- Bailey K. A., F. Marc, K. Sandman, and J. N. Reeve, 2002 Both DNA and histone fold sequences contribute to archaeal nucleosome stability. *J. Biol. Chem.* 277: 9293–9301. <https://doi.org/10.1074/jbc.M110029200>
- Balasubramanian R., M. G. Pray-Grant, W. Selleck, P. A. Grant, and S. Tan, 2002 Role of the Ada2 and Ada3 Transcriptional Coactivators in Histone Acetylation *. *J. Biol. Chem.* 277: 7989–7995. <https://doi.org/10.1074/jbc.M110849200>
- Baluapuri A., J. Hofstetter, N. Dudvarski Stankovic, T. Endres, P. Bhandare, *et al.*, 2019 MYC Recruits SPT5 to RNA Polymerase II to Promote Processive Transcription Elongation. *Mol. Cell* 74: 674-687.e11. <https://doi.org/10.1016/j.molcel.2019.02.031>
- Bannister A. J., and T. Kouzarides, 2011 Regulation of chromatin by histone modifications. *Cell Res.* 21: 381–395. <https://doi.org/10.1038/cr.2011.22>

- Baptista T., S. Grünberg, N. Minoungou, M. J. E. Koster, H. T. M. Timmers, *et al.*, 2017 SAGA Is a General Cofactor for RNA Polymerase II Transcription. *Mol. Cell* 68: 130-143.e5. <https://doi.org/10.1016/j.molcel.2017.08.016>
- Barba-Aliaga M., P. Alepuz, and J. E. Pérez-Ortín, 2021 Eukaryotic RNA Polymerases: The Many Ways to Transcribe a Gene. *Front. Mol. Biosci.* 8: 663209. <https://doi.org/10.3389/fmolb.2021.663209>
- Bernecky C., J. M. Plitzko, and P. Cramer, 2017 Structure of a transcribing RNA polymerase II–DSIF complex reveals a multidentate DNA–RNA clamp. *Nat. Struct. Mol. Biol.* 24: 809–815. <https://doi.org/10.1038/nsmb.3465>
- Bhat W., G. Boutin, A. Rufiange, and A. Nourani, 2013 Casein kinase 2 associates with the yeast chromatin reassembly factor Spt2/Sin1 to regulate its function in the repression of spurious transcription. *Mol. Cell. Biol.* 33: 4198–4211. <https://doi.org/10.1128/MCB.00525-13>
- Bhaumik S. R., and M. R. Green, 2001 SAGA is an essential in vivo target of the yeast acidic activator Gal4p. *Genes Dev.* 15: 1935–1945. <https://doi.org/10.1101/gad.911401>
- Bian C., C. Xu, J. Ruan, K. K. Lee, T. L. Burke, *et al.*, 2011 Sgf29 binds histone H3K4me2/3 and is required for SAGA complex recruitment and histone H3 acetylation. *EMBO J.* 30: 2829–2842. <https://doi.org/10.1038/emboj.2011.193>
- Biernat E., J. Kinney, K. Dunlap, C. Rizza, and C. K. Govind, 2021 The RSC complex remodels nucleosomes in transcribed coding sequences and promotes transcription in *Saccharomyces cerevisiae*. *Genetics* 217: iyab021. <https://doi.org/10.1093/genetics/iyab021>
- Bintu L., M. Kopaczynska, C. Hodges, L. Lubkowska, M. Kashlev, *et al.*, 2011 The elongation rate of RNA polymerase determines the fate of transcribed nucleosomes. *Nat. Struct. Mol. Biol.* 18: 1394–1399. <https://doi.org/10.1038/nsmb.2164>
- Bintu L., T. Ishibashi, M. Dangkulwanich, Y.-Y. Wu, L. Lubkowska, *et al.*, 2012 Nucleosomal elements that control the topography of the barrier to transcription. *Cell* 151: 738–749. <https://doi.org/10.1016/j.cell.2012.10.009>
- Blythe A. J., B. Yazar-Klosinski, M. W. Webster, E. Chen, M. Vandevenne, *et al.*, 2016 The yeast transcription elongation factor Spt4/5 is a sequence-specific RNA binding protein. *Protein Sci.* 25: 1710–1721. <https://doi.org/10.1002/pro.2976>
- Boeger H., J. Griesenbeck, J. S. Strattan, and R. D. Kornberg, 2004 Removal of promoter nucleosomes by disassembly rather than sliding in vivo. *Mol. Cell* 14: 667–673. <https://doi.org/10.1016/j.molcel.2004.05.013>

- Bondarenko V. A., L. M. Steele, A. Újvári, D. A. Gaykalova, O. I. Kulaeva, *et al.*, 2006 Nucleosomes Can Form a Polar Barrier to Transcript Elongation by RNA Polymerase II. *Mol. Cell* 24: 469–479. <https://doi.org/10.1016/j.molcel.2006.09.009>
- Bonnet J., C.-Y. Wang, T. Baptista, S. D. Vincent, W.-C. Hsiao, *et al.*, 2014 The SAGA coactivator complex acts on the whole transcribed genome and is required for RNA polymerase II transcription. *Genes Dev.* 28: 1999–2012. <https://doi.org/10.1101/gad.250225.114>
- Booth G. T., I. X. Wang, V. G. Cheung, and J. T. Lis, 2016 Divergence of a conserved elongation factor and transcription regulation in budding and fission yeast. *Genome Res.* 26: 799–811. <https://doi.org/10.1101/gr.204578.116>
- Brown C. R., C. Mao, E. Falkovskaia, M. S. Jurica, and H. Boeger, 2013 Linking stochastic fluctuations in chromatin structure and gene expression. *PLoS Biol.* 11: e1001621. <https://doi.org/10.1371/journal.pbio.1001621>
- Brown C. R., J. A. Eskin, S. Hamperl, J. Griesenbeck, M. S. Jurica, *et al.*, 2015 Chromatin structure analysis of single gene molecules by psoralen cross-linking and electron microscopy. *Methods Mol. Biol. Clifton NJ* 1228: 93–121. https://doi.org/10.1007/978-1-4939-1680-1_9
- Burckin T., R. Nagel, Y. Mandel-Gutfreund, L. Shiue, T. A. Clark, *et al.*, 2005 Exploring functional relationships between components of the gene expression machinery. *Nat. Struct. Mol. Biol.* 12: 175–182. <https://doi.org/10.1038/nsmb891>
- Burgess R. J., H. Zhou, J. Han, and Z. Zhang, 2010 A role for Gcn5 in replication-coupled nucleosome assembly. *Mol. Cell* 37: 469–480. <https://doi.org/10.1016/j.molcel.2010.01.020>
- Buszczak M., S. Paterno, and A. C. Spradling, 2009 *Drosophila* Stem Cells Share a Common Requirement for the Histone H2B Ubiquitin Protease Scrawny. *Science* 323: 248–251. <https://doi.org/10.1126/science.1165678>
- Carey M., B. Li, and J. L. Workman, 2006 RSC exploits histone acetylation to abrogate the nucleosomal block to RNA polymerase II elongation. *Mol. Cell* 24: 481–487. <https://doi.org/10.1016/j.molcel.2006.09.012>
- Chandrasekharan M. B., F. Huang, and Z.-W. Sun, 2009 Ubiquitination of histone H2B regulates chromatin dynamics by enhancing nucleosome stability. *Proc. Natl. Acad. Sci.* 106: 16686–16691. <https://doi.org/10.1073/pnas.0907862106>
- Chandrasekharan M. B., F. Huang, and Z.-W. Sun, 2010 Histone H2B ubiquitination and beyond: Regulation of nucleosome stability, chromatin dynamics and the trans-

- histone H3 methylation. *Epigenetics* 5: 460–468.
<https://doi.org/10.4161/epi.5.6.12314>
- Chang C.-H., and D. S. Luse, 1997 The H3/H4 Tetramer Blocks Transcript Elongation by RNA Polymerase II in Vitro *. *J. Biol. Chem.* 272: 23427–23434.
<https://doi.org/10.1074/jbc.272.37.23427>
- Chatterjee N., D. Sinha, M. Lemma-Dechassa, S. Tan, M. A. Shogren-Knaak, *et al.*, 2011 Histone H3 tail acetylation modulates ATP-dependent remodeling through multiple mechanisms. *Nucleic Acids Res.* 39: 8378–8391. <https://doi.org/10.1093/nar/gkr535>
- Chen S., A. Rufiange, H. Huang, K. R. Rajashankar, A. Nourani, *et al.*, 2015 Structure–function studies of histone H3/H4 tetramer maintenance during transcription by chaperone Spt2. *Genes Dev.* 29: 1326–1340. <https://doi.org/10.1101/gad.261115.115>
- Chen Z., R. Gabizon, A. I. Brown, A. Lee, A. Song, *et al.*, 2019 High-resolution and high-accuracy topographic and transcriptional maps of the nucleosome barrier. *eLife* 8: e48281. <https://doi.org/10.7554/eLife.48281>
- Cheng B., and D. H. Price, 2008 Analysis of factor interactions with RNA polymerase II elongation complexes using a new electrophoretic mobility shift assay. *Nucleic Acids Res.* 36: e135. <https://doi.org/10.1093/nar/gkn630>
- Cheung V., G. Chua, N. N. Batada, C. R. Landry, S. W. Michnick, *et al.*, 2008 Chromatin- and Transcription-Related Factors Repress Transcription from within Coding Regions throughout the *Saccharomyces cerevisiae* Genome. *PLOS Biol.* 6: e277.
<https://doi.org/10.1371/journal.pbio.0060277>
- Chiu Y.-L., C. K. Ho, N. Saha, B. Schwer, S. Shuman, *et al.*, 2002 Tat stimulates cotranscriptional capping of HIV mRNA. *Mol. Cell* 10: 585–597.
[https://doi.org/10.1016/s1097-2765\(02\)00630-5](https://doi.org/10.1016/s1097-2765(02)00630-5)
- Clark-Adams C. D., and F. Winston, 1987 The SPT6 gene is essential for growth and is required for delta-mediated transcription in *Saccharomyces cerevisiae*. *Mol. Cell. Biol.* 7: 679–686. <https://doi.org/10.1128/mcb.7.2.679-686.1987>
- Clark-Adams C. D., D. Norris, M. A. Osley, J. S. Fassler, and F. Winston, 1988 Changes in histone gene dosage alter transcription in yeast. *Genes Dev.* 2: 150–159.
<https://doi.org/10.1101/gad.2.2.150>
- Crickard J. B., J. Fu, and J. C. Reese, 2016 Biochemical Analysis of Yeast Suppressor of Ty 4/5 (Spt4/5) Reveals the Importance of Nucleic Acid Interactions in the Prevention of RNA Polymerase II Arrest*♦. *J. Biol. Chem.* 291: 9853–9870.
<https://doi.org/10.1074/jbc.M116.716001>

- Crickard J. B., J. Lee, T.-H. Lee, and J. C. Reese, 2017 The elongation factor Spt4/5 regulates RNA polymerase II transcription through the nucleosome. *Nucleic Acids Res.* 45: 6362–6374. <https://doi.org/10.1093/nar/gkx220>
- Dame R. T., and M. Tark-Dame, 2016 Bacterial chromatin: converging views at different scales. *Curr. Opin. Cell Biol.* 40: 60–65. <https://doi.org/10.1016/j.ceb.2016.02.015>
- Decker T.-M., 2020 Mechanisms of Transcription Elongation Factor DSIF (Spt4-Spt5). *J. Mol. Biol.* 166657. <https://doi.org/10.1016/j.jmb.2020.09.016>
- Diamant G., A. Bahat, and R. Dikstein, 2016 The elongation factor Spt5 facilitates transcription initiation for rapid induction of inflammatory-response genes. *Nat. Commun.* 7: 11547. <https://doi.org/10.1038/ncomms11547>
- Diebold M.-L., M. Koch, E. Loeliger, V. Cura, F. Winston, *et al.*, 2010a The structure of an Iws1/Spt6 complex reveals an interaction domain conserved in TFIIIS, Elongin A and Med26. *EMBO J.* 29: 3979–3991. <https://doi.org/10.1038/emboj.2010.272>
- Diebold M.-L., E. Loeliger, M. Koch, F. Winston, J. Cavarelli, *et al.*, 2010b Noncanonical tandem SH2 enables interaction of elongation factor Spt6 with RNA polymerase II. *J. Biol. Chem.* 285: 38389–38398. <https://doi.org/10.1074/jbc.M110.146696>
- Dijk E. L. van, C. L. Chen, Y. d’Aubenton-Carafa, S. Gourvennec, M. Kwapisz, *et al.*, 2011 XUTs are a class of Xrn1-sensitive antisense regulatory non-coding RNA in yeast. *Nature* 475: 114–117. <https://doi.org/10.1038/nature10118>
- Dion M. F., T. Kaplan, M. Kim, S. Buratowski, N. Friedman, *et al.*, 2007 Dynamics of replication-independent histone turnover in budding yeast. *Science* 315: 1405–1408. <https://doi.org/10.1126/science.1134053>
- Downey M., J. R. Johnson, N. E. Davey, B. W. Newton, T. L. Johnson, *et al.*, 2015 Acetylome profiling reveals overlap in the regulation of diverse processes by sirtuins, gcn5, and esa1. *Mol. Cell. Proteomics MCP* 14: 162–176. <https://doi.org/10.1074/mcp.M114.043141>
- Dronamraju R., J. L. Kerschner, S. A. Peck, A. J. Hepperla, A. T. Adams, *et al.*, 2018 Casein Kinase II Phosphorylation of Spt6 Enforces Transcriptional Fidelity by Maintaining Spn1-Spt6 Interaction. *Cell Rep.* 25: 3476–3489.e5. <https://doi.org/10.1016/j.celrep.2018.11.089>
- Du H.-N., and S. D. Briggs, 2010 A Nucleosome Surface Formed by Histone H4, H2A, and H3 Residues Is Needed for Proper Histone H3 Lys36 Methylation, Histone Acetylation, and Repression of Cryptic Transcription*. *J. Biol. Chem.* 285: 11704–11713. <https://doi.org/10.1074/jbc.M109.085043>

- Duina A. A., and F. Winston, 2004 Analysis of a Mutant Histone H3 That Perturbs the Association of Swi/Snf with Chromatin. *Mol. Cell. Biol.* 24: 561–572. <https://doi.org/10.1128/MCB.24.2.561-572.2004>
- Duina A. A., A. Rufiange, J. Bracey, J. Hall, A. Nourani, *et al.*, 2007 Evidence that the localization of the elongation factor Spt16 across transcribed genes is dependent upon histone H3 integrity in *Saccharomyces cerevisiae*. *Genetics* 177: 101–112. <https://doi.org/10.1534/genetics.106.067140>
- Durairaj G., R. Sen, B. Uprety, A. Shukla, and S. R. Bhaumik, 2014 Sus1p facilitates pre-initiation complex formation at the SAGA-regulated genes independently of histone H2B de-ubiquitylation. *J. Mol. Biol.* 426: 2928–2941. <https://doi.org/10.1016/j.jmb.2014.05.028>
- Durand A., J. Bonnet, M. Fournier, V. Chavant, and P. Schultz, 2014 Mapping the deubiquitination module within the SAGA complex. *Struct. Lond. Engl.* 1993 22: 1553–1559. <https://doi.org/10.1016/j.str.2014.07.017>
- Eberharter A., D. E. Sterner, D. Schieltz, A. Hassan, J. R. Yates, *et al.*, 1999 The ADA complex is a distinct histone acetyltransferase complex in *Saccharomyces cerevisiae*. *Mol. Cell. Biol.* 19: 6621–6631. <https://doi.org/10.1128/MCB.19.10.6621>
- Ehara H., T. Yokoyama, H. Shigematsu, S. Yokoyama, M. Shirouzu, *et al.*, 2017 Structure of the complete elongation complex of RNA polymerase II with basal factors. *Science* 357: 921–924. <https://doi.org/10.1126/science.aan8552>
- Ehara H., T. Kujirai, Y. Fujino, M. Shirouzu, H. Kurumizaka, *et al.*, 2019 Structural insight into nucleosome transcription by RNA polymerase II with elongation factors. *Science* 363: 744–747. <https://doi.org/10.1126/science.aav8912>
- Elsaesser S. J., A. D. Goldberg, and C. D. Allis, 2010 New functions for an old variant: no substitute for histone H3.3. *Curr. Opin. Genet. Dev.* 20: 110–117. <https://doi.org/10.1016/j.gde.2010.01.003>
- Erickson B., R. M. Sheridan, M. Cortazar, and D. L. Bentley, 2018 Dynamic turnover of paused Pol II complexes at human promoters. *Genes Dev.* 32: 1215–1225. <https://doi.org/10.1101/gad.316810.118>
- Evrin C., A. Serra-Cardona, S. Duan, P. P. Mukherjee, Z. Zhang, *et al.*, 2022 Spt5 histone binding activity preserves chromatin during transcription by RNA polymerase II. *EMBO J.* 41: e109783. <https://doi.org/10.15252/embj.2021109783>
- Farnung L., M. Ochmann, M. Engeholm, and P. Cramer, 2021 Structural basis of nucleosome transcription mediated by Chd1 and FACT. *Nat. Struct. Mol. Biol.* 28: 382–387. <https://doi.org/10.1038/s41594-021-00578-6>

- Fazly A., Q. Li, Q. Hu, G. Mer, B. Horazdovsky, *et al.*, 2012 Histone chaperone Rtt106 promotes nucleosome formation using (H3-H4)₂ tetramers. *J. Biol. Chem.* 287: 10753–10760. <https://doi.org/10.1074/jbc.M112.347450>
- Fei J., S. E. Torigoe, C. R. Brown, M. T. Khuong, G. A. Kassavetis, *et al.*, 2015 The prenucleosome, a stable conformational isomer of the nucleosome. *Genes Dev.* 29: 2563–2575. <https://doi.org/10.1101/gad.272633.115>
- Feng J., H. Gan, M. L. Eaton, H. Zhou, S. Li, *et al.*, 2016 Noncoding Transcription Is a Driving Force for Nucleosome Instability in *spt16* Mutant Cells. *Mol. Cell. Biol.* 36: 1856–1867. <https://doi.org/10.1128/MCB.00152-16>
- Ferreira H., A. Flaus, and T. Owen-Hughes, 2007 Histone modifications influence the action of Snf2 family remodelling enzymes by different mechanisms. *J. Mol. Biol.* 374: 563–579. <https://doi.org/10.1016/j.jmb.2007.09.059>
- Fleming A. B., C.-F. Kao, C. Hillyer, M. Pikaart, and M. A. Osley, 2008 H2B ubiquitylation plays a role in nucleosome dynamics during transcription elongation. *Mol. Cell* 31: 57–66. <https://doi.org/10.1016/j.molcel.2008.04.025>
- Fletcher T. M., and J. C. Hansen, 1995 Core Histone Tail Domains Mediate Oligonucleosome Folding and Nucleosomal DNA Organization through Distinct Molecular Mechanisms (*). *J. Biol. Chem.* 270: 25359–25362. <https://doi.org/10.1074/jbc.270.43.25359>
- Francette A. M., S. A. Tripplehorn, and K. M. Arndt, 2021 The Paf1 Complex: A Keystone of Nuclear Regulation Operating at the Interface of Transcription and Chromatin. *J. Mol. Biol.* 433: 166979. <https://doi.org/10.1016/j.jmb.2021.166979>
- Fujinaga K., D. Irwin, Y. Huang, R. Taube, T. Kurosu, *et al.*, 2004 Dynamics of Human Immunodeficiency Virus Transcription: P-TEFb Phosphorylates RD and Dissociates Negative Effectors from the Transactivation Response Element. *Mol. Cell. Biol.* 24: 787–795. <https://doi.org/10.1128/MCB.24.2.787-795.2004>
- Gallego-Sánchez A., S. Andrés, F. Conde, P. A. San-Segundo, and A. Bueno, 2012 Reversal of PCNA Ubiquitylation by Ubp10 in *Saccharomyces cerevisiae*. *PLOS Genet.* 8: e1002826. <https://doi.org/10.1371/journal.pgen.1002826>
- Gangaraju V. K., P. Prasad, A. Srour, M. N. Kagalwala, and B. Bartholomew, 2009 Conformational changes associated with template commitment in ATP-dependent chromatin remodeling by ISW2. *Mol. Cell* 35: 58–69. <https://doi.org/10.1016/j.molcel.2009.05.013>
- Gangloff Y. G., S. Werten, C. Romier, L. Carré, O. Poch, *et al.*, 2000 The human TFIID components TAF(II)135 and TAF(II)20 and the yeast SAGA components ADA1 and

- TAF(II)68 heterodimerize to form histone-like pairs. *Mol. Cell. Biol.* 20: 340–351. <https://doi.org/10.1128/MCB.20.1.340-351.2000>
- Gardner R. G., Z. W. Nelson, and D. E. Gottschling, 2005 Ubp10/Dot4p regulates the persistence of ubiquitinated histone H2B: distinct roles in telomeric silencing and general chromatin. *Mol. Cell. Biol.* 25: 6123–6139. <https://doi.org/10.1128/MCB.25.14.6123-6139.2005>
- Gebala M., S. L. Johnson, G. J. Narlikar, and D. Herschlag, 2019 Ion counting demonstrates a high electrostatic field generated by the nucleosome, (S. Deindl, J. Kuriyan, and R. V. Pappu, Eds.). *eLife* 8: e44993. <https://doi.org/10.7554/eLife.44993>
- Ghoneim M., H. A. Fuchs, and C. A. Musselman, 2021 Histone Tail Conformations: A Fuzzy Affair with DNA. *Trends Biochem. Sci.* 46: 564–578. <https://doi.org/10.1016/j.tibs.2020.12.012>
- Gkikopoulos T., P. Schofield, V. Singh, M. Pinskaya, J. Mellor, *et al.*, 2011 A Role for Snf2-Related Nucleosome-Spacing Enzymes in Genome-Wide Nucleosome Organization. *Science* 333: 1758–1760. <https://doi.org/10.1126/science.1206097>
- Gossett A. J., and J. D. Lieb, 2012 In Vivo Effects of Histone H3 Depletion on Nucleosome Occupancy and Position in *Saccharomyces cerevisiae*. *PLOS Genet.* 8: e1002771. <https://doi.org/10.1371/journal.pgen.1002771>
- Gouot E., W. Bhat, A. Rufiange, E. Fournier, E. Paquet, *et al.*, 2018 Casein kinase 2 mediated phosphorylation of Spt6 modulates histone dynamics and regulates spurious transcription. *Nucleic Acids Res.* 46: 7612–7630. <https://doi.org/10.1093/nar/gky515>
- Grainger D. C., 2016 Structure and function of bacterial H-NS protein. *Biochem. Soc. Trans.* 44: 1561–1569. <https://doi.org/10.1042/BST20160190>
- Grohmann D., J. Nagy, A. Chakraborty, D. Klose, D. Fielden, *et al.*, 2011 The Initiation Factor TFE and the Elongation Factor Spt4/5 Compete for the RNAP Clamp during Transcription Initiation and Elongation. *Mol. Cell* 43: 263–274. <https://doi.org/10.1016/j.molcel.2011.05.030>
- Grover P., J. S. Asa, and E. I. Campos, 2018 H3-H4 Histone Chaperone Pathways. *Annu. Rev. Genet.* 52: 109–130. <https://doi.org/10.1146/annurev-genet-120417-031547>
- Guo M., F. Xu, J. Yamada, T. Egelhofer, Y. Gao, *et al.*, 2008 Core Structure of the Yeast Spt4-Spt5 Complex: A Conserved Module for Regulation of Transcription Elongation. *Structure* 16: 1649–1658. <https://doi.org/10.1016/j.str.2008.08.013>

- Hada A., S. K. Hota, J. Luo, Y.-C. Lin, S. Kale, *et al.*, 2019 Histone Octamer Structure Is Altered Early in ISW2 ATP-Dependent Nucleosome Remodeling. *Cell Rep.* 28: 282-294.e6. <https://doi.org/10.1016/j.celrep.2019.05.106>
- Hainer S. J., and J. A. Martens, 2011 Identification of Histone Mutants That Are Defective for Transcription-Coupled Nucleosome Occupancy. *Mol. Cell. Biol.* 31: 3557–3568. <https://doi.org/10.1128/MCB.05195-11>
- Hainer S. J., B. A. Charsar, S. B. Cohen, and J. A. Martens, 2012 Identification of Mutant Versions of the Spt16 Histone Chaperone That Are Defective for Transcription-Coupled Nucleosome Occupancy in *Saccharomyces cerevisiae*. *G3 Bethesda Md* 2: 555–567. <https://doi.org/10.1534/g3.112.002451>
- Hainer S. J., and J. A. Martens, 2016 Regulation of chaperone binding and nucleosome dynamics by key residues within the globular domain of histone H3. *Epigenetics Chromatin* 9: 17. <https://doi.org/10.1186/s13072-016-0066-4>
- Han M., and M. Grunstein, 1988 Nucleosome loss activates yeast downstream promoters in vivo. *Cell* 55: 1137–1145. [https://doi.org/10.1016/0092-8674\(88\)90258-9](https://doi.org/10.1016/0092-8674(88)90258-9)
- Han Y., J. Luo, J. Ranish, and S. Hahn, 2014 Architecture of the *Saccharomyces cerevisiae* SAGA transcription coactivator complex. *EMBO J.* 33: 2534–2546. <https://doi.org/10.15252/embj.201488638>
- Hartzog G. A., T. Wada, H. Handa, and F. Winston, 1998 Evidence that Spt4, Spt5, and Spt6 control transcription elongation by RNA polymerase II in *Saccharomyces cerevisiae*. *Genes Dev.* 12: 357–369. <https://doi.org/10.1101/gad.12.3.357>
- Hartzog G. A., and J. Fu, 2013 The Spt4–Spt5 complex: A multi-faceted regulator of transcription elongation. *Biochim. Biophys. Acta BBA - Gene Regul. Mech.* 1829: 105–115. <https://doi.org/10.1016/j.bbagr.2012.08.007>
- Hauk G., and G. D. Bowman, 2011 Structural insights into regulation and action of SWI2/SNF2 ATPases. *Curr. Opin. Struct. Biol.* 21: 719–727. <https://doi.org/10.1016/j.sbi.2011.09.003>
- Heijden T. van der, J. J. F. A. van Vugt, C. Logie, and J. van Noort, 2012 Sequence-based prediction of single nucleosome positioning and genome-wide nucleosome occupancy. *Proc. Natl. Acad. Sci.* 109: E2514–E2522. <https://doi.org/10.1073/pnas.1205659109>
- Henneman B., C. van Emmerik, H. van Ingen, and R. T. Dame, 2018 Structure and function of archaeal histones. *PLOS Genet.* 14: e1007582. <https://doi.org/10.1371/journal.pgen.1007582>

- Henriques T., B. S. Scruggs, M. O. Inouye, G. W. Muse, L. H. Williams, *et al.*, 2018 Widespread transcriptional pausing and elongation control at enhancers. *Genes Dev.* 32: 26–41. <https://doi.org/10.1101/gad.309351.117>
- Herbert K. M., J. Zhou, R. A. Mooney, A. L. Porta, R. Landick, *et al.*, 2010 E. coli NusG Inhibits Backtracking and Accelerates Pause-Free Transcription by Promoting Forward Translocation of RNA Polymerase. *J. Mol. Biol.* 399: 17–30. <https://doi.org/10.1016/j.jmb.2010.03.051>
- Hickman M. J., D. Spatt, and F. Winston, 2011 The Hog1 mitogen-activated protein kinase mediates a hypoxic response in *Saccharomyces cerevisiae*. *Genetics* 188: 325–338. <https://doi.org/10.1534/genetics.111.128322>
- Hirschhorn J. N., S. A. Brown, C. D. Clark, and F. Winston, 1992 Evidence that SNF2/SWI2 and SNF5 activate transcription in yeast by altering chromatin structure. *Genes Dev.* 6: 2288–2298. <https://doi.org/10.1101/gad.6.12a.2288>
- Hou L., Y. Wang, Y. Liu, N. Zhang, I. Shamovsky, *et al.*, 2019 Paf1C regulates RNA polymerase II progression by modulating elongation rate. *Proc. Natl. Acad. Sci. U. S. A.* 116: 14583–14592. <https://doi.org/10.1073/pnas.1904324116>
- Hsieh F.-K., M. Fisher, A. Ujvári, V. M. Studitsky, and D. S. Luse, 2010 Histone H3 mutations promote nucleosome traversal and histone displacement by RNA polymerase II. *EMBO Rep.* 11: 705–710. <https://doi.org/10.1038/embor.2010.113>
- Hsieh F.-K., O. I. Kulaeva, S. S. Patel, P. N. Dyer, K. Luger, *et al.*, 2013 Histone chaperone FACT action during transcription through chromatin by RNA polymerase II. *Proc. Natl. Acad. Sci. U. S. A.* 110: 7654–7659. <https://doi.org/10.1073/pnas.1222198110>
- Hsieh T.-H. S., A. Weiner, B. Lajoie, J. Dekker, N. Friedman, *et al.*, 2015 Mapping Nucleosome Resolution Chromosome Folding in Yeast by Micro-C. *Cell* 162: 108–119. <https://doi.org/10.1016/j.cell.2015.05.048>
- Huang H., A. M. Maertens, E. M. Hyland, J. Dai, A. Norris, *et al.*, 2009 HistoneHits: a database for histone mutations and their phenotypes. *Genome Res.* 19: 674–681. <https://doi.org/10.1101/gr.083402.108>
- Huisinga K. L., and B. F. Pugh, 2004 A genome-wide housekeeping role for TFIID and a highly regulated stress-related role for SAGA in *Saccharomyces cerevisiae*. *Mol. Cell* 13: 573–585. [https://doi.org/10.1016/s1097-2765\(04\)00087-5](https://doi.org/10.1016/s1097-2765(04)00087-5)
- Ibars E., G. Bellí, C. Casas, J. Codina-Fabra, M. Tarrés, *et al.*, 2021 Ubiquitin proteomics reveals critical targets of the Nse1 RING domain in rDNA and genome stability. 2021.12.11.472054.

- Irwin N. A. T., B. J. E. Martin, B. P. Young, M. J. G. Browne, A. Flaus, *et al.*, 2018 Viral proteins as a potential driver of histone depletion in dinoflagellates. *Nat. Commun.* 9: 1535. <https://doi.org/10.1038/s41467-018-03993-4>
- Isasa M., C. M. Rose, S. Elsasser, J. Navarrete-Perea, J. A. Paulo, *et al.*, 2015 Multiplexed, Proteome-Wide Protein Expression Profiling: Yeast Deubiquitylating Enzyme Knockout Strains. *J. Proteome Res.* 14: 5306–5317. <https://doi.org/10.1021/acs.jproteome.5b00802>
- Iwasaki W., Y. Miya, N. Horikoshi, A. Osakabe, H. Taguchi, *et al.*, 2013 Contribution of histone N-terminal tails to the structure and stability of nucleosomes. *FEBS Open Bio* 3: 363–369. <https://doi.org/10.1016/j.fob.2013.08.007>
- Izban M. G., and D. S. Luse, 1991 Transcription on nucleosomal templates by RNA polymerase II in vitro: inhibition of elongation with enhancement of sequence-specific pausing. *Genes Dev.* 5: 683–696. <https://doi.org/10.1101/gad.5.4.683>
- Jeronimo C., S. Watanabe, C. D. Kaplan, C. L. Peterson, and F. Robert, 2015 The Histone Chaperones FACT and Spt6 Restrict H2A.Z from Intragenic Locations. *Mol. Cell* 58: 1113–1123. <https://doi.org/10.1016/j.molcel.2015.03.030>
- Jeronimo C., C. Poitras, and F. Robert, 2019 Histone Recycling by FACT and Spt6 during Transcription Prevents the Scrambling of Histone Modifications. *Cell Rep.* 28: 1206–1218.e8. <https://doi.org/10.1016/j.celrep.2019.06.097>
- Jeronimo C., A. Angel, V. Q. Nguyen, J. M. Kim, C. Poitras, *et al.*, 2021 FACT is recruited to the +1 nucleosome of transcribed genes and spreads in a Chd1-dependent manner. *Mol. Cell* 81: 3542–3559.e11. <https://doi.org/10.1016/j.molcel.2021.07.010>
- Jones G. M., J. Stalker, S. Humphray, A. West, T. Cox, *et al.*, 2008 A systematic library for comprehensive overexpression screens in *Saccharomyces cerevisiae*. *Nat. Methods* 5: 239–241. <https://doi.org/10.1038/nmeth.1181>
- Joo Y. J., S. B. Ficarro, Y. Chun, J. A. Marto, and S. Buratowski, 2019 In vitro analysis of RNA polymerase II elongation complex dynamics. *Genes Dev.* 33: 578–589. <https://doi.org/10.1101/gad.324202.119>
- Jumper J., R. Evans, A. Pritzel, T. Green, M. Figurnov, *et al.*, 2021 Highly accurate protein structure prediction with AlphaFold. *Nature* 596: 583–589. <https://doi.org/10.1038/s41586-021-03819-2>
- Kachaev Z. M., L. A. Lebedeva, E. N. Kozlov, and Y. V. Shidlovskii, 2020 Interplay of mRNA capping and transcription machineries. *Biosci. Rep.* 40: BSR20192825. <https://doi.org/10.1042/BSR20192825>

- Kahana A., and D. E. Gottschling, 1999 DOT4 links silencing and cell growth in *Saccharomyces cerevisiae*. *Mol. Cell. Biol.* 19: 6608–6620.
<https://doi.org/10.1128/MCB.19.10.6608>
- Kang J. Y., R. A. Mooney, Y. Nedialkov, J. Saba, T. V. Mishanina, *et al.*, 2018 Structural Basis for Transcript Elongation Control by NusG Family Universal Regulators. *Cell* 173: 1650–1662.e14. <https://doi.org/10.1016/j.cell.2018.05.017>
- Kaplan C. D., L. Laprade, and F. Winston, 2003 Transcription Elongation Factors Repress Transcription Initiation from Cryptic Sites. *Science* 301: 1096–1099.
<https://doi.org/10.1126/science.1087374>
- Kaplan C. D., M. J. Holland, and F. Winston, 2005 Interaction between transcription elongation factors and mRNA 3'-end formation at the *Saccharomyces cerevisiae* GAL10-GAL7 locus. *J. Biol. Chem.* 280: 913–922.
<https://doi.org/10.1074/jbc.M411108200>
- Kaplan N., I. K. Moore, Y. Fondufe-Mittendorf, A. J. Gossett, D. Tillo, *et al.*, 2009 The DNA-encoded nucleosome organization of a eukaryotic genome. *Nature* 458: 362–366.
<https://doi.org/10.1038/nature07667>
- Kasten M., H. Szerlong, H. Erdjument-Bromage, P. Tempst, M. Werner, *et al.*, 2004 Tandem bromodomains in the chromatin remodeler RSC recognize acetylated histone H3 Lys14. *EMBO J.* 23: 1348–1359. <https://doi.org/10.1038/sj.emboj.7600143>
- Kemble D. J., L. L. McCullough, F. G. Whitby, T. Formosa, and C. P. Hill, 2015 FACT Disrupts Nucleosome Structure by Binding H2A-H2B with Conserved Peptide Motifs. *Mol. Cell* 60: 294–306. <https://doi.org/10.1016/j.molcel.2015.09.008>
- Kiely C. M., S. Marguerat, J. F. Garcia, H. D. Madhani, J. Bähler, *et al.*, 2011 Spt6 is required for heterochromatic silencing in the fission yeast *Schizosaccharomyces pombe*. *Mol. Cell. Biol.* 31: 4193–4204. <https://doi.org/10.1128/MCB.05568-11>
- Kim J. B., and P. A. Sharp, 2001 Positive Transcription Elongation Factor b Phosphorylates hSPT5 and RNA Polymerase II Carboxyl-terminal Domain Independently of Cyclin-dependent Kinase-activating Kinase*. *J. Biol. Chem.* 276: 12317–12323.
<https://doi.org/10.1074/jbc.M010908200>
- Kim J.-H., A. Saraf, L. Florens, M. Washburn, and J. L. Workman, 2010 Gcn5 regulates the dissociation of SWI/SNF from chromatin by acetylation of Swi2/Snf2. *Genes Dev.* 24: 2766–2771. <https://doi.org/10.1101/gad.1979710>
- Kim M., Y. Choi, H. Kim, and D. Lee, 2019 SAGA DUBm-mediated surveillance regulates prompt export of stress-inducible transcripts for proteostasis. *Nat. Commun.* 10: 2458. <https://doi.org/10.1038/s41467-019-10350-6>

- Kireeva M. L., W. Walter, V. Tchernajenko, V. Bondarenko, M. Kashlev, *et al.*, 2002 Nucleosome remodeling induced by RNA polymerase II: loss of the H2A/H2B dimer during transcription. *Mol. Cell* 9: 541–552. [https://doi.org/10.1016/s1097-2765\(02\)00472-0](https://doi.org/10.1016/s1097-2765(02)00472-0)
- Kireeva M. L., B. Hancock, G. H. Cremona, W. Walter, V. M. Studitsky, *et al.*, 2005 Nature of the Nucleosomal Barrier to RNA Polymerase II. *Mol. Cell* 18: 97–108. <https://doi.org/10.1016/j.molcel.2005.02.027>
- Klöckner C., M. Schneider, S. Lutz, D. Jani, D. Kressler, *et al.*, 2009 Mutational uncoupling of the role of Sus1 in nuclear pore complex targeting of an mRNA export complex and histone H2B deubiquitination. *J. Biol. Chem.* 284: 12049–12056. <https://doi.org/10.1074/jbc.M900502200>
- Knezetic J. A., and D. S. Luse, 1986 The presence of nucleosomes on a DNA template prevents initiation by RNA polymerase II in vitro. *Cell* 45: 95–104. [https://doi.org/10.1016/0092-8674\(86\)90541-6](https://doi.org/10.1016/0092-8674(86)90541-6)
- Koehler C., J. Bonnet, M. Stierle, C. Romier, D. Devys, *et al.*, 2014 DNA Binding by Sgf11 Protein Affects Histone H2B Deubiquitination by Spt-Ada-Gcn5-Acetyltransferase (SAGA)*. *J. Biol. Chem.* 289: 8989–8999. <https://doi.org/10.1074/jbc.M113.500868>
- Köhler A., P. Pascual-García, A. Llopis, M. Zapater, F. Posas, *et al.*, 2006 The mRNA export factor Sus1 is involved in Spt/Ada/Gcn5 acetyltransferase-mediated H2B deubiquitylation through its interaction with Ubp8 and Sgf11. *Mol. Biol. Cell* 17: 4228–4236. <https://doi.org/10.1091/mbc.e06-02-0098>
- Köhler A., M. Schneider, G. G. Cabal, U. Nehrbaas, and E. Hurt, 2008 Yeast Ataxin-7 links histone deubiquitination with gene gating and mRNA export. *Nat. Cell Biol.* 10: 707–715. <https://doi.org/10.1038/ncb1733>
- Komori T., N. Inukai, T. Yamada, Y. Yamaguchi, and H. Handa, 2009 Role of human transcription elongation factor DSIF in the suppression of senescence and apoptosis. *Genes Cells* 14: 343–354. <https://doi.org/10.1111/j.1365-2443.2008.01273.x>
- Konev A. Y., M. Tribus, S. Y. Park, V. Podhraski, C. Y. Lim, *et al.*, 2007 CHD1 motor protein is required for deposition of histone variant H3.3 into chromatin in vivo. *Science* 317: 1087–1090. <https://doi.org/10.1126/science.1145339>
- Korber P., and S. Barbaric, 2014 The yeast PHO5 promoter: from single locus to systems biology of a paradigm for gene regulation through chromatin. *Nucleic Acids Res.* 42: 10888–10902. <https://doi.org/10.1093/nar/gku784>
- Kotlajich M. V., D. R. Hron, B. A. Boudreau, Z. Sun, Y. L. Lyubchenko, *et al.*, 2015 Bridged filaments of histone-like nucleoid structuring protein pause RNA polymerase and aid

- termination in bacteria, (N. J. Proudfoot, Ed.). eLife 4: e04970.
<https://doi.org/10.7554/eLife.04970>
- Kramer N. J., Y. Carlomagno, Y.-J. Zhang, S. Almeida, C. N. Cook, *et al.*, 2016 Spt4 selectively regulates the expression of C9orf72 sense and antisense mutant transcripts. *Science* 353: 708–712. <https://doi.org/10.1126/science.aaf7791>
- Krogan N. J., J. Dover, S. Khorrani, J. F. Greenblatt, J. Schneider, *et al.*, 2002a COMPASS, a histone H3 (Lysine 4) methyltransferase required for telomeric silencing of gene expression. *J. Biol. Chem.* 277: 10753–10755.
<https://doi.org/10.1074/jbc.C200023200>
- Krogan N. J., M. Kim, S. H. Ahn, G. Zhong, M. S. Kobor, *et al.*, 2002b RNA polymerase II elongation factors of *Saccharomyces cerevisiae*: a targeted proteomics approach. *Mol. Cell. Biol.* 22: 6979–6992. <https://doi.org/10.1128/MCB.22.20.6979-6992.2002>
- Kruger W., C. L. Peterson, A. Sil, C. Coburn, G. Arents, *et al.*, 1995 Amino acid substitutions in the structured domains of histones H3 and H4 partially relieve the requirement of the yeast SWI/SNF complex for transcription. *Genes Dev.* 9: 2770–2779.
<https://doi.org/10.1101/gad.9.22.2770>
- Kujirai T., H. Ehara, Y. Fujino, M. Shirouzu, S.-I. Sekine, *et al.*, 2018 Structural basis of the nucleosome transition during RNA polymerase II passage. *Science* 362: 595–598.
<https://doi.org/10.1126/science.aau9904>
- Kulaeva O. I., D. A. Gaykalova, N. A. Pestov, V. V. Golovastov, D. G. Vassilyev, *et al.*, 2009 Mechanism of chromatin remodeling and recovery during passage of RNA polymerase II. *Nat. Struct. Mol. Biol.* 16: 1272–1278.
<https://doi.org/10.1038/nsmb.1689>
- Kuo Y.-M., and A. J. Andrews, 2013 Quantitating the specificity and selectivity of Gcn5-mediated acetylation of histone H3. *PLoS One* 8: e54896.
<https://doi.org/10.1371/journal.pone.0054896>
- Kwon H., A. N. Imbalzano, P. A. Khavari, R. E. Kingston, and M. R. Green, 1994 Nucleosome disruption and enhancement of activator binding by a human SW1/SNF complex. *Nature* 370: 477–481. <https://doi.org/10.1038/370477a0>
- Kyrpides N. C., C. R. Woese, and C. A. Ouzounis, 1996 KOW: a novel motif linking a bacterial transcription factor with ribosomal proteins. *Trends Biochem. Sci.* 21: 425–426.
[https://doi.org/10.1016/s0968-0004\(96\)30036-4](https://doi.org/10.1016/s0968-0004(96)30036-4)
- Larschan E., and F. Winston, 2001 The *S. cerevisiae* SAGA complex functions in vivo as a coactivator for transcriptional activation by Gal4. *Genes Dev.* 15: 1946–1956.
<https://doi.org/10.1101/gad.911501>

- Larson M. H., R. A. Mooney, J. M. Peters, T. Windgassen, D. Nayak, *et al.*, 2014 A pause sequence enriched at translation start sites drives transcription dynamics in vivo. *Science* 344: 1042–1047. <https://doi.org/10.1126/science.1251871>
- Laursen S. P., S. Bowerman, and K. Luger, 2021 Archaea: The Final Frontier of Chromatin. *J. Mol. Biol.* 433: 166791. <https://doi.org/10.1016/j.jmb.2020.166791>
- Lee K. K., S. K. Swanson, L. Florens, M. P. Washburn, and J. L. Workman, 2009 Yeast Sgf73/Ataxin-7 serves to anchor the deubiquitination module into both SAGA and Slik(SALSA) HAT complexes. *Epigenetics Chromatin* 2: 2. <https://doi.org/10.1186/1756-8935-2-2>
- Lee K. K., M. E. Sardi, S. K. Swanson, J. M. Gilmore, M. Torok, *et al.*, 2011 Combinatorial depletion analysis to assemble the network architecture of the SAGA and ADA chromatin remodeling complexes. *Mol. Syst. Biol.* 7: 503. <https://doi.org/10.1038/msb.2011.40>
- Li G., M. Levitus, C. Bustamante, and J. Widom, 2005 Rapid spontaneous accessibility of nucleosomal DNA. *Nat. Struct. Mol. Biol.* 12: 46–53. <https://doi.org/10.1038/nsmb869>
- Li B., M. Gogol, M. Carey, S. G. Pattenden, C. Seidel, *et al.*, 2007 Infrequently transcribed long genes depend on the Set2/Rpd3S pathway for accurate transcription. *Genes Dev.* 21: 1422–1430. <https://doi.org/10.1101/gad.1539307>
- Libuda D. E., and F. Winston, 2006 Amplification of histone genes by circular chromosome formation in *Saccharomyces cerevisiae*. *Nature* 443: 1003–1007. <https://doi.org/10.1038/nature05205>
- Lieberman P. M., 2008 Chromatin organization and virus gene expression. *J. Cell. Physiol.* 216: 295–302. <https://doi.org/10.1002/jcp.21421>
- Lindstrom D. L., S. L. Squazzo, N. Muster, T. A. Burckin, K. C. Wachter, *et al.*, 2003 Dual roles for Spt5 in pre-mRNA processing and transcription elongation revealed by identification of Spt5-associated proteins. *Mol. Cell. Biol.* 23: 1368–1378. <https://doi.org/10.1128/MCB.23.4.1368-1378.2003>
- Ling X., T. A. Harkness, M. C. Schultz, G. Fisher-Adams, and M. Grunstein, 1996 Yeast histone H3 and H4 amino termini are important for nucleosome assembly in vivo and in vitro: redundant and position-independent functions in assembly but not in gene regulation. *Genes Dev.* 10: 686–699. <https://doi.org/10.1101/gad.10.6.686>
- Lisica A., C. Engel, M. Jahnel, É. Roldán, E. A. Galburt, *et al.*, 2016 Mechanisms of backtrack recovery by RNA polymerases I and II. *Proc. Natl. Acad. Sci.* 113: 2946–2951. <https://doi.org/10.1073/pnas.1517011113>

- Liu Y., K. Zhou, N. Zhang, H. Wei, Y. Z. Tan, *et al.*, 2020 FACT caught in the act of manipulating the nucleosome. *Nature* 577: 426–431.
<https://doi.org/10.1038/s41586-019-1820-0>
- Liu Y., H. Bisio, C. M. Toner, S. Jeudy, N. Philippe, *et al.*, 2021 Virus-encoded histone doublets are essential and form nucleosome-like structures. *Cell* 184: 4237–4250.e19.
<https://doi.org/10.1016/j.cell.2021.06.032>
- Lorch Y., J. W. LaPointe, and R. D. Kornberg, 1987 Nucleosomes inhibit the initiation of transcription but allow chain elongation with the displacement of histones. *Cell* 49: 203–210. [https://doi.org/10.1016/0092-8674\(87\)90561-7](https://doi.org/10.1016/0092-8674(87)90561-7)
- Lorch Y., J. Griesenbeck, H. Boeger, B. Maier-Davis, and R. D. Kornberg, 2011 Selective removal of promoter nucleosomes by the RSC chromatin-remodeling complex. *Nat. Struct. Mol. Biol.* 18: 881–885. <https://doi.org/10.1038/nsmb.2072>
- Lorch Y., B. Maier-Davis, and R. D. Kornberg, 2018 Histone Acetylation Inhibits RSC and Stabilizes the +1 Nucleosome. *Mol. Cell* 72: 594–600.e2.
<https://doi.org/10.1016/j.molcel.2018.09.030>
- Luger K., A. W. Mäder, R. K. Richmond, D. F. Sargent, and T. J. Richmond, 1997 Crystal structure of the nucleosome core particle at 2.8 Å resolution. *Nature* 389: 251–260.
<https://doi.org/10.1038/38444>
- Mack A. H., D. J. Schlingman, R. P. Ilagan, L. Regan, and S. G. J. Mochrie, 2012 Kinetics and Thermodynamics of Phenotype: Unwinding and Rewinding the Nucleosome. *J. Mol. Biol.* 423: 687–701. <https://doi.org/10.1016/j.jmb.2012.08.021>
- Mann R. K., and M. Grunstein, 1992 Histone H3 N-terminal mutations allow hyperactivation of the yeast GAL1 gene in vivo. *EMBO J.* 11: 3297–3306.
- Marshall N. F., J. Peng, Z. Xie, and D. H. Price, 1996 Control of RNA Polymerase II Elongation Potential by a Novel Carboxyl-terminal Domain Kinase *. *J. Biol. Chem.* 271: 27176–27183. <https://doi.org/10.1074/jbc.271.43.27176>
- Martens J. A., L. Laprade, and F. Winston, 2004 Intergenic transcription is required to repress the *Saccharomyces cerevisiae* SER3 gene. *Nature* 429: 571–574.
<https://doi.org/10.1038/nature02538>
- Martire S., and L. A. Banaszynski, 2020 The roles of histone variants in fine-tuning chromatin organization and function. *Nat. Rev. Mol. Cell Biol.* 21: 522–541.
<https://doi.org/10.1038/s41580-020-0262-8>
- Materne P., E. Vázquez, M. Sánchez, C. Yague-Sanz, J. Anandhakumar, *et al.*, 2016 Histone H2B ubiquitylation represses gametogenesis by opposing RSC-dependent chromatin

- remodeling at the *ste11* master regulator locus. *eLife* 5: e13500.
<https://doi.org/10.7554/eLife.13500>
- Mattioli F., S. Bhattacharyya, P. N. Dyer, A. E. White, K. Sandman, *et al.*, 2017 Structure of histone-based chromatin in Archaea. *Science* 357: 609–612.
<https://doi.org/10.1126/science.aaj1849>
- Mayer A., M. Lidschreiber, M. Siebert, K. Leike, J. Söding, *et al.*, 2010 Uniform transitions of the general RNA polymerase II transcription complex. *Nat. Struct. Mol. Biol.* 17: 1272–1278. <https://doi.org/10.1038/nsmb.1903>
- McCormick M. A., A. G. Mason, S. J. Guyenet, W. Dang, R. M. Garza, *et al.*, 2014 The SAGA histone deubiquitinase module controls yeast replicative lifespan via Sir2 interaction. *Cell Rep.* 8: 477–486. <https://doi.org/10.1016/j.celrep.2014.06.037>
- McCullough L., B. Poe, Z. Connell, H. Xin, and T. Formosa, 2013 The FACT histone chaperone guides histone H4 into its nucleosomal conformation in *Saccharomyces cerevisiae*. *Genetics* 195: 101–113. <https://doi.org/10.1534/genetics.113.153080>
- McCullough L., Z. Connell, C. Petersen, and T. Formosa, 2015 The Abundant Histone Chaperones Spt6 and FACT Collaborate to Assemble, Inspect, and Maintain Chromatin Structure in *Saccharomyces cerevisiae*. *Genetics* 201: 1031–1045.
<https://doi.org/10.1534/genetics.115.180794>
- McCullough L. L., Z. Connell, H. Xin, V. M. Studitsky, A. V. Feofanov, *et al.*, 2018 Functional roles of the DNA-binding HMGB domain in the histone chaperone FACT in nucleosome reorganization. *J. Biol. Chem.* 293: 6121–6133.
<https://doi.org/10.1074/jbc.RA117.000199>
- McCullough L. L., T. H. Pham, T. J. Parnell, Z. Connell, M. B. Chandrasekharan, *et al.*, 2019 Establishment and Maintenance of Chromatin Architecture Are Promoted Independently of Transcription by the Histone Chaperone FACT and H3-K56 Acetylation in *Saccharomyces cerevisiae*. *Genetics* 211: 877–892.
<https://doi.org/10.1534/genetics.118.301853>
- McDonald S. M., D. Close, H. Xin, T. Formosa, and C. P. Hill, 2010 Structure and biological importance of the Spn1-Spt6 interaction, and its regulatory role in nucleosome binding. *Mol. Cell* 40: 725–735. <https://doi.org/10.1016/j.molcel.2010.11.014>
- Meyer P. A., S. Li, M. Zhang, K. Yamada, Y. Takagi, *et al.*, 2015 Structures and Functions of the Multiple KOW Domains of Transcription Elongation Factor Spt5. *Mol. Cell. Biol.* 35: 3354–3369. <https://doi.org/10.1128/MCB.00520-15>
- Missra A., and D. S. Gilmour, 2010 Interactions between DSIF (DRB sensitivity inducing factor), NELF (negative elongation factor), and the *Drosophila* RNA polymerase II

- transcription elongation complex. *Proc. Natl. Acad. Sci.* 107: 11301–11306.
<https://doi.org/10.1073/pnas.1000681107>
- Moehle E. A., C. J. Ryan, N. J. Krogan, T. L. Kress, and C. Guthrie, 2012 The yeast SR-like protein Npl3 links chromatin modification to mRNA processing. *PLoS Genet.* 8: e1003101. <https://doi.org/10.1371/journal.pgen.1003101>
- Mooney R. A., S. E. Davis, J. M. Peters, J. L. Rowland, A. Z. Ansari, *et al.*, 2009 Regulator trafficking on bacterial transcription units in vivo. *Mol. Cell* 33: 97–108.
<https://doi.org/10.1016/j.molcel.2008.12.021>
- Morgan M. T., M. Haj-Yahya, A. E. Ringel, P. Bandi, A. Brik, *et al.*, 2016 Structural basis for histone H2B deubiquitination by the SAGA DUB module. *Science* 351: 725–728.
<https://doi.org/10.1126/science.aac5681>
- Morgunova E., and J. Taipale, 2021 Structural insights into the interaction between transcription factors and the nucleosome. *Curr. Opin. Struct. Biol.* 71: 171–179.
<https://doi.org/10.1016/j.sbi.2021.06.016>
- Myers C. N., G. B. Berner, J. H. Holthoff, K. Martinez-Fonts, J. A. Harper, *et al.*, 2011 Mutant versions of the *S. cerevisiae* transcription elongation factor Spt16 define regions of Spt16 that functionally interact with histone H3. *PloS One* 6: e20847.
<https://doi.org/10.1371/journal.pone.0020847>
- Nagai S., R. E. Davis, P. J. Mattei, K. P. Eagen, and R. D. Kornberg, 2017 Chromatin potentiates transcription. *Proc. Natl. Acad. Sci. U. S. A.* 114: 1536–1541.
<https://doi.org/10.1073/pnas.1620312114>
- Nakatani Y., D. Ray-Gallet, J.-P. Quivy, H. Tagami, and G. Almouzni, 2004 Two distinct nucleosome assembly pathways: dependent or independent of DNA synthesis promoted by histone H3.1 and H3.3 complexes. *Cold Spring Harb. Symp. Quant. Biol.* 69: 273–280. <https://doi.org/10.1101/sqb.2004.69.273>
- Nodelman I. M., and G. D. Bowman, 2021 Biophysics of Chromatin Remodeling. *Annu. Rev. Biophys.* 50: 73–93. <https://doi.org/10.1146/annurev-biophys-082520-080201>
- Nourani A., F. Robert, and F. Winston, 2006 Evidence that Spt2/Sin1, an HMG-like factor, plays roles in transcription elongation, chromatin structure, and genome stability in *Saccharomyces cerevisiae*. *Mol. Cell. Biol.* 26: 1496–1509.
<https://doi.org/10.1128/MCB.26.4.1496-1509.2006>
- Nune M., M. T. Morgan, Z. Connell, L. McCullough, M. Jbara, *et al.*, 2019 FACT and Ubp10 collaborate to modulate H2B deubiquitination and nucleosome dynamics. *eLife* 8: e40988. <https://doi.org/10.7554/eLife.40988>

- Ocampo J., R. V. Chereji, P. R. Eriksson, and D. J. Clark, 2016 The ISW1 and CHD1 ATP-dependent chromatin remodelers compete to set nucleosome spacing in vivo. *Nucleic Acids Res.* 44: 4625–4635. <https://doi.org/10.1093/nar/gkw068>
- Orphanides G., G. LeRoy, C.-H. Chang, D. S. Luse, and D. Reinberg, 1998 FACT, a Factor that Facilitates Transcript Elongation through Nucleosomes. *Cell* 92: 105–116. [https://doi.org/10.1016/S0092-8674\(00\)80903-4](https://doi.org/10.1016/S0092-8674(00)80903-4)
- Papai G., A. Frechard, O. Kolesnikova, C. Crucifix, P. Schultz, *et al.*, 2020 Structure of SAGA and mechanism of TBP deposition on gene promoters. *Nature* 577: 711–716. <https://doi.org/10.1038/s41586-020-1944-2>
- Park J.-H., M. S. Cosgrove, E. Youngman, C. Wolberger, and J. D. Boeke, 2002 A core nucleosome surface crucial for transcriptional silencing. *Nat. Genet.* 32: 273–279. <https://doi.org/10.1038/ng982>
- Park Y.-J., K. B. Sudhoff, A. J. Andrews, L. A. Stargell, and K. Luger, 2008 Histone chaperone specificity in Rtt109 activation. *Nat. Struct. Mol. Biol.* 15: 957–964. <https://doi.org/10.1038/nsmb.1480>
- Park D., A. R. Morris, A. Battenhouse, and V. R. Iyer, 2014 Simultaneous mapping of transcript ends at single-nucleotide resolution and identification of widespread promoter-associated non-coding RNA governed by TATA elements. *Nucleic Acids Res.* 42: 3736–3749. <https://doi.org/10.1093/nar/gkt1366>
- Patel A. B., C. M. Moore, B. J. Greber, J. Luo, S. A. Zukin, *et al.*, 2019 Architecture of the chromatin remodeler RSC and insights into its nucleosome engagement. *eLife* 8: e54449. <https://doi.org/10.7554/eLife.54449>
- Pavri R., B. Zhu, G. Li, P. Trojer, S. Mandal, *et al.*, 2006 Histone H2B monoubiquitination functions cooperatively with FACT to regulate elongation by RNA polymerase II. *Cell* 125: 703–717. <https://doi.org/10.1016/j.cell.2006.04.029>
- Peters J. M., R. A. Mooney, J. A. Grass, E. D. Jessen, F. Tran, *et al.*, 2012 Rho and NusG suppress pervasive antisense transcription in *Escherichia coli*. *Genes Dev.* 26: 2621–2633. <https://doi.org/10.1101/gad.196741.112>
- Prather D., N. J. Krogan, A. Emili, J. F. Greenblatt, and F. Winston, 2005 Identification and characterization of Elf1, a conserved transcription elongation factor in *Saccharomyces cerevisiae*. *Mol. Cell. Biol.* 25: 10122–10135. <https://doi.org/10.1128/MCB.25.22.10122-10135.2005>
- Prelich G., and F. Winston, 1993 Mutations That Suppress the Deletion of an Upstream Activating Sequence in Yeast: Involvement of a Protein Kinase and Histone H3 in Repressing Transcription in Vivo. *Genetics* 135: 665–676.

- Pruneski J. A., S. J. Hainer, K. O. Petrov, and J. A. Martens, 2011 The Paf1 complex represses SER3 transcription in *Saccharomyces cerevisiae* by facilitating intergenic transcription-dependent nucleosome occupancy of the SER3 promoter. *Eukaryot. Cell* 10: 1283–1294. <https://doi.org/10.1128/EC.05141-11>
- Qiu C., O. C. Erinne, J. M. Dave, P. Cui, H. Jin, *et al.*, 2016 High-Resolution Phenotypic Landscape of the RNA Polymerase II Trigger Loop. *PLOS Genet.* 12: e1006321. <https://doi.org/10.1371/journal.pgen.1006321>
- Quan T. K., and G. A. Hartzog, 2010 Histone H3K4 and K36 methylation, Chd1 and Rpd3S oppose the functions of *Saccharomyces cerevisiae* Spt4-Spt5 in transcription. *Genetics* 184: 321–334. <https://doi.org/10.1534/genetics.109.111526>
- Radman-Livaja M., K. F. Verzijlbergen, A. Weiner, T. van Welsem, N. Friedman, *et al.*, 2011 Patterns and Mechanisms of Ancestral Histone Protein Inheritance in Budding Yeast. *PLOS Biol.* 9: e1001075. <https://doi.org/10.1371/journal.pbio.1001075>
- Radman-Livaja M., T. K. Quan, L. Valenzuela, J. A. Armstrong, T. van Welsem, *et al.*, 2012 A Key Role for Chd1 in Histone H3 Dynamics at the 3' Ends of Long Genes in Yeast. *PLOS Genet.* 8: e1002811. <https://doi.org/10.1371/journal.pgen.1002811>
- Rahl P. B., C. Y. Lin, A. C. Seila, R. A. Flynn, S. McCuine, *et al.*, 2010 c-Myc regulates transcriptional pause release. *Cell* 141: 432–445. <https://doi.org/10.1016/j.cell.2010.03.030>
- Rando O. J., and F. Winston, 2012 Chromatin and Transcription in Yeast. *Genetics* 190: 351–387. <https://doi.org/10.1534/genetics.111.132266>
- Rasmussen E. B., and J. T. Lis, 1993 In vivo transcriptional pausing and cap formation on three *Drosophila* heat shock genes. *Proc. Natl. Acad. Sci. U. S. A.* 90: 7923–7927. <https://doi.org/10.1073/pnas.90.17.7923>
- Ray-Gallet D., and G. Almouzni, 2021 The Histone H3 Family and Its Deposition Pathways. *Adv. Exp. Med. Biol.* 1283: 17–42. https://doi.org/10.1007/978-981-15-8104-5_2
- Richardson L. A., B. J. Reed, J. M. Charette, E. F. Freed, E. K. Fredrickson, *et al.*, 2012 A conserved deubiquitinating enzyme controls cell growth by regulating RNA polymerase I stability. *Cell Rep.* 2: 372–385. <https://doi.org/10.1016/j.celrep.2012.07.009>
- Ricketts M. D., B. Frederick, H. Hoff, Y. Tang, D. C. Schultz, *et al.*, 2015 Ubinuclein-1 confers histone H3.3-specific-binding by the HIRA histone chaperone complex. *Nat. Commun.* 6: 7711. <https://doi.org/10.1038/ncomms8711>
- Rodríguez-Navarro S., T. Fischer, M.-J. Luo, O. Antúnez, S. Brettschneider, *et al.*, 2004 Sus1, a functional component of the SAGA histone acetylase complex and the nuclear pore-

- associated mRNA export machinery. *Cell* 116: 75–86.
[https://doi.org/10.1016/s0092-8674\(03\)01025-0](https://doi.org/10.1016/s0092-8674(03)01025-0)
- Rosen G. A., I. Baek, L. J. Friedman, Y. J. Joo, S. Buratowski, *et al.*, 2020 Dynamics of RNA polymerase II and elongation factor Spt4/5 recruitment during activator-dependent transcription. *Proc. Natl. Acad. Sci.* 117: 32348–32357.
<https://doi.org/10.1073/pnas.2011224117>
- Rössl A., A. Denoncourt, M.-S. Lin, and M. Downey, 2019 A synthetic non-histone substrate to study substrate targeting by the Gcn5 HAT and sirtuin HDACs. *J. Biol. Chem.* 294: 6227–6239. <https://doi.org/10.1074/jbc.RA118.006051>
- Rufiange A., P.-E. Jacques, W. Bhat, F. Robert, and A. Nourani, 2007 Genome-wide replication-independent histone H3 exchange occurs predominantly at promoters and implicates H3 K56 acetylation and Asf1. *Mol. Cell* 27: 393–405.
<https://doi.org/10.1016/j.molcel.2007.07.011>
- Samara N. L., A. E. Ringel, and C. Wolberger, 2012 A role for intersubunit interactions in maintaining SAGA deubiquitinating module structure and activity. *Struct. Lond. Engl.* 1993 20: 1414–1424. <https://doi.org/10.1016/j.str.2012.05.015>
- Sanders T. J., M. Lammers, C. J. Marshall, J. E. Walker, E. R. Lynch, *et al.*, 2019 TFS and Spt4/5 accelerate transcription through archaeal histone-based chromatin. *Mol. Microbiol.* 111: 784–797. <https://doi.org/10.1111/mmi.14191>
- Sansó M., R. S. Levin, J. J. Lipp, V. Y.-F. Wang, A. K. Greifenberg, *et al.*, 2016 P-TEFb regulation of transcription termination factor Xrn2 revealed by a chemical genetic screen for Cdk9 substrates. *Genes Dev.* 30: 117–131.
<https://doi.org/10.1101/gad.269589.115>
- Schlichter A., M. M. Kasten, T. J. Parnell, and B. R. Cairns, 2020 Specialization of the chromatin remodeler RSC to mobilize partially-unwrapped nucleosomes, (S. Buratowski, K. Struhl, and B. Bartholomew, Eds.). *eLife* 9: e58130.
<https://doi.org/10.7554/eLife.58130>
- Schoberleitner I., I. Bauer, A. Huang, E. N. Andreyeva, J. Sebald, *et al.*, 2021 CHD1 controls H3.3 incorporation in adult brain chromatin to maintain metabolic homeostasis and normal lifespan. *Cell Rep.* 37: 109769. <https://doi.org/10.1016/j.celrep.2021.109769>
- Schulze J. M., T. Hentrich, S. Nakanishi, A. Gupta, E. Emberly, *et al.*, 2011 Splitting the task: Ubp8 and Ubp10 deubiquitinate different cellular pools of H2BK123. *Genes Dev.* 25: 2242–2247. <https://doi.org/10.1101/gad.177220.111>
- Shen Y., D. E. H. F. Mevius, R. Caliandro, B. Carrozzini, Y. Roh, *et al.*, 2019 Set7 Is a H3K37 Methyltransferase in *Schizosaccharomyces pombe* and Is Required for Proper

- Gametogenesis. *Struct. Lond. Engl.* 1993 27: 631-638.e8.
<https://doi.org/10.1016/j.str.2019.01.011>
- Shetty A., S. P. Kallgren, C. Demel, K. C. Maier, D. Spatt, *et al.*, 2017 Spt5 Plays Vital Roles in the Control of Sense and Antisense Transcription Elongation. *Mol. Cell* 66: 77-88.e5.
<https://doi.org/10.1016/j.molcel.2017.02.023>
- Shukla A., P. Bajwa, and S. R. Bhaumik, 2006 SAGA-associated Sgf73p facilitates formation of the preinitiation complex assembly at the promoters either in a HAT-dependent or independent manner in vivo. *Nucleic Acids Res.* 34: 6225–6232.
<https://doi.org/10.1093/nar/gkl844>
- Siggens L., L. Cordeddu, M. Rönnerblad, A. Lennartsson, and K. Ekwall, 2015 Transcription-coupled recruitment of human CHD1 and CHD2 influences chromatin accessibility and histone H3 and H3.3 occupancy at active chromatin regions. *Epigenetics Chromatin* 8: 4. <https://doi.org/10.1186/1756-8935-8-4>
- Silva A. C., X. Xu, H.-S. Kim, J. Fillingham, T. Kislinger, *et al.*, 2012 The Replication-independent Histone H3-H4 Chaperones HIR, ASF1, and RTT106 Co-operate to Maintain Promoter Fidelity. *J. Biol. Chem.* 287: 1709–1718.
<https://doi.org/10.1074/jbc.M111.316489>
- Simic R., D. L. Lindstrom, H. G. Tran, K. L. Roinick, P. J. Costa, *et al.*, 2003 Chromatin remodeling protein Chd1 interacts with transcription elongation factors and localizes to transcribed genes. *EMBO J.* 22: 1846–1856.
<https://doi.org/10.1093/emboj/cdg179>
- Sinha K. K., J. D. Gross, and G. J. Narlikar, 2017 Distortion of histone octamer core promotes nucleosome mobilization by a chromatin remodeler. *Science* 355.
<https://doi.org/10.1126/science.aaa3761>
- Sivkina A. L., M. G. Karlova, M. E. Valieva, L. L. McCullough, T. Formosa, *et al.*, 2022 Electron microscopy analysis of ATP-independent nucleosome unfolding by FACT. *Commun. Biol.* 5: 2. <https://doi.org/10.1038/s42003-021-02948-8>
- Smolle M., S. Venkatesh, M. M. Gogol, H. Li, Y. Zhang, *et al.*, 2012 Chromatin remodelers Isw1 and Chd1 maintain chromatin structure during transcription by preventing histone exchange. *Nat. Struct. Mol. Biol.* 19: 884–892.
<https://doi.org/10.1038/nsmb.2312>
- Smollett K., F. Blombach, R. Reichelt, M. Thomm, and F. Werner, 2017 A global analysis of transcription reveals two modes of Spt4/5 recruitment to archaeal RNA polymerase. *Nat. Microbiol.* 2: 1–11. <https://doi.org/10.1038/nmicrobiol.2017.21>

- Somers J., and T. Owen-Hughes, 2009 Mutations to the histone H3 α N region selectively alter the outcome of ATP-dependent nucleosome-remodelling reactions. *Nucleic Acids Res.* 37: 2504–2513. <https://doi.org/10.1093/nar/gkp114>
- Song Y., J.-H. Seol, J.-H. Yang, H.-J. Kim, J.-W. Han, *et al.*, 2013 Dissecting the roles of the histone chaperones reveals the evolutionary conserved mechanism of transcription-coupled deposition of H3.3. *Nucleic Acids Res.* 41: 5199–5209. <https://doi.org/10.1093/nar/gkt220>
- Spain M. M., S. A. Ansari, R. Pathak, M. J. Palumbo, R. H. Morse, *et al.*, 2014 The RSC Complex Localizes to Coding Sequences to Regulate Pol II and Histone Occupancy. *Mol. Cell* 56: 653–666. <https://doi.org/10.1016/j.molcel.2014.10.002>
- Squazzo S. L., P. J. Costa, D. L. Lindstrom, K. E. Kumer, R. Simic, *et al.*, 2002 The Paf1 complex physically and functionally associates with transcription elongation factors in vivo. *EMBO J.* 21: 1764–1774. <https://doi.org/10.1093/emboj/21.7.1764>
- Sterner D. E., P. A. Grant, S. M. Roberts, L. J. Duggan, R. Belotserkovskaya, *et al.*, 1999 Functional organization of the yeast SAGA complex: distinct components involved in structural integrity, nucleosome acetylation, and TATA-binding protein interaction. *Mol. Cell. Biol.* 19: 86–98. <https://doi.org/10.1128/MCB.19.1.86>
- Stormberg T., S. Vemulapalli, S. Filliaux, and Y. L. Lyubchenko, 2021 Effect of histone H4 tail on nucleosome stability and internucleosomal interactions. *Sci. Rep.* 11: 24086. <https://doi.org/10.1038/s41598-021-03561-9>
- Swanson M. S., E. A. Malone, and F. Winston, 1991 SPT5, an essential gene important for normal transcription in *Saccharomyces cerevisiae*, encodes an acidic nuclear protein with a carboxy-terminal repeat. *Mol. Cell. Biol.* 11: 3009–3019. <https://doi.org/10.1128/MCB.11.6.3009>
- Swanson M. S., and F. Winston, 1992 SPT4, SPT5 and SPT6 interactions: effects on transcription and viability in *Saccharomyces cerevisiae*. *Genetics* 132: 325–336.
- Tennyson C. N., H. J. Klamut, and R. G. Worton, 1995 The human dystrophin gene requires 16 hours to be transcribed and is cotranscriptionally spliced. *Nat. Genet.* 9: 184–190. <https://doi.org/10.1038/ng0295-184>
- Thebault P., G. Boutin, W. Bhat, A. Rufiange, J. Martens, *et al.*, 2011 Transcription regulation by the noncoding RNA SRG1 requires Spt2-dependent chromatin deposition in the wake of RNA polymerase II. *Mol. Cell. Biol.* 31: 1288–1300. <https://doi.org/10.1128/MCB.01083-10>

- Torigoe S. E., A. Patel, M. T. Khuong, G. D. Bowman, and J. T. Kadonaga, 2013 ATP-dependent chromatin assembly is functionally distinct from chromatin remodeling. *eLife* 2: e00863. <https://doi.org/10.7554/eLife.00863>
- Tse C., E. I. Georgieva, A. B. Ruiz-García, R. Sendra, and J. C. Hansen, 1998 Gcn5p, a transcription-related histone acetyltransferase, acetylates nucleosomes and folded nucleosomal arrays in the absence of other protein subunits. *J. Biol. Chem.* 273: 32388–32392. <https://doi.org/10.1074/jbc.273.49.32388>
- Tsunaka Y., Y. Fujiwara, T. Oyama, S. Hirose, and K. Morikawa, 2016 Integrated molecular mechanism directing nucleosome reorganization by human FACT. *Genes Dev.* 30: 673–686. <https://doi.org/10.1101/gad.274183.115>
- Uzun Ü., T. Brown, H. Fischl, A. Angel, and J. Mellor, 2021 Spt4 facilitates the movement of RNA polymerase II through the +2 nucleosomal barrier. *Cell Rep.* 36: 109755. <https://doi.org/10.1016/j.celrep.2021.109755>
- Valieva M. E., G. A. Armeev, K. S. Kudryashova, N. S. Gerasimova, A. K. Shaytan, *et al.*, 2016 Large-scale ATP-independent nucleosome unfolding by a histone chaperone. *Nat. Struct. Mol. Biol.* 23: 1111–1116. <https://doi.org/10.1038/nsmb.3321>
- VanDemark A. P., M. M. Kasten, E. Ferris, A. Heroux, C. P. Hill, *et al.*, 2007 Autoregulation of the rsc4 tandem bromodomain by gcn5 acetylation. *Mol. Cell* 27: 817–828. <https://doi.org/10.1016/j.molcel.2007.08.018>
- Varadi M., S. Anyango, M. Deshpande, S. Nair, C. Natassia, *et al.*, 2022 AlphaFold Protein Structure Database: massively expanding the structural coverage of protein-sequence space with high-accuracy models. *Nucleic Acids Res.* 50: D439–D444. <https://doi.org/10.1093/nar/gkab1061>
- Venkatesh S., and J. L. Workman, 2015 Histone exchange, chromatin structure and the regulation of transcription. *Nat. Rev. Mol. Cell Biol.* 16: 178–189. <https://doi.org/10.1038/nrm3941>
- Venkatesh S., H. Li, M. M. Gogol, and J. L. Workman, 2016 Selective suppression of antisense transcription by Set2-mediated H3K36 methylation. *Nat. Commun.* 7: 13610. <https://doi.org/10.1038/ncomms13610>
- Viktorovskaya O. V., K. L. Engel, S. L. French, P. Cui, P. J. Vandeventer, *et al.*, 2013 Divergent Contributions of Conserved Active Site Residues to Transcription by Eukaryotic RNA Polymerases I and II. *Cell Rep.* 4: 974–984. <https://doi.org/10.1016/j.celrep.2013.07.044>

- Viktorovskaya O., J. Chuang, D. Jain, N. I. Reim, F. López-Rivera, *et al.*, 2021 Essential histone chaperones collaborate to regulate transcription and chromatin integrity. *Genes Dev.* 35: 698–712. <https://doi.org/10.1101/gad.348431.121>
- Vitaliano-Prunier A., A. Babour, L. Hérisant, L. Apponi, T. Margaritis, *et al.*, 2012 H2B ubiquitylation controls the formation of export-competent mRNP. *Mol. Cell* 45: 132–139. <https://doi.org/10.1016/j.molcel.2011.12.011>
- Vos S. M., L. Farnung, H. Urlaub, and P. Cramer, 2018 Structure of paused transcription complex Pol II–DSIF–NELF. *Nature* 560: 601–606. <https://doi.org/10.1038/s41586-018-0442-2>
- Wada T., T. Takagi, Y. Yamaguchi, A. Ferdous, T. Imai, *et al.*, 1998 DSIF, a novel transcription elongation factor that regulates RNA polymerase II processivity, is composed of human Spt4 and Spt5 homologs. *Genes Dev.* 12: 343–356.
- Wada T., G. Orphanides, J. Hasegawa, D. K. Kim, D. Shima, *et al.*, 2000 FACT relieves DSIF/NELF-mediated inhibition of transcriptional elongation and reveals functional differences between P-TEFb and TFIIF. *Mol. Cell* 5: 1067–1072. [https://doi.org/10.1016/s1097-2765\(00\)80272-5](https://doi.org/10.1016/s1097-2765(00)80272-5)
- Wang H., C. Dienemann, A. Stützer, H. Urlaub, A. C. M. Cheung, *et al.*, 2020 Structure of the transcription coactivator SAGA. *Nature* 577: 717–720. <https://doi.org/10.1038/s41586-020-1933-5>
- Wang B., and I. Artsimovitch, 2021 NusG, an Ancient Yet Rapidly Evolving Transcription Factor. *Front. Microbiol.* 11.
- White C. L., R. K. Suto, and K. Luger, 2001 Structure of the yeast nucleosome core particle reveals fundamental changes in internucleosome interactions. *EMBO J.* 20: 5207–5218. <https://doi.org/10.1093/emboj/20.18.5207>
- Winston F., D. T. Chaleff, B. Valent, and G. R. Fink, 1984 Mutations Affecting Ty-Mediated Expression of the HIS4 Gene of *SACCHAROMYCES CEREVISIAE*. *Genetics* 107: 179–197.
- Winston F., and D. Koshland, 2016 Back to the Future: Mutant Hunts Are Still the Way To Go. *Genetics* 203: 1007–1010. <https://doi.org/10.1534/genetics.115.180596>
- Wood A., N. J. Krogan, J. Dover, J. Schneider, J. Heidt, *et al.*, 2003 Bre1, an E3 ubiquitin ligase required for recruitment and substrate selection of Rad6 at a promoter. *Mol. Cell* 11: 267–274. [https://doi.org/10.1016/s1097-2765\(02\)00802-x](https://doi.org/10.1016/s1097-2765(02)00802-x)
- Wu P.-Y. J., and F. Winston, 2002 Analysis of Spt7 function in the *Saccharomyces cerevisiae* SAGA coactivator complex. *Mol. Cell. Biol.* 22: 5367–5379. <https://doi.org/10.1128/MCB.22.15.5367-5379.2002>

- Wu P.-Y. J., C. Ruhlmann, F. Winston, and P. Schultz, 2004 Molecular architecture of the *S. cerevisiae* SAGA complex. *Mol. Cell* 15: 199–208.
<https://doi.org/10.1016/j.molcel.2004.06.005>
- Wyrick J. J., F. C. P. Holstege, E. G. Jennings, H. C. Causton, D. Shore, *et al.*, 1999 Chromosomal landscape of nucleosome-dependent gene expression and silencing in yeast. *Nature* 402: 418–421. <https://doi.org/10.1038/46567>
- Xiao T., C.-F. Kao, N. J. Krogan, Z.-W. Sun, J. F. Greenblatt, *et al.*, 2005 Histone H2B ubiquitylation is associated with elongating RNA polymerase II. *Mol. Cell. Biol.* 25: 637–651. <https://doi.org/10.1128/MCB.25.2.637-651.2005>
- Xu F., Q. Zhang, K. Zhang, W. Xie, and M. Grunstein, 2007 Sir2 Deacetylates Histone H3 Lysine 56 to Regulate Telomeric Heterochromatin Structure in Yeast. *Mol. Cell* 27: 890–900. <https://doi.org/10.1016/j.molcel.2007.07.021>
- Xu Z., W. Wei, J. Gagneur, F. Perocchi, S. Clauder-Münster, *et al.*, 2009 Bidirectional promoters generate pervasive transcription in yeast. *Nature* 457: 1033–1037. <https://doi.org/10.1038/nature07728>
- Yakhnin A. V., P. C. FitzGerald, C. McIntosh, H. Yakhnin, M. Kireeva, *et al.*, 2020 NusG controls transcription pausing and RNA polymerase translocation throughout the *Bacillus subtilis* genome. *Proc. Natl. Acad. Sci. U. S. A.* 117: 21628–21636. <https://doi.org/10.1073/pnas.2006873117>
- Yamada T., Y. Yamaguchi, N. Inukai, S. Okamoto, T. Mura, *et al.*, 2006 P-TEFb-Mediated Phosphorylation of hSpt5 C-Terminal Repeats Is Critical for Processive Transcription Elongation. *Mol. Cell* 21: 227–237. <https://doi.org/10.1016/j.molcel.2005.11.024>
- Yan C., H. Chen, and L. Bai, 2018 Systematic Study of Nucleosome-Displacing Factors in Budding Yeast. *Mol. Cell* 71: 294-305.e4. <https://doi.org/10.1016/j.molcel.2018.06.017>
- Yang Y., C. Liu, W. Zhou, W. Shi, M. Chen, *et al.*, 2021 Structural visualization of transcription activated by a multidrug-sensing MerR family regulator. *Nat. Commun.* 12: 2702. <https://doi.org/10.1038/s41467-021-22990-8>
- Yang C., R. Fujiwara, H. J. Kim, P. Basnet, Y. Zhu, *et al.*, 2022 Structural visualization of de novo transcription initiation by *Saccharomyces cerevisiae* RNA polymerase II. *Mol. Cell* 82: 660-676.e9. <https://doi.org/10.1016/j.molcel.2021.12.020>
- Ye Y., H. Wu, K. Chen, C. R. Clapier, N. Verma, *et al.*, 2019 Structure of the RSC complex bound to the nucleosome. *Science* 366: 838–843. <https://doi.org/10.1126/science.aay0033>

- Zentner G. E., T. Tsukiyama, and S. Henikoff, 2013 ISWI and CHD Chromatin Remodelers Bind Promoters but Act in Gene Bodies. *PLOS Genet.* 9: e1003317. <https://doi.org/10.1371/journal.pgen.1003317>
- Zhang K., S. K. Rajput, S. Wang, J. K. Folger, J. G. Knott, *et al.*, 2016 CHD1 Regulates Deposition of Histone Variant H3.3 During Bovine Early Embryonic Development. *Biol. Reprod.* 94: 140. <https://doi.org/10.1095/biolreprod.116.138693>
- Zhang L., A. Serra-Cardona, H. Zhou, M. Wang, N. Yang, *et al.*, 2018 Multisite Substrate Recognition in Asf1-Dependent Acetylation of Histone H3 K56 by Rtt109. *Cell* 174: 818-830.e11. <https://doi.org/10.1016/j.cell.2018.07.005>
- Zofall M., J. Persinger, S. R. Kassabov, and B. Bartholomew, 2006 Chromatin remodeling by ISW2 and SWI/SNF requires DNA translocation inside the nucleosome. *Nat. Struct. Mol. Biol.* 13: 339–346. <https://doi.org/10.1038/nsmb1071>
- Zuber P. K., L. Hahn, A. Reinl, K. Schweimer, S. H. Knauer, *et al.*, 2018 Structure and nucleic acid binding properties of KOW domains 4 and 6–7 of human transcription elongation factor DSIF. *Sci. Rep.* 8: 11660. <https://doi.org/10.1038/s41598-018-30042-3>
- Žumer K., K. C. Maier, L. Farnung, M. G. Jaeger, P. Rus, *et al.*, 2021 Two distinct mechanisms of RNA polymerase II elongation stimulation in vivo. *Mol. Cell* 81: 3096-3109.e8. <https://doi.org/10.1016/j.molcel.2021.05.028>
- Zunder R. M., A. J. Antczak, J. M. Berger, and J. Rine, 2012 Two surfaces on the histone chaperone Rtt106 mediate histone binding, replication, and silencing. *Proc. Natl. Acad. Sci. U. S. A.* 109: E144-153. <https://doi.org/10.1073/pnas.1119095109>